

**POWER SYSTEM INTENTIONAL ISLANDING FOR
DIFFERENT CONTINGENCY SCENARIOS USING
DISCRETE OPTIMIZATION TECHNIQUE**

NUR ZAWANI BINTI SAHARUDDIN

**COLLEGE OF GRADUATE STUDIES
UNIVERSITI TENAGA NASIONAL**

2020

**POWER SYSTEM INTENTIONAL ISLANDING FOR
DIFFERENT CONTINGENCY SCENARIOS USING DISCRETE
OPTIMIZATION TECHNIQUE**

NUR ZAWANI BINTI SAHARUDDIN

**A Thesis Submitted to the College of Graduate Studies, Universiti
Tenaga Nasional, in Fulfilment of the Requirements for the Degree
of**

Doctor of Philosophy (Engineering)

FEBRUARY 2020

DECLARATION

I hereby declare that the thesis is my original work except for quotations and citations which have been duly acknowledged. I also declare that it has not been previously, and is not concurrently submitted for any other degree at Universiti Tenaga Nasional or at any other institutions. This thesis may be made available within the university library and may be photocopied and loaned to other libraries for the purpose of consultation.

NUR ZAWANI BINTI SAHARUDDIN

Date:

ABSTRACT

Power systems are susceptible to unavoidable failures or outages. One of these incidents is critical line outage, which can lead to the occurrence of severe cascading failures. These cascading failures can cause the system to split in an uncontrollable manner, forming unbalanced islands, which results in severe instability problems before the system completely collapses. Intentional islanding is one of the remedial actions that can be implemented to prevent severe cascading failures following a critical line outage. This approach splits the system to form balanced, stand-alone islands in order to continuously supply electricity to the consumers until the system is completely restored. However, an optimal intentional islanding strategy is required for this purpose. Hence, this thesis proposed a Modified Discrete Evolutionary Programming (MDEP) to determine the optimal intentional islanding strategies for different large-scale power systems following a critical line outage. First, N-1 contingency analysis was performed to identify the critical line outages. Next, graph theory was used to map the network, where the physical connections of the network were represented by edges and vertices. The initial intentional islanding solution was determined using graph theory approach, to facilitate the proposed MDEP algorithm in determining the optimal intentional islanding strategy. Once the optimal solution was obtained, the power balance for each island was checked to ensure that the load-generation balance criterion was met. If there was power imbalance in a particular island, the MDEP-based load shedding scheme developed in this research was executed for that island. Finally, the bus voltage was checked and transmission line power flow analysis was performed to ensure that the solution did not violate the allowable voltage and transmission line capacity limits. The performance of the proposed MDEP algorithm was evaluated using the IEEE 30-bus, IEEE 39-bus, and IEEE 118-bus test systems. The results showed that the MDEP algorithm was capable of determining the optimal intentional islanding strategy (without critical line outage) with a lower total power flow disruption compared to those of other published works. In addition, the results of the case studies (with critical line outage) showed that the MDEP algorithm was able to obtain the optimal intentional islanding strategy with minimal power flow disruption.

ACKNOWLEDGMENT

In the Name of Allah, the Most Gracious, the Most Merciful

Firstly, I would like to express my infinite thank and praise to Allah the Almighty, for ease me to complete my PhD thesis. I would like to express my deepest appreciation to my supervisor, Prof. Ir. Dr. Izham Bin Zainal Abidin, Universiti Tenaga Nasional (UNITEN) for his sincere and excellent supervision, motivations and sharing valuable ideas during completion of this thesis. My sincere gratitude goes to my co-supervisor, Prof Ir. Dr. Hazlie Bin Mokhlis, University Malaya for his guidance, help and support throughout completing this thesis. May Allah reward both of them with more success and happiness in life. My honest appreciation goes to my colleague, Dr. Kanendra Naidu, lecturer in UniKL BMI, Kuala Lumpur, who gave me a helping hand and insightful comments to complete this PhD research.

My sincere appreciation goes to the Malaysian Ministry of Higher Education (MOHE) and FRGS Grant (FRGS/1/2018/TK07/UNITEN/01/1) for the financial and technical support throughout my PhD study. Not forgotten, many thanks to the Universiti Tenaga Nasional (UNITEN) and Universiti Teknikal Malaysia Melaka (UTeM) for giving a great opportunity to further and complete this PhD study.

My special and heartfelt gratitude goes to my beloved husband, Mr. Khalid Ahmad, for his continuous support, motivations, and endless love throughout this wonderful journey. To my pillar of strength, my parents, Hj. Saharuddin and Hj. Usemah, thank you for your endless love, supports and prayers to make my PhD study completed successfully. Not to forget, I am grateful to my adorable children, Alya Adawiyah, Ahmad Irfan and Amira Aleesya, for their love and understanding. I heartily thank to my siblings, and my grandfather, Hj Samsudin for their endless supports and prayers. Lastly, thank you to all my colleagues, friends and everyone in the impact to the completion of this PhD thesis.

TABLE OF CONTENTS

DECLARATION	ii
ABSTRACT	iii
ACKNOWLEDGMENT	iv
TABLE OF CONTENTS	v
LIST OF TABLES	ix
LIST OF FIGURES	xiv
LIST OF SYMBOLS	xix
LIST OF ABBREVIATIONS	xx
LIST OF PUBLICATIONS	xxi
CHAPTER 1 INTRODUCTION	1
1.1 Background of the Research	1
1.2 Problem Statement	2
1.3 Research Objectives	4
1.4 Research Scope	5
1.5 Significant Contributions of the Research	5
1.6 Organization of the Thesis	6
CHAPTER 2 LITERATURE REVIEW	8
2.1 Introduction	8
2.2 Power System Network	8
2.3 Power System Failures	9
2.4 Power System Security	10
2.4.1 Contingency Analysis	14
2.5 Power System Blackouts	16
2.5.1 Blackout in Canada and Some States in the North-Eastern Region of the United States of America	18
2.5.2 Blackout in the United States of America and Canada	18
2.5.3 Blackout in Southern Sweden and Eastern Denmark	19
2.5.4 Blackout in Italy	19
2.5.5 Blackout in India	20
2.5.6 Blackout in Malaysia	20

2.5.7	Summary of Power System Blackouts	21
2.6	Blackout Mitigation Techniques	22
2.6.1	Preventive Control Action: Generator Rescheduling	22
2.6.2	Load Shedding Scheme	23
2.6.3	Automatic Voltage Regulators and Power System Stabilizers	25
2.6.4	Intentional Islanding	26
2.6.5	Summary of Blackout Mitigation Techniques	27
2.7	Intentional Islanding as a Remedial Action for Power Systems	28
2.7.1	Ordered Binary Decision Diagram-Based Techniques	30
2.7.2	Slow Coherency-Based Techniques	33
2.7.3	Clustering-Based Techniques	34
2.7.4	Linear Programming-Based Techniques	35
2.7.5	Heuristic and Metaheuristic-Based Techniques	36
2.7.6	Summary of Intentional Islanding Techniques	38
2.8	Graph Theory	39
2.8.1	Application of Graph Theory in Modelling Power Systems	41
2.8.2	Application of Graph Theory in Intentional Islanding	42
2.9	Optimization and Metaheuristic Techniques	42
2.9.1	Evolutionary Programming	44
2.9.2	Particle Swarm Optimization	45
2.10	Load Shedding Scheme for Intentional Islanding	46
2.11	Chapter Summary	49
 CHAPTER 3 METHODOLOGY		 51
3.1	Introduction	51
3.2	Overall Research Methodology	51
3.2.1	Stage 1: Preliminary Study	52
3.2.2	Stage 2: Data Collection and Extraction	52
3.2.3	Stage 3: Development of the intentional islanding algorithms and load shedding algorithm	52
3.2.4	Stage 4: Evaluation and validation of the intentional islanding algorithms and load shedding algorithm using case studies	53
3.3	Proposed Methodology	53
3.3.1	Modelling of the Large-Scale Power Systems	55

3.3.2	N-1 Contingency Analysis	57
3.3.3	Determination of the Initial Intentional Islanding Solution Using the Graph Theory Approach	59
3.3.4	Metaheuristic Discrete Optimization Algorithms	65
3.3.5	Modified Discrete Evolutionary Programming (MDEP) Algorithm	66
3.3.6	Modified Discrete Particle Swarm Optimization (MDPSO) Algorithm	74
3.3.7	Load Shedding Scheme Based on the Modified Discrete Evolutionary Programming (MDEP) Technique	76
3.4	Chapter Summary	80

CHAPTER 4 VALIDATION OF THE DEVELOPED INTENTIONAL ISLANDING ALGORITHMS WITHOUT CONTINGENCY ANALYSIS 82

4.1	Introduction	82
4.2	IEEE Test Systems	82
4.2.1	IEEE 30-Bus Test System	83
4.2.2	IEEE 39-Bus Test System	83
4.2.3	IEEE 118-Bus Test System	84
4.3	Analysis of the IEEE 30-Bus Test System	85
4.3.1	Case Study 1	86
4.3.2	Case Study 2	93
4.3.3	Case Study 3	98
4.4	Analysis of the IEEE 39-Bus Test System	104
4.4.1	Case Study 4	104
4.4.2	Case Study 5	110
4.4.3	Case Study 6	115
4.5	Analysis of the IEEE 118-Bus Test System	122
4.5.1	Case Study 7	123
4.5.2	Case Study 8	129
4.5.3	Case Study 9	134
4.6	Chapter Summary	140

CHAPTER 5	PROPOSED INTENTIONAL ISLANDING ALGORITHM WITH CONTINGENCY ANALYSIS AND LOAD SHEDDING SCHEME	142
5.1	Introduction	142
5.2	IEEE Test Systems	142
5.3	N-1 Contingency Analysis and Determination of Critical Lines	143
5.4	Critical Line Outages for the IEEE 30-Bus Test System	143
5.4.1	Case Study C1	144
5.4.2	Case Study C2	150
5.4.3	Case Study C3	155
5.5	Critical Line Outages for the IEEE 39-Bus Test System	160
5.5.1	Case Study C4	161
5.5.2	Case Study C5	166
5.5.3	Case Study C6	171
5.6	Critical Line Outages for the IEEE 118-Bus Test System	177
5.6.1	Case Study C7	178
5.6.2	Case Study C8	183
5.6.3	Case Study C9	188
5.7	Validation of the MDEP-Based Load Shedding Scheme	194
5.8	Chapter Summary	198
CHAPTER 6	CONCLUSIONS AND RECOMMENDATIONS FOR FUTURE WORK	200
6.1	Conclusions	200
6.2	Recommendations for Future Work	202
	REFERENCES	204
	APPENDIX A	217
	APPENDIX B	256

LIST OF TABLES

Table 2.1. Main Causes of Failures and Their Effects on the Power System	10
Table 3.1. Transmission Line Data for IEEE 14-bus test system	65
Table 3.2. Step 1 of Mutation Technique 1	68
Table 3.3. Step 2 of Mutation Technique 1	68
Table 3.4. Step 1 of Mutation Technique 2	69
Table 3.5. Step 2 of Mutation Technique 2	70
Table 3.6. Step 1 of Mutation Technique 3	70
Table 3.7. Step 2 of Mutation Technique 3	71
Table 3.8. Example of Initial Populations Generated for Load Shedding Using the MDEP-Based Load Shedding Scheme	79
Table 4.1. Initial Intentional Islanding Solution for Case Study 1	87
Table 4.2. Comparison of the Optimal Intentional Islanding Strategies for Case Study	88
Table 4.3. Comparison of the Performance between the MDEP and MDPSO Algorithms	89
Table 4.4. Results for Island 1 and Island 2 Before and After Intentional Islanding Implementation: Case Study 1	91
Table 4.5. Initial Intentional Islanding Solution for Case Study 2	94
Table 4.6. Comparison of the Optimal Intentional Islanding Strategies for Case Study 2	94
Table 4.7. Comparison of the Performance between the MDEP and MDPSO Algorithms	95
Table 4.8. Results for Island 1 and Island 2 Before and After Intentional Islanding Implementation: Case Study 2	97
Table 4.9. Initial Intentional Islanding Solution for Case Study 3	99
Table 4.10. Comparison of the Optimal Intentional Islanding Strategies for Case Study 3	99
Table 4.11. Comparison of the Performance Between the MDEP and MDPSO Algorithms	100
Table 4.12. Results for Islands 1–3 Before and After Intentional Islanding Implementation: Case Study 3	102
Table 4.13. Initial Intentional Islanding Solution for Case Study 4	105

Table 4.14. Comparison of the Optimal Intentional Islanding Strategies for Case Study 4	106
Table 4.15. Comparison of the Performance Between the MDEP and MDPSO Algorithms	107
Table 4.16. Results for Island 1 and Island 2 Before and After Intentional Islanding Implementation: Case Study 4	109
Table 4.17. Initial Intentional Islanding Solution for Case Study 5	110
Table 4.18. Comparison of the Optimal Intentional Islanding Strategies for Case Study 5	111
Table 4.19. Comparison of the Performance Between the MDEP and MDPSO Algorithms	112
Table 4.20. Results for Islands 1–3 Before and After Intentional Islanding Implementation: Case Study 5	114
Table 4.21. Initial Intentional Islanding Solution for Case Study 6	117
Table 4.22. Comparison of the Optimal Intentional Islanding Strategies for Case Study 6	117
Table 4.23. Comparison of the Performance Between the MDEP and MDPSO Algorithms	118
Table 4.24. Results for Islands 1–4 Before and After Intentional Islanding Implementation: Case Study 6	120
Table 4.25. Initial Intentional Islanding Solution for Case Study 7	124
Table 4.26. Comparison of the Optimal Intentional Islanding Strategies for Case Study 7	125
Table 4.27. Comparison of the Performance between the MDEP and MDPSO Algorithms	126
Table 4.28. Results for Island 1 and Island 2 Before and After Intentional Islanding Implementation: Case Study 7	128
Table 4.29. Initial Intentional Islanding Solution for Case Study 8	130
Table 4.30. Comparison of the Optimal Intentional Islanding Strategies for Case Study 8	131
Table 4.31. Results for Island 1 and Island 2 Before and After Intentional Islanding Implementation: Case Study 8	133
Table 4.32. Initial Intentional Islanding Solution for Case Study 9	135

Table 4.33. Comparison of the Optimal Intentional Islanding Strategies for Case Study 9	136
Table 4.34. Results for Islands 1–3 Before and After Intentional Islanding Implementation: Case Study 9	138
Table 5.1. Three Most Critical Line Outages for the IEEE 30-Bus Test System	143
Table 5.2. Initial Intentional Islanding Solution for Case Study C1	145
Table 5.3. Comparison of the Optimal Intentional Islanding Strategies for Case Study C1	146
Table 5.4. Comparison of the Performance between the MDEP and MDPSO Algorithms	147
Table 5.5. Results for Island 1 and Island 2 Before and After Intentional Islanding Implementation: Case Study C1	149
Table 5.6. Initial Intentional Islanding Solution for Case Study C2	151
Table 5.7. Comparison of the Optimal Intentional Islanding Strategies for Case Study C2	151
Table 5.8. Comparison of the Performance between the MDEP and MDPSO Algorithms	152
Table 5.9. Results for Island 1 and Island 2 Before and After Intentional Islanding Implementation: Case Study C2	153
Table 5.10. Initial Intentional Islanding Solution for Case Study C3	155
Table 5.11. Comparison of the Optimal Intentional Islanding Strategies for Case Study C3	156
Table 5.12. Comparison of the Performance Between the MDEP and MDPSO Algorithms	156
Table 5.13. Results for Islands 1–3 Before and After Intentional Islanding Implementation: Case Study C3	158
Table 5.14. Three Most Critical Line Outages for the IEEE 39-Bus Test System	160
Table 5.15. Initial Intentional Islanding Solution for Case Study C4	161
Table 5.16. Comparison of the Optimal Intentional Islanding Strategies for Case Study C4	162
Table 5.17. Comparison of the Performance Between the MDEP and MDPSO Algorithms	163
Table 5.18. Results for Island 1 and Island 2 Before and After Intentional Islanding Implementation: Case Study C4	165

Table 5.19. Initial Intentional Islanding Solution for Case Study C5	166
Table 5.20. Comparison of the Optimal Intentional Islanding Strategies for Case Study C5	167
Table 5.21. Comparison of the Performance Between the MDEP and MDPSO Algorithms	168
Table 5.22. Results for Islands 1–3 Before and After Intentional Islanding Implementation: Case Study C5	170
Table 5.23. Initial Intentional Islanding Solution for Case Study C6	172
Table 5.24. Comparison of the Optimal Intentional Islanding Strategies for Case Study C6	172
Table 5.25. Comparison of the Performance Between the MDEP and MDPSO Algorithms	173
Table 5.26. Results for Islands 1–4 Before and After Intentional Islanding Implementation: Case Study C6	175
Table 5.27. Three Most Critical Line Outages for the IEEE 118-Bus Test System	178
Table 5.28. Initial Intentional Islanding Solution for Case Study C7	179
Table 5.29. Comparison of the Optimal Intentional Islanding Strategies for Case Study C7	179
Table 5.30. Comparison of the Performance Between the MDEP and MDPSO Algorithms	180
Table 5.31. Results for Island 1 and Island 2 Before and After Intentional Islanding Implementation: Case Study C7	182
Table 5.32. Initial Intentional Islanding Solution for Case Study C8	184
Table 5.33. Comparison of the Optimal Intentional Islanding Strategies for Case Study C8	184
Table 5.34. Results for Islands 1–3 Before and After Intentional Islanding Implementation: Case Study C8	187
Table 5.35. Initial Intentional Islanding Solution for Case Study C9	189
Table 5.36. Comparison of the Optimal Intentional Islanding Strategies for Case Study C9	189
Table 5.37. Results for Islands 1–4 Before and After Intentional Islanding Implementation: Case Study C9	192

Table 5.38. Comparison of the Performance between the Conventional EP, Exhaustive Search, and MDEP Algorithms for Case Study 6 (Island 2) – Chapter 4	194
Table 5.39. Comparison of the Performance between the Conventional EP, Exhaustive Search, and MDEP Algorithms for Case Study 6 (Island 4) – Chapter 4	195
Table 5.40. Comparison of the Performance between the Conventional EP, Exhaustive Search, and MDEP Algorithms for Case Study C1 (Island 2) – Chapter 5	196
Table 5.41. Comparison of the Performance between the Conventional EP, Exhaustive Search, and MDEP Algorithms for Case Study C4 (Island 1) – Chapter 5	197

LIST OF FIGURES

Figure 2.1. Basic Power System [14]	8
Figure 2.2. Operating States of a Power System [25]	11
Figure 2.3. General Process that Leads to a Power System Blackout [28]	13
Figure 2.4. Steps Involved in a Contingency Analysis [33]	16
Figure 2.5. Consequences of Power System Blackouts [44].	17
Figure 2.6. Flow Chart of the Undervoltage Load Shedding (UVLS) Scheme [66]	24
Figure 2.7. Intentional Islanding Strategy Obtained from the Ordered Binary Decision Diagram (OBDD)-Based Approach for the IEEE 30-Bus Test System [80]	27
Figure 2.8. Intentional Islanding Techniques	30
Figure 2.9. Steps Involved in the Three-Phase Ordered Binary Decision Diagram (OBDD)-Based Intentional Islanding Technique [89]	31
Figure 2.10. Concept of the Multi-Level Kernel k -means Intentional Islanding Algorithm [2]	34
Figure 2.11. (a) Schematic of an Electrical Circuit, (b) Graph Theory Representation [103]	40
Figure 2.12. Schematic of a Directed Graph	40
Figure 2.13. Schematic of an Undirected Graph	40
Figure 2.14. Depth First Search Graph Traversal Technique	41
Figure 2.15. Steps Involved in the Evolutionary Programming (EP) Algorithm [121]	45
Figure 2.16. Steps Involved in the Particle Swarm Optimization (PSO) Algorithm [128]	46
Figure 3.1. Flow Chart of the Overall Research Methodology	52
Figure 3.2. Flow Chart of the Proposed Methodology	54
Figure 3.3. IEEE 9-Bus Test System	56
Figure 3.4. Representation of the IEEE 9-Bus Test System as a Graph Model	56
Figure 3.5. Flow Chart of the N-1 Contingency Analysis	58
Figure 3.6. Determination of the Initial intentional islanding solution using the Graph Theory Approach	61
Figure 3.7. IEEE 14-Bus Test System	62
Figure 3.8. IEEE 14-Bus Test System after Disconnecting the Critical Line	62

Figure 3.9. Formation of the Coherent Groups of Generators	63
Figure 3.10. Identification of the Next-Nearest Vertices for the Vertices in Group 1 and Group 2 after the 2 nd Iteration of Graph Theory-Based Initialization	64
Figure 3.11. Final Result (Initial Intentional Islanding Solution) Obtained from the Graph Theory Approach	64
Figure 3.12. Flow Chart of the Developed MDEP Algorithm	72
Figure 3.13. Flow Chart of the Developed MDPSO Algorithm	75
Figure 3.14. Steps Involved in a Load Shedding Scheme	77
Figure 3.15. Steps Involved in the MDEP-Based Load Shedding Scheme	79
Figure 4.1. Schematic of the IEEE 30-Bus Test System	83
Figure 4.2. Schematic of the Original IEEE 39-Bus Test System	84
Figure 4.3. Schematic of the Modified IEEE 39-Bus Test System	84
Figure 4.4. Schematic of the IEEE 118-Bus Test System	85
Figure 4.5. Representation of the IEEE 30-Bus Test System as a Graph Model	86
Figure 4.6. Graph Model of the Initial Intentional Islanding Solution (Red Lines) for Case Study 1	87
Figure 4.7. Convergence Curves for the MDEP and MDPSO Algorithms for Case Study 1	88
Figure 4.8. One-Line Diagram for Case Study 1	90
Figure 4.9. Graph Model of the Islanded Islands for Case Study 1	90
Figure 4.10. Graph Model of the Initial Intentional Islanding Solution (Red Lines) for Case Study 2	93
Figure 4.11. Convergence Curves for the MDEP and MDPSO Algorithms for Case Study 2	95
Figure 4.12. Optimal Intentional Islanding Strategy (Red Dashed Lines) for Case Study 2	96
Figure 4.13. Graph Model of the Initial Intentional Islanding Solution (Red Lines) for Case Study 3	98
Figure 4.14. Convergence Curves for the MDEP and MDPSO Algorithms for Case Study 3	100
Figure 4.15. Optimal Intentional Islanding Strategy (Red Dashed Lines) for Case Study 3	101
Figure 4.16. Representation of the Original IEEE 39-Bus Test System as a Graph Model	104

Figure 4.17. Graph Model of the Initial Intentional Islanding Solution (Red Lines) for Case Study 4	105
Figure 4.18. Convergence Curves for the MDEP and MDPSO Algorithms for Case Study 4	106
Figure 4.19. Optimal Intentional Islanding Strategy (Red Dashed Lines) for Case Study 4	108
Figure 4.20. Graph Model of the Initial Intentional Islanding Solution (Red Lines) for Case Study 5	110
Figure 4.21. Convergence Curves for the MDEP and MDPSO Algorithms for Case Study 5	112
Figure 4.22. Optimal Intentional Islanding Strategy (Red Dashed Lines) for Case Study 5	113
Figure 4.23. Representation of the Modified IEEE 39-Bus Test System as a Graph Model	116
Figure 4.24. Graph Model of the Initial Intentional Islanding Solution (Red Lines) for Case Study 6	116
Figure 4.25. Convergence Curves for the MDEP and MDPSO Algorithms for Case Study 6	118
Figure 4.26. Optimal Intentional Islanding Strategy (Red Dashed Lines) for Case Study 6	119
Figure 4.27. Representation of the IEEE 118-Bus Test System as a Graph Model	123
Figure 4.28. Graph Model of the Initial Intentional Islanding Solution (Red Lines) for Case Study 7	124
Figure 4.29. Convergence Curves for the MDEP and MDPSO Algorithms for Case Study 7	126
Figure 4.30. Optimal Intentional Islanding Strategy (Red Dashed Lines) for Case Study 7	127
Figure 4.31. Graph Model of the Initial Intentional Islanding Solution (Red Lines) for Case Study 8	130
Figure 4.32. Convergence Curves for the MDEP and MDPSO Algorithms for Case Study 8	131
Figure 4.33. Optimal Intentional Islanding Strategy (Red Dashed Lines) for Case Study 8	132

Figure 4.34. Graph Model of the Initial Intentional Islanding Solution (Red Lines) for Case Study 9	135
Figure 4.35. Convergence Curves for the MDEP and MDPSO Algorithms for Case Study 9	136
Figure 4.36. Optimal Intentional Islanding Strategy (Red Dashed Lines) for Case Study 9	137
Figure 5.1. Initial Intentional Islanding Solution (Red Lines) for Case Study C1	145
Figure 5.2. Convergence Curves for the MDEP and MDPSO Algorithms for Case Study C1	146
Figure 5.3. One-Line Diagram for Case Study C1	147
Figure 5.4. Graph Model of the Islanded Islands for Case Study C1	148
Figure 5.5. Convergence Curves for the MDEP and MDPSO Algorithms for Case Study C2	152
Figure 5.6. One-Line Diagram for Case Study C2	153
Figure 5.7. Convergence Curves for the MDEP and MDPSO Algorithms for Case Study C3	156
Figure 5.8. One-Line Diagram for Case Study C3	157
Figure 5.9. Convergence Curves for the MDEP and MDPSO Algorithms for Case Study C4	162
Figure 5.10. One-Line Diagram for Case Study C4	164
Figure 5.11. Convergence Curves for the MDEP and MDPSO Algorithms for Case Study C5	167
Figure 5.12. One-Line Diagram for Case Study C5	169
Figure 5.13. Convergence Curves for the MDEP and MDPSO Algorithms for Case Study C6	173
Figure 5.14. One-Line Diagram for Case Study C6	174
Figure 5.15. Convergence Curves for the MDEP and MDPSO Algorithms for Case Study C7	180
Figure 5.16. One-Line Diagram for Case Study C7	181
Figure 5.17. Convergence Curves for the MDEP and MDPSO Algorithms for Case Study C8	185
Figure 5.18. One-Line Diagram for Case Study C8	186
Figure 5.19. Convergence Curves for the MDEP and MDPSO Algorithms for Case Study C9	190

LIST OF SYMBOLS

Variables

$P_{i,gen}$	Generated active power
$P_{i,load}$	Supplied active power
$P_{i,line}$	Active power flow for line i
$P_{i,max}$	Maximum allowable limit of active power flow for line i
V_{min}	Minimum voltage magnitude
V_{max}	Maximum voltage magnitude
V_{line}	Operating voltage magnitude
g_{best}	Global best particle
p_{best}	Local best position
$S_{ij(critical)}$	Critical loading of the transmission line between line i and line j
$S_{ij(max)}$	Maximum limit of MVA loading of the transmission line between line i and line j
$2^n - 1$	Search space, n =total number of transmission line in the system
$IS(x)$	Mutated islanding solution
P_{imb}	Power Imbalance
P_{loss}	Power losses

LIST OF ABBREVIATIONS

AC	Alternating Current
AMPSO	Angle Modulated Particle Swarm Optimization
AVR	Automatic Voltage Regulator
BFS	Breadth first search
BPSO	Binary Particle Swarm Optimization
DC	Direct Current
DC-OPF	Direct Current Optimal Power Flow
DFS	Depth first search
EP	Evolutionary Programming
ER	Eastern Regional Grid
MDEP	Modified Discrete Evolutionary Programming
MDPSO	Modified Discrete Particle Swarm Optimization
MILP	Mixed-Integer Linear Programming
MVA	Mega Volt Amp
MW	Mega Watt
NERC	North American Electric Reliability Corporation
NER	North- Eastern Regional Grid
NR	Northern Regional Grid
OBDD	Ordered Binary Decision Diagram
PBC	Power balance constraint
PSO	Particle Swarm Optimization
PSS	Power System Stabilizer
RAS	Remedial Action Scheme
RLC	Rated value and limit constraints
SR	Southern Regional Grid
SSC	Separation and synchronization constraint
TVC	Threshold value constraint
UCTE	Union for the Coordination of the Transmission of Electricity
UFLS	Under Frequency Load Shedding
UVLS	Under Voltage Load Shedding
WR	Western Regional Grid

LIST OF PUBLICATIONS

Journal paper

N. Saharuddin, I. Zainal Abidin, H. Mohklis, A. Abdullah, and K. Naidu, "A Power System Network Splitting Strategy Based on Contingency Analysis," *Energies*, vol. 11, no. 2, pp. 434, 2018. (ISI Journal).

N. Saharuddin, I. Zainal Abidin, H. Mohklis, K. Naidu, "Intentional Islanding Methods as Post Fault Remedial Action : A Review", *Indonesian Journal of Electrical Engineering and Computer Science*, 12(1), pp. 182-192, 2019. (SCOPUS Journal).

N. Saharuddin, I. Zainal Abidin, H. Mohklis, "Discrete Evolutionary Programming for Network Splitting Strategy : Different Mutation Technique", *Indonesian Journal of Electrical Engineering and Computer Science*, 12(1), pp. 261-268, 2018. (SCOPUS Journal).

Conference Proceedings

N. Saharuddin, I. Zainal Abidin, H. Mohklis, "Intentional Islanding Solution Based on Modified Discrete Particle Swarm Optimization Technique," in 2018 IEEE 7th International Conference on Power and Energy (PECon), pp. 399-404, 2018. (SCOPUS indexed).

CHAPTER 1

INTRODUCTION

1.1 Background of the Research

Electricity is one of the necessities in today's world and it is used in various sectors such as residential, transportation, and industrial sectors. Electricity is delivered to the consumers through an interconnected network, which is called a power system. A power system typically consists of three main elements, which are generation, transmission, and distribution systems. With increasing dependency on electricity, there is a critical need for reliable and secure operation of power systems to ensure a stable, continuous supply of electricity to the consumers.

In general, power systems are designed to withstand contingencies and minimize the unfavourable consequences of these contingencies. However, it is not possible to maintain the security of power systems in all contingencies. Some critical contingencies may cause the power system to deviate from its normal operating conditions and initiate cascading failures event. One of the common causes of cascading failures is line overloading [1]. When a certain line is disconnected from the power system because of a severe outage, this will cause other lines to overload and trip. This process continues and causes the system eventually splits into several unbalanced electrical islands. This phenomenon is known as unintentional islanding. Unintentional islanding can cause instability in the power system, which will lead to a partial or total system blackout [2].

Most of the major blackout incidents worldwide are caused by cascading failures [3], [4], [5]. The most detrimental impact of cascading failures (e.g. sequence of line tripping) is blackouts. Blackouts can have a significant effect on a nation's economic growth [6]. For instance, a major blackout that occurred in Northern India in July 2012 for two consecutive days was initiated by cascading failures because of line overloading. These cascading failures culminated in a total system blackout, which affected more than 600 million consumers [7].

One of the remedial actions implemented to prevent blackouts in power systems is intentional islanding. Intentional islanding is a planned islanding process, which preserves the stable areas in the power system from further cascading failures. Moreover, intentional islanding speeds up the restoration process by minimizing transient instability during system reconnection [8]. In general, intentional islanding is a process of splitting the power system into a number of balanced, stand-alone islands. These islands must be balanced in terms of the total generated power and total load to ensure a continuous supply of electricity to the consumers even though the power system has deviated from its normal state. It is important to devise a suitable intentional islanding technique for cases where there is a high possibility for severe cascading failures to occur. One of the important criteria for intentional islanding is to disconnect the appropriate transmission lines (cutset candidates). The huge number of possible combinations of lines ($2^{\text{total_no_of_transmission_lines}} - 1$) that can be considered as the cutset candidates further complicates the islanding problem. Therefore, it is crucial to determine the optimal intentional islanding strategy to ensure that the implementation of intentional islanding does not cause further stability problems in the power system.

To date, a number of intentional islanding techniques have been proposed by previous researchers. Some of these techniques consider contingencies whereas others do not during the intentional islanding implementation. However, none of these techniques consider the possibility of severe cascading failures due to critical line outages in determining the optimal intentional islanding strategy [9]. It is important to develop intentional islanding algorithms that are capable of determining the optimal intentional islanding strategies for different scale of power systems following a critical line outage, which is known to cause severe cascading failures that can lead to a partial or total system blackout. These algorithms will be greatly beneficial for system operators to simulate and implement successful intentional islanding during contingencies.

1.2 Problem Statement

Intentional islanding is executed when the system is exposed to severe cascading failure following a critical line outage. However, it is impossible to obtain the

intentional islanding strategy without precise and reliable information on critical line outages. Due to the fact that power system consists of many transmission lines and some outages may be vulnerable to severe cascading failures, which can lead to a partial or total system blackout, the identification of critical line outages is crucial [1]. Contingency analysis based on N-1 contingency analysis (MVA violation) is one of the primary contingency analyzes used in the planning and control stage of a power system to identify the critical line outages that can initiate severe cascading failures. Based on this information, the suitable intentional islanding strategy following a critical line outage can be determined using the appropriate optimization technique.

One of the aspects that pose a significant challenge in determining the optimal intentional islanding strategy is the huge number of possible intentional islanding strategies, especially for large-scale power systems [10]. Other constraints such as the desired number of islands, coherent groups of generators, load-generation balance, and transmission line capacity further complicates the determination of the optimal intentional islanding strategy [9]. Without a feasible initial population that fulfils all of the specified constraints, the optimization technique may not be able to determine the optimal intentional islanding strategy. Hence, a randomly generated initial population may not be a feasible approach to solve intentional islanding problems. Therefore, a suitable technique needs to be devised to generate a feasible initial population, which will facilitate the optimization technique in determining the optimal intentional islanding strategy following critical line outage. Graph theory-based initialization is one of the approaches that can be used to determine a feasible initial solution, which will be used as an initial population for the optimization technique.

Since intentional islanding is a discrete problem in nature, continuous optimization technique is not suitable to solve intentional islanding problem [11]. Therefore, a suitable discrete based optimization technique is required to determine the optimal intentional islanding strategy following a critical line outage.

The power balance (also known as the load-generation balance) is a criterion that needs to be fulfilled for each island formed after intentional islanding [12]. The total generated power and total load in each island must be balanced to ensure successful intentional islanding implementation [8]. However, there may be cases where certain islands are not balanced (i.e. the total generated power is less than the total demand) after intentional islanding and a load shedding scheme is needed to shed to the suitable amount of load from these islands. In general, conventional load shedding schemes based on expert knowledge or exhaustive search are used to determine the best combination of loads to be shed. However, expert knowledge-based load shedding schemes do not guarantee that the optimal amount of load is shed from the unbalanced islands at all times [13]. Likewise, exhaustive search-based load shedding schemes are not really efficient because the time taken to determine the optimal amount of load to be shed will increase with an increase in the network size. Hence, it is crucial to devise an efficient load shedding scheme, which will determine the optimal amount of load to be shed within a shorter computational time. The number of interrupted loads can be reduced by shedding the optimal amount of load after intentional islanding.

1.3 Research Objectives

The main aim of this research is to determine the optimal intentional islanding strategies for different large-scale power systems following a critical line outage. The following objectives were set to achieve this aim:

1. To develop an algorithm to determine the best initial islanding solution, which will facilitate the intentional islanding algorithms in determining the optimal intentional islanding strategy for a power system following a critical line outage.
2. To develop intentional islanding algorithms to determine the optimal intentional islanding strategy for a power system (considering critical line outages) using the Modified Discrete Evolutionary Programming (MDEP) and Modified Discrete Particle Swarm Optimization (MDPSO) techniques.
3. To develop a load shedding scheme based on the MDEP technique to determine the optimal amount of load that needs to be shed in order to obtain balanced, stand-alone islands after intentional islanding.

1.4 Research Scope

The scope and limitations of this research are presented as follows:

- The main aim of this research is to determine the optimal intentional islanding strategies for different large-scale power systems following a critical line outage, which can be used for planning and control action purposes. Thus, the time constraints in determining the optimal solutions are not considered.
- Contingency analysis is important to determine the critical line outages for a power system, which can trigger cascading failures. In this research, only N-1 contingency analysis is considered to determine the three most critical line outages for a particular power system because it is sufficient for primary contingencies (single-element outages).
- The power systems studied in this research are the IEEE 30-bus, IEEE 39-bus, and IEEE 118-bus test systems.
- The coherent group of generators and the desired number of islands to be formed are defined based on previously published works.
- Because the deficits in the reactive power, Q of the power system could be compensated locally, the proposed intentional islanding and load shedding algorithms only consider the active power (real power), P in this research.

1.5 Significant Contributions of the Research

The significant contributions of this research are summarized as follows:

- **Development of intentional islanding algorithm for planning and control action purposes:** The intentional islanding algorithms (MDEP and MDPSO algorithms) developed in this research can be used to plan and implement the appropriate control actions in the event of a contingency (single-element outage). With these algorithms (particularly the MDEP algorithm), the optimal intentional islanding strategy (i.e. the suitable transmission lines to be disconnected) can be determined, which will facilitate system operators in managing the conditions of the power system. With this algorithm, the system operators can simulate and plan successful intentional islanding in order to prevent severe cascading failures and blackouts.

- **Development of the graph theory-based algorithm to determine a feasible initial intentional islanding solution, considering critical line outages:** In this research, graph theory approach is used to determine the initial intentional islanding solution for a power system following a critical line outage. This algorithm provides a feasible initial solution after the first critical line is disconnected from the network. This emulates the scenario where the critical line is disconnected because of an outage, which can cause severe cascading failures to occur. The initial solution reduces the huge search space of possible intentional islanding strategies without making any simplifications to the original power system. The initial islanding solution is then used in the MDEP and MDPSO algorithms to determine the optimal intentional islanding strategy.
- **Development of intentional islanding algorithms taking into account the critical line outages:** In this research, two intentional islanding algorithms (MDEP and MDPSO algorithms) are developed and the proposed algorithm (MDEP algorithm) is used to determine the optimal intentional islanding strategy taking into consideration the critical line outages. The N-1 contingency analysis is used to identify the critical line outages, which will trigger severe cascading failures. Since intentional islanding is a discrete problem, discrete mutation techniques are used in the developed algorithms to determine the optimal intentional islanding strategies. The advantage of this approach is that all of the system constraints can be embedded into the intentional islanding algorithms.
- **Development of the MDEP-based load shedding scheme:** In this research, a load shedding scheme is developed based on the MDEP technique to determine the optimal amount of load that needs to be shed from the unbalanced islands after intentional islanding in order to islands that fulfil the load-generation balance criteria.

1.6 Organization of the Thesis

This thesis is focused on determining the optimal intentional islanding strategies for large-scale power systems, taking into account critical line outages, by means of discrete optimization technique. This thesis starts with Chapter 1 which presents a

brief introduction on the importance of intentional islanding as a blackout mitigation technique. Then, the problem statement is presented, followed by the research objectives, scope, limitations, and significant contributions of the research. The organization of the thesis is presented at the end of this chapter. Chapter 2 describes on the power system network and power system failures. The power system security and contingency analysis in power system are also discussed in this chapter. Numerous worldwide major blackouts are further reviewed and discussed. Common mitigations technique used to prevent blackouts are also highlighted in detail. This chapter also examines numerous intentional islanding techniques and load shedding schemes, which are related to the research topic. Chapter 3 presents the methodology adopted in this research to develop the MDEP and MDPSO intentional islanding algorithms and the MDEP-based load shedding scheme. Chapter 4 further presents the validation of the developed MDEP and MDPSO algorithms based on nine case studies (three case studies for the IEEE 30-bus, IEEE 39-bus, and IEEE 118-bus test systems, respectively). These algorithms were used to determine the optimal intentional islanding strategies for these case studies without contingency analysis and the results are presented and discussed in detail in this chapter. Chapter 5 presents the evaluation of the developed MDEP and MDPSO algorithms based on nine case studies (three case studies for the IEEE 30-bus, IEEE 39-bus, and IEEE 118-bus test systems, respectively). These algorithms were used to determine the optimal intentional islanding strategies for these case studies, where N-1 contingency analysis was used to identify the three most critical line outages for each test system. The results obtained for these case studies are presented and discussed in detail in this chapter. The validation of the MDEP-based load shedding scheme is also presented in this chapter. Finally, Chapter 6 presents the key findings of this research, along with recommendations for future work, particularly the areas that can be improved for the MDEP algorithm.

CHAPTER 2

LITERATURE REVIEW

2.1 Introduction

This chapter begins by describing a power system and the processes involved in the power system. The main causes of power system failures and their effects on the power system operation are also presented. The importance of power system security to prevent the occurrence of cascading failures and blackouts is highlighted. Several major blackout cases that occurred worldwide are reviewed and the techniques used to mitigate cascading failures and blackouts are discussed. Various intentional islanding techniques commonly used as remedial actions in the event of contingencies are reviewed in this chapter. The graph theory approach and its application on intentional islanding determination are also discussed. Load shedding scheme for intentional islanding applications are also elaborated in this chapter.

2.2 Power System Network

A power system is a network of electrical elements that generate, transmit, and distribute electricity to consumers. A basic power system is illustrated in Figure 2.1.

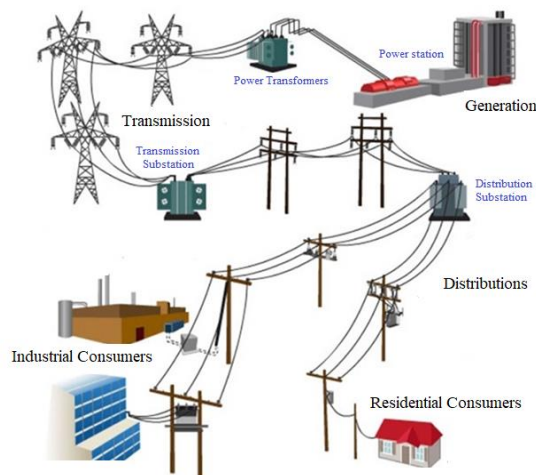


Figure 2.1. Basic Power System [14]

In general, electricity is generated at the power station by electrical generators. The generated electricity is then transferred through the transmission system to the distribution system. Finally, the distribution system delivers electricity to the residential and industrial consumers, as shown in Figure 2.1. In between these processes, the electricity passes through several substations at different voltage levels. These substations convert the high transmission voltages into lower distribution voltages using power transformers.

Power systems are essential because they enable all of the technologies which consumers (individuals or organizations) use to perform their daily activities. Electricity consumption is increasing with each passing year and it is projected that electricity demands will increase further in the near future. According to the International Energy Outlook 2017 report [15], the world energy consumption is expected to increase by 28% between 2015 and 2040, which is driven by strong economic and technology growth in developed countries.

Hence, reliable power systems are essential to fulfil the ever-increasing electricity demands. To ensure reliable electricity supply at all times, electric utility companies consistently perform preventive measures on all electrical elements in power systems.

2.3 Power System Failures

In general, failures or outages can occur in a power system because of various factors such as natural disasters, technical failures, and human errors. The main causes of failures and their effects on the power system are summarized in Table 2.1 [16], [17].

All of these failures occur unexpectedly, which can cause tripping of major elements in the power system such as generators, transmission lines, and transformers. A single-element outage can cause other elements (which share a common bus) to overload and trip in a continuous cycle. This event is known as cascading failures, which is highly detrimental to the power system. Cascading failures are uncontrollable and they can result in a partial or total system collapse. Cascading

failures have a significant effect on the power system such that the network is exposed to various risks. The main causes of cascading failures are transmission line overloads, voltage violations, and hidden failures (e.g. misoperation of relays during a failure) [18], [19].

Table 2.1. Main Causes of Failures and Their Effects on the Power System

Main causes of failures		Effects
Natural disasters	Lightning	<ul style="list-style-type: none"> - Can cause flashovers on electrical elements in power lines - Electrical equipment/element failure
	Earthquakes	<ul style="list-style-type: none"> - Disruptions to major elements in the power system because of stresses
	Floods	<ul style="list-style-type: none"> - Short circuits in the power system - Equipment damage
	Storms	<ul style="list-style-type: none"> - Electrical equipment/element damage because of atmospheric discharge
Technical failures	Equipment failures	<ul style="list-style-type: none"> - Breakdown of electrical equipment - Technical failures in the power system owing to ageing of the equipment
	Inadequate power reserves and production capacities	<ul style="list-style-type: none"> - Power generation deficits, making it difficult to fulfil high load demands
	Poor control and communication systems	<ul style="list-style-type: none"> - Communication breakdowns and misinformation between operators and dispatchers
Human errors	Errors and negligence of operators	<ul style="list-style-type: none"> - Errors in decision-making, especially when the system faces a high probability of failure - Fail to perform inspections of equipment and devices in a timely manner
	Vandalism	<ul style="list-style-type: none"> - Destruction of network infrastructure such as insulators in overhead lines

2.4 Power System Security

Power system security assessment is vital for power system planning and operation in order to ensure reliable and continuous availability of electricity supply. Power system security assessment is used to evaluate the capability of a power system in severe contingencies and propose suitable remedial actions to maintain normal operating conditions [20]. In general, power system security is defined as the ability of a power system to continuously operate without violating its normal operating conditions during any contingency [21]. Contingency refers to the failure or outage of important elements (e.g. generators, transformers, buses, or transmission lines), which will significantly affect the operating conditions of the power system [22].

The operating conditions are dependent on two important operating constraints: (1) Equality constraints and (2) Inequality constraints. Equality constraints refer to power balance constraints, where the total generated power must be more than the total load and total power loss [23]. Inequality constraints refer to the maximum allowable limits of the physical devices in the power system such as the bus voltage limits and power flow limits of transmission lines. When failures or outages occur, the power system must be capable of operating in its normal operating conditions and fulfil the specified operating constraints. Otherwise, there will be disruptions in the power system such that the system is unable to supply electricity to the consumers. In addition, violations of the operating constraints can initiate severe cascading failures, culminating in a partial or total system blackout [24].

Therefore, it is important to understand and identify the operating states of a power system. These operating states can be identified based on the definitions provided in [25]. This information is essential so that the proper control or remedial actions can be implemented to ensure reliable power system operations.

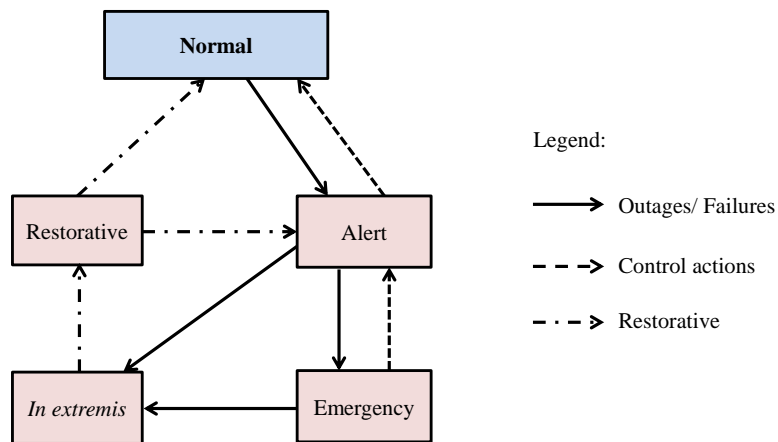


Figure 2.2. Operating States of a Power System [25]

There are five operating states for a power system, as shown in Figure 2.2 [25], [26]. The solid arrows indicate the failures or outages that occur from unavoidable events whereas the dashed arrows indicate the proper control actions to bring the system back to its normal operating state. Each of these operating states is briefly described as follows:

- a) Normal state: In this state, the equality and inequality constraints are satisfied and there is a sufficient level of stability margins in transmission and generation. The power system is able to withstand one possible contingency and ensure continuous electricity supply to the consumers. None of the control actions are implemented.
- b) Alert state: In this state, the equality and inequality constraints are still satisfied; however, there is an insufficient level of stability margins in transmission and generation. Even though electricity is still supplied to the consumers, at least one inequality constraint will be violated in the event of a contingency. For example, the transmission line capacity will be violated because of overload. Hence, the proper control actions need to be implemented to return the system to the normal state.
- c) Emergency state: The power system goes into this state because of contingencies when the system is in the alert state. The power system is intact and power is still supplied to the consumers although the inequality constraints are violated. Proper control actions are needed to revert system to (at least) the alert state. Failing to do so will lead to severe instability, which will force the system into the *in extremis* state. Load shedding, tripping of the transmission lines or generator units are the control actions that can be taken to prevent the system from entering into the *in extremis* state.
- d) *In extremis* state: In this state, the equality and inequality constraints are violated and the system is no longer intact. Most areas in the power system will suffer from a power cut. The appropriate remedial actions need to be implemented swiftly to prevent the power system from further collapse.
- e) Restorative state: In this state, restorative actions need to be implemented to restore and reconnect the power system so that the system returns to the normal operating state. The power system may return to the normal state or alert state, depending on its conditions.

Certain failures or outages that occur in a power system are unexpected and unavoidable. The severe impact of these failures or outages can be reduced by the power system operators through proper planning and implementing the suitable control actions. In general, an insufficient degree of security can lead to catastrophic failures of the power system, significant financial losses, and even loss of lives [27].

Figure 2.3 shows the general process that leads to a power system blackout [28]. Based on Figure 2.3, the power system is initially in the normal state. The equality and inequality constraints are fulfilled and therefore, electricity supply is continuously delivered to the consumers. When failures or outages occur, which disrupt the normal operating conditions of the power system, the operators will monitor changes of important parameters such as voltage, current, frequency, and power flow. Based on this information, the operators will implement the suitable remedial actions (which can be manual or automated) to return the power system to the normal state. The power system will revert to the normal state if the remedial actions are successful. However, the power system will be in the emergency state for a certain period. Once the power system is found to be stable and safe for normal operation, readjustment is executed and the system will return to the normal state. However, if a second major failure or outage occurs before the power system reverts to the normal state, cascading failures will be initiated owing to the violation of many lines.

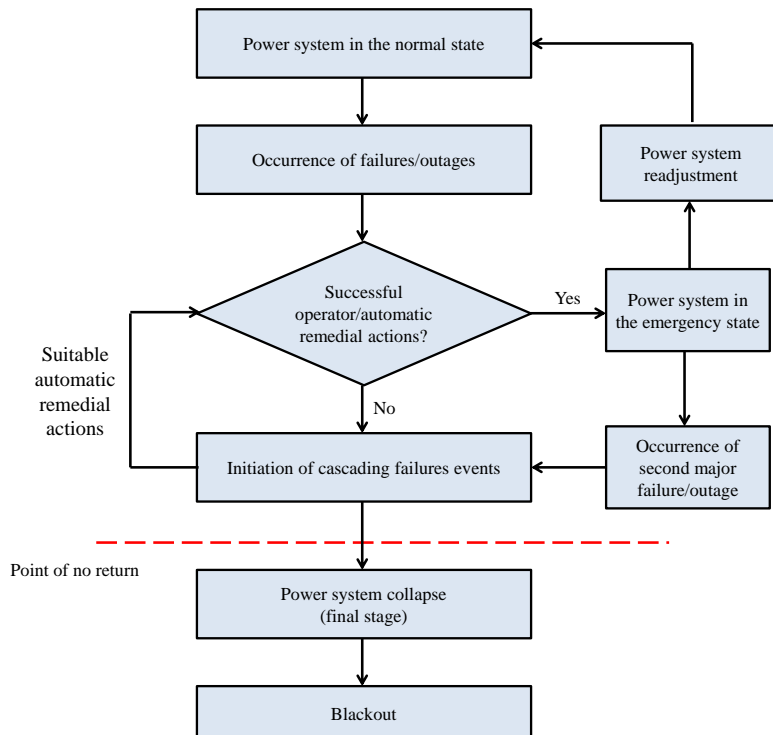


Figure 2.3. General Process that Leads to a Power System Blackout [28]

Cascading failures can occur in the power system if the remedial actions implemented after the first failures or outages are unsuccessful. These cascading failures can cause other elements in the power system (initially in their normal states) to overload and trip. Therefore, a suitable remedial action scheme (e.g. load shedding scheme) is needed to return the power state to a secure operating state.

However, if the remedial action scheme is not successful in mitigating the cascading failures, the power system will eventually collapse (point of no return). In this stage, the equality and inequality constraints are violated and system is separated into uncontrollable islands because of severe cascading failures. There are no control action schemes that can save the system from a partial or total system blackout.

2.4.1 Contingency Analysis

In order to evaluate the ability of the power system to withstand contingencies, power system security assessment known as contingency analysis is performed. In general, power systems are designed to fulfil a particular contingency criterion such as the N-1, N-2, or N-1-1 contingency criterion [29], [30], [31]. Each of these criteria enables the power system to operate continuously to deliver reliable electricity to the consumers in such a way that reliable power is delivered during a single-element outage (N-1), two-element outage (N-2), or a sequence of outages (N-1-1) at a time. In other words, the power system must operate in a secure operating state in the event of failures or outages.

Contingency analysis is an offline analysis used to analyze the conditions of a power system immediately after the occurrence of failures or outages [32], [33]. Failures or outages can occur due to sudden tripping of major transmission lines, variations of electricity generation, and increase/decrease of loads [34], which will subject the whole system or part of the system under stress.

N-1 contingency analysis (single-element outage) is the primary contingency analysis used to assess the security of a power system [35], [36]. This analysis involves analysing load flow information following a single-element outage such as

the outage of a transmission line, transformer, bus, or generator [37]. The N-1 contingency analysis provides information on critical contingency lists and subsequent violations, which may lead to cascading failures and system blackouts. Therefore, this analysis is crucial for system operators to identify the effect of a specific contingency on the power system and propose suitable control or remedial actions to ensure reliable power system operation. There are two types of violations that can occur following a contingency, which are briefly described as follows [35], [38]:

- a) Voltage violation: The acceptable voltage is typically within a range of 0.8–1.1 p.u. If the bus voltage exceeds or falls below this range, the bus is said to have violated the allowable voltage limits. In general, low-voltage and high-voltage problems in a power system are rectified by the reactive power flow. If the bus voltage falls below the allowable voltage limit, reactive power is supplied to that particular bus to increase its voltage profile. Conversely, the reactive power is absorbed if the bus voltage exceeds the allowable voltage limit to decrease its voltage profile.
- b) Transmission line capacity (MVA) violation: If the transmission line exceeds the maximum MVA limit of 130%, then the transmission line is considered to have violated the allowable MVA limit.

Figure 2.4 shows the steps involved in a contingency analysis [33]. The steps involved to determine the critical contingency list can be summarized as follows [39]:

- a) Contingency creation: A list of possible contingencies that can occur in the power system is created.
- b) Contingency selection/screening: The severe contingencies are identified and selected from the overall list of possible contingencies that violate the system voltage and power flow limits.
- c) Contingency ranking: The severe contingencies are ranked in descending order.
- d) Contingency evaluation: The suitable control or remedial actions are implemented to return the power system to the normal state.

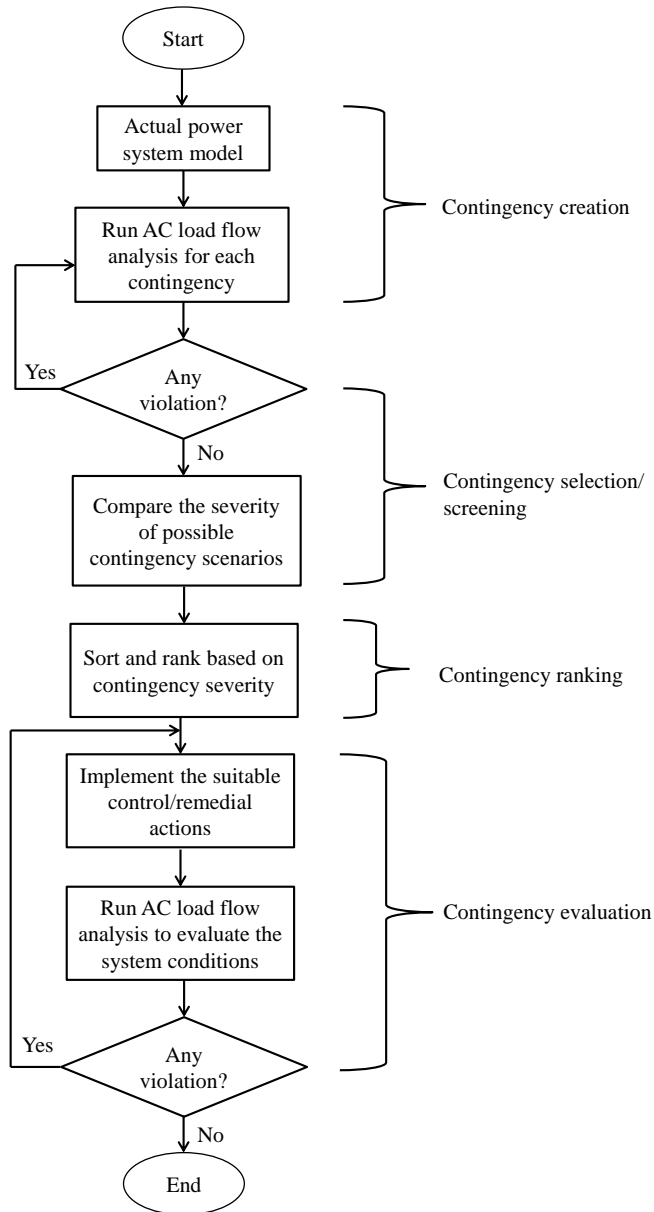


Figure 2.4. Steps Involved in a Contingency Analysis [33]

2.5 Power System Blackouts

Even if contingency analysis is performed to ensure continuous operation of the power system, failures can still occur in the system. These failures are caused by various factors, as described in Section 2.2. In addition, the increasing electricity

demands in developing countries caused power systems to be operated near their maximum limits, which increases the risk of outages that finally trigger the cascading failures [40]. Cascading failures will cause the power system to deviate from its normal operating conditions, which eventually lead to blackout. Blackout is one of the main problems for power systems and many blackout cases occur annually worldwide [41]. In general, blackout is the situation where there is power outage in certain parts or throughout the power system. Blackout is the worst-case scenario and it can last over short or long periods, depending on the severity of the outage. Blackouts have a significant effect on communication networks, production lines, healthcare facilities and other daily operations, and they can result in significant economic losses [42], [43]. The consequences of power system blackouts are presented in Figure 2.5.

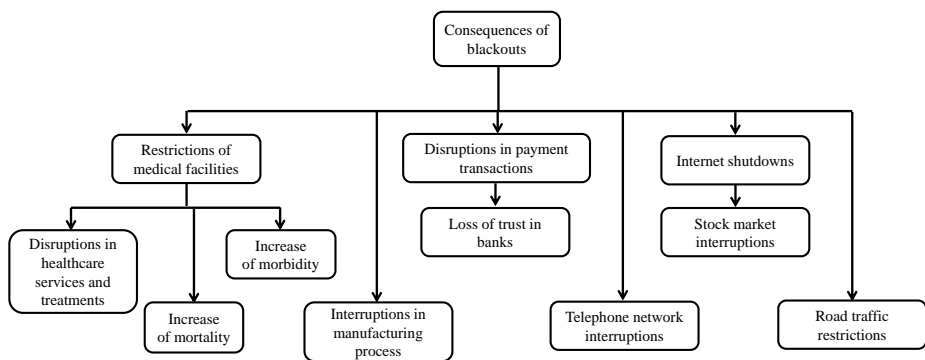


Figure 2.5. Consequences of Power System Blackouts [44].

As described in the previous subsection, the consequences of power system blackouts can be severe. Referring to Figure 2.5, blackouts can cause restrictions in medical facilities (e.g. clinics and hospitals) and disruptions in healthcare services and treatments, which can promote morbidity and mortality rates. Blackouts can cause disruptions in manufacturing processes (production lines), which will affect the economic growth of a nation. The social impacts of power system blackouts include telephone network interruptions which can cause communication breakdowns, internet shutdowns that can cause problems in stock market updates, disruptions in banking services and payment transactions, and road traffic restrictions that can lead to accidents and cause great inconvenience to road users.

There are many blackout cases reported in the world, which have significant effects on various parties. Some of the major blackout cases are presented in the following subsections, including the causes and effects of the incident as a whole.

2.5.1 Blackout in Canada and Some States in the North-Eastern Region of the United States of America

The blackout that occurred in Canada and certain states in the north-eastern region of the United States of America is one of the earlier severe blackouts that occurred in the world. This blackout occurred on 9th November 1965, which affected about 30 million people, where there was no electricity supply for almost 13 hours. This blackout occurred because of wrong relay settings, which caused one of the main transmission lines to trip. This caused other lines to overload, which initiated cascading failures in the power system such that the system eventually split into a few islands. Owing to the large load-generation imbalance, the system could not be saved, resulting in a total blackout. The affected areas were Connecticut, Rhode Island, Massachusetts, Vermont, parts of New Hampshire, New Jersey, New York, and Pennsylvania, as well as a major part of Ontario, Canada [45].

2.5.2 Blackout in the United States of America and Canada

A major blackout occurred in the United States of America and Canada on 14th August 2003, which affected almost 50 million people with a total interrupted load of 63 GW. This incident caused 400 transmission lines and 531 generators in 261 power stations to trip. The problem originated from reactive power supply problems in Indiana and Ohio. However, the state estimator software developed by Midwest Independent System Operator, Inc. (now known as Midcontinent Independent System Operator, Inc.) failed to detect the problem, which caused the generator in Eastlake to trip. This further caused many transmission lines to overload, resulting in cascading failures. The generators in the power system could not fulfil the load-generation balance criteria and therefore, more generators began to trip. Consequently, many major tie lines tripped, resulting in reserve power flow in the system and a complete voltage collapse. Other transmission lines became heavily loaded and the cascading failures resulted in a catastrophic system blackout. In this

incident, reactive power problems was not only the contributor towards the blackout, but also poor planning and practices, inadequate training to respond to failure, and delays in making a proper decision (lack of situational awareness) by the system operators [28], [46], [47].

2.5.3 Blackout in Southern Sweden and Eastern Denmark

A major blackout occurred in southern Sweden and eastern Denmark on 23rd September 2003. The failure was initiated from the loss of a 1200-MW nuclear unit in southern Sweden, which caused a surge of power transfer from the north. Five minutes after this outage, a double busbar fault caused by disconnecter damage occurred in the southern Sweden substation, which resulted in a loss of a few lines and two 900-MW nuclear units. These outages caused a voltage collapse in the southwest grid in Stockholm. Consequently, the grid was split into two parts, which isolated southern Sweden from the northern grid and eastern Denmark from the central grid. The isolated systems experienced voltage and frequency collapse within a few seconds, which eventually led to a blackout. This incident affected 1.6 million people in southern Sweden with a load loss of 470 MW whereas it affected 2.4 million people in eastern Denmark with a load loss of 1850 MW [3].

2.5.4 Blackout in Italy

The power system in Italy is an interconnected system, which is connected to other grids in France, Switzerland, Austria, and Slovenia that are part of the Union for the Coordination of the Transmission of Electricity (UCTE). On 28th September 2003, the main 380-kV tie line that connected Italy and Switzerland tripped in Switzerland because of line flashover. Other available transmission lines were assigned to cater for the load demands in order to revert the system to the normal state. However, other transmission lines were already heavily loaded, resulting in overloading and overheating (voltage sag) and hence, a sequence of line tripping (cascading tripping). This further isolated the power system in Italy from other systems in the grid. Within a few seconds of isolation, the power system in Italy faced many overloads and undervoltage problems, which eventually caused the system to collapse. In this

incident, about 45 million people were affected. The time taken for system restoration was approximately 19 hours [48], [49], [50], [51].

2.5.5 Blackout in India

The blackouts on 30th and 31st July 2012 were the two largest blackouts that occurred in the grid system in India. The power system consisted of five regional grids, namely, the Northern (NR), North- Eastern (NER), Eastern (ER), Western (WR) and Southern (SR) regional grids. The NER, NR, ER, and WR grids were synchronously connected to each other (known as the NEW grid) whereas the SR grid was asynchronously connected to other regions. The Northern region imported power from the Eastern and Western regions. Before the blackout on 30th July 2012, two major lines between the NR and WR grids were undergoing scheduled maintenance (shutdown). The NR grid experienced a large power surge from the ER and WR grids and consequently, the 765-kV line in Gwalior–Agra tripped due to false relay tripping. The huge power imbalance in the NR and ER grids led to severe cascading failures. This blackout affected over 300 million people across nine states in the Northern region. Another blackout occurred on the following day, 31st July 2012. Before this incident, many lines were undergoing scheduled maintenance and therefore, the system was not secured. Similar tripping events occurred again, where large amounts of power were imported from the ER and WR grids, resulting in tripping of many transmission lines due to false relay tripping. Severe cascading failures took place and many lines tripped because of overvoltage and power imbalance problems. Many generators were shut down because of underfrequency problems. This caused the NR region to isolate from other grid systems following the total blackout of the ER and NER grids. In this blackout, 670 million people were affected across 22 states in the NR, ER, and NER regions [52], [53].

2.5.6 Blackout in Malaysia

Malaysia is also among the countries that have experienced severe blackouts. One of the severe blackouts occurred on 29th September 1992, where there was no electricity supply in Peninsular Malaysia for almost 48 hours. The blackout was initiated by a lightning strike on the transmission facility, which cascaded further and caused

failure of the transmission and distribution systems. Another severe blackout occurred on 3rd August 1996 due to the switchgear breakdown near the Sultan Ismail Power Station in Paka, Terengganu. This breakdown initiated cascading tripping effects, which caused all of the power stations in Peninsular Malaysia to trip and the power failure lasted for about 7 hours. In September 2003, a blackout occurred in southern Peninsular Malaysia, resulting in a power outage for almost 5 hours in a few states (Wilayah Persekutuan, Selangor, Negeri Sembilan, Melaka, and Johor). Another blackout occurred on 13th January 2005 due to switchgear breakdown at the Sultan Salahuddin Abdul Aziz Shah Power Station in Kapar, Selangor. This incident caused power outage in a few states in Peninsular Malaysia (Wilayah Persekutuan, Melaka, Negeri Sembilan, and Selangor) for about 5 hours [54], [55].

2.5.7 Summary of Power System Blackouts

The major blackout cases presented in the preceding subsections indicate the causes that trigger the occurrence of blackouts and their effects on the consumers. There are a few important observations made from the major blackout cases, as outlined below:

- a) Blackout is initiated by a single event (i.e. critical element outage), which leads to severe cascading failures and eventually a total system collapse. By identifying the critical component outages (contingencies), which can cause severe cascading failures, it is possible to devise and implement the appropriate control or remedial actions to save the system from severe cascading failures and partial or total blackouts.
- b) The failure of important components, devices, and/or equipment within the power system due to severe cascading failures results in system islanding. This phenomenon is known as unintentional islanding, where unbalanced, stand-alone islands are formed. There are large load-generation imbalances in these islands and eventually, the system completely collapses, resulting in a blackout.
- c) Voltage violation often occurs when major transmission lines trip. This is evident from previous blackout cases, where voltage violation/collapse was one of the causes of system blackouts. When major transmission lines trip, the power system splits into unbalanced, stand-alone islands. Thus, it is

essential to select the appropriate transmission lines to be disconnected to ensure stability of the isolated islands.

- d) Delays and uncertainties in making the proper decision by the system operators in the event of failures will further aggravate the operating conditions of the power system. Hence, there is a need for a well-devised management system for power system planning and control action, which will facilitate the system operators to respond swiftly to failure events.

2.6 Blackout Mitigation Techniques

In general, power systems must be equipped with proper control/remedial action plans in the event of a failure in order to minimize or prevent cascading failures and blackouts. Various remedial action schemes have been developed for this purpose based on critical analyzes of past blackout cases. The implementation of suitable blackout mitigation techniques in the event of a contingency helps to minimize or eliminate cascading failures by reverting the system to the normal state and thereby preventing a catastrophic system collapse. Several blackout mitigation techniques have been implemented to date, which will be detailed in the following subsections.

2.6.1 Preventive Control Action: Generator Rescheduling

Preventive control action is one of the standard practices in power system security in order to maintain secure operating conditions when the power system is at risk of instability during a contingency [56]. Generator rescheduling is one of the preventive control actions taken to maintain the normal operating states of the power system by shifting the generated power between the generators without violating the transmission line capacities during a contingency. This action prevents the system from further severe outages, which can culminate in blackouts.

A generator rescheduling technique was proposed in [57], where graph theory was used to reallocate the generated power for multiple unstable contingencies. Graph theory was used to determine the actual amount of power transferred between the individual generators and loads, which is vital for power system control. Coherency-based generator rescheduling was proposed in [58], where the generator coherency

behavior improved the transient stability of the power system during contingencies. Another generator rescheduling technique based on rotor trajectory index was proposed in [56] as a preventive control measure. This technique will help guide the system operators in making the right decision to achieve a generation configuration with better transient security dispatch. Even though this technique help to maintain the secure operating conditions in the power system, however, it is not suitable to be executed during severe contingency scenarios. This is because it cannot be implemented for immediate execution due to the dynamic behavior of the system (e.g. governor response time), which requires some time to perform the action.

2.6.2 Load Shedding Scheme

Load shedding scheme is one of the common techniques used to prevent severe cascading failures. As the name implies, load shedding scheme involves removing a suitable amount of load from the power system to achieve stable operation [59]. Various load shedding schemes have been proposed in recent years. The selection of a suitable load shedding scheme is generally dependent on the conditions of the system or contingency scenario [60].

The common types of load shedding schemes are the (1) Under Voltage Load Shedding (UVLS) scheme, and the (2) Under Frequency Load Shedding (UFLS) scheme [61]. The UVLS scheme is implemented to prevent voltage collapse in the power system. Most of the major blackouts worldwide were caused by voltage instability, as discussed in Section 2.4. The UVLS scheme is executed when the bus voltage drops below the allowable voltage limits. Delays in addressing voltage instability problems (voltage drops) can cause significant changes in the reactive power demands, which can result in blackouts. Therefore, the UVLS scheme is executed to ensure that the voltage profiles for all buses are always within the allowable voltage limits during any contingency scenarios[62]. The UVLS scheme prevents further voltage collapse in the power system. The application and advantages of the UVLS scheme are highlighted in [63], [64]. An effective linear UVLS scheme was developed in [65], in order to determine the global optimal amount and the best location of the load that needs to be shed. The steps involved in

the UVLS scheme to prevent cascading failures are summarized in the form of a flow chart, as shown in Figure 2.6.

Referring to Figure 2.6, the system conditions are continuously monitored and the UVLS relays are activated if there are any voltage violations, which may result in voltage collapse. The suitable load bus and the appropriate amount of load to be shed are identified. The voltage profiles for all buses in the power system are checked to determine whether there are voltage violations. If the system is able to operate within the allowable voltage limits, the system is in the normal state (i.e. load-generation balance criterion is fulfilled). Otherwise, the next suitable load bus and the appropriate amount of load to be shed is identified and the process continues until the normal state is achieved.

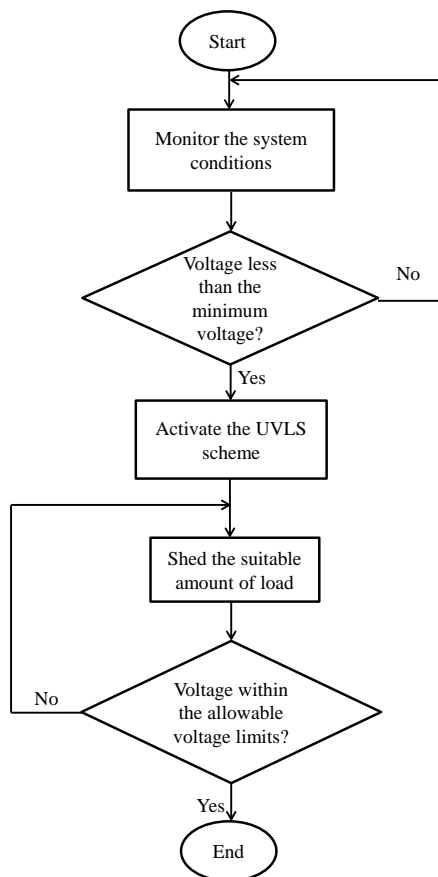


Figure 2.6. Flow Chart of the Undervoltage Load Shedding (UVLS) Scheme [66]

The UFLS scheme is another common load shedding scheme, which is used by many utility companies to prevent drastic frequency drops caused by power imbalances [67]. This scheme is specifically designed to identify any deficits in the generated power based on the rate of frequency change of the system. The UFLS scheme determines the suitable amount of load to be shed in order to keep the power system balanced and secure, which is calculated based on the rate of frequency change (df/dt) of the power system [68]. The application of the UFLS scheme as an adaptive load shedding scheme is described in [69], [70]. Another load shedding technique has been proposed in [71], where the load shedding decisions were made based on the measured voltage and frequency. This approach helps to enhance the security of the power system during severe disturbances and prevent further outages.

However, load shedding technique cannot guarantee for successful cascading failures prevention at all times. Inaccuracies in executing load shedding scheme can cause instability problem in the system if less load is removed whereas shedding to much load can cause unnecessary power failures [72], [73]. This situation will further result in severe cascading failures which will lead to system blackout.

2.6.3 Automatic Voltage Regulators and Power System Stabilizers

Instability occurs in the power system because of large disturbances, which may cause the generators to lose their synchronization, resulting in a partial or total blackout. Severe disturbances such as a sudden loss of major transmission lines, sudden increase in loads, or sudden loss of major transformer units will impose significant burden on the generators to maintain a constant electrical speed in the power system. In such cases, some of the generators will speed up whereas others will slow down to compensate for these disturbances [74].

The use of fast excitation control systems or Automatic Voltage Regulators (AVR) can facilitate in maintaining the steady-state and transient stability of generators in the power system [75]. The use of AVR helps to maintain the terminal voltages of the generators within their allowable limits. Furthermore, the use of AVRs helps to improve the transient stability of the system and maintain synchronization of the generators in the event of disturbances. However, it is not possible to fine tune in

order to control oscillations in speed using fast AVRs. In such cases, Power System Stabilizers (PSS) are used to fine tune the damping of electromechanical oscillations and inter-area oscillations in the power system [76]. The optimal tuning of AVR and PSS in order to prevent power system blackouts is presented in [75]. A novel AVR and PSS analysis method has also been proposed in [77] based on the bode frequency response. However, even if the optimal settings of AVR and PSS are used, there are circumstances where the system will deviate from the normal state and therefore, additional remedial actions are needed to revert the system to the normal state [78].

2.6.4 Intentional Islanding

Intentional islanding (also known as controlled islanding or network splitting) is one of the effective remedial actions taken to prevent severe cascading failures, which can lead to major blackouts [79]. Intentional islanding is a process where the original power system is split into a few balanced, stand-alone islands by disconnecting suitable transmission lines based on a specific fitness function and system constraints.

In most major blackout cases, cascading failures often result in unintentional islanding, where unbalanced islands are formed due to load-generation imbalance before the system completely collapses. This unfavourable situation can be prevented by implementing an optimal intentional islanding strategy and a suitable load shedding scheme. The balanced, stand-alone islands obtained from the optimal intentional islanding strategy ensure continuous electricity supply to the consumers even though the power system is not in the normal condition.

An intentional islanding approach was proposed in [80], where the Ordered Binary Decision Diagram (OBDD) was employed to split the network into feasible stand-alone islands. The intentional islanding strategy obtained from this approach must fulfil the following constraints: (1) Separation and Synchronization Constraints (SSC), (2) Power Balance Constraints (PBC), and (3) Rated value and Limit Constraints (RLC). Figure 2.7 shows the intentional islanding strategy obtained from the OBDD-based approach for the IEEE 30-bus test system. In this strategy, the

power system is separated into three balanced islands that satisfy the specified constraints.

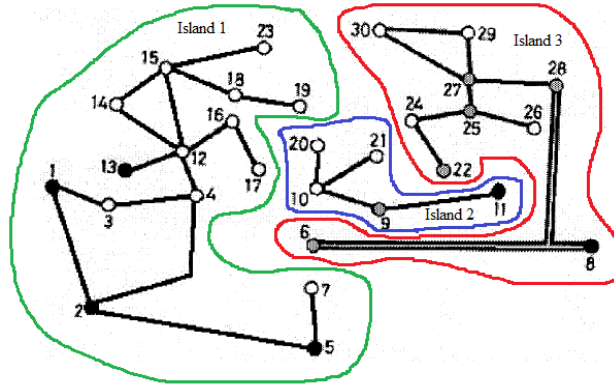


Figure 2.7. Intentional Islanding Strategy Obtained from the Ordered Binary Decision Diagram (OBDD)-Based Approach for the IEEE 30-Bus Test System [80]

Another intentional islanding approach was proposed in [81], where slow coherency was used to group the coherent generators. Subsequently, automatic islanding was carried out, where the least load-generation imbalance was the criterion for island formation. The slow coherency-based intentional islanding approach was used to demonstrate real blackout cases in the United States of America-Canadian borders in 2003 [82]. The results showed that the implementation of intentional islanding can prevent the power system from severe blackouts. Similar works have also been carried out [11], [83] to determine the suitable intentional islanding strategies. In [83], intentional islanding was carried out based on the slow coherency approach with minimal cutsets and minimal net flow. In [11], a Binary Particle Swarm Optimization (BPSO) algorithm was developed to determine the optimal intentional islanding strategy, where the minimal power imbalance was used as the fitness function.

2.6.5 Summary of Blackout Mitigation Techniques

The blackout mitigation techniques discussed in the preceding subsections are implemented during contingencies to prevent cascading failures from spreading

throughout the power system, which can result in a partial or total blackout. Among them, intentional islanding is the preferred blackout mitigation technique. Intentional islanding takes into account important criteria to ensure that the power system is stable during and after its implementation. This technique does not only prevent the system from experiencing further severe outages, but it also speeds up restoration during system reconnection [8]. Furthermore, intentional islanding helps to prevent unintentional islanding events, considering that the cascading failures in most of the past blackout cases resulted in the formation of uncontrollable islands during severe contingencies before the power systems completely collapsed. In addition, a suitable load shedding scheme can be incorporated into the intentional islanding algorithm to ensure the formation of balanced, stand-alone islands, which can continuously supply electricity to the consumers. This makes intentional islanding a robust technique to prevent the occurrence of cascading failures and blackouts in a power system. The Northern Regional Power Committee (NRPC) had also advised to implement an intentional islanding scheme in the Delhi Transmission Utility Network in order to prevent severe blackouts during grid failures, which was the case in July 2012 [44]. In addition, intentional islanding has been proven to be a robust remedial action because it prevented the occurrence of blackout when an aeroplane crashed in Tokyo, which severed a 275-kV overhead tie transmission line [84].

2.7 Intentional Islanding as a Remedial Action for Power Systems

The implementation of intentional islanding as a remedial action for power systems has gained considerable attention from researchers in the last few years. Various intentional islanding approaches have been proposed by previous researchers. In general, the main objective of intentional islanding is to isolate the power system into a feasible set of islands by disconnecting suitable transmission lines, which satisfy a certain fitness function and the specified system constraints.

There are two types of fitness functions typically used to determine the best transmission line candidates (cutsets), namely: (1) Minimal power imbalance and (2) Minimal power flow disruption. The first fitness function (minimal power imbalance) emphasizes on a small tolerance between the total generated power and total load in each island during the islanding process. The objective of this fitness function is to

minimize the amount of load that needs to be shed. The objective of the second fitness function (minimal power flow disruption) is to minimize changes in the power flow pattern of the power system during the islanding process [85].

In addition, the intentional islanding strategy needs to satisfy certain a number of constraints in order to produce balanced, stand-alone islands. These constraints are briefly described as follows [86]:

- (a) Integrity constraints: All of the buses in an island must be connected as one integrated subsystem.
- (b) Steady-state constraints:
 - i) Load-generation balance: Each island must fulfil the load-generation balance criterion in order to produce balanced, stand-alone islands. A suitable load shedding scheme should be used for cases where the total load is greater than the total generated power. The load-generation balance criterion is expressed as:

$$\sum_i^n P_{i,gen} \geq \sum_i^n P_{i,load} \quad (\text{Equation 2.1})$$

where $P_{i,gen}$ is the generated active power for Line i , $P_{i,load}$ is the supplied active power for line i , and n is the total number of buses in the island.

- ii) Transmission line loading: The transmission line loading should not exceed the maximum allowable limit during the islanding process. This criterion is given by:

$$P_{i,line} < 1.3 \times P_{i,max} \quad (\text{Equation 2.2})$$

where $P_{i,line}$ is the active power flow for line i , and $P_{i,max}$ is the maximum allowable active power flow limit for line i .

- iii) Bus voltage limit: The voltage of each bus in the island must be within the allowable voltage limits. This criterion is given by:

$$0.8V_{min} \leq V_{line} \leq 1.1V_{max} \quad (\text{Equation 2.3})$$

where V_{line} is the operating voltage of the power system, V_{min} is the minimum voltage, and V_{max} is the maximum voltage.

(c) Dynamic constraints:

Generator coherency: All of the generators in each island must be coherent and synchronized.

Figure 2.8 shows the intentional islanding techniques that have been proposed and implemented by previous researchers. These techniques can be categorized into five main groups: (1) Ordered Binary Decision Diagram (OBDD)-based, (2) Slow Coherency-based, (3) Clustering-based, (4) Linear Programming-based, and (5) Heuristic and Metaheuristic-based techniques. Each of these techniques is described in detail in the following subsections.

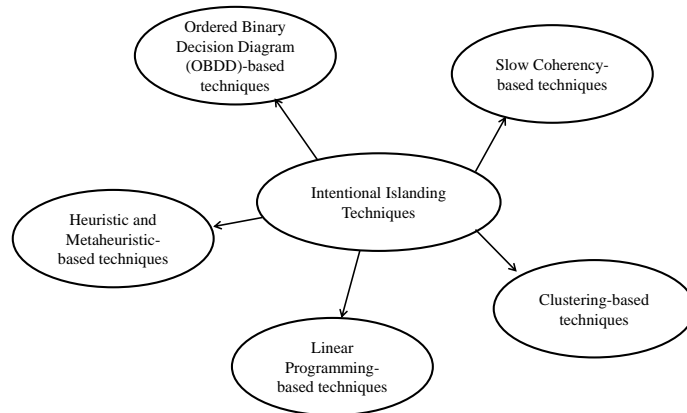


Figure 2.8. Intentional Islanding Techniques

2.7.1 Ordered Binary Decision Diagram-Based Techniques

Ordered Binary Decision Diagram (OBDD) is a Boolean function representation developed by Bryant [87], which is widely used to simplify complex problems. OBDD is a decision diagram obtained by imposing the relationship between the variables in an ordered manner, resulting in the canonical form of Boolean representation [88]. OBDD has been used to obtain the suitable intentional islanding

strategies for power systems. In [80], two-phase OBDD was used to identify the possible intentional islanding strategies. First, the intentional islanding strategies that fulfilled the power balance criterion were determined based on a node-weighted graph model. Second, the intentional islanding strategies from the previous phase were checked to verify whether they violated the transmission line capacity criterion. The intentional islanding strategy must satisfy the following steady-state constraints:

- a) Separation and synchronization constraint (SSC): The generators in each island must be coherent and synchronized. Asynchronous generators must be separated according to their coherent groups.
- b) Power balance constraint (PBC): The total generated power and total load in each island must be balanced to ensure stability of the power system after intentional islanding.
- c) Rated value and limit constraint (RLC): The transmission line capacity and transmission thermal limit must not exceed the allowable limits.

The OBDD-based intentional islanding technique was further upgraded to a three-phase technique in order to determine the suitable intentional islanding strategies for large-scale power systems in [89]. The steps involved in the three-phase OBDD-based intentional islanding technique are presented in Figure 2.9.

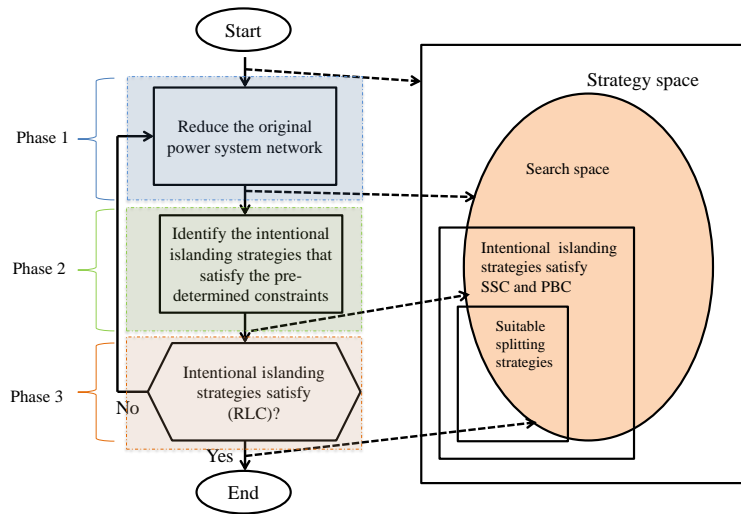


Figure 2.9. Steps Involved in the Three-Phase Ordered Binary Decision Diagram (OBDD)-Based Intentional Islanding Technique [89]

In the three-phase OBDD-based intentional islanding technique, the strategy space represents all of the possible intentional islanding strategies available for a particular power system. In Phase 1, this strategy space is reduced to a smaller search space by reducing the original power system. This is done by eliminating irrelevant vertices and edges, and combining the relevant vertices based on their groups. In Phase 2, the intentional islanding strategies that fulfil the SSC and PBC are determined. The search space of the intentional islanding strategies is further reduced in this phase. In Phase 3, the intentional islanding strategies are checked to verify whether they fulfil the RLC. The approaches used for the two-stage OBDD-based technique [80] are also used for Phase 2 and Phase 3 of the three-phase OBDD-based technique. The threshold value constraint (TVC) was introduced in [90] to determine whether the intentional islanding strategies obtained from the OBDD-based technique were feasible solutions. The TVC (which is selected offline) restricts the degree of allowable disturbances caused by the intentional islanding strategies. If the intentional islanding strategy produced by the OBDD-based technique [80], [89] satisfies the TVC, then the solution is a feasible strategy that satisfies the transient stability constraints.

Even though OBDD-based intentional islanding techniques [80], [89], [90] are capable of obtaining feasible solutions, these techniques combine offline and online computations in real-time islanding determination, which will lead to inaccurate intentional islanding solutions. Furthermore, OBDD-based intentional islanding techniques simplify the original network into a smaller network in order to reduce the search space of possible solutions. In such cases, the optimal solution cannot be obtained because the network is not truly representative of the original network as a result of the simplification process. Moreover, these techniques did not consider the critical line outages when determining the intentional islanding solutions where these solutions would not be a viable solution during any contingency. The load shedding scheme that needs to be implemented (in some cases) after intentional islanding execution are not highlighted in these techniques.

2.7.2 Slow Coherency-Based Techniques

Slow coherency-based techniques have been employed to determine intentional islanding strategies when there are large disturbances in the power system. A slow-coherency-based intentional islanding scheme was proposed in [81], where a two-timescale technique was used to determine the weakest connections between the coherent groups of generators when the power system was subjected to large disturbances. The weakest connections between the coherent groups of generators were used as the criteria to obtain the best candidates (lines to be disconnected) during the islanding process. The following assumptions were made in this technique: (1) The coherent groups of generators do not rely on size of the disturbance; (2) The coherent groups of generators were independent of the level of detail deployed to model the generating units. Then, the brute force search was conducted to obtain the intentional islanding strategies and load-generation balance information, taking into account the boundary topology conditions.

A slow coherency-based intentional islanding technique was also developed in [83] which determine an islanding strategy considering minimal cutsets and minimal net flow. The main purpose of this approach was to obtain better intentional islanding strategies with a minimal number of transmission lines to be disconnected, which fulfilled various criteria such as generator coherency, minimal power imbalance, and quick system restoration. A slow coherency-based graph theoretic intentional islanding technique was proposed in [91] to reduce the large-scale power system into a small-scale power system without compromising the optimal solutions. This technique consisted of a graph simplification method and a multi-level recursive bisection graph partitioning method. With this approach, the original network can be reduced to a smaller size, which will minimize the computational burden during intentional islanding. Another slow coherency-based technique was proposed in [92], where a black start unit was allocated to each island during the islanding process. Black start units were considered because the islands formed may be unstable, which could lead to local blackouts. Therefore, a black start unit allocated on each island ensures the load-generation balance in the island is achieved. In this technique, the final cutsets were determined based on the minimum power exchange across the weak lines.

However, slow coherency-based intentional islanding techniques [81], [83], [91], [92] are unideal for intentional islanding solution determination because these techniques use a linearized electromechanical model to determine the coherent groups of generators. This will lead to inaccurate solutions owing to the inherent non-linear characteristics of the power system. Similar to OBDD-based techniques, slow coherency-based techniques simplify the original network into a smaller network to reduce the search space of the possible solutions, which will result in inaccurate intentional islanding strategies. Furthermore, the intentional islanding determination following critical line outages did not emphasize in these techniques. The UFLS load shedding scheme used in these techniques is also not discussed in detail.

2.7.3 Clustering-Based Techniques

Several clustering-based intentional islanding techniques have been proposed over the years. In clustering-based techniques, the intentional islanding problem is solved based on the graph partitioning method. The *k-way* spectral clustering technique was proposed in [93] to split the power system into stand-alone islands, where the minimal power imbalance was used as the fitness function. A multi-level kernel *k*-means intentional islanding algorithm was developed in [2] for a large-scale power system. The minimal power flow disruption was used as the fitness function to determine the intentional islanding strategy. This algorithm consisted of three main phases, namely: (1) Aggregation, (2) Partitioning, and (3) Retrieval. In Phase 1, the original network was reduced to a manageable size through specific rules and assumptions. In Phase 2, graph partitioning was performed for a short period. In Phase 3, the retrieval process was carried out using the kernel *k*-means algorithm. Figure 2.10 illustrates the concept of the multi-level kernel *k*-means intentional islanding algorithm.

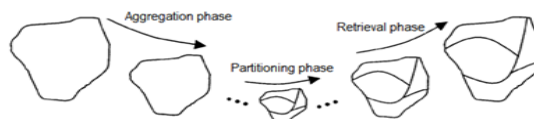


Figure 2.10. Concept of the Multi-Level Kernel *k*-means Intentional Islanding Algorithm [2]

A two-step spectral clustering-based intentional islanding technique was then proposed in [85]. In this technique, the coherent generators were grouped based on their dynamic models by normalized spectral clustering. Following this, the intentional islanding strategies were determined based on the fitness function and specified constraints. Another intentional islanding technique was proposed in [94] based on constrained spectral clustering. In this technique, graph theory was used to convert the optimization problem into graph-cut problems. The constraints (including coherent groups of generators and available transmission lines) were included in the graph-cut problems. Next, spectral clustering was applied to solve the graph-cut problems to determine the feasible intentional islanding solutions. Furthermore, an improved spectral clustering-based intentional islanding technique was proposed in [12]. This improved technique was capable of obtaining better islanding solutions within a shorter computational time. Another spectral clustering-based intentional islanding technique was proposed in [8]. The k -medoids algorithm was used, which could flexibly adjust the clustering and partitioning process and produced balanced, stand-alone islands.

Even though clustering-based techniques [2], [8], [12], [85], [93], [94], have also been developed to solve islanding problems, these techniques are inherently complex and need to be improved in order to determine the optimal intentional islanding strategies. Moreover, these techniques did not consider the critical line outages with proper contingency analysis when determining the intentional islanding strategy. The load shedding scheme used were slightly mentioned without any detail explanation. For instance, the UVLS scheme used in [8] was not clearly explained in their work.

2.7.4 Linear Programming-Based Techniques

Linear programming (also known as linear optimization) is a mathematical approach used to determine the best possible solution (maximum or minimum) for a given problem based on linear constraints [95]. Linear programming has been used for intentional islanding because it can provide the best intentional islanding strategy for a given objective function and a specific set of constraints. A mixed integer programming approach was developed in [96], where the direct current optimal power flow (DC-OPF) model was used to determine the optimal intentional islanding

strategy. The minimal power imbalance was used as the objective function to split the power system into the desired number of islands.

Then, a mixed integer linear programming (MILP) approach was developed in [97] to determine the optimal intentional islanding strategy by isolating the affected area from the network. This approach consisted of two stages. In the first stage, the feasible intentional islanding strategy was obtained by solving the DC power flow equation. In the second stage, the AC load shedding scheme was executed to determine the feasible intentional islanding strategy. This approach was then improved by using a piecewise linear AC power flow model to obtain better solutions [98]. The results proved that the AC power flow model was capable of obtaining balanced islands compared with the DC power flow model. Another MILP-based intentional islanding technique was proposed in [99], where the intentional islanding strategies were determined by ensuring that each island consisted of coherent generators. Another MILP-based intentional islanding technique was also developed in [100], which reduced the search space of possible solutions.

The linear programming-based techniques [96], [97], [98], [99], [100] have also been developed to solve islanding problems, however, these techniques involved with complex mathematical modelling. Furthermore, the DC-OPF model was used in the linear programming-based intentional islanding technique proposed in [96], which produce an inaccurate solution. Furthermore, these techniques did not identify the critical line outages with proper contingency analysis for intentional islanding determination. Similar to clustering-based techniques, the load shedding scheme utilized in these techniques was not explained in detail.

2.7.5 Heuristic and Metaheuristic-Based Techniques

Heuristic techniques are practical problem-solving techniques, which give quick, immediate solutions that are not necessarily the optimal solutions. Trial and error is the most fundamental heuristic technique used to obtain the possible solutions for a problem. A heuristic technique was developed in [101] to determine the intentional islanding strategy, where the minimal power imbalance was used as the objective

function. This technique consisted of three phases. In Phase 1, a power flow tracing algorithm was to identify the domain for each generator (i.e. the load buses attached to each generator). In Phase 2, the initial islanding boundaries were determined based on the coherent groups of generators. Finally, in Phase 3, the initial intentional islanding solution was refined to obtain the final intentional islanding strategy.

Another heuristic technique based on the ant search mechanism was developed in [86] to determine the feasible intentional islanding strategies. In this technique, the possible intentional islanding strategies were searched simultaneously in parallel with the number of initial points. The number of initial points was equal to the number of coherent groups of generators. The searching process was executed many times until the feasible intentional islanding strategy was obtained. The load-generation balance and transmission line loading were chosen as the constraints. Linear programming and the DC load flow model were used in this work.

A metaheuristic technique was proposed in [11] to determine the optimal intentional islanding strategy, where Binary Particle Swarm Optimization (BPSO) was used to split the large-scale power system. The minimum power imbalance was used as the objective function. The important loads and the desired number of islands were prioritized in this work. A load shedding scheme was also incorporated into the BPSO algorithm to produce balanced islands after intentional islanding. This technique was then improved [102] using Angle Modulated Particle Swarm Optimization (AMPSO), where the coherent groups of generators were determined using the slow coherency technique. The AMPSO algorithm was used to optimize the objective function (minimal power imbalance) based on the coherent groups of generators. The results showed that the AMPSO algorithm produced better optimal intentional islanding strategies compared with the BPSO algorithm [11]. A similar metaheuristic technique, namely, the Tabu search algorithm was developed in [10] to determine the optimal intentional strategies, where the minimal power imbalance was used as the objective function. This algorithm is based on neighbourhood search to determine if a better solution is available. A metaheuristic-based intentional islanding technique was also developed in [9] using Artificial Bee Colony (ABC) algorithm. The edge reduction method was used to reduce the huge search space of possible

intentional islanding strategies. The minimal power flow disruption was used as the objective function to determine the optimal intentional islanding strategies.

In general, the heuristic and metaheuristic-based techniques have also been proposed to solve islanding problems. However, the heuristic technique proposed in [86] uses the DC load flow model, which will not produce the optimal intentional islanding strategies. The minimal power imbalance is typically used as the objective function in both heuristic-based and metaheuristic-based intentional islanding techniques [10], [11], [101], [102]. Nevertheless, the minimal power flow disruption is an important criterion in order to determine the feasible intentional islanding strategies. This objective function helps to maintain the transient stability of each island during the islanding process. Although the ABC-based intentional islanding technique developed in [9] uses the minimal power flow disruption as the objective function to determine the optimal solution, this technique does not consider contingency scenarios during the islanding process. Nevertheless, it is important to consider contingency scenarios so that intentional islanding can be executed appropriately in critical contingencies.

2.7.6 Summary of Intentional Islanding Techniques

Various techniques have been developed over the years to determine the feasible intentional islanding strategies, as discussed in the preceding subsections. Each of these techniques has its own advantages and disadvantages. Among these, metaheuristic techniques are ideal for this research because the main objective is to develop optimization algorithms for intentional islanding strategy. Metaheuristic techniques are capable of determining the optimal intentional islanding strategies, taking into consideration contingencies. In addition, post-islanding schemes can be integrated with these techniques to verify whether the intentional islanding strategies fulfil the load-generation balance, allowable bus voltage limits, and other criteria.

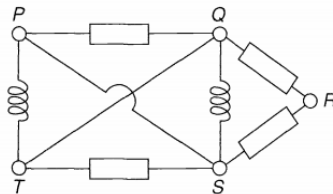
Since intentional islanding is a discrete problem in nature, metaheuristic optimization algorithms with discrete mutation were adopted in this research to solve intentional islanding problems. Graph theory is the most suitable tool to accurately represent large-scale power systems and therefore, this approach was used in this research to

represent the IEEE test systems for intentional islanding. Furthermore, graph theory can be used conjunction with other schemes such as load shedding and transmission line power flow analysis schemes to determine if there were violations in the specified constraints. For this reason, graph theory was used in conjunction with the intentional islanding algorithms proposed in this research.

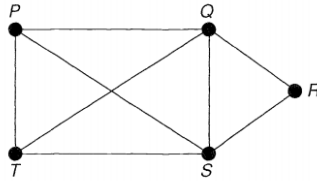
2.8 Graph Theory

Graph theory involves the use of mathematical structures to represent the connections between interacting elements. The elements are modelled in the graph as nodes or vertices, V , and their connections are represented as edges, E . The relationship between the vertices and edges can be represented as a graph, $G(V, E)$ [103].

Figure 2.11(a) shows the schematic of an electrical circuit whereas Figure 2.11(b) shows its representation obtained from the graph theory approach. Points P , Q , R , S , and T denote the vertices, which are connected by lines (edges). It shall be noted that the intersection of Edges PS and QT is not the vertex because it is not a meeting point between two lines. In the graph model, the vertices are $\{P, Q, R, S, T\}$ while the edges are $\{PS, PQ, PT, QT, QS, QR, RS, ST\}$. This example clearly shows how a set of points is connected as a graph model.



(a)



(b)

Figure 2.11. (a) Schematic of an Electrical Circuit, (b) Graph Theory Representation [103]

There are two types of graph models commonly used in graph theory: (1) Directed Graph and (2) Undirected Graph. The primary difference between these graph models is that the edges in a directed graph have a particular direction whereas the edges in an undirected graph do not have any particular direction. Hence, directed graph is a one-way communication in which each edge traverses in a single direction whereas undirected graph is a two-way communication where each edge can traverse in both directions [104].

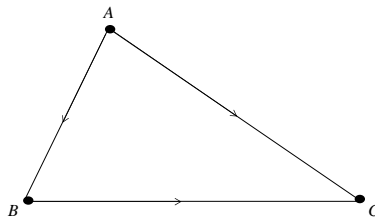


Figure 2.12. Schematic of a Directed Graph

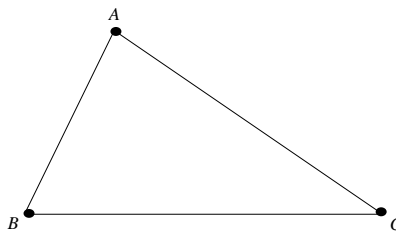


Figure 2.13. Schematic of an Undirected Graph

Figure 2.12 and Figure 2.13 show an arbitrary directed graph and undirected graph, respectively, each with three vertices (marked by Points *A*, *B*, and *C*) and three edges. It is evident that the traverse for the directed graph is only in one direction whereas the traverse for the undirected graph is from any direction between two vertices.

2.8.1 Application of Graph Theory in Modelling Power Systems

When the graph theory approach is used to model the power system, the vertices represent electrical elements such as generators and load buses. The edges that connect the vertices represent the transmission lines. Each vertex connected in the graph model can be identified by graph traversal. Graph traversal is a process of visiting or checking each vertex in a graph model. The common graph traversal techniques are depth first search (DFS) and breadth first search (BFS). In these techniques, all of the vertices in the graph model are visited based on a different approach.

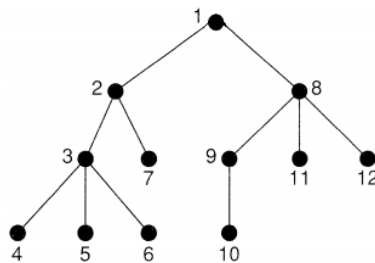


Figure 2.14. Depth First Search Graph Traversal Technique

Figure 2.14 shows the concept of the DFS graph traversal technique, where the algorithm traverses deep into the graph structure, beginning from the parent vertex and proceeding downwards to the children and grandchildren vertices in other levels in a single path. This process continues until there are no more vertices to be visited in that path. In this case, the algorithm will backtrack to a vertex in order to select another path to traverse and the process is iterated until all of the vertices in the graph structure are visited. For example, in Figure 2.14, the DFS algorithm begins the graph traversal from the parent vertex (Vertex 1). The sequence of vertices

visited by the DFS algorithm for this example is: $1 \rightarrow 2 \rightarrow 3 \rightarrow 4 \rightarrow 5 \rightarrow 6 \rightarrow 7 \rightarrow 8 \rightarrow 9 \rightarrow 10 \rightarrow 11 \rightarrow 12$.

In the BFS graph traversal technique, the algorithm traverses into the graph structure breadthwise, beginning from the parent vertex and proceeding to the children vertices in the following level. The algorithm will visit all of the children vertices before moving on to the next level, which consists of the grandchildren vertices. The process continues in this fashion until all of the vertices in the graph structure are visited. Based on Figure 2.14, if the graph traversal begins from the parent vertex (Vertex 1), the sequence of vertices visited by the BFS algorithm will be: $1 \rightarrow 2 \rightarrow 8 \rightarrow 3 \rightarrow 7 \rightarrow 9 \rightarrow 11 \rightarrow 12 \rightarrow 4 \rightarrow 5 \rightarrow 6 \rightarrow 10$.

In general, graph theory is used to study and model various systems [105]. Graph theory has also been used to model intentional islanding problems, which will be described in the following subsection.

2.8.2 Application of Graph Theory in Intentional Islanding

The diverse applications of graph theory have enabled researchers to solve complex problems, including intentional islanding problems. In intentional islanding, graph theory has been used to represent the power system as a graph model [80], [89], partition the network into islands by removing a set of edges (also known as cutsets) [10], and partition the network with a minimal number of cutsets [83].

In this research, graph theory was used to model the power system network and determine the initial intentional islanding solution by partitioned the network into a number of feasible islands by disconnecting the suitable edges (cutsets). Metaheuristic optimization algorithms were developed to determine the optimal intentional islanding strategy, with the aid of graph theory.

2.9 Optimization and Metaheuristic Techniques

Optimization and metaheuristic techniques are related to one another. Optimization techniques are widely used in power system operation and planning by searching for

the ‘best’ solutions for a particular problem. Optimization techniques can be categorized into two groups: (1) Exact and (2) Approximate techniques. As the name implies, exact techniques (also known as analytical techniques or classical optimization techniques) provide an exact solution to the optimization problem. However, these techniques are not suitable to solve large, complex systems. In this regard, approximate techniques overcome the limitations of exact techniques, producing efficient and effective solutions by means of simple and compact theoretical approaches. As the name implies, approximate techniques provide approximate solutions for a particular problem. These techniques can be further classified as heuristic and metaheuristic techniques. Metaheuristic techniques typically produce better solutions compared with heuristic techniques [106], [107].

Metaheuristic is a combination of the prefix ‘meta’ (which means ‘beyond’ or ‘a higher level’) and the word ‘heuristic’ (which means ‘to find or discover by trial and error’) [108]. Hence, metaheuristic techniques can be essentially defined as searching algorithms to solve complex optimization problems by means of one or more heuristics. In other words, metaheuristic techniques are high-level heuristic-based algorithms used to obtain better solutions in the search space [109]. These techniques are based on an iterative process of modifying the initial population in order to obtain a near-optimal solution and they are usually more computationally efficient compared with the exhaustive search algorithm. The ability of metaheuristic techniques to solve practical problems of different complexities with reasonably acceptable solutions is the main reason these techniques are widely used. Hence, metaheuristic techniques were chosen to determine the optimal intentional islanding strategies for different IEEE test systems in this research.

There are various types of metaheuristic techniques, some of which are still being improved ever since they were first introduced in the mid-1980s. Most metaheuristic techniques are developed based on natural, physical, or biological principles, and various operators were used to emulate these principles at the fundamental level [110]. The development of various metaheuristic techniques over the years help to identify and solve a large number of complex problems [109].

Metaheuristic techniques can be classified based on the domain that they emulate. Terms such as ‘nature-inspired’, ‘bio-inspired’, and ‘physical-inspired’ are often used to classify metaheuristic techniques. Evolutionary algorithms such as genetic algorithms, differential evolution, and evolutionary programming are examples of bio-inspired metaheuristic techniques. These techniques mimic various aspects of natural evolution such as survival of the fittest, mutation, and genetic mutation. Swarm intelligence algorithms are nature-inspired metaheuristic techniques because they emulate the group behavior or interactions of living organisms such as ants, bees, birds, and bacteria or non-living things such as river systems and masses under gravity. Physical-inspired metaheuristic techniques such as simulated annealing and musical aesthetics (harmony) emulate physical phenomena [110].

Each of these metaheuristic techniques has its own advantages and disadvantages, depending on the optimization problem that it is used to solve. In this research, evolutionary programming (EP) and particle swarm optimization (PSO) with discrete mutation were used to develop the intentional islanding algorithms. EP and PSO techniques are chosen due to its simplicity and reliable convergence [111], [112]. In addition, these optimization techniques are a robust and flexible techniques suitable to solve large, complex systems and discrete optimization problems [113], [114], [115]. These techniques are briefly described in the following subsections. However, the Modified Discrete Evolutionary Programming (MDEP) and Modified Discrete Particle Swarm Optimization (MDPSO) algorithms developed in this research to determine the optimal intentional islanding strategies will be elaborated in Chapter 3.

2.9.1 Evolutionary Programming

Evolutionary programming (EP) is a robust optimization technique used to solve a large number of power system problems [116], [117], [118]. EP belongs to a class of evolutionary algorithms and it was introduced by Dr Lawrence Jerome Fogel in an attempt to generate artificial intelligence using simulated evolution [119]. EP is inspired based on the theory of evolution at the macro level, where each individual is regarded as a producer and the behavioral relationship between the parents and children (offspring) is emphasized [110], [120]. The steps involved in EP are summarized in the form of a flow chart, as shown in Figure 2.15.

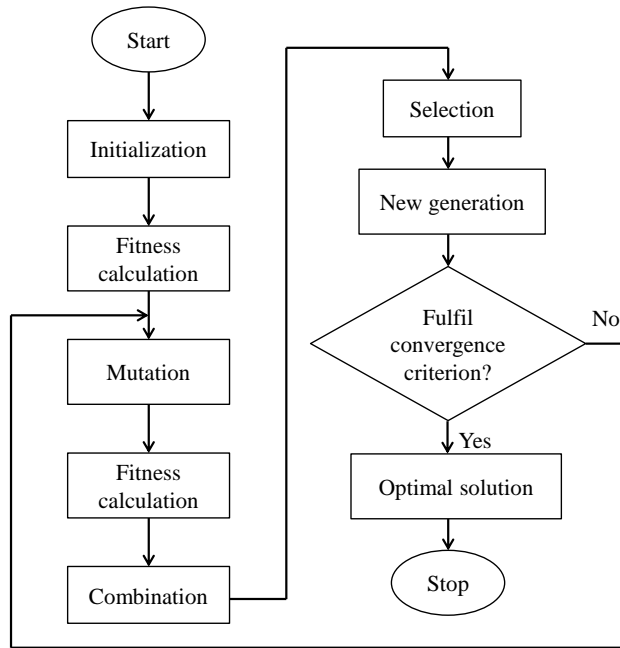


Figure 2.15. Steps Involved in the Evolutionary Programming (EP) Algorithm [121]

In the EP algorithm, the initial population (parents) is first generated randomly. Next, the fitness function value is calculated for each member using a specific fitness function. Each member is mutated using a specific mutation operator in order to produce the new population (offspring). The fitness function value for each member in the new population is calculated based on the fitness function. Next, the parents and offspring are combined and a selection process is carried out to identify the fittest candidates for the new generation. The mutation process is repeated until the convergence criterion is met. The optimal solution is obtained once the convergence criterion is met, as shown in Figure 2.15.

2.9.2 Particle Swarm Optimization

Particle Swarm Optimization (PSO) is a nature-inspired metaheuristic technique that has been widely used to solve power system problems [122], [123], [124], [125]. PSO was introduced by Kennedy and Eberhart in the mid-1990s [126]. As the name implies, PSO is inspired from the swarming behavior of animals such as birds or insects [127]. PSO solves a problem by iteratively improving the candidate solution at any given moment. The steps involved in PSO are presented in Figure 2.16.

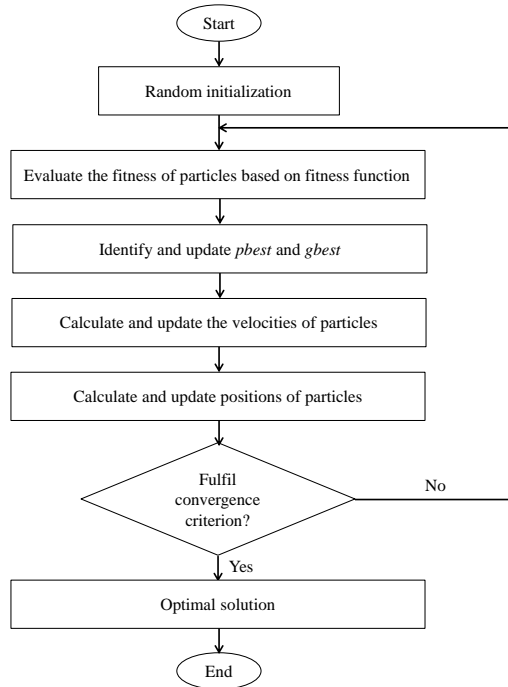


Figure 2.16. Steps Involved in the Particle Swarm Optimization (PSO) Algorithm [128]

In the PSO algorithm, the initial population is initialized randomly based on the potential solutions (particles) for the optimization problem. Each particle with a given velocity can move around the search space. The PSO algorithm tracks the global best position, g_{best} , and the personal best position, p_{best} , of the particles by carrying out the following steps in an iterative process: (1) Evaluate the fitness function value for each particle based on the fitness function; (2) Identify and update g_{best} and p_{best} ; (3) Calculate and update the velocity for each particle; (4) Calculate and update the position for each particle. The optimal solution is the global best position, g_{best} , obtained once the convergence criterion is fulfilled. In general, the PSO algorithm combines local search and global search methods in order to balance exploration and exploitation [129].

2.10 Load Shedding Scheme for Intentional Islanding

In general, power imbalance can occur in the islands formed after intentional islanding when the total load is more than the total generated power. Hence, a

suitable load shedding scheme is needed to ensure that these islands can function as balanced, stand-alone islands. Load shedding is a process of removing a suitable amount of load from the power system to prevent the system from catastrophic failures. One of the common load shedding schemes used for steady-state analysis is the UVLS scheme, which can be executed by exhaustive search, conventional or computational intelligence approaches.

Exhaustive search is a general problem solving technique that considers all the possible solutions in order to determine the optimal solution (optimal amount of load to be shed), which is given by the following equation:

$$\text{Possible load shedding solutions} = 2^n - 1 \quad (\text{Equation 2.4})$$

where n is the total number of buses available in the power system. Exhaustive search is a simple and effective technique to determine the optimal solution [130]. However, this method is not suitable for large scale power systems with a huge number of possible solutions as it will take a longer time to determine the optimal solution [131]. The delay in determining the optimal load to be shed will trigger other stability issues within the system which further lead the system towards partial or total system blackout.

Meanwhile, the conventional approach works by shedding a fixed amount of load within a fixed time delay when undervoltage is detected in the power system. This approach is typically used to prevent the system from voltage collapse. However, this approach does not estimate the actual amount of power imbalance in the system, which may result in overshedding or undershedding of loads. This unnecessary load shedding may lead to other problems in the system such as voltage collapse and power outages [132]. Furthermore, conventional load shedding is not efficient for modern, complex power systems because it does not provide the optimal amount of load that needs to be shed from the system [133].

The optimal amount of load to be shed is important to produce balanced islands after intentional islanding. Computational intelligence approaches are ideal for this

purpose because they are robust and flexible to solve complex, non-linear problems such as load shedding problems. Metaheuristic algorithms are one of the computational intelligence techniques that can be used to determine the optimal amount of load that needs to be shed, which will prevent severe cascading failures in the power system.

A number of metaheuristic-based load shedding schemes have been proposed for power systems. A PSO-based load shedding scheme was proposed in [134] to determine the optimal amount of load to be shed and the optimal power loss in order to establish secure operating conditions. A load shedding scheme was developed in [135] based on the firefly algorithm (which is a metaheuristic technique) and the results showed that the algorithm was capable of determining the global optimal solution, which minimized the amount of load to be shed. Other metaheuristic-based load shedding schemes have also been developed such as ant colony optimization [136], genetic algorithm [137], and ant lion optimizer [113]. These load shedding schemes determine the optimal amount and appropriate locations of loads to be shed so that the power system can operate in the normal state.

To date, there are no detailed discussions on the types of load shedding schemes used with the intentional islanding algorithms in previous works. For instance, in [80], [89], [90], there were no details on the types of load shedding schemes used with the OBDD-based intentional islanding algorithms. Even though UFLS schemes were used with the slow coherency-based intentional islanding algorithms in [81], [83], [91], there were no specific details on these schemes in these works.

The conventional load shedding scheme was used with the clustering-based intentional islanding algorithm in [93]; however, it was not mentioned whether the load shedding scheme was UVLS or UFLS. Likewise, a load shedding scheme was developed in [12] to determine the optimal amount of load to be shed, but the type of load shedding scheme was not stated explicitly in their work. The UVLS scheme was used with the intentional islanding algorithm in [8], but there was no detailed explanation on the UVLS scheme used in their work.

AC load shedding schemes were used with the MILP-based intentional islanding algorithm [97] and piecewise linear AC power flow model [98]. However, there were no specific details on the type of load shedding scheme used in these works. Likewise, there are no detailed descriptions on the types of load shedding schemes used with other intentional islanding techniques presented in Section 2.7.

Based on the literature survey, it can be deduced that none of the previous studies provide details on a suitable load shedding scheme for intentional islanding. Since the load shedding scheme is essential for successful intentional islanding, it is crucial to develop a suitable load shedding scheme that fulfils the specific criteria for a power system in order to prevent cascading failures and blackouts. In this research, EP optimization based discrete mutation was chosen to develop the load shedding scheme.

2.11 Chapter Summary

The main causes of power system failures and their effects have been discussed in this chapter. The importance of power system security and contingency analysis in ensuring continuous electricity supply to the consumers has also been presented. The causes and effects of several severe blackout cases worldwide were analyzed in order to study the proper mitigation techniques that can be carried out in the event of severe power system failures. The techniques used to mitigate cascading failures and blackouts of power systems have been described in detail in this chapter.

Based on the objectives of this research, intentional islanding is the best technique to be implemented when there is a high possibility that severe cascading failures will occur during a contingency. Even though various intentional islanding techniques have been proposed over the years, to date, there are no studies on the development of intentional islanding algorithms to determine the optimal intentional islanding strategy following a critical line outage. To fulfil this gap, two metaheuristic-based intentional islanding algorithms (MDEP and MDPSO algorithms) were developed, taking into account critical line outages. These algorithms will greatly facilitate system operators to simulate and plan successful intentional islanding in order to

prevent severe cascading failures and blackouts of large-scale power systems during severe contingency.

The huge search space of all possible intentional islanding strategies (cutset candidates) is another problem that needs to be addressed in order to determine the optimal intentional islanding strategy within a shorter computational time. The number of possible solutions increases proportionally with an increase in the network size. Therefore, it is crucial to obtain a proper initial intentional islanding solution, which will facilitate the algorithms in searching for the optimal solution. To solve the aforementioned problem, graph theory was used in this research to determine the initial intentional islanding solution.

The general metaheuristic techniques (EP and PSO) used to develop the intentional islanding algorithms have also been described briefly in this chapter. The modified versions of these metaheuristic techniques (MDEP and MDPSO algorithms with a load shedding scheme) will be elaborated in Chapter 3. The purpose of these algorithms was to determine the optimal intentional islanding strategies (i.e. transmission lines to be disconnected) for different large-scale power systems in order to produce balanced, stand-alone islands.

CHAPTER 3

METHODOLOGY

3.1 Introduction

In general, failure of a certain critical line can cause severe cascading failures in the power system, culminating in a partial or total system blackout. Based on the literature review as described in Chapter 2, intentional islanding is the best remedial action that can be implemented to save the power system from such catastrophic events. This chapter presents in detail the methodology adopted to develop the initial intentional islanding solution algorithm, two intentional islanding algorithms based on metaheuristic optimization techniques and load shedding scheme based metaheuristic optimization techniques. MATLAB 10 (R2015a) software was used to code the developed algorithms.

3.2 Overall Research Methodology

Two metaheuristic algorithms were developed in this research to determine the optimal intentional islanding strategy following a critical line outage, where the objective function (fitness function) was the minimal power flow disruption. Minimal power flow disruption was selected to achieve the fitness objective as explained in Section 2.7 (Chapter 2) and it refers to the arithmetical sum of active power flow on each islanding cutsets. Figure 3.1 shows the flow chart of the overall research methodology. The methodology adopted in this research consisted of four stages: (1) Preliminary study, (2) Data collection and extraction, (3) Development of the MDEP and MDPSO algorithms, and (4) Testing and validation of the MDEP and MDPSO algorithms using case studies.

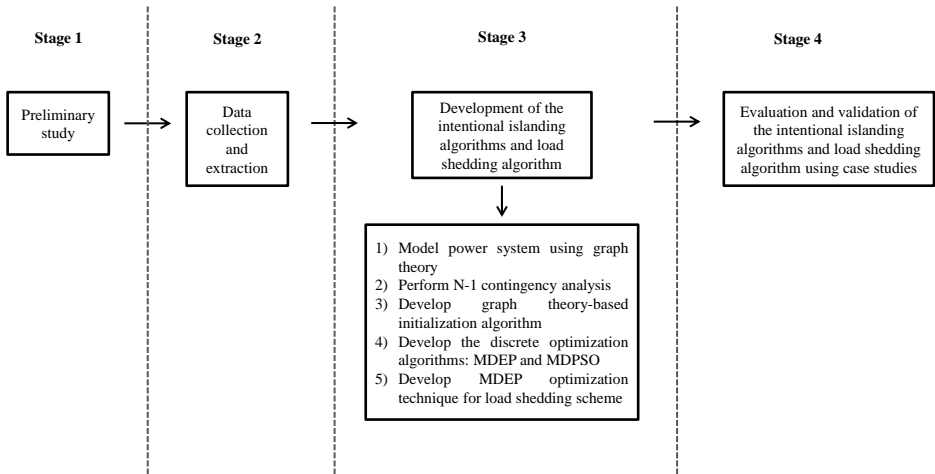


Figure 3.1. Flow Chart of the Overall Research Methodology

3.2.1 Stage 1: Preliminary Study

In this stage, information pertaining to the research topic was collected from scholarly journals, books, theses, and other authoritative sources and a detailed literature survey was carried out. The research problem was identified and the objectives were set in order to address the research problem, as presented in Chapter 1. This research is focused on intentional islanding strategies, techniques, and methodologies.

3.2.2 Stage 2: Data Collection and Extraction

In this stage, the data used for analysis were obtained from the database of IEEE test systems. Three test systems were used for data collection and extraction: (1) IEEE 30-bus, (2) IEEE 39-bus, and (3) IEEE 118-bus test systems.

3.2.3 Stage 3: Development of the intentional islanding algorithms and load shedding algorithm

In this stage, two metaheuristic optimization algorithms (MDEP and MDPSO) and MDEP based load shedding scheme were developed to determine the optimal intentional islanding strategy and optimal amount of load to be shed. MATLAB 10

(R2015a) software was used to code the developed algorithms. The steps involved in the development of these algorithms will be described in detail in this chapter.

3.2.4 Stage 4: Evaluation and validation of the intentional islanding algorithms and load shedding algorithm using case studies

In this stage, the MDEP and MDPSO algorithms developed in Stage 3 were evaluated and validated using several case studies. The evaluation and validation processes consisted of two main parts. In Part 1, nine case studies from three IEEE test systems were used to evaluate and validate the developed algorithms and the results were compared with those obtained by other researchers. The performance of the developed algorithms was compared in order to select the best algorithm. The same IEEE test systems with similar coherent groups of generators used in previous studies were used in this research. It shall be noted that critical line outages were not considered in the previous studies.

In Part 2, another nine case studies from three IEEE test systems were further used to evaluate and validate the proposed algorithm to determine the optimal intentional islanding strategy following a critical line outage. The developed load shedding scheme was further evaluated and validated with the conventional EP and exhaustive search algorithms, based on the case studies conducted in Part 1 and Part 2. The detailed analyzes and results for Part 1 and Part 2 are presented in Chapter 4 and Chapter 5, respectively.

3.3 Proposed Methodology

In this research, the MDEP and MDPSO algorithms were developed to determine the optimal intentional islanding strategy following a critical line outage. In general, the proposed methodology consisted of five main phases: (1) Modelling the power systems (IEEE test systems) using graph theory, (2) Performing N-1 contingency analysis, (3) Determining the initial intentional islanding solution using graph theory, (4) Developing the MDEP and MDPSO algorithms (which are both metaheuristic optimization techniques) to determine the optimal intentional islanding strategy, and (5) Developing the MDEP-based load shedding scheme. Figure 3.2 shows the

correlation between the research objectives and phases involved in the proposed methodology.

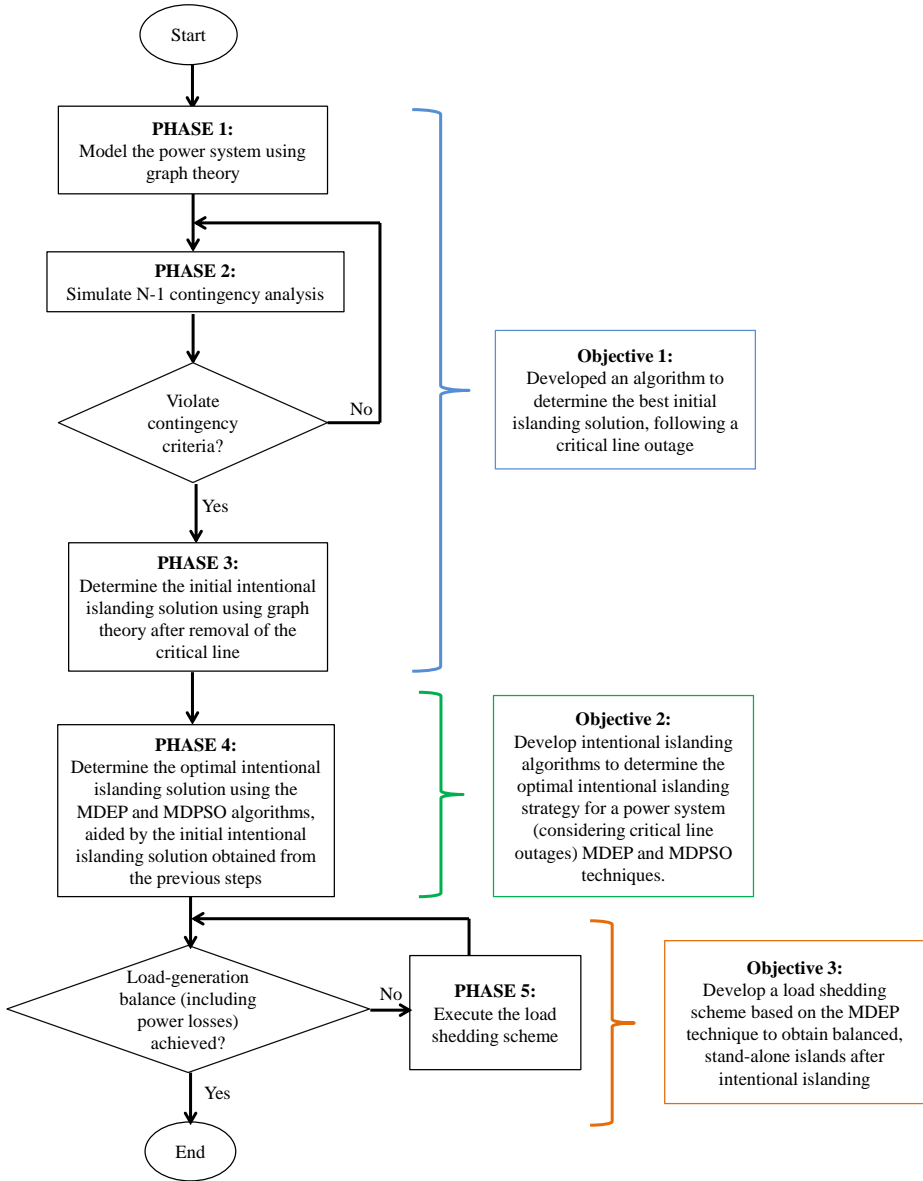


Figure 3.2. Flow Chart of the Proposed Methodology

As shown in Figure 3.2, in Phase 1, the large-scale power systems (IEEE test systems) were modelled using graph theory. In Phase 2, N-1 contingency analysis was simulated to identify the critical lines. Here, the critical lines refer to those that

violate the contingency criteria in contingency scenarios. In Phase 3, graph theory was used to determine the initial intentional islanding solution (i.e. initial cutsets for the islanding problem) following a critical line outage. To achieve Objective 1, these three phases must be accomplished. Next, Objective 2 is achieved in Phase 4, where the MDEP and MDPSO algorithms developed in this research were used to determine the optimal intentional islanding strategy, aided by the initial intentional islanding solution obtained from the previous phase. The power balance (load-generation balance) criterion was checked for each island. If there were any islands that violated the power balance criterion, the developed MDEP-based load shedding scheme (Objective 3) was executed in Phase 5 until the power balance criterion in each island was fulfilled. Each of these phases is described in more detail in the following subsections.

3.3.1 Modelling of the Large-Scale Power Systems

The large-scale power systems were based on the IEEE test systems and modelled using graph theory in MATLAB software. In the graph theory approach, all of the elements in the power system are described in a graphical representation by means of edges, E , and vertices, V . When modelling the power system, the major electrical element nodes (e.g., generators, buses, and load buses) are represented by vertices, V , whereas the transmission lines are represented by edges, E . In this research, graph theory was essential to represent the physical connections of the power system in a graph model. Furthermore, graph theory is very useful for detailed analysis of intentional islanding implementation because the buses and transmission lines in the power system can be easily recognized.

3.3.1.1 Application of Graph Theory for Intentional Islanding

In general, the graph $G(V, E)$ illustrates the relationship between a set of points (edges, E) and a set of lines (vertices, V). In the graph theory approach, the adjacency matrix, $A(G) = [a_{ij}]$, represents the connection between vertex i and vertex j for each pair in the graph. If two vertices are connected by the same edge, they are said to be adjacent. The element of the adjacency matrix is $a_{ij} = 1$ if vertex

i is connected to vertex j by an edge whereas $a_{ij} = 0$ if there is no connection between vertex i and vertex j , where $(i, j) \in E$ [138]. In an intentional islanding problem, the power flow is bidirectional ($a_{ij} = a_{ji} = 1$, where $(i, j) \in E$) and thus, an undirected graph was employed in this research. To gain a better understanding on the graph theory approach, the graph theory was applied to the IEEE 9-bus system, as shown in Figure 3.3. The system comprises three generators (G_1 , G_2 , and G_3), three loads (LD_5 , LD_7 , and LD_9), and nine transmission lines (l_{1-4} , l_{2-8} , l_{3-6} , l_{4-5} , l_{4-9} , l_{5-6} , l_{6-7} , l_{7-8} , and l_{8-9}).

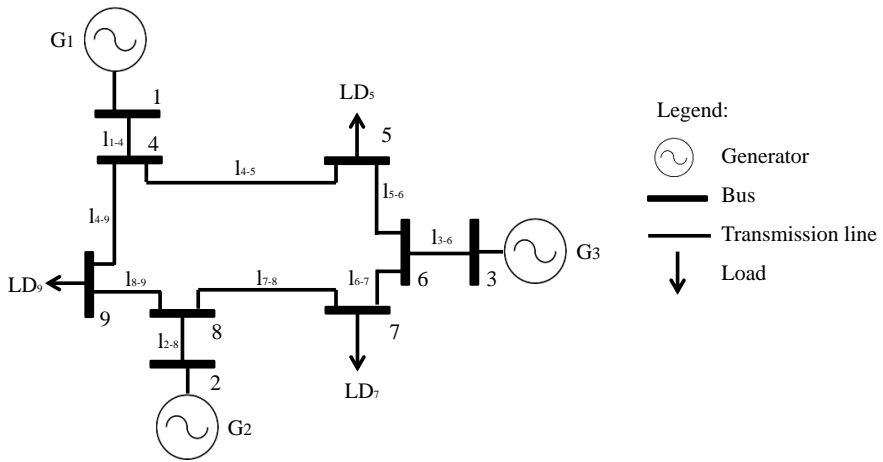


Figure 3.3. IEEE 9-Bus Test System

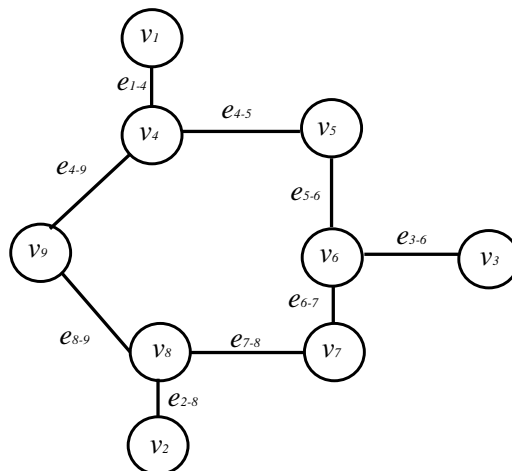


Figure 3.4. Representation of the IEEE 9-Bus Test System as a Graph Model

Figure 3.4 shows the representation of the IEEE 9-bus test system as a graph model. The vertices ($v_1, v_2, v_3, v_4, v_5, v_6, v_7, v_8,$ and v_9) represent the bus nodes (generator buses or load buses) in the power system while the edges ($e_{1-4}, e_{2-8}, e_{3-6}, e_{4-5}, e_{4-9}, e_{5-6}, e_{6-7}, e_{7-8},$ and e_{8-9}) represent the transmission lines. The adjacency matrix, $A(G)$, of this system is given by:

$$A(G) = \begin{bmatrix} 0 & 0 & 0 & 1 & 0 & 0 & 0 & 0 & 0 \\ 0 & 0 & 0 & 0 & 0 & 0 & 0 & 1 & 0 \\ 0 & 0 & 0 & 0 & 0 & 1 & 0 & 0 & 0 \\ 1 & 0 & 0 & 0 & 1 & 0 & 0 & 0 & 1 \\ 0 & 0 & 0 & 1 & 0 & 1 & 0 & 0 & 0 \\ 0 & 0 & 1 & 0 & 1 & 0 & 1 & 0 & 0 \\ 0 & 0 & 0 & 0 & 0 & 1 & 0 & 1 & 0 \\ 0 & 0 & 0 & 0 & 0 & 0 & 1 & 0 & 1 \\ 0 & 0 & 0 & 1 & 0 & 0 & 0 & 1 & 0 \end{bmatrix} \quad (\text{Equation 3.1})$$

The 1s and 0s in the adjacency matrix $A(G)$ represent the connections between the vertices (bus nodes) in the system. This information is vital to determine the optimal intentional islanding strategy because the connections between the buses and transmission lines are crucial in the formation of islands.

3.3.2 N-1 Contingency Analysis

Contingency analysis is important for power system planning and operation. This analysis gives information on the state of a power system in the event of contingencies or outages. Outages of the elements in the power system such as generators, transmission lines, and transformers can trigger overloading problems or can cause a sudden surge/drop in the system voltage [32]. Contingency analysis is carried out by removing each transmission line per cycle (in sequence) to study the effect of outage on the power system operation. It was conducted without considering the current network condition; therefore the outage done is considered to be planned outage. Based on the information gleaned from the contingency analysis, the operators can implement the appropriate remedial action to prevent system instability following a critical line outage.

In this research, N-1 contingency analysis was carried out to identify the critical line outages in different power systems. According to the North American Electric Reliability Corporation (NERC) standard [139], the power system must be secure,

with only one element failure. However, certain line (critical line) outages can trigger cascading failures. Critical line outage is the scenario where the failure of this ‘critical line’ will result in severe cascading failures. A line is defined as a critical line when it reaches a maximum overload (MVA) of 130% [38], as given by the following equation:

$$S_{ij(critical)} > 1.3 \times S_{ij(max)} \quad (\text{Equation 3.2})$$

where $S_{ij(critical)}$ is the critical loading of the transmission line between line i and line j , $S_{ij(max)}$ is the maximum MVA limit of the transmission line between line i and line j . Figure 3.5 shows the flow chart of the N-1 contingency analysis.

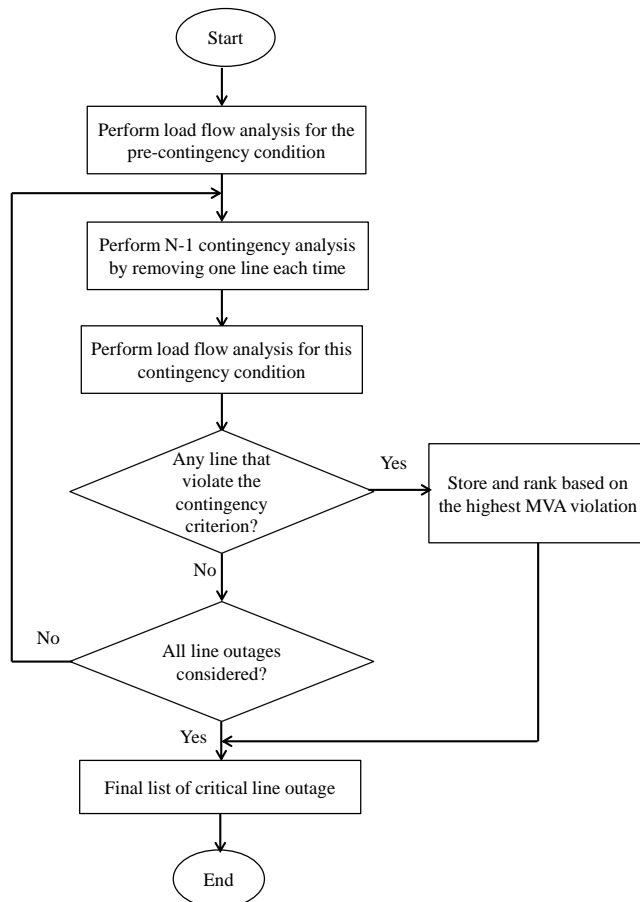


Figure 3.5. Flow Chart of the N-1 Contingency Analysis

As shown in Figure 3.5, the N-1 contingency analysis was initiated by performing load flow analysis on the pre-contingency condition of the power system in order to obtain the system parameters in the initial state. Next, the N-1 contingency analysis was performed by removing one transmission line each time. For each N-1 contingency analysis, load flow analysis was carried out to identify if there were any lines that violated the contingency criterion (Equation 3.2). All the lines that violated the contingency criterion were ranked based on the highest MVA violation and then stored. The process continued until all of the possible line outages were considered. The outcome of the N-1 contingency analysis was the final list of critical line outages that emulate cascading failures leading to blackouts.

3.3.3 Determination of the Initial Intentional Islanding Solution Using the Graph Theory Approach

One of the challenges in intentional islanding is to determine the optimal intentional islanding strategy because of the huge search space of possible solutions. This search space increases proportionally with an increase in the network size. The search space for a given power system is defined as:

$$\text{Search space} = 2^n - 1 \quad (\text{Equation 3.3})$$

where n is the total number of transmission lines in the system. It is apparent from Equation 3.3 that the search space (total number of possible intentional islanding strategies) will significantly increase with an increase in the number of transmission lines (network size).

For instance, the IEEE 30-bus test system has 41 transmission lines. Therefore, the search space for the system is $2^{41}-1 = 2.19902 \times 10^{12}$. Meanwhile, the search space of the IEEE 39-bus test system with 46 transmission lines is 7.03687×10^{13} whereas the search space of the IEEE 118-bus test system with 186 transmission lines is significantly higher, with a value of 9.80797×10^{55} . The huge search space of all possible intentional islanding strategies makes the determination of the optimal intentional islanding strategy highly complex and time-consuming. Therefore, it is

crucial to narrow down the huge search space to speed up the determination of the optimal intentional islanding strategy [89], [140].

In this research, the initial intentional islanding solution obtained from the graph theory approach was used to facilitate the MDEP and MDPSO algorithms to determine the optimal intentional islanding strategy. The initial solution was determined by searching for the possible lines that can be disconnected to form the islands. The graph theory can provide a good initial intentional islanding solution (cutsets) based on certain constraints. Without the initial solution, determining the optimal intentional islanding strategy using optimization algorithms will be an arduous task owing to the huge search space of possible intentional islanding strategies. With the initial solution, the search space can be significantly reduced, which will speed up convergence of the MDEP and MDPSO algorithms in determining the optimal intentional islanding strategy.

Figure 3.6 shows the procedure used in this research to determine the initial intentional islanding solution using the graph theory approach. First, the power system was modelled using graph theory, as described in Section 3.3.1. Next, the critical line outages were identified from the N-1 contingency analysis, as described in Section 3.3.2. The initial intentional islanding solution (cutsets) was determined using graph theory after the critical lines were removed from the power system. The coherent groups of generators were the input parameters supplied to the algorithm. Initially, all of the edges and vertices were set at 0 and the values were updated once the group for each edge and vertex was identified. The process was initiated by forming the backbone of the network, where the coherent generators were grouped into a particular group based on the shortest path configuration. The next-nearest vertices for each group were then assigned to their nearest group. This process was repeated until all of the edges and vertices were assigned to their respective groups. If there was a line that lies in between two different vertices, then the edge would be the cutset candidate. In this research, the shortest path configuration was determined based on Dijkstra's algorithm [141]. The grouping process based on the shortest path configuration was performed in sequence, beginning from Group 1, followed by Group 2, and so on. The rationale of this approach is to facilitate coordination

between the coherent generators in order to control the generated power to meet the total load in a particular island. With this approach, the coherent groups are grouped in the same island, which helps to maintain the stability of each island after intentional islanding implementation.

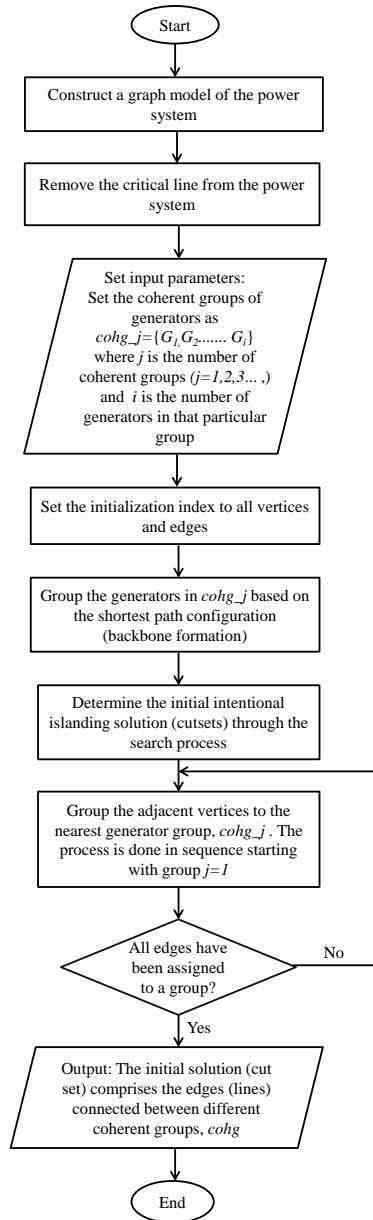


Figure 3.6. Determination of the Initial intentional islanding solution using the Graph Theory Approach

An arbitrary power system based on the IEEE 14-bus test system is used to demonstrate the determination of the initial intentional islanding solution, as shown in Figure 3.7. In this example, the critical line obtained from the N-1 contingency analysis is Line 6-13, as indicated by the blue dashed line in Figure 3.7. The process to determine the initial cutsets is carried out after this line is removed from the system, as shown in Figure 3.8.

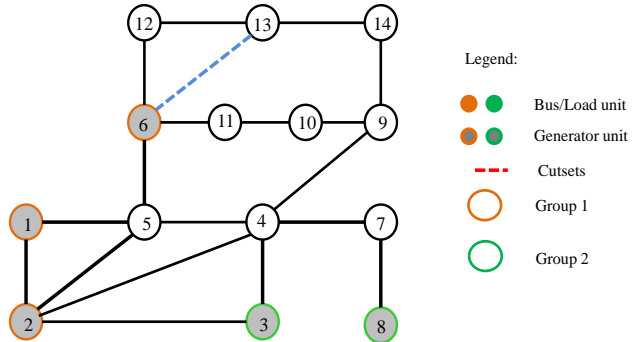


Figure 3.7. IEEE 14-Bus Test System

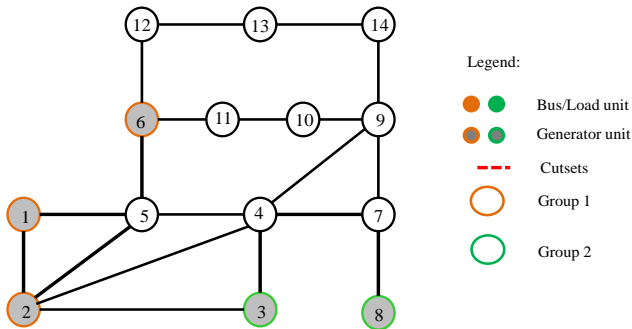


Figure 3.8. IEEE 14-Bus Test System after Disconnecting the Critical Line

The coherent groups of generators are provided as the input parameters of the algorithm. In this example, the coherent groups of generators are as follows:

- a) Group 1: Generators 1, 2, and 6.
- b) Group 2: Generators 3 and 8.

Once the input parameters are supplied to the algorithm, the process begins by grouping the coherent generators in each group based on the shortest path

configuration between the vertices. This forms the backbone of the network, as indicated by the orange lines (Group 1) and green lines (Group 2) in Figure 3.9. Here, the grouping process is performed in sequence, beginning from Group 1, followed by Group 2, and so on.

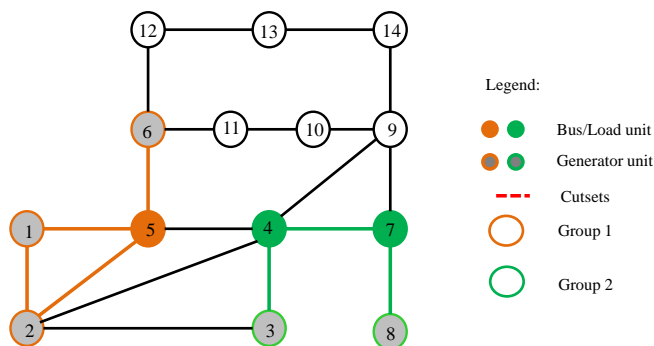


Figure 3.9. Formation of the Coherent Groups of Generators

As shown in Figure 3.9, edges 1–2, 1–5, 2–5, and 5–6 belong to Group 1 whereas edges 3–4, 4–7, and 7–8 belong to Group 2. Next, identification of the next-nearest vertices for the vertices in each group is carried out sequentially, beginning from Group 1. The vertices in Group 1 are assigned to the next-nearest vertices in their group. Likewise, the vertices in Group 2 are assigned to the next-nearest vertices in their group. The edge (line) that lies in between two different vertices (vertices from different groups) is identified as the cutset candidate. Figure 3.10 shows the identification of the next-nearest vertices for the vertices in Group 1 and Group 2 after the 2nd iteration of graph theory-based initialization. The edges indicated by the red dashed lines are lines 2–3, 2–4, and 4–5 and these edges represent the cutset candidates because they are connected between two different groups of vertices.

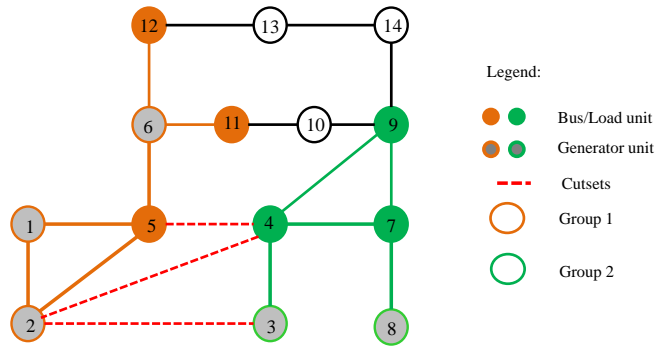


Figure 3.10. Identification of the Next-Nearest Vertices for the Vertices in Group 1 and Group 2 after the 2nd Iteration of Graph Theory-Based Initialization

In the next iteration, the process is repeated and the vertices in each group are assigned to their nearest group sequentially, beginning from Group 1. This process continues until all the vertices are grouped into the appropriate group. The final result, which is the initial intentional islanding solution obtained from the graph theory approach is shown in Figure 3.11. Edges 2–3, 2–4, 4–5, 9–10, and 13–14 (indicated by the red dashed lines) are the initial cutsets obtained from this approach.

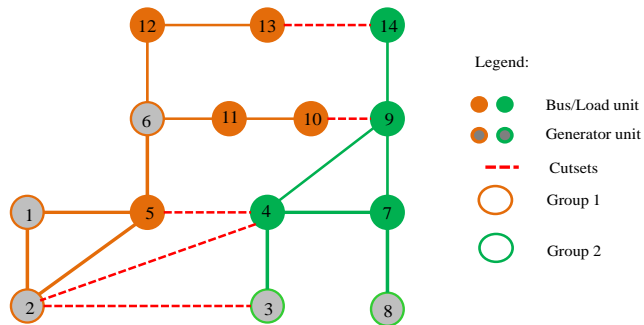


Figure 3.11. Final Result (Initial Intentional Islanding Solution) Obtained from the Graph Theory Approach

Applying the explained concept, the initial cutsets obtained are compared with the transmission line data of the IEEE test system to determine the disconnected lines (initial intentional islanding solution). The initial intentional islanding solution, *in_sol*, is obtained by referring to the number given for each transmission line in the data.

Referring to Table 3.1 that shows the transmission line data for IEEE 14-bus test system, the *in_sol* for the initial cutsets is [3, 4, 7, 15, 19], which is obtained by comparing each initial cutset with each transmission line. If the initial cutset matches the transmission line, the corresponding number is taken as the *in_sol* variable. The *in_sol* variables will be used as the initial population for the MDEP and MDPSO algorithms in this research.

Table 3.1. Transmission Line Data for IEEE 14-bus test system

No.	Transmission Line
1	1-2
2	1-5
3	2-3
4	2-4
5	2-5
6	3-4
7	4-5
8	4-7
9	4-9
10	5-6
11	6-11
12	6-12
13	6-13
14	7-8
15	9-10
16	9-14
17	10-11
18	12-13
19	13-14

3.3.4 Metaheuristic Discrete Optimization Algorithms

As mentioned previously, intentional islanding is a discrete problem because determination of the optimal intentional islanding strategy (cutsets) involves discrete numbers (i.e. Lines 2-4, 6-7, 9-12, and 9-14). Therefore, continuous optimization approaches are not suitable to solve intentional islanding problems. In this research, two metaheuristic discrete optimization algorithms: MDEP and MDPSO algorithms were developed to determine the optimal intentional islanding strategy following a critical line outage, facilitated by the initial solution obtained from the graph theory approach, as described in the preceding section. The best algorithm was selected from both of these algorithms based on the evaluation and validation results for nine case studies, which will be presented in Chapter 4.

3.3.5 Modified Discrete Evolutionary Programming (MDEP) Algorithm

The MDEP algorithm was developed in this research to determine the optimal intentional islanding strategy following a critical line outage. There are a number of aspects that need to be considered in the MDEP algorithm such as the system constraints, fitness function, and mutation techniques, which will be described in detail in this section.

3.3.5.1 System Constraints

The optimal intentional islanding strategy produced by the MDEP algorithm must satisfy the following constraints:

- a) Coherent groups of generators
- b) Desired number of islands
- c) Load-generation balance (including power losses)

However, if the algorithm was unable to determine an intentional islanding strategy that fulfilled the load-generation balance criterion within the specified number of counts (*count_num*), the intentional islanding strategy was further processed, provided that Constraints 1 and 2 were fulfilled. It shall be noted that the coherent groups of generators and the desired number of islands used in this research were obtained based on previously published works [9], [10], [11], [80], [86], [92], [96], [102].

3.3.5.2 Fitness Function

In this research, the minimal power flow disruption was used as the fitness function. This fitness function produces islands with improved transient stability owing to the minimal changes in the power flow patterns [85]. The fitness function is given by:

$$\min \left\{ f(x) = \left(\sum_{cut=1}^{n_{cut}} |P_{ij}| \right) \right\} \quad (\text{Equation 3.4})$$

where P_{ij} is the active power flow in the transmission line from Vertex i to Vertex j and n_{cut} is the total number of cutsets (i.e. the total number of transmission lines to be disconnected). The optimal intentional islanding strategy was selected based on the minimal fitness value. The minimal fitness value represents the minimal arithmetic sum of the active power flow in each line that is disconnected from the system. The fitness value for each candidate was calculated from the fitness function and stored during the optimization process. The fitness values were ranked in order to determine the minimal fitness value.

3.3.5.3 Developed Mutation Techniques

In general, the mutation technique for MDEP optimization is different from that for conventional EP optimization. In this research, the mutation technique was modified to suit the intentional islanding problem because of its discrete nature. Conventional mutation techniques are not suitable for intentional islanding problems because it involves with the floating number that needs to be rounded off, which will lead to slow convergence. Hence, the use of discrete variables is more effective because this approach involves whole numbers (positive integers) in the mutation process. In this research, three mutation techniques were used to mutate the initial intentional islanding solution, in_sol , to produce the optimal intentional islanding strategy, $islanding_sol$. The mutation techniques used in each iteration of the MDEP algorithm are described as follows:

i) Technique 1

In this technique, the mutation process was carried out by replacing a cutset in the initial intentional islanding solution, in_sol , with a new random value x in diagonal manner to produce new populations. The random value x was selected from the search space, S of the power system. The variable $cutsets_mut$ was created to set the maximum number of cutsets to be mutated, which would be replaced in this technique.

- a) **Step 1:** The variable $cutsets_mut$ was initially set at 1 and one cutset in in_sol was mutated and replaced with a new random value x in a diagonal manner as shown in Table 3.2.

Table 3.2. Step 1 of Mutation Technique 1

Initial solution, in_sol	A_1	A_2	A_3	...	A_n	in_sol
1 st mutated in_sol	x_{11}	A_2	A_3	...	A_n	in_sol
2 nd mutated in_sol	A_1	x_{22}	A_3	...	A_n	in_sol
...	A_n	in_sol
...	A_n	in_sol
n^{th} mutated in_sol	A_1	A_2	A_3	...	x_n	in_sol

The variables A_1, A_2, \dots, A_n (variables of in_sol) represent the initial intentional islanding solutions (lines to be disconnected) for a particular line configuration. The new population, $x_{11}, x_{22}, \dots, x_n$, was produced by replacing the variables of in_sol with a new random value x in a diagonal manner. For example, if the line configuration consists of six edges to be disconnected (cutsets), a new six-line configuration is produced by random replacement of the diagonal edges from the 1st edge to the 6th edge. The replacement technique was conducted in such a manner to maintain a certain level of heuristic value based on the last feasible solution. This will speed up convergence of the algorithm during the optimization process.

- b) **Step 2:** The variable $cutsets_mut$ was set at 2 and two cutsets in in_sol were mutated and replaced with a random value x in a diagonal manner as shown in Table 3.3.

Table 3.3. Step 2 of Mutation Technique 1

Initial solution, in_sol	A_1	A_2	A_3	...	A_{n-1}	in_sol	A_n	in_sol
1 st mutated in_sol	x_{11}	x_{12}	A_3	...	A_{n-1}	in_sol	A_n	in_sol
2 nd mutated in_sol	A_1	x_{22}	x_{23}	...	A_{n-1}	in_sol	A_n	in_sol
...	A_{n-1}	in_sol	A_n	in_sol
...	A_{n-1}	in_sol	A_n	in_sol
n^{th} mutated in_sol	A_1	A_2	A_3	...	x_{n-1}	in_sol	x_n	in_sol

The new populations were produced by mutating two cutsets in a diagonal manner. The replacement technique employed here was similar to that in Step 1.

Finally, all of the new populations, mutated in_sol , generated from Step 1 and Step 2 were combined and stored as mutated $islanding_sol$, $IS(x)$, which can be expressed as:

$$IS(x) = \sum_{x=cutsets_mut=1}^2 \text{mutated } in_sol_x \quad (\text{Equation 3.5})$$

ii) Technique 2

In this technique, the total number of initial intentional islanding solutions (total number of *in_sol*) was reduced by a pre-determined number, *reduce_c*, and the new populations were produced by mutating the cutsets, *cutsets_mut*, and replaced with a new random value in a diagonal manner, as performed in Technique 1. The maximum value for *reduce_c* was 3. The steps involved in this technique are outlined as follows:

- a) **Step 1:** The pre-determined number, *reduce_c*, was initially set at 1 and therefore, one cutset was reduced from the original *in_sol*. The variable *cutsets_mut* was set at 1, the mutation process was carried out, and the variables of *in_sol* were replaced with a new random value *x* in a diagonal manner, as shown in Table 3.4.

Table 3.4. Step 1 of Mutation Technique 2

Initial solution, <i>in_sol</i>	A_1	A_2		A_5	A_n <i>in_sol</i>
1 st mutated <i>in_sol</i>	x_{11}	A_2	0
2 nd mutated <i>in_sol</i>	A_1	x_{22}	0
...	0
...	0
n^{th} mutated <i>in_sol</i>	A_1	A_2	...	x_{55}	0

The rationale of mutating *in_sol* by reducing one cutset from the original *in_sol* is to search for new possible intentional islanding solutions, *islanding_sol*, with a fewer number of cutsets (lines to be disconnected). For instance, by performing this step, if the original *in_sol* has six cutsets, the algorithm will search for other feasible *islanding_sol* based on the new *in_sol* with five cutsets. Step 1 was repeated by setting *reduce_c* at 2 and 3.

- b) **Step 2:** This step was similar to Step 1; however, the variable *cutsets_mut* was set at 2. The mutation process was carried out and the variables of *in_sol* were replaced with a random value *x* in a diagonal manner as shown in Table 3.5.

Table 3.5. Step 2 of Mutation Technique 2

Initial solution, in_sol	A_1	A_2	A_3	A_4	$A_{n_in_sol-1}$	$A_{n_in_sol}$
1 st mutated in_sol	x_{11}	x_{22}	A_3	A_4	$A_{n_in_sol-1}$	0
2 nd mutated in_sol	A_1	x_{22}	x_{33}	A_4	$A_{n_in_sol-1}$	0
...	0
n^{th} mutated in_sol	A_1	A_2	A_3	A_4	$x_{n_in_sol-1}$	0

Step 2 was repeated by setting $reduce_c$ at a different value (2 and 3). These processes produced a new series of mutated $islanding_sol$, $IS(x)$, which can be expressed as:

$$IS(x) = \sum_{x=cutsets_mut=1}^2 \left(\sum_{n=1}^3 mutated\ in_sol_x - n \right) \quad (\text{Equation 3.6})$$

iii) Technique 3

In this technique, a pre-determined number of cutsets, $added_c$, was added randomly to in_sol , producing new populations by mutating the cutsets, $cutsets_mut$, and replaced with a new random value in a diagonal manner, as performed in Technique 1. The maximum value for $added_c$ was 3. The steps involved in this technique are outlined as follows:

- a) **Step 1:** The pre-determined number of cutsets, $added_c$, was initially set at 1 and thus, one random cutset was added to the original in_sol . The variable $cutsets_mut$ was set as 1, the mutation process was carried out, and the variables of in_sol were replaced with a new random value x in a diagonal manner, as shown in Table 3.6.

Table 3.6. Step 1 of Mutation Technique 3

Initial solution, in_sol	A_1	A_2	A_7
1 st mutated in_sol	x_{11}	A_2	x_{17}
2 nd mutated in_sol	A_1	x_{22}	x_{27}
3 rd mutated in_sol	x_{37}
4 th mutated in_sol	x_{47}
5 th mutated in_sol	x_{57}
6 th mutated in_sol	x_{67}
n^{th} mutated in_sol	A_1	A_2	x_{77}

The rationale of adding a random number of cutsets into the original *in_sol* is to search for new possible *islanding_sol* with more cutsets but lower fitness function values. For instance, by performing this step, if the original *in_sol* has six cutsets, the algorithm will search for other feasible *islanding_sol* based on the new *in_sol* with seven cutsets. The new *in_sol* may yield possible *islanding_sol* with better fitness function values compared with that obtained based on the original *in_sol*. Step 1 was repeated by setting a different value for *added_c* (2 and 3). These processes produced a new series of mutated *islanding_sol*.

- b) **Step 2:** Step 2 was similar to Step 1; however, the variable *cutsets_mut* was set at 2. The mutation process was carried out and the variables of *in_sol* were replaced with a new random value *x* in a diagonal fashion, as shown in Table 3.7.

Table 3.7. Step 2 of Mutation Technique 3

Initial solution, <i>in_sol</i>	A_1	A_2	A_3	A_6	A_7
1 st mutated <i>in_sol</i>	x_{11}	x_{22}	A_3	A_6	x_{17}
2 nd mutated <i>in_sol</i>	A_1	x_{22}	x_{33}	A_6	x_{27}
3 rd mutated <i>in_sol</i>
4 th mutated <i>in_sol</i>
5 th mutated <i>in_sol</i>
6 th mutated <i>in_sol</i>
n^{th} mutated <i>in_sol</i>	A_1	A_2	A_3	x_{66}	x_{77}

Step 2 was repeated by setting *added_c* at a different value (2 and 3). These processes produced a new series of mutated intentional islanding solutions, *IS(x)*, which can be expressed as:

$$IS(x) = \sum_{x=cutsets_mut=1}^2 \left(\sum_{n=1}^3 mutated\ in_sol_x + n \right) \quad (\text{Equation 3.7})$$

3.3.5.4 Flow Chart of the Modified Discrete Evolutionary Programming (MDEP) Algorithm

Figure 3.12 shows the flow chart of the MDEP algorithm developed in this research to determine the optimal intentional islanding strategy.

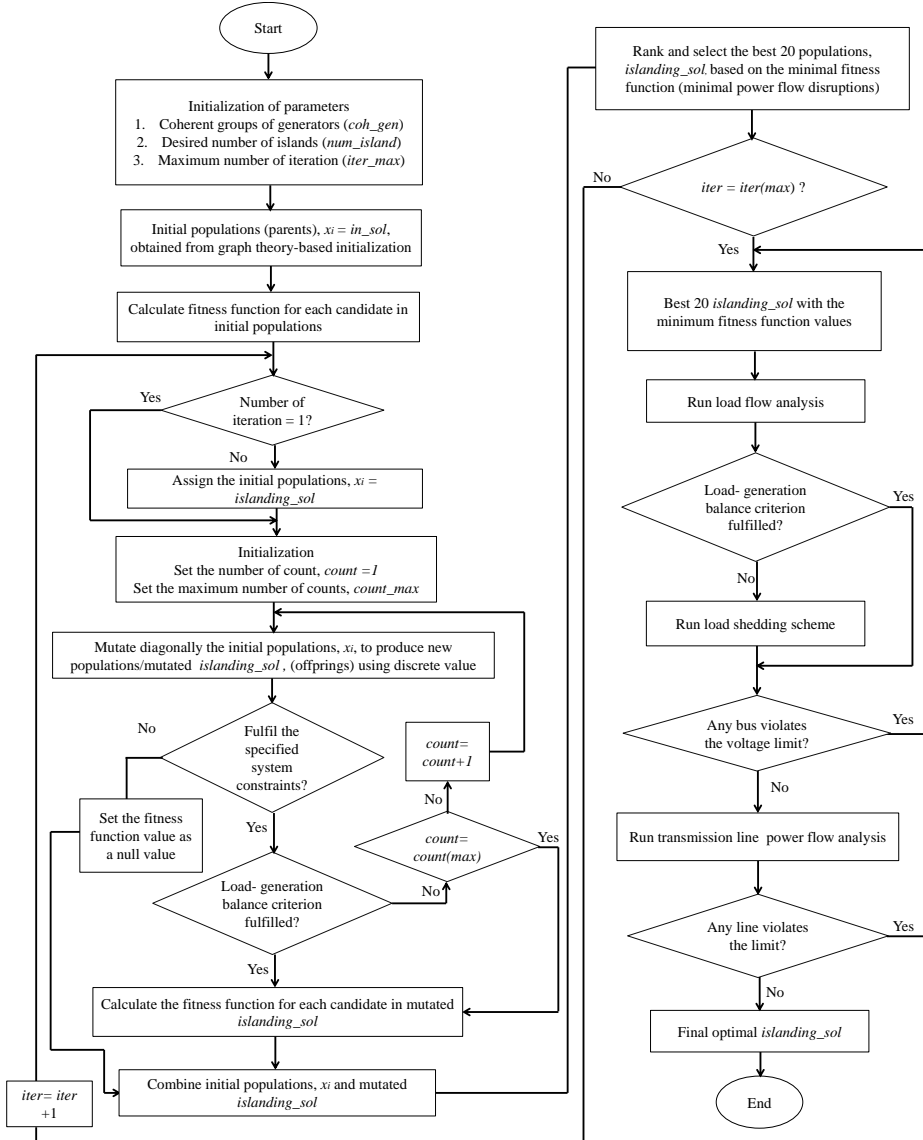


Figure 3.12. Flow Chart of the Developed MDEP Algorithm

In the initialization phase, the initial values were provided for the coherent groups of generators, *coh_gen*, desired number of islands, *num_island*, and the maximum

number of iterations, *iter_max*. Next, the initial intentional islanding solution, *in_sol*, obtained from graph theory-based initialization was assigned as the initial population in the MDEP algorithm. The fitness function values for the initial population were calculated using the fitness function (Equation 3.4) and then stored.

Subsequently, the initial values for the number of counts, *count*, and the maximum number of counts, *count_max*, were provided to check for violations of the load-generation balance criterion. The mutation process was initiated after these values were supplied to the algorithm. In this phase, the initial population was mutated (based on the three techniques described in Section 3.3.5.3) to produce new populations, namely, the mutated *islanding_sol* (offspring). If the mutated *islanding_sol* fulfilled the specified system constraints (i.e. the coherent groups of generators, *coh_gen*, and desired number of islands, *num_island*), the algorithm would proceed to check whether the mutated *islanding_sol* fulfilled the load-generation balance criterion. Otherwise, a null value is given to the fitness value indicating that the mutated *islanding_sol* was unable to produce a feasible intentional islanding solution. If the mutated *islanding_sol* was unable to fulfil the load-generation balance criterion, a new search was executed for the mutated *islanding_sol* until *count_max* was reached. Once *count_max* was reached, the latest mutated *islanding_sol* was selected for evaluation, assuming that the load-generation balance criterion can be fulfilled after performing intentional islanding with the load shedding scheme.

The fitness function values for the mutated *islanding_sol* were calculated using the fitness function as shown in Equation 3.4 and then stored. Next, the mutated *islanding_sol* was combined with the initial population (parents). The best population was selected by ranking all of the combined populations based on their calculated fitness function values (minimal power flow disruption values). The best 20 populations known as best *islanding_sol* were selected as the initial populations for the next iteration. The process of producing new populations continued until the maximum number of iterations was reached. The best 20 *islanding_sol* were selected based on their fitness function values, which were minimal power flow disruption values and stored in the final list.

The first *islanding_sol* in the final list was selected and load flow analysis was performed for each island. This process was carried out because the original network was already partitioned and it was necessary to obtain information from the load flow analysis for the new network configuration, the post-islanding. In the original network, only one slack bus was available. Hence, only one island had a slack bus and the other islands consisted of generator (PV) buses and load buses. Therefore, a slack bus was assigned to other islands in order to perform the load flow analysis. In this research, the slack bus was selected based on the highest maximum power limit ($P_{gen,max}$) among the PV buses. If there were two or more PV buses with the same $P_{gen,max}$ value, then the preceding PV bus was selected. The load flow analysis was then performed to determine whether each island fulfilled the power balance criterion. It shall be noted that the total loads and total generated power must be balanced in each island. If any of the islands did not fulfil the power balance criterion, the developed load shedding scheme was implemented to ensure that the power balance criterion was met. These procedures will be elaborated in Section 3.3.7.

Once the load-generation balance criterion was satisfied, the voltage profile was checked for each island. The voltage of each bus for all islands must be within the allowable voltage limit, as stated in Section 2.3.1, Chapter 2. If there was any bus that violated the allowable voltage limit, then the algorithm would evaluate the next best *islanding_sol*. However, transmission line power flow analysis would be carried out if the bus voltages in all islands were within the allowable voltage limit. In this phase, the power flow in each transmission line for all islands was checked to determine if there were violations in the transmission line capacity. If there was any transmission line that violated its allowable limit, the solution was not the optimal solution and the algorithm would evaluate the next best *islanding_sol*. Otherwise, the *islanding_sol* was the optimal islanding strategy.

3.3.6 Modified Discrete Particle Swarm Optimization (MDPSO) Algorithm

The MDPSO algorithm was also developed in this research to compare its performance in determining the optimal intentional islanding strategy with the MDEP algorithm. The mutation techniques as described in Section 3.3.5.3 were

applied to the MDPSO algorithm in order to update the particles. Figure 3.13 shows the flow chart of the MDPSO algorithm developed in this research work to determine the optimal intentional islanding strategy.

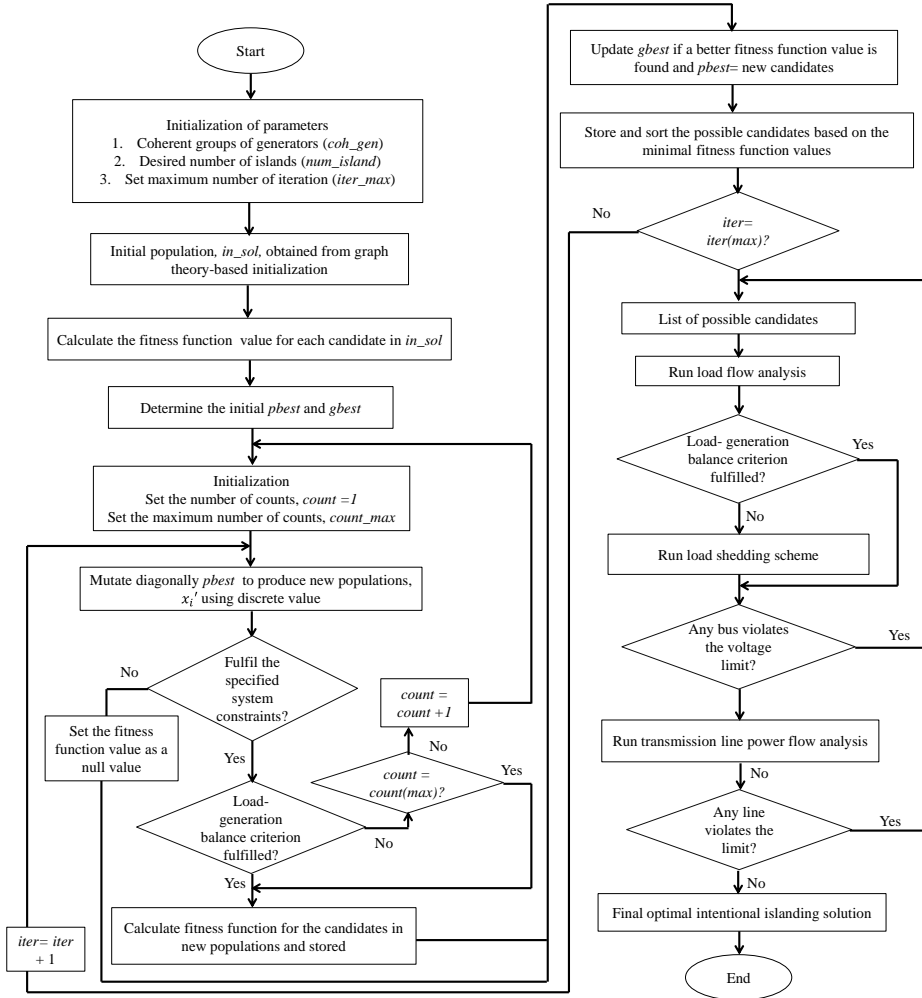


Figure 3.13. Flow Chart of the Developed MDPSO Algorithm

The optimization process was initiated by initializing the parameters, which was the same as that for the MDEP algorithm. The initial population, in_sol , was the initial intentional islanding solution obtained from the graph theory-based initialization. Next, the fitness function values for the initial population were calculated, where the fitness function was the minimal power flow disruption. In this stage, the initial values were assigned for $pbest$ and $gbest$.

Following this, the initial values for the number of counts, *count*, and the maximum number of counts, *count_max*, were provided to check if there were violations in the balance, as in the MDEP algorithm. The mutation techniques used to produce new populations (mutated *islanding_sol*) in the MDPSO algorithm were the same as those used in the MDEP algorithm. Each of the new populations was checked to determine whether the new population fulfilled the system constraints. The fitness function values for the mutated *islanding_sol* were subsequently calculated and then stored. The mutated *islanding_sol* candidates were ranked based on their fitness function values (minimal power flow disruption values) and then stored. The *gbest* values was compared and updated if a better fitness function value was found. Here, *pbest* is the local best position known as mutated *islanding_sol* and *gbest* is the global best position among the mutated *islanding_sol*. The iteration condition was checked and the process continued until the maximum number iterations was reached.

Once the maximum number of iterations was reached, the *islanding_sol* was further evaluated, as in the MDEP algorithm. Load flow analysis was carried out to obtain the new system parameters for each island formed. The load-generation balance and voltage profile for each island were checked to ensure that each island fulfilled the load-generation balance criterion and allowable voltage limit. Finally, transmission line power flow analysis was carried out to determine whether the power flow in each transmission line for all islands fulfilled the allowable limit. The *islanding_sol* that satisfied the load-generation balance criterion, allowable bus voltage limit, and transmission line capacity was the optimal *islanding_sol*.

3.3.7 Load Shedding Scheme Based on the Modified Discrete Evolutionary Programming (MDEP) Technique

Power generation deficit is a scenario that may occur after intentional islanding. This scenario occurs when the total generated power, P_{gen} , is lower than the total load, P_{load} . Hence, a load shedding scheme is needed to maintain the load-generation balance and voltage profile of each island. Figure 3.14 shows the steps involved in a load shedding scheme.

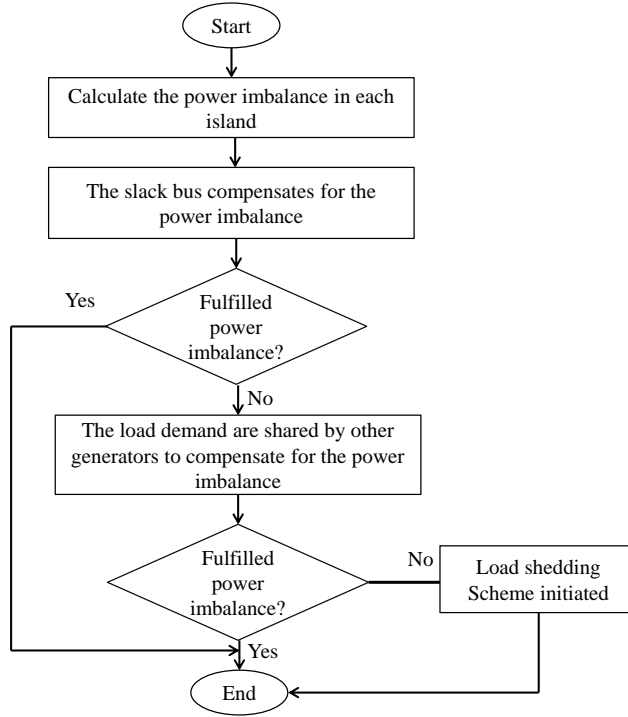


Figure 3.14. Steps Involved in a Load Shedding Scheme

Based on Figure 3.14, the steps involved in a load shedding scheme can be summarized as follows:

- a) **Step 1:** Calculate the total power imbalance, P_{imb} , for each island using the following equation:

$$\sum P_{imb} = \sum P_{gen} - (\sum P_{load} + \sum P_{loss}) \quad (\text{Equation 3.8})$$

where P_{gen} is the total generated power and P_{load} is the total load for a particular island.

- b) **Step 2:** The slack bus will compensate for the power generation deficit if there is power imbalance in the island. The generated power of the slack bus can be increased up to its maximum power rating, $P_{max(slack)}$. If power imbalance is still present, then the loads will be shared by other generators in the island. The total power imbalance, P_{imb} , is divided equally between the

generators. This process is carried out until the maximum power limits of all generators are reached.

- c) **Step 3:** If power imbalance is still present in the island after Step 2, the load shedding scheme is executed. In this research, the load shedding scheme was developed based on a metaheuristic approach in order to determine the optimal amount of load to be shed. It shall be noted that for transmission level, the load is shed based on the optimal amount of load to be shed. Priority of load shed can be only considered in the distribution level. The details of the MDEP-based load shedding scheme are presented in the following section.

3.3.7.1 Developed MDEP-Based Load Shedding Scheme

In this research, the MDEP-based load shedding scheme was developed to determine the optimal amount of load to be shed. The use of discrete optimization is preferable because the selection of buses for load shedding is a discrete problem (i.e. Buses 4, 6, and 8). The flow chart of the MDEP-based load shedding scheme is shown in Figure 3.15.

Referring to Figure 3.15, the initial populations were generated from random combinations and different number of buses. Table 3.8 shows an example of the initial populations generated for load shedding. Random bus, B_i , is chosen from the total number of buses available for load shedding.

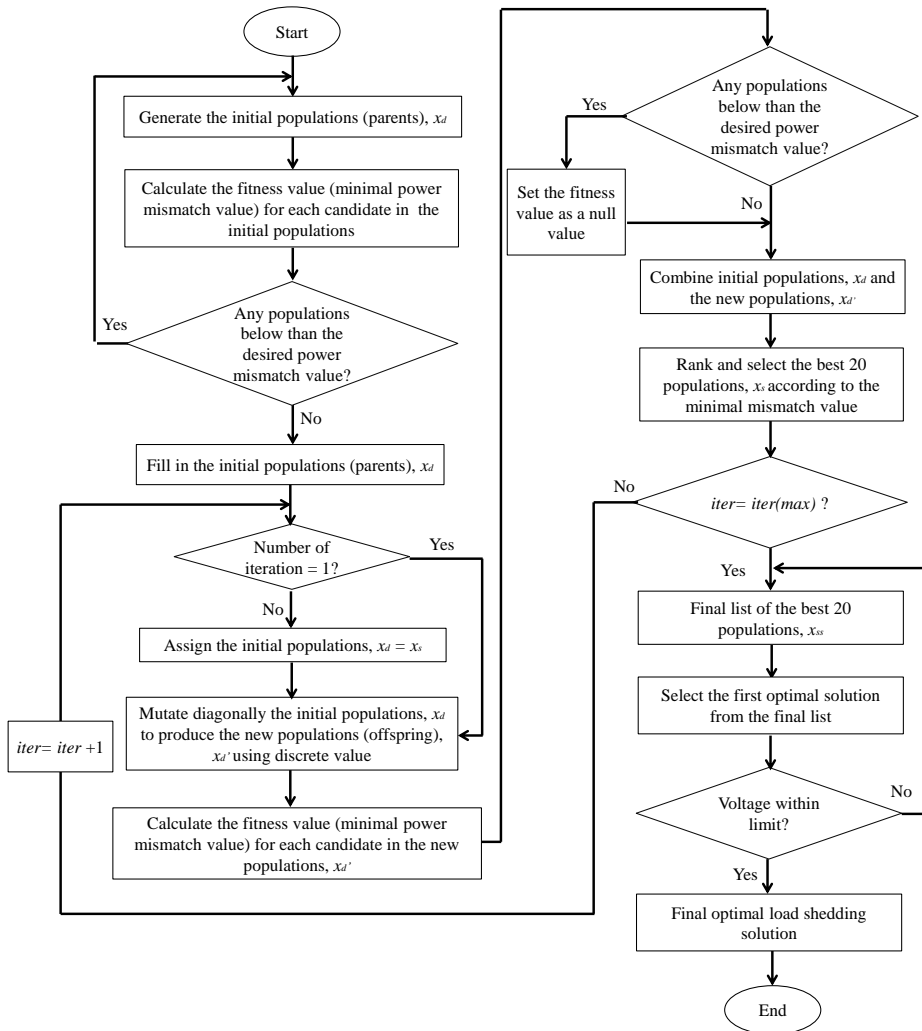


Figure 3.15. Steps Involved in the MDEP-Based Load Shedding Scheme

Table 3.8. Example of Initial Populations Generated for Load Shedding Using the MDEP-Based Load Shedding Scheme

No. of buses randomly chosen	1 st bus	2 nd bus	3 rd bus	4 th bus	n th bus
1	B_1				
2	B_2	B_3			
3	B_4	B_5	B_6		
4	B_7	B_8	B_9	B_{10}	
n	B_{11}	B_{12}	B_{13}	B_{14}	B_n

Next, the fitness function value was calculated for each population. The minimal power mismatch value (minimal power imbalance) was used as the fitness function in the MDEP-based load shedding scheme. Once the fitness function values were calculated, the algorithm would check to determine if there were populations whose fitness function values were less than the desired power mismatch value. If a population fulfilled this criterion, its fitness function value was set as a null value, indicating that this population was not a feasible load shedding solution.

Applying the concept, the initial populations, x_d , were combined with the new populations, x_d' . The combined populations were ranked based on their minimal power mismatch values and the best 20 populations were selected as the initial populations (parents) for the next iteration. The mutation process continued until the maximum number of iterations was reached. The MDEP-based load shedding scheme then produced the final list of the best 20 populations, x_{SS} . The first solution from the final list was checked to determine if there were violations in the allowable voltage limit. The solution was regarded as the considered as the optimal load shedding solution if the voltages for all buses in the island were within the allowable voltage limit. Otherwise, the algorithm would select the next best solution from the final list and the process was repeated until the optimal load shedding solution was obtained for that particular island.

3.4 Chapter Summary

The methodology adopted in this research to determine the optimal intentional islanding strategy following a critical line outage has been described in detail in this chapter. The methodology consisted of five main phases. In Phase 1, graph theory was used to model large-scale power systems (IEEE test systems). In Phase 2, N-1 contingency analysis based on MVA violation was carried out for a single element (transmission line) outage to obtain the list of critical lines that can trigger cascading failures. In Phase 3, the initial intentional islanding solution (cutsets) was determined by removing these critical lines from the power system. The initial intentional islanding solution obtained from Phase 3 was used in the MDEP and MDPSO algorithms in Phase 4.

This initial intentional islanding solution was crucial to facilitate the MDEP and MDPSO algorithms to determine the optimal intentional islanding strategy. Once the specified system constraints were fulfilled, the possible intentional islanding strategies were checked to determine whether they fulfilled the load-generation balance criterion. If there was power imbalance in any island, the MDEP-based load shedding scheme was executed in Phase 5. With the load shedding scheme, the optimal amount of load to be shed was obtained in order to fulfil the power balance criterion in all islands formed.

Finally, the voltage of each bus was checked and transmission line power flow analysis was performed to determine if there were violations in the allowable voltage limit and power flow rating for all islands. The final optimal intentional islanding strategy was obtained when the voltages of all buses did not exceed the allowable voltage limit and the power flow in all transmission lines did not exceed the allowable power rating. The developed MDEP and MDPSO algorithms were further analyzed, validated, and evaluated using nine case studies, which will be described in Chapter 4 and Chapter 5.

CHAPTER 4

VALIDATION OF THE DEVELOPED INTENTIONAL ISLANDING ALGORITHMS WITHOUT CONTINGENCY ANALYSIS

4.1 Introduction

This chapter presents a detailed analysis and discussion in determining the optimal intentional islanding strategy using the developed intentional islanding algorithms (MDEP and MDPSO algorithms) outlined in the previous chapter. Nine case studies using three different IEEE test systems: IEEE 30-bus, IEEE 39-bus, and IEEE 118-bus test systems were employed for this purpose. Critical line outages were not considered in this chapter so that the results of the proposed algorithms could be compared with those in previously published works, where critical line outages were also not considered. The process began with modelling the test systems using graph theory. The initial solution obtained from the graph theory approach was used as the initial solution for the intentional islanding algorithm. Then, the Modified Discrete Evolutionary Programming (MDEP) and Modified Discrete Particle Swarm Optimization (MDPSO) algorithms were analyzed in order to determine the optimal intentional islanding strategy. The effectiveness of these algorithms was validated by comparing the results with those obtained in published works. The best algorithm was chosen from these algorithms based on the convergence curve and computational time.

4.2 IEEE Test Systems

In this research, three IEEE test systems: IEEE 30-bus, IEEE 39-bus and IEEE 118-bus test systems were used to evaluate and validate the effectiveness of the proposed MDEP and MDPSO algorithms in determining the optimal intentional islanding strategy. Three different sets of coherent groups of generators were evaluated for each test system, which gives a total of nine case studies. All data including buses, transmission lines, and maximum line rating for these test systems were obtained from [142] and [143]. The generator data for each test system are provided in Appendix A (Table A.1- Table A.3).

4.2.1 IEEE 30-Bus Test System

The IEEE 30-bus test system consists of six generators, 24 load buses, and 41 transmission lines. The network diagram of the IEEE 30-bus test system is shown in Figure 4.1. The load flow analysis for this system is presented in Appendix A (Table A.4).

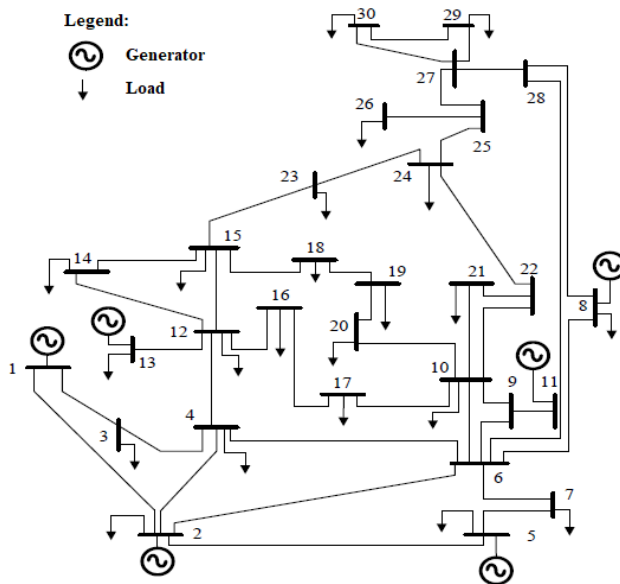


Figure 4.1. Schematic of the IEEE 30-Bus Test System

4.2.2 IEEE 39-Bus Test System

The IEEE 39-bus test system consists of 10 generators, 29 load buses, and 46 transmission lines. The original IEEE 39-bus test system is shown in Figure 4.2. Another modified IEEE-39 bus test system is also utilized in this research for analysis purposes [86]. The modified version of IEEE-39 bus test system uses the same system parameters; however, there are some amendments in the transmission line configuration, as marked by the green regions in Figure 4.3. The results of load flow analysis for both systems are provided in Appendix A (Table A.5) and Appendix A (Table A.6) respectively.

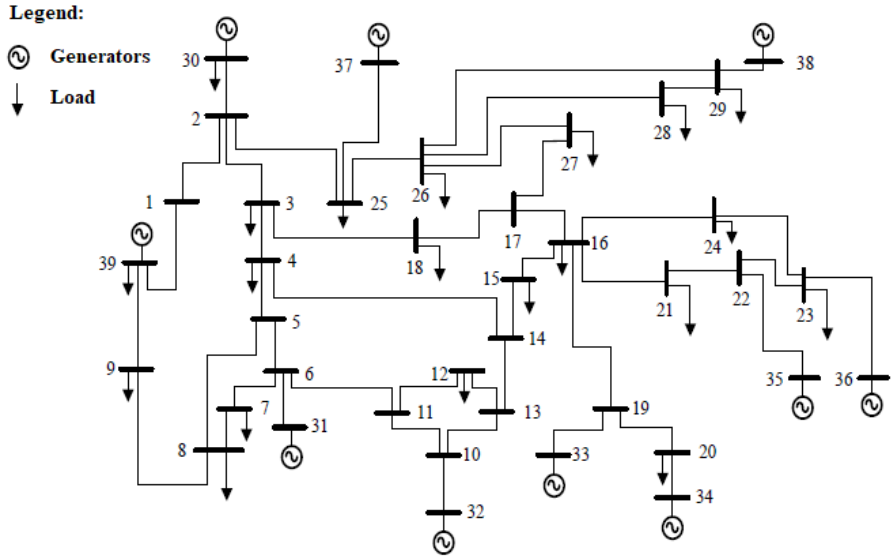


Figure 4.2. Schematic of the Original IEEE 39-Bus Test System

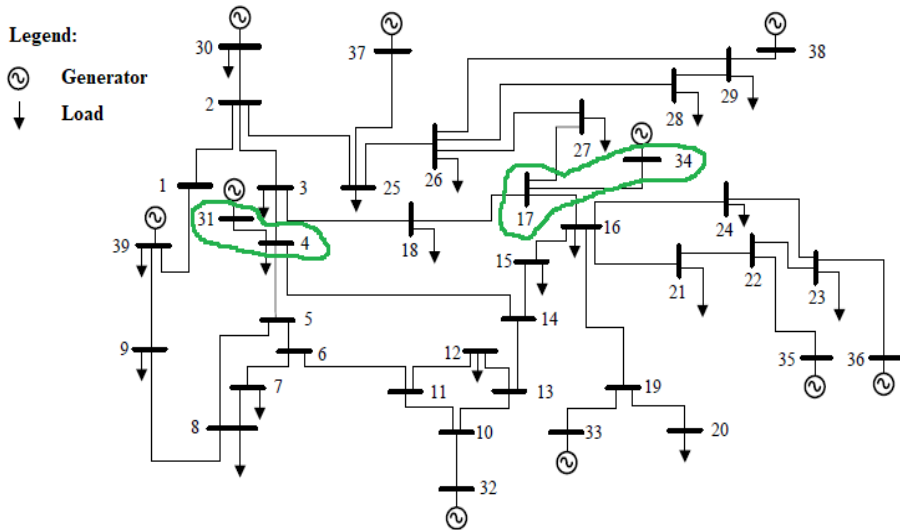


Figure 4.3. Schematic of the Modified IEEE 39-Bus Test System

4.2.3 IEEE 118-Bus Test System

The IEEE 118-bus test system consists of 19 generators, 35 synchronous condensers, 64 load buses, and 186 transmission lines, as shown in Figure 4.4. However, in this research, the 35 synchronous condensers were regarded as the load buses for analysis

purposes. The result of load flow analysis for this system is provided in Appendix A (Table A.7).

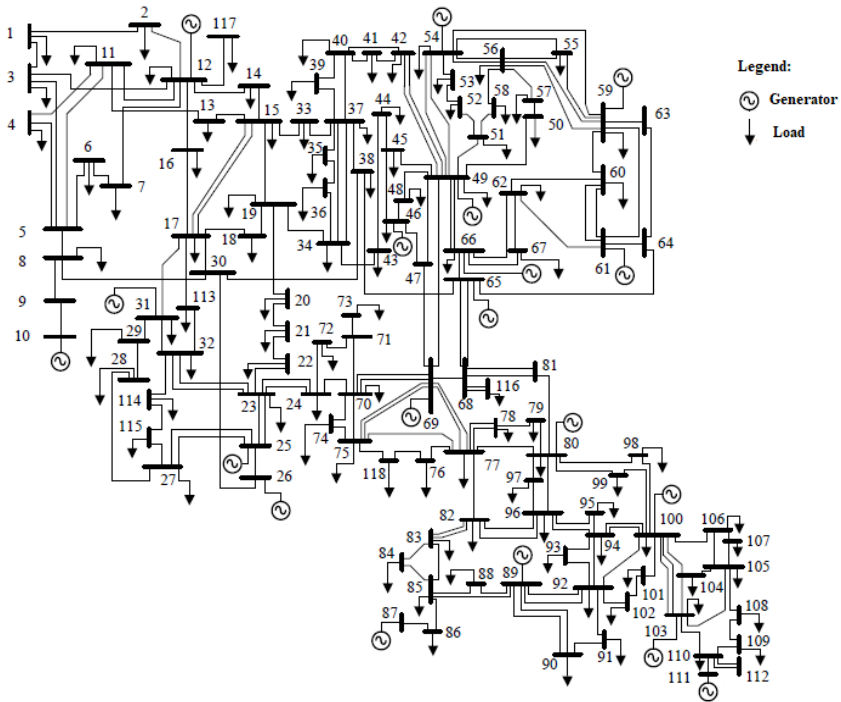


Figure 4.4. Schematic of the IEEE 118-Bus Test System

4.3 Analysis of the IEEE 30-Bus Test System

Three case studies were carried out using the IEEE 30-bus test system in order to evaluate the MDEP and MDPSO algorithms. The results, including the initial solution obtained from the graph theory approach and the optimal intentional islanding strategy determined from the proposed intentional islanding algorithms for each case study are presented and discussed in this section. The results were also compared with previously published works to assess the performance of the MDEP and MDPSO algorithms. Initially, the IEEE 30-bus test system was first modelled using the graph theory approach, as shown in Figure 4.5. In this graph model, the vertices represent the buses in the test system while the edges represent the transmission line connections.

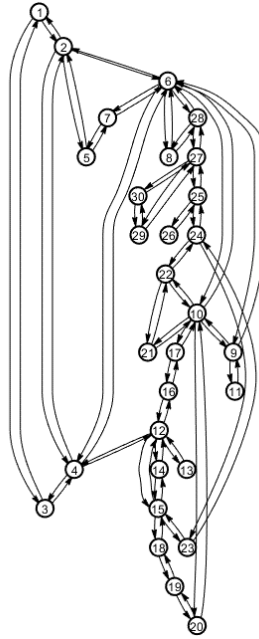


Figure 4.5. Representation of the IEEE 30-Bus Test System as a Graph Model

4.3.1 Case Study 1

In Case Study 1, the optimal intentional islanding strategy was analyzed based on previous works reported in [9], [11]. In this case study, intentional islanding was executed by splitting the system into two islands based on the coherent groups of generators: $G_1 = \{1, 2, 5, 13\}$ and $G_2 = \{8, 11\}$.

4.3.1.1 Determination of the Initial Intentional Islanding Solution

Once the number of islands and coherent groups of generators were known, the initial intentional islanding solution was determined using graph theory approach. In general, this approach determines the total number of transmission lines that needs to be disconnected in order to form the desired number of islands based on the coherent groups of generators. Figure 4.6 shows the graph model of the initial intentional islanding solution (red lines) for the IEEE 30-bus test system. The initial intentional islanding solution and the corresponding total power flow disruption, P_{disrup} , obtained for Case Study 1 are shown in Table 4.1.

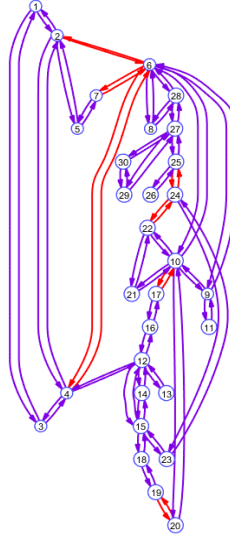


Figure 4.6. Graph Model of the Initial Intentional Islanding Solution (Red Lines) for Case Study 1

Table 4.1. Initial Intentional Islanding Solution for Case Study 1

Initial intentional islanding solution	Total power flow disruption, P_{disrup} (MW)
2-6, 4-6, 6-7, 19-20, 10-17, 22-24, 24-25	188.641

The initial intentional islanding solution consisting of seven cutsets obtained from the graph theory approach, which produced a total power flow disruption, P_{disrup} , of 188.641 MW, as shown in Table 4.1. This shows that the graph theory approach is capable of reducing the initial search space of all possible transmission lines ($2^{41}-1 \approx 2.199 \times 10^{12}$) to seven lines as the initial solution. This initial solution was used to facilitate the MDEP and MDPSO algorithms in determining the optimal intentional islanding strategy.

4.3.1.2 Evaluation of the MDEP and MDPSO Algorithms

The MDEP and MDPSO algorithms were analyzed using the IEEE 30-bus test system and the results are presented in Table 4.2. Both of these algorithms provided the same optimal intentional islanding strategy, with a total power flow disruption, P_{disrup} , of 154.442 MW. The total number of disconnected lines (cutsets) was reduced to six in the optimal solution whereas the initial solution consisted of seven

cutsets. The results were compared with those of previously published works [9], [11]. It is evident from Table 4.2 that the MDEP and MDPSO algorithms were capable of obtaining a better optimal intentional islanding strategy compared with the BPSO algorithm [11] and similar islanding strategy with the modified ABC algorithm [9]. The identical optimal intentional islanding strategies determined from the developed algorithms and modified ABC algorithm [9] are likely because this strategy are the most optimal solution that can be obtained for this case study.

Table 4.2. Comparison of the Optimal Intentional Islanding Strategies for Case Study

Algorithm	Optimal intentional islanding strategy	$\sum P_{disrup}$ (MW)
BPSO [11]	2-6, 4-6, 6-7, 19-20, 10-17, 22-24, 24-25	188.641
Modified ABC [9]	2-6, 4-6, 5-7, 16-17, 18-19, 23-24	154.442
MDPSO	2-6, 4-6, 5-7, 16-17, 18-19, 23-24	154.442
MDEP	2-6, 4-6, 5-7, 16-17, 18-19, 23-24	154.442

Since the MDEP and MDPSO algorithms developed in this research produced the same optimal intentional islanding strategy, the performance of these algorithms was assessed to identify which was the best algorithm. As mentioned previously, the best algorithm was chosen based on the convergence curve and computational time. The maximum number of iterations for the convergence test was set at 50 and the convergence curves for the MDEP and MDPSO algorithms are shown in Figure 4.7. It can be observed that both of the algorithms reached convergence within 50 iterations.

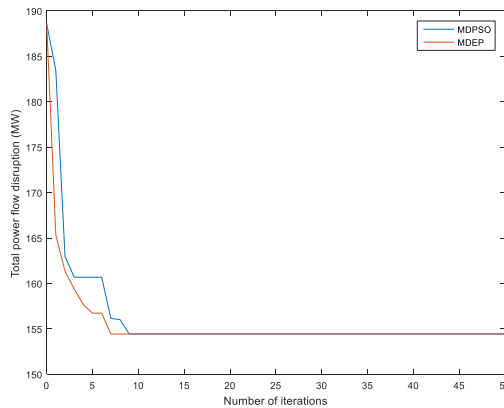


Figure 4.7. Convergence Curves for the MDEP and MDPSO Algorithms for Case Study 1

Although both algorithms produced the same optimal intentional islanding strategy, the MDEP algorithm converged faster compared with the MDPSO algorithm. The performance of the MDEP and MDPSO algorithms was analyzed in terms of the number of iterations required by the algorithm to reach convergence and computational time, and the results are summarized in Table 4.3.

Table 4.3. Comparison of the Performance between the MDEP and MDPSO Algorithms

Algorithm	No. of iterations required by the algorithm to reach convergence	Computational time (sec)
MDEP	7	506.780
MDPSO	9	664.592

It can be seen from Table 4.3 that the MDEP algorithm achieved convergence on the 7th iteration whereas the MDPSO algorithm achieved convergence on the 9th iteration. Furthermore, the MDEP algorithm consumed less computational time, which is 506.780 sec to achieve convergence compared to the MDPSO algorithm with 664.592 sec. Thus, the MDEP algorithm was the best algorithm to implement intentional islanding for Case Study 1.

4.3.1.3 Determination of the Optimal Intentional Islanding Strategy Using the MDEP Algorithm

The optimal intentional islanding strategy obtained from the MDEP algorithm produced two stand-alone islands with 12 and 18 buses in Island 1 and Island 2, respectively. The optimal intentional islanding strategy for Case Study 1 was 2–6, 4–6, 5–7, 16–17, 18–19, and 23–24, resulting in a total power flow disruption of 154.442 MW. The one-line diagram and the graph model of the islanded islands for this case study are shown in Figure 4.8 and Figure 4.9, respectively.

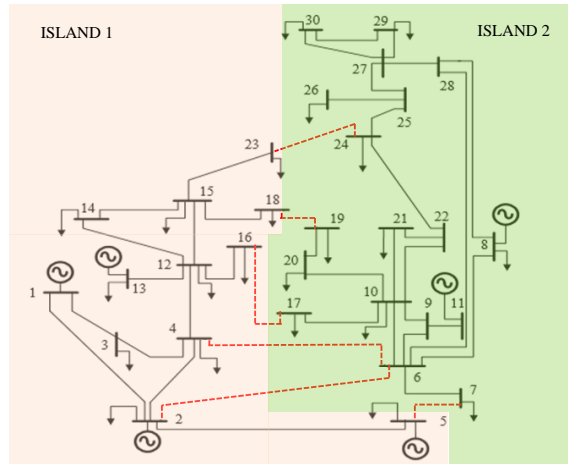


Figure 4.8. One-Line Diagram for Case Study 1

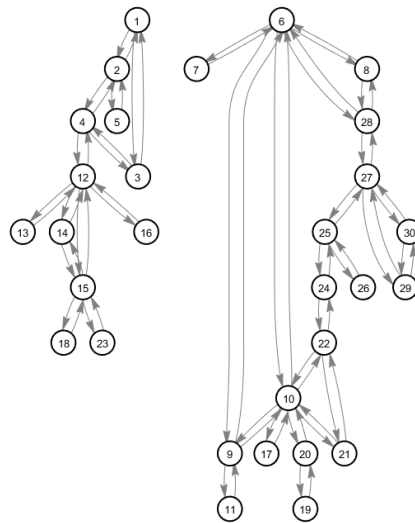


Figure 4.9. Graph Model of the Islanded Islands for Case Study 1

In this case study, the two stand-alone islands formed after intentional islanding must be balanced in terms of the total generated power and total load. Hence, the power balance criterion was assessed for each island. Table 4.4 shows the results for Island 1 and Island 2 before and after intentional islanding implementation.

Table 4.4. Results for Island 1 and Island 2 Before and After Intentional Islanding Implementation: Case Study 1

Island 1				
Buses in Island 1	Generator information		Active power (MW)	
	Generator	Max. limit (MW)	Pre-islanding	Post-islanding
			ΣP_{gen}	ΣP_{gen}
1–5, 12–16, 18, 23	G _{1*}	360	260.998	128.075
	G ₂	140	40.000	40.000
	G ₅	100	0.000	0.000
	G ₁₃	100	0.000	0.000
Total generated power, P_{gen} (MW)			300.998	168.075
Total load, P_{load} (MW)			161.400	161.400
Total power loss, P_{loss} (MW)			13.566	6.675
Total power imbalance, P_{imb} (MW)			126.032	0.000
Total amount of load to be shed, P_{shed} (MW)			—	—
Island 2				
Buses in Island 2	Generator information		Active power (MW)	
	Generator	Max. limit (MW)	Pre-islanding	Post-islanding
			ΣP_{gen}	ΣP_{gen}
6–11, 17, 19–22, 24–30	G _{8*}	100	0.000	62.189
	G ₁₁	100	0.000	61.000
Total generated power, P_{gen} (MW)			0.000	123.189
Total load, P_{load} (MW)			122.000	122.000
Total power loss, P_{loss} (MW)			1.207	1.189
Total power imbalance, P_{imb} (MW)			-123.207	0.000
Total amount of load to be shed, P_{shed} (MW)			—	—

*slack bus

The total generated power, P_{gen} , total load, P_{load} , total power loss, P_{losses} , and total power imbalance, P_{imb} , before and after intentional islanding are presented in the ‘pre-islanding’ and ‘post-islanding’ columns of Table 4.4, respectively, for both Island 1 and Island 2.

In Island 1, there was a power surplus of 126.032 MW before intentional islanding. This can be attributed to the slack bus, G₁ (located in Island 1), which generated a high amount of power in the pre-islanding condition. Load flow analysis was then carried out to obtain the new system parameters for Island 1. It can be seen from Table 4.4 (post-islanding column for Island 1) that the slack bus, G₁, reduced its generated power from 260.998 MW to 128.075 MW in order to fulfil the power balance criterion in the island. After intentional islanding, the power balance criterion was met and therefore, the load shedding scheme was not executed. Island 1 could operate as a balanced, stand-alone island.

In contrast, there was a power deficit of 123.207 MW in Island 2. This may be attributed to the absence of a slack bus in this island, considering that the original slack bus was located in Island 1. Therefore, it was necessary to assign a new slack bus in Island 2. The slack bus was selected based on the highest maximum power limit ($P_{gen,max}$) among the available generator (PV) buses. This criterion was used to select a new slack bus for all case studies presented in Chapter 4 and Chapter 5. Since the generators buses available in this island had the same maximum power limit, either one of them could be selected as the slack bus. In this case, generator bus, G_8 was selected as the slack bus. The total power generated, P_{gen} , in this island was 0.000 MW while the total load, P_{load} , was 122.000 MW in the pre-islanding condition. However, the maximum power limit for generator bus, G_8 was 100 MW. Therefore, both generator buses, G_8 and G_{11} shared the loads equally to compensate for the power deficit in Island 2. Finally, the power balance criterion was met for Island 2, as shown in Table 4.4 (post-islanding column for Island 2) and therefore, the load shedding scheme was not executed. Island 2 could operate as a balanced, stand-alone island. Detail information on the load, P_{load} and generated power, P_{gen} connected to each bus for each island are shown in Appendix A (Table A.8).

The voltage profile was checked for each island after intentional islanding to ensure that there were no voltage violations. The voltage of each bus for all islands was found to be within the allowable voltage limits, as shown in Appendix A (Table A.9).

In addition, the power flow in each transmission line was analyzed for both islands to ensure that there were no violations in the transmission line capacity. The power flow, P_{flow} , in each transmission line for both islands was found to be less than the transmission line capacity limit. The results of the transmission line power flow analysis for Case Study 1 are shown in Appendix A (Table A.10).

Overall, the results indicate that the proposed MDEP algorithm is capable of reducing the huge search space of possible intentional islanding solutions and determine the optimal intentional islanding strategy that fulfils the specified system constraints. The intentional islanding strategy is considered successful when the

power balance, bus voltage, and transmission line capacity criteria are fulfilled for each island formed.

4.3.2 Case Study 2

For Case Study 2, a different set of coherent groups of generators was investigated using the IEEE 30-bus test system to obtain the optimal intentional islanding strategy. This case study was performed based on the information obtained from a previous work [96]. In this case study, the desired number of islands to be formed was two islands based on the coherent groups of generators: $G_1 = \{1, 2, 5, 8\}$ and $G_2 = \{11, 13\}$. The steps implemented in Case Study 1 were also implemented in this case study and in other case studies presented in this chapter.

4.3.2.1 Determination of the Initial Intentional Islanding Solution

The graph model of the initial intentional islanding solution (red lines) for the IEEE 30-bus test system (Case Study 2) is shown in Figure 4.10. The corresponding total power flow disruption, P_{disrup} , is shown in Table 4.5.

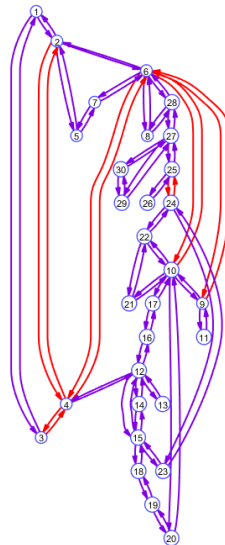


Figure 4.10. Graph Model of the Initial Intentional Islanding Solution (Red Lines) for Case Study 2

Table 4.5. Initial Intentional Islanding Solution for Case Study 2

Initial intentional islanding solution	Total power flow disruption, P_{disrup} (MW)
2-4, 3-4, 4-6, 6-9, 6-10, 24-25	238.690

Table 4.5 shows the initial intentional islanding solution with six cutsets obtained from the graph theory approach, where the corresponding total power flow disruption, P_{disrup} , was 238.690 MW. This initial solution was then used to facilitate the MDEP and MDPSO algorithms in determining the optimal intentional islanding strategy.

4.3.2.2 Evaluation of the MDEP and MDPSO Algorithms

The MDEP and MDPSO algorithms were then analyzed using the IEEE 30-bus test system. As in the previous case study, both of the algorithms produced the same optimal intentional islanding strategy with a total power flow disruption of 88.962 MW, as shown in Table 4.6. The number of cutsets was reduced from six cutsets (initial intentional islanding solution) to four cutsets (optimal intentional islanding strategy). The results were compared with those of [96], as shown in Table 4.6. It is evident that the proposed MDEP and MDPSO algorithms were able to determine a superior intentional islanding strategy and significantly reduce the number of cutsets compared with the mixed integer algorithm [96].

Table 4.6. Comparison of the Optimal Intentional Islanding Strategies for Case Study 2

Algorithm	Optimal intentional islanding strategy	$\sum P_{disrup}$ (MW)
Mixed integer [96]	1-3, 2-4, 4-6, 6-9, 6-10, 6-28, 10-22, 10-21, 15-18, 12-15, 14-15	309.214
MDPSO	6-9, 6-10, 4-12, 24-25	88.962
MDEP	6-9, 6-10, 4-12, 24-25	88.962

As in the previous case study, the MDEP and MDPSO algorithms yielded the same optimal intentional islanding strategy. Therefore, the best algorithm was selected based on the convergence curve and computational time. Both of these algorithms reached convergence within 50 iterations, as shown in Figure 4.11.

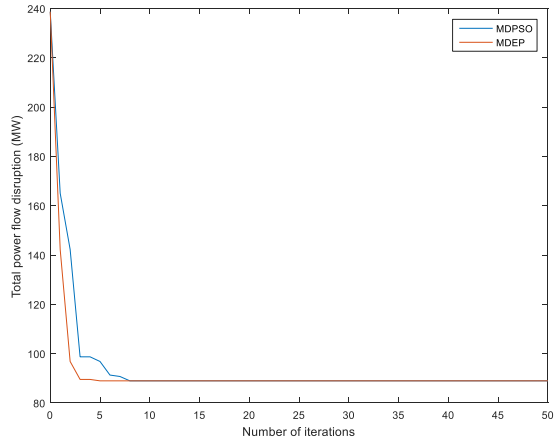


Figure 4.11. Convergence Curves for the MDEP and MDPSO Algorithms for Case Study 2

It is apparent that the MDEP algorithm converged faster compared with the MDPSO algorithm. The performance of these algorithms was analyzed and the results are tabulated in Table 4.7.

Table 4.7. Comparison of the Performance between the MDEP and MDPSO Algorithms

Algorithm	No. of iterations required by the algorithm to reach convergence	Computational time (sec)
MDEP	5	321.878
MDPSO	8	519.715

It can be seen from Table 4.7 that the MDEP algorithm attained convergence on the 5th iteration whereas the MDPSO attained convergence on the 8th iteration. Moreover, the MDEP algorithm attained convergence within a shorter time, which is 321.878 sec compared to the MDPSO algorithm of 519.715 sec. Therefore, MDEP algorithm was the best algorithm for intentional islanding implementation.

4.3.2.3 Determination of the Optimal Intentional Islanding Strategy Using the MDEP Algorithm

For Case Study 2, the optimal intentional islanding strategy obtained from the MDEP algorithm produced two stand-alone islands with 14 and 16 buses in Island 1 and

Island 2, respectively. The optimal intentional islanding strategy for this case study was 6–9, 6–10, 4–12, and 24–25 and the corresponding total power flow disruption was 89.962 MW. The one-line diagram of the optimal intentional islanding strategy is shown in Figure 4.12 while the graph model of the islanded islands is given in Appendix A (Figure A.1).

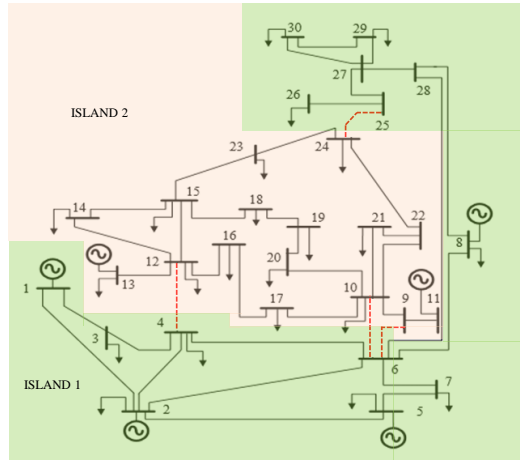


Figure 4.12. Optimal Intentional Islanding Strategy (Red Dashed Lines) for Case Study 2

Next, the power balance criterion was evaluated for each island. Table 4.8 shows the results for Island 1 and Island 2 before and after intentional islanding implementation.

Referring to Table 4.8, the total generated power, P_{gen} , was 300.998 MW and the total load, P_{load} , was 195.200 MW prior to intentional islanding in Island 1. There was a power surplus of 88.9690 MW in the pre-islanding condition. The slack bus was situated in Island 1 and therefore, load flow analysis was performed to obtain the system parameters for the island. The slack bus, G_1 reduced its generated power from 260.998 MW to 163.809 MW to fulfil the power balance criterion in the island, as shown in Table 4.8 referring to post-islanding column for Island 1. Since, the power balance criterion was met, the load shedding scheme was not executed. Island 1 was capable of operating as a balanced, stand-alone island.

Table 4.8. Results for Island 1 and Island 2 Before and After Intentional Islanding Implementation: Case Study 2

Island 1				
Buses in Island 1	Generator information		Active power (MW)	
	Generator	Max. limit (MW)	Pre-islanding	Post-islanding
			ΣP_{gen}	ΣP_{gen}
1–8, 25–30	G _{1*}	360	260.998	163.809
	G ₂	140	40.000	40.000
	G ₅	100	0.000	0.000
	G ₈	100	0.000	0.000
Total generated power, P_{gen} (MW)			300.998	203.809
Total load, P_{load} (MW)			195.200	195.200
Total power loss, P_{loss} (MW)			16.829	8.609
Total power imbalance, P_{imb} (MW)			88.969	0.000
Total amount of load to be shed, P_{shed} (MW)			—	—
Island 2				
Buses in Island 2	Generator information		Active power (MW)	
	Generator	Max. limit (MW)	Pre-islanding	Post-islanding
			ΣP_{gen}	ΣP_{gen}
9–24	G _{11*}	100	0.000	90.455
	G ₁₃	100	0.000	0.000
Total generated power, P_{gen} (MW)			0.000	90.455
Total load, P_{load} (MW)			88.200	88.200
Total power loss, P_{loss} (MW)			0.762	2.255
Total power imbalance, P_{imb} (MW)			–88.962	0.000
Total amount of load to be shed, P_{shed} (MW)			—	—

*slack bus

It can be seen from Table 4.8 that there was a power deficit of 88.962 MW prior to intentional islanding in Island 2. A new slack bus was assigned because there was no slack bus available in the island. Since both generator buses, G₁₁ and G₁₃ had the same maximum power limit, either one of these buses could be selected as the slack bus. In this case, generator bus, G₁₁ was selected as the slack bus. Referring to Table 4.8, the total generated power, P_{gen} , was 0.000 MW and the total load, P_{load} , was 88.200 MW before intentional islanding. Since P_{load} was less than the maximum power limit of generator bus, G₁₁, this generator was adjusted to compensate for the power deficit in this island. After performing load flow analysis, P_{gen} was found to be 90.455 MW in order to fulfil the total load. Finally, the power balance criterion in Island 2 was met and thus, the load shedding scheme was not executed. Island 2 could operate as a balanced, stand-alone island. Detail information on the load, P_{load} and generated power, P_{gen} connected to each bus for each island are shown in Appendix A (Table A.11).

After intentional islanding, the voltage profile was checked for each island to ensure that there were no voltage violations. The voltage of each bus for all islands was determined to be within the allowable voltage limits, as shown in Appendix A (Table A.12). Next, transmission line power flow analysis was performed for both islands to ensure that there were no violations in the transmission line capacity. It was found that the power flow in each transmission line for these islands was less than the transmission line capacity limit. The results of transmission line power flow analysis for Case Study 2 are provided in Appendix A (Table A.13).

4.3.3 Case Study 3

For Case Study 3, a different set of coherent groups of generators was investigated using the IEEE 30-bus test system in order to determine the optimal intentional islanding strategy. This case study was carried out based on previously published works reported in [9], [11], [80]. The system was partitioned into three islands based on the coherent groups of generators: $G_1 = \{1, 2, 5, 13\}$, $G_2 = \{8\}$, and $G_3 = \{11\}$.

4.3.3.1 Determination of the Initial Intentional Islanding Solution

The graph model of the initial solution of intentional islanding is shown with red lines for the IEEE 30-bus test system (Case Study 3) and the corresponding total power flow disruption, P_{disrup} , are shown in Figure 4.13 and Table 4.9, respectively.

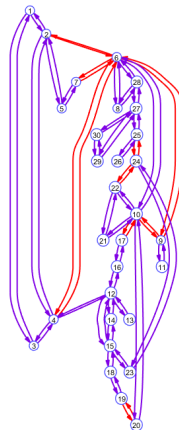


Figure 4.13. Graph Model of the Initial Intentional Islanding Solution (Red Lines) for Case Study 3

Table 4.9. Initial Intentional Islanding Solution for Case Study 3

Initial intentional islanding solution	Total power flow disruption, P_{disrup} (MW)
2-6, 4-6, 6-7, 6-9, 9-10, 19-20, 10-17, 22-24, 24-25	244.027

It can be seen from Table 4.9 that the initial intentional islanding solution obtained from the graph theory approach consisted of nine cutsets, producing a total power flow disruption, P_{disrup} , of 244.027 MW. This initial solution was used to facilitate the MDEP and MDPSO algorithms in determining the optimal intentional islanding strategy.

4.3.3.2 Evaluation of the MDEP and MDPSO Algorithms

The MDEP and MDPSO algorithms were then analyzed using the IEEE 30-bus test system. As in the previous case studies, both of these algorithms provided the same optimal intentional islanding strategy with a total power flow disruption, P_{disrup} , of 199.283 MW. The results obtained were compared with those of previously published works [9], [11], [80] as shown in Table 4.10. The proposed MDEP and MDPSO algorithms were capable of finding a better optimal intentional islanding strategy compared with the OBDD [80], BPSO [11], and modified ABC [9] algorithms.

Table 4.10. Comparison of the Optimal Intentional Islanding Strategies for Case Study 3

Algorithm	Optimal intentional islanding strategy	$\sum P_{disrup}$ (MW)
BPSO [11], OBDD [80]	2-6, 4-6, 6-7, 6-9, 6-28, 10-17, 10-22, 19-20, 21-22, 23-24	239.404
Modified ABC [9]	2-6, 4-6, 5-7, 6-9, 9-10, 16-17, 18-19, 23-24	209.828
MDPSO	2-6, 4-6, 5-7, 6-9, 6-10, 16-17, 18-19, 23-24, 24-25	199.283
MDEP	2-6, 4-6, 5-7, 6-9, 6-10, 16-17, 18-19, 23-24, 24-25	199.283

Since the MDEP and MDPSO algorithms produced the same optimal intentional islanding strategy, the best algorithm was chosen based on the convergence curve and computational time. Both of these algorithms reached convergence within 50 iterations, as shown in Figure 4.14.

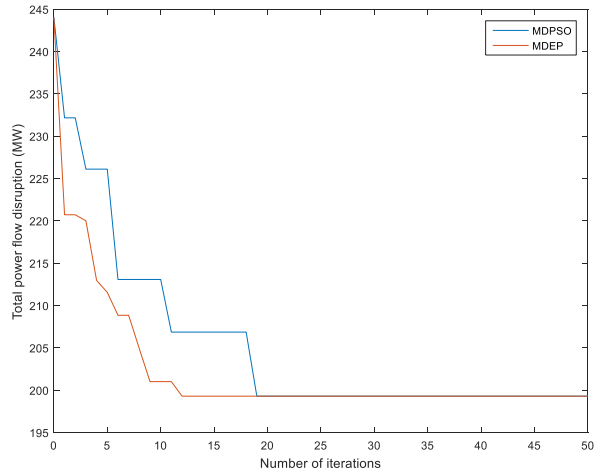


Figure 4.14. Convergence Curves for the MDEP and MDPSO Algorithms for Case Study 3

Although both of the proposed algorithms produced the same optimal intentional islanding strategy, the MDEP algorithm converged faster compared with the MDPSO algorithm, as shown in Figure 4.14. The detailed comparisons of these techniques are as shown in Table 4.11.

Table 4.11. Comparison of the Performance Between the MDEP and MDPSO Algorithms

Algorithm	No. of iterations required by the algorithm to reach convergence	Computational time (sec)
MDEP	12	1115.417
MDPSO	19	1777.961

It can be observed from Table 4.11 that the MDEP algorithm achieved convergence on the 12th iteration whereas the MDPSO algorithm was slightly slower, where convergence was achieved on the 19th iteration. In addition, the MDEP algorithm achieved convergence within a shorter time of (1115.417 sec) compared with the MDPSO algorithm (1777.961 sec). Hence, the MDEP algorithm was selected as the best algorithm for intentional islanding implementation.

4.3.3.3 Determination of the Optimal Intentional Islanding Strategy Using the MDEP Algorithm

The optimal intentional islanding strategy obtained from the MDEP algorithm produced three stand-alone islands with 12, 9, and 9 buses in Island 1, Island 2, and Island 3 respectively. The optimal intentional islanding strategy for this case study was 2–6, 4–6, 5–7, 6–9, 6–10, 16–17, 18–19, 23–24, and 24–25, resulting in a total power flow disruption of 199.283 MW. The one-line diagram for the optimal intentional islanding strategy is shown in Figure 4.15. The graph model of the islanded islands is given in Appendix A (Figure A.2).

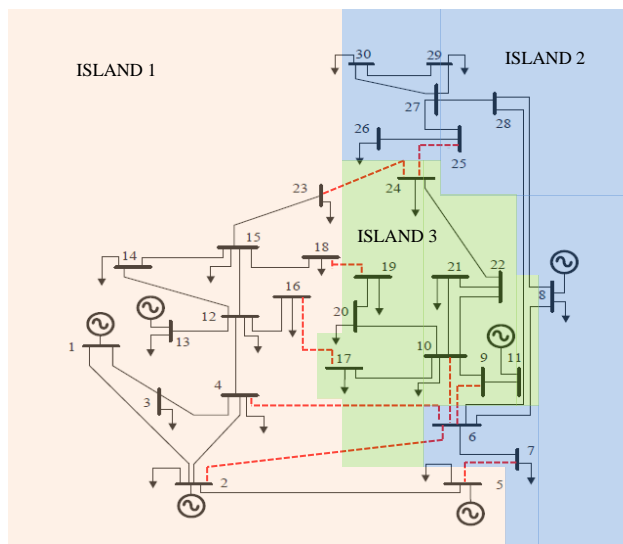


Figure 4.15. Optimal Intentional Islanding Strategy (Red Dashed Lines) for Case Study 3

Next, the power balance criterion was assessed for each island. Table 4.12 shows the results for Islands 1–3 before and after intentional islanding implementation.

Table 4.12. Results for Islands 1–3 Before and After Intentional Islanding Implementation: Case Study 3

Island 1				
Buses in Island 1	Generator information		Active power (MW)	
	Generator	Max. limit (MW)	Pre-islanding	Post-islanding
1–5, 12–16, 18, 23	G _{1*}	360	260.998	128.075
	G ₂	140	40.000	40.000
	G ₅	100	0.000	0.000
	G ₁₃	100	0.000	0.000
Total generated power, P_{gen} (MW)			300.998	168.075
Total load, P_{load} (MW)			161.400	161.400
Total power loss, P_{loss} (MW)			13.566	6.675
Total power imbalance, P_{imb} (MW)			126.032	0.000
Total amount of load to be shed, P_{shed} (MW)			—	—
Island 2				
Buses in Island 2	Generator information		Active power (MW)	
	Generator	Max. limit (MW)	Pre-islanding	Post-islanding
6–8, 25–30	G _{8*}	100	0.000	69.996
Total generated power, P_{gen} (MW)			0.000	69.996
Total load, P_{load} (MW)			69.300	69.300
Total power loss, P_{loss} (MW)			0.89	0.696
Total power imbalance, P_{imb} (MW)			-70.190	0.000
Total amount of load to be shed, P_{shed} (MW)			—	—
Island 3				
Buses in Island 3	Generator information		Active power (MW)	
	Generator	Max. limit (MW)	Pre-islanding	Post-islanding
9–11, 17, 19–22, 24	G _{11*}	100	0.000	53.189
Total generated power, P_{gen} (MW)			0.000	53.189
Total load, P_{load} (MW)			52.700	52.700
Total power loss, P_{loss} (MW)			0.325	0.489
Total power imbalance, P_{imb} (MW)			-53.025	0.000
Total amount of load to be shed, P_{shed} (MW)			—	—

*slack bus

In Island 1, the total generated power, P_{gen} , the total load, P_{load} , and the total power imbalance, P_{imb} , were 300.998 MW, 161.400 MW, and 126.032 MW, respectively, before intentional islanding. The slack bus was located in Island 1 and load flow analysis was carried out to obtain the system parameters in the island. It was found that the slack bus, G₁, reduced its generated power from 260.998 MW to 128.075 MW to fulfil the power balance criterion for the island, as shown in Table 4.12 referring to post-islanding column for Island 1. Because the power balance criterion

was met, the load shedding scheme was not executed. Island 1 could operate as a balanced, stand-alone island.

In Island 2, there was a power deficit of 70.190 MW in the pre-islanding condition. Since there was no slack bus, the only generator bus available in this island, G_8 , was chosen as the slack bus to perform the load flow analysis. It can be seen from Table 4.12 referring to post-islanding column for Island 2 that the value of P_{gen} for G_8 was 69.996 MW, which was slightly higher than that for P_{load} with 69.300 MW and P_{losses} of 0.696MW. Thus, the load shedding scheme was not executed and the island could operate as a balanced, stand-alone island.

A similar case can be observed for Island 3, where there was a power deficit of 53.025 MW in the pre-islanding condition. Furthermore, there was no slack bus available in Island 3. Therefore, generator bus, G_{11} was chosen as the slack bus because it was the only generator available in the island. Based on the load flow analysis, P_{gen} was found to be 53.189 MW in order to cater for the P_{load} value of 52.700 MW including P_{losses} of 0.489MW. The power balance criterion in Island 3 was met, as shown in Table 4.12 with respect to post-islanding column for Island 3. Therefore, the load shedding scheme was not executed and the island was capable of operating as a balanced, stand-alone island. Detail information on the load, P_{load} and generated power, P_{gen} connected to each bus for each island are shown in Appendix A (Table A.14).

Next, the voltage of each bus for all islands was checked, as in the previous case studies. The voltage of each bus for all islands was found to be within the allowable voltage limits, as shown in Appendix A (Table A.15). The power system was also checked to ensure that there were no violations in the transmission line capacity. It was found that the power flow in each transmission line for Islands 1–3 was less than transmission line capacity limit. The results of the transmission line power flow analysis are presented in Appendix A (Table A.16).

4.4 Analysis of the IEEE 39-Bus Test System

Similar analyzes were performed on the IEEE 39-bus test system and the results are presented in this section. The graph model of the original IEEE 39-bus test system obtained from the graph theory approach is shown in Figure 4.16.

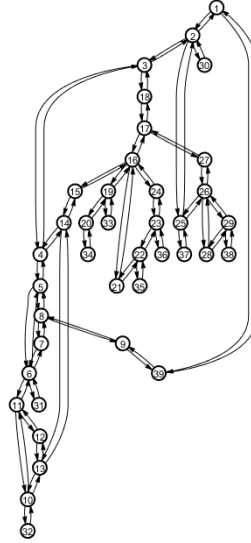


Figure 4.16. Representation of the Original IEEE 39-Bus Test System as a Graph Model

4.4.1 Case Study 4

For Case Study 4, the optimal intentional islanding strategy was analyzed based on previously published works [9], [11]. In this case study, the system was partitioned into two islands based on the coherent groups of generators: $G_1 = \{30, 31, 32, 37, 38, 39\}$ and $G_2 = \{33, 34, 35, 36\}$.

4.4.1.1 Determination of the Initial Intentional Islanding Solution

Similar to the previous case studies, the initial intentional islanding solution was first determined using the graph theory approach. This approach determines the total number of transmission lines that needs to be disconnected in order to form the desired number of islands based on the coherent groups of generators. The graph

model of the initial intentional islanding solution (red lines) for the IEEE 39-bus test system and the corresponding total power flow disruption, P_{disrup} , are shown in Figure 4.17 and Table 4.13, respectively.

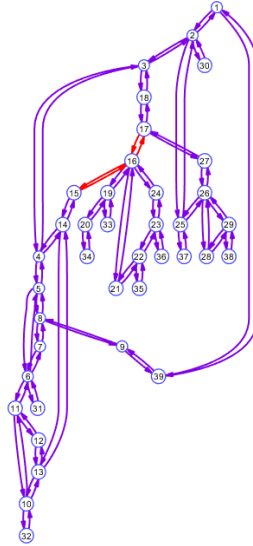


Figure 4.17. Graph Model of the Initial Intentional Islanding Solution (Red Lines) for Case Study 4

Table 4.13. Initial Intentional Islanding Solution for Case Study 4

Initial intentional islanding solution	Total power flow disruption, P_{disrup} (MW)
15–16, 16–17	493.3603

It can be seen from Table 4.13 that the initial intentional islanding solution consisted of two cutsets, producing a total power flow disruption, P_{disrup} , of 493.3603 MW. This indicates that the graph theory approach is capable of reducing the initial search space of all possible transmission lines ($2^{46}-1 \approx 7.0369 \times 10^{13}$) to two lines as the initial solution. This initial solution was used to aid the MDEP and MDPSO algorithms in determining the optimal intentional islanding strategy.

4.4.1.2 Evaluation of the MDEP and MDPSO Algorithms

The MDEP and MDPSO algorithms were analyzed using the IEEE 39-bus test system and the results are tabulated in Table 4.14. It can be observed that both of the

proposed algorithms were able to determine the same optimal intentional islanding strategy with three cutsets, producing a total power flow disruption, P_{disrup} , of 115.867 MW. The results were compared with those of [11] and [9]. It can be deduced from the results that the MDEP and MDPSO algorithms were capable of obtaining a better optimal intentional islanding strategy with a significantly lower total power flow disruption compared with the BPSO [11] and modified ABC [9] algorithms.

Table 4.14. Comparison of the Optimal Intentional Islanding Strategies for Case Study 4

Algorithm	Optimal intentional islanding strategy	$\sum P_{disrup}$ (MW)
BPSO [11]	3–18, 15–16, 17–27	334.541
Modified ABC [9]	14–15, 16–17	274.686
MDPSO	3–18, 14–15, 17–27	115.867
MDEP	3–18, 14–15, 17–27	115.867

Since both of the proposed algorithms yielded the same optimal intentional islanding strategies for Case Study 4, the best algorithm for intentional islanding was selected based on the convergence curve and computational time. The maximum number of iterations was set at 50 and it can be observed from Figure 4.18 that the MDEP and MDPSO algorithms reached convergence within 50 iterations.

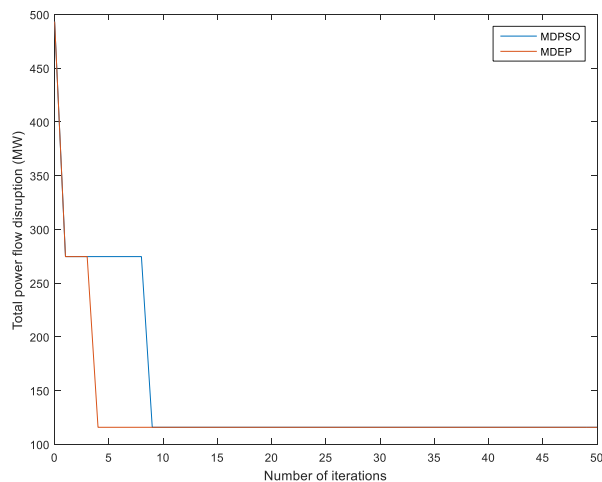


Figure 4.18. Convergence Curves for the MDEP and MDPSO Algorithms for Case Study 4

It is evident that the MDEP algorithm converged faster compared with the MDPSO algorithm. The performance of these algorithms was analyzed and the results are tabulated in Table 4.15.

Table 4.15. Comparison of the Performance Between the MDEP and MDPSO Algorithms

Algorithm	No. of iterations required by the algorithm to reach convergence	Computational time (sec)
MDEP	4	169.757
MDPSO	9	386.446

It can be observed from Table 4.15 that the MDEP algorithm attained convergence on the 4th iteration while the MDPSO algorithm attained convergence on the 9th iteration. In addition, the MDEP algorithm consumed less computational time to attain convergence (169.757 sec) compared with the MDPSO algorithm (386.446 sec). Thus, the MDEP algorithm was selected as the best algorithm for intentional islanding implementation.

4.4.1.3 Determination of the Optimal Intentional Islanding Strategy Using the MDEP Algorithm

For Case Study 4, the optimal islanding strategy obtained from the MDEP algorithm produced two stand-alone islands with 25 and 14 buses in Island 1 and Island 2, respectively. The optimal intentional islanding strategy (cutsets) for this case study was 3–18, 14–15, and 17–27, with a total power flow disruption of 115.867 MW. The one-line diagram of the islanding strategy is shown in Figure 4.19 while the graph model of the islanded islands is given in Appendix A (Figure A.3).

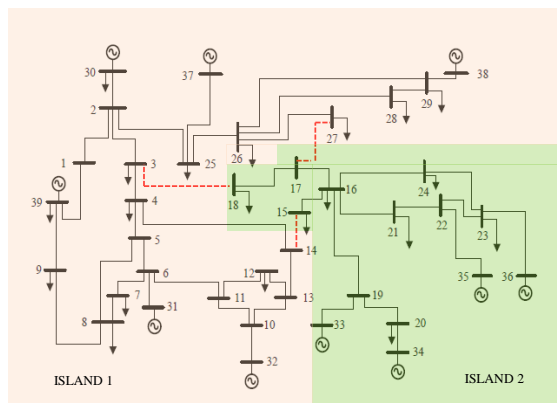


Figure 4.19. Optimal Intentional Islanding Strategy (Red Dashed Lines) for Case Study 4

As in the previous case studies, the two stand-alone islands formed after intentional islanding must be balanced in terms of the total generated power and total load. Thus, the power balance criterion was evaluated for each island. Table 4.16 shows the results for Island 1 and Island 2 before and after intentional islanding implementation.

Based on the results in Table 4.16, there was a power deficit of 114.313 MW prior to intentional islanding in Island 1. Because the slack bus was situated in Island 1, load flow analysis was carried out to obtain the system parameters in this island. It was found that the slack bus, G_{31} , was not able to compensate for the power deficit because the maximum power limit for generator bus, G_{31} was 646 MW. Hence, all of the generator buses shared the loads in order to overcome this problem. The generated power increased for all generators, as shown in Table 4.16 (post-islanding column for Island 1). Finally, the power balance criterion was met for Island 1 and load shedding scheme was not executed. Island 1 could operate as a balanced, stand-alone island.

In Island 2, there was a power surplus of 14.558 MW in the pre-islanding condition. There was no slack bus available on this island and therefore, generator bus, G_{31} was selected as the slack bus because it had the highest maximum power limit (687 MW). Load flow analysis was performed upon selection of the slack bus. The results showed that the slack bus reduced its generated power to overcome the power

surplus problem in Island 2. Finally, the power balance criterion was met ($P_{imb} = 0.000$ MW), as shown in Table 4.16 (post-islanding column for Island 2). The load shedding scheme was not executed and the island could operate as a balanced, stand-alone island. Detail information on the load, P_{load} and generated power, P_{gen} connected to each bus for each island are presented in Appendix A (Table A.17).

Table 4.16. Results for Island 1 and Island 2 Before and After Intentional Islanding Implementation: Case Study 4

Island 1				
Buses in Island 1	Generator information		Active power (MW)	
	Generator	Max. limit (MW)	Pre-islanding ΣP_{gen}	Post-islanding ΣP_{gen}
1–14, 25–32, 37–39	G ₃₀	1040	250.000	269.052
	G _{31*}	646	579.539	601.060
	G ₃₂	725	650.000	669.052
	G ₃₇	564	540.000	559.052
	G ₃₈	865	830.000	849.052
	G ₃₉	1100	1000.000	1019.052
Total generated power, P_{gen} (MW)			3849.539	3966.320
Total load, P_{load} (MW)			3937.130	3937.130
Total power loss, P_{loss} (MW)			26.722	29.190
Total power imbalance, P_{imb} (MW)			-114.313	0.000
Total amount of load to be shed, P_{shed} (MW)			—	—
Island 2				
Buses in Island 2	Generator information		Active power (MW)	
	Generator	Max. limit (MW)	Pre-islanding ΣP_{gen}	Post-islanding ΣP_{gen}
15–24, 33–36	G ₃₃	652	632.000	632.000
	G ₃₄	508	508.000	508.000
	G _{35*}	687	650.000	635.223
	G ₃₆	580	560.000	560.000
Total generated power, P_{gen} (MW)			2350.000	2335.223
Total load, P_{load} (MW)			2317.100	2317.100
Total power loss, P_{loss} (MW)			18.342	18.123
Total power imbalance, P_{imb} (MW)			14.558	0.000
Total amount of load to be shed, P_{shed} (MW)			—	—

*slack bus

The steps performed in previous case studies were also performed in this case study. The voltage of each bus for all islands was checked to ensure that there were no voltage violations. The voltage of each bus for all islands was determined to be within the allowable voltage limits, as shown in Appendix A (Table A.18). The power system was also checked to determine if there were violations in the transmission line capacity. The power flow in each transmission line for Island 1 and Island 2 was

less than the transmission line capacity limit. The results of the transmission line power flow analysis for Case Study 4 are presented in Appendix A (Table A.19).

4.4.2 Case Study 5

The optimal intentional islanding strategy for Case Study 5 was analyzed based on previously published works [9], [11]. In this case study, the system was partitioned into three islands based on the coherent groups of generators: $G_1 = \{30, 37, 38\}$, $G_2 = \{31, 32, 39\}$, and $G_3 = \{33, 34, 35, 36\}$.

4.4.2.1 Determination of the Initial Intentional Islanding Solution

The graph model of the initial intentional islanding solution (red lines) for the IEEE 39-bus test system (Case Study 5) is shown in Figure 4.20. The corresponding total power flow disruption, P_{disrup} , is presented in Table 4.17.

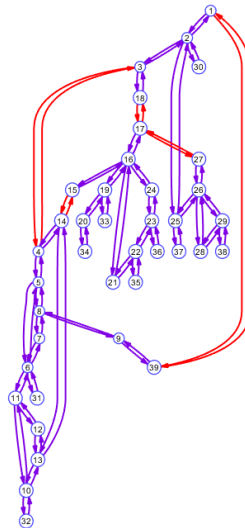


Figure 4.20. Graph Model of the Initial Intentional Islanding Solution (Red Lines) for Case Study 5

Table 4.17. Initial Intentional Islanding Solution for Case Study 5

Initial intentional islanding solution	Total power flow disruption, P_{disrup} (MW)
1–39, 3–4, 14–15, 17–18, 17–27	386.232

It can be seen from Table 4.17 that the initial intentional islanding solution obtained from the graph theory approach consisted of five cutsets, resulting in a total power flow disruption, P_{disrup} , of 386.232 MW. This initial solution was used to facilitate the MDEP and MDPSO algorithms in determining the optimal intentional islanding strategy.

4.4.2.2 Evaluation of the MDEP and MDPSO Algorithms

The developed MDEP and MDPSO algorithms were analyzed using the IEEE 39-bus test system. As in the previous case studies, both of these algorithms produced the same optimal intentional islanding strategy with a total power flow disruption, P_{disrup} , of 227.951 MW. The results were compared with those of previously published works [9], [11]. It is apparent that the proposed islanding algorithms were capable of determining a better islanding strategy with a significantly lower total power flow disruption compared with the BPSO [11] and modified ABC [9] algorithms, as shown in Table 4.18.

Table 4.18. Comparison of the Optimal Intentional Islanding Strategies for Case Study 5

Algorithm	Optimal intentional islanding strategy	ΣP_{disrup} (MW)
BPSO [11]	1-39, 3-4, 15-16, 16-17	605.444
Modified ABC [9]	1-39, 3-4, 14-15, 16-17	386.77
MDPSO	1-39, 3-4, 3-18, 14-15, 17-27	227.951
MDEP	1-39, 3-4, 3-18, 14-15, 17-27	227.951

Next, the best algorithm was determined based on the convergence curve and computational time. It can be seen from Figure 4.21 that the MDEP and MDPSO algorithms reached convergence within 50 iterations.

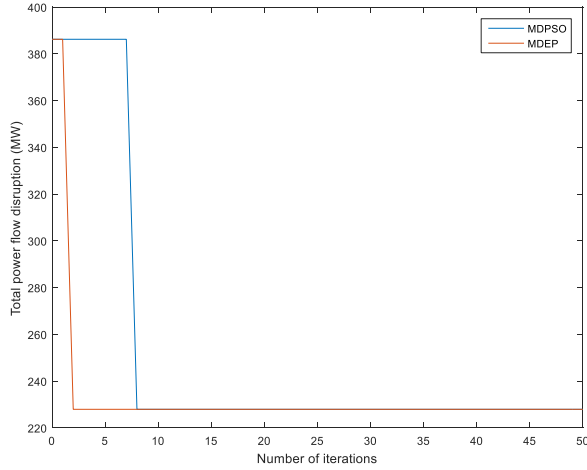


Figure 4.21. Convergence Curves for the MDEP and MDPSO Algorithms for Case Study 5

It is evident that the MDEP algorithm converged faster compared with the MDPSO algorithm. The performance of these algorithms was analyzed and the results are summarized in Table 4.19.

Table 4.19. Comparison of the Performance Between the MDEP and MDPSO Algorithms

Algorithm	No. of iterations required by the algorithm to reach convergence	Computational time (sec)
MDEP	2	150.081
MDPSO	8	612.634

Referring to Table 4.19, the MDEP algorithm achieved convergence on the 2nd iteration whereas the MDPSO achieved convergence only on the 8th iteration. Furthermore, the MDEP algorithm achieved convergence within a shorter time (150.081 sec) compared with the MDPSO algorithm (612.634 sec). For these reasons, the MDEP algorithm was the best algorithm to implement intentional islanding for Case Study 5.

4.4.2.3 Determination of the Optimal Intentional Islanding Strategy Using the MDEP Algorithm

The optimal intentional islanding strategy determined from the proposed MDEP algorithm produced two stand-alone islands with 11, 14, and 14 buses in Island 1, Island 2, and Island 3, respectively. The optimal intentional islanding strategy for this case was 1–39, 3–4, 3–18, 14–15 and 17–27, with a total power flow disruption of 227.951 MW. The one-line diagram of the optimal intentional islanding strategy is shown in Figure 4.22. The graph model of the islanded islands is shown in Appendix A (Figure A.4).

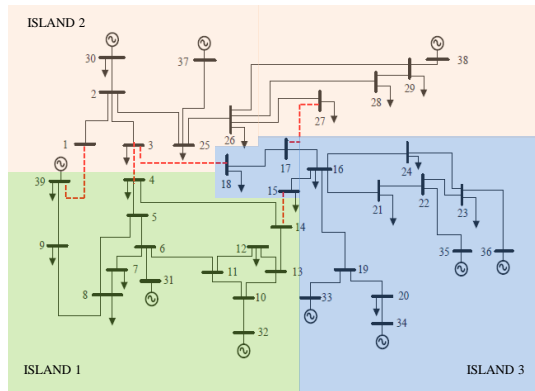


Figure 4.22. Optimal Intentional Islanding Strategy (Red Dashed Lines) for Case Study 5

Next, the power balance criterion was evaluated for each island. Table 4.20 shows the results for Islands 1–3 before and after intentional islanding implementation.

Referring to Table 4.20, there was a power deficit of 161.884 MW prior to intentional islanding in Island 1. The slack bus was located in this island and therefore, load flow analysis was carried out to obtain the system parameters. It was found that the slack bus, G_{31} , was not able to compensate for the power deficit in the island because the maximum power limit for slack bus, G_{31} was 646 MW. Thus, all of the generators shared the loads equally to compensate for the power deficit in Island 1. The power generated by each generator increased, as shown in Table 4.20 (post-islanding column for Island 1). The power balance criterion in Island 1 was met

and therefore, the load shedding scheme was not executed. Island 1 was capable of operating as a balanced, stand-alone island.

Table 4.20. Results for Islands 1–3 Before and After Intentional Islanding Implementation: Case Study 5

Island 1				
Buses in Island 1	Generator information		Active power (MW)	
			Pre-islanding	Post-islanding
	Generator	Max. limit (MW)	ΣP_{gen}	ΣP_{gen}
4–14, 31–32, 39	G _{31*}	646	579.539	635.807
	G ₃₂	725	650.000	703.961
	G ₃₉	1100	1000.000	1053.961
Total generated power, P_{gen} (MW)			2229.539	2393.729
Total load, P_{load} (MW)			2384.030	2384.000
Total power loss, P_{loss} (MW)			7.393	9.729
Total power imbalance, P_{imb} (MW)			-161.884	0.000
Total amount of load to be shed, P_{shed} (MW)			—	—
Island 2				
Buses in Island 2	Generator information		Active power (MW)	
			Pre-islanding	Post-islanding
	Generator	Max. limit (MW)	ΣP_{gen}	ΣP_{gen}
1–3, 25–30, 37–38	G _{30*}	1040	250.000	200.675
	G ₃₇	564	540.000	540.000
	G ₃₈	865	830.000	830.000
Total generated power, P_{gen} (MW)			1620.000	1570.675
Total load, P_{load} (MW)			1553.100	1553.100
Total power loss, P_{loss} (MW)			19.795	17.575
Total power imbalance, P_{imb} (MW)			47.105	0.000
Total amount of load to be shed, P_{shed} (MW)			—	—
Island 3				
Buses in Island 3	Generator information		Active power (MW)	
			Pre-islanding	Post-islanding
	Generator	Max. limit (MW)	ΣP_{gen}	ΣP_{gen}
15–24, 33–36	G ₃₃	652	632.000	632.000
	G ₃₄	508	508.000	508.000
	G _{35*}	687	650.000	635.223
	G ₃₆	580	560.000	560.000
Total generated power, P_{gen} (MW)			2350.000	2335.223
Total load, P_{load} (MW)			2317.100	2317.100
Total power loss, P_{loss} (MW)			18.337	18.123
Total power imbalance, P_{imb} (MW)			14.563	0.000
Total amount of load to be shed, P_{shed} (MW)			—	—

*slack bus

In contrast, it can be seen from Table 4.20 that there was a power surplus of 47.105 MW in Island 2 in the pre-islanding condition. There was no slack bus available in this island and thus, generator bus, G₃₀ was selected as the slack bus to perform the

load flow analysis because it had the highest maximum power limit of 1040 MW. The slack bus reduced its generated power from 250.000 MW to 200.675 MW to compensate for the power surplus in Island 2. Finally, the power balance criterion was met ($P_{imb} = 0.000$ MW), as shown in Table 4.20 (post-islanding column for Island 2). Thus, the load shedding scheme was not executed and the island could operate as a balanced, stand-alone island.

Likewise, there was a small power surplus of 14.563 MW in Island 3 in the pre-islanding condition. Similar to Island 2, there was no slack bus available in this island. Hence, Generator Bus G_{35} was selected as the slack bus to perform the load flow analysis. The slack bus reduced its generated power from 650.000 MW to 635.223 MW to compensate for the power surplus in Island 3. The power balance criterion in Island 3 was met ($P_{imb} = 0.000$ MW), as shown in Table 4.20 (post-islanding column for Island 3). Thus, the load shedding scheme was not executed and the island could operate as a balanced, stand-alone island. Detail information on the load, P_{load} and generated power, P_{gen} connected to each bus for each island are presented in Appendix A (Table A.20).

Next, the voltage of each bus was checked for all islands, as in the previous case studies. The voltage of each bus for Islands 1–3 was obtained to be within the allowable voltage limits, as shown in Appendix A (Table A.21). Following this, transmission line power flow analysis was performed for all three islands to ascertain that there were no violations in the transmission line capacity. The power flow in each transmission line for all islands was found to be less than the transmission line capacity limit. The results of the transmission line power flow analysis for Case Study 5 are given in Appendix A (Table A.22).

4.4.3 Case Study 6

For Case Study 6, the optimal intentional islanding strategy was analyzed using the modified IEEE 39-bus test system as utilized in [9], [86]. In this case study, the system was partitioned into four islands based on the coherent groups of generators: $G_1 = \{30, 31, 37\}$, $G_2 = \{33, 35, 36\}$, $G_3 = \{34, 38\}$, and $G_4 = \{32, 39\}$. The graph model of the modified IEEE 39-bus test system is shown in Figure 4.23.

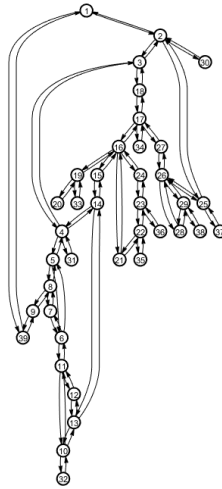


Figure 4.23. Representation of the Modified IEEE 39-Bus Test System as a Graph Model

4.4.3.1 Determination of the Initial Intentional Islanding Solution

In this case study, the graph model of the initial intentional islanding solution (red lines) for the IEEE 39-bus test system and the corresponding total power flow disruption, P_{disrup} , are shown in Figure 4.24 and Table 4.21, respectively.

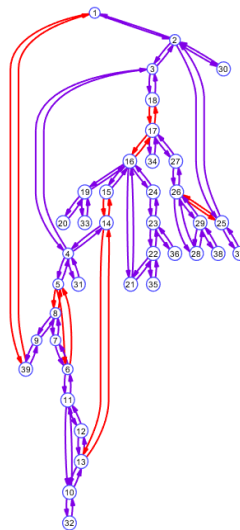


Figure 4.24. Graph Model of the Initial Intentional Islanding Solution (Red Lines) for Case Study 6

Table 4.21. Initial Intentional Islanding Solution for Case Study 6

Initial intentional islanding solution	Total power flow disruption, P_{disrup} (MW)
1-39, 5-6, 5-8, 13-14, 14-15, 16-17, 17-18, 25-26	1343.832

It can be seen from Table 4.21 that the initial intentional islanding solution with eight cutsets obtained from the graph theory approach produced a total power flow disruption, P_{disrup} , of 1343.832 MW. This initial solution was used to aid the MDEP and MDPSO algorithms in determining the optimal intentional islanding strategy.

4.4.3.2 Evaluation of the MDEP and MDPSO Algorithms

The MDEP and MDPSO algorithms were then analyzed using the modified IEEE 39-bus test system. Both of these algorithms produced the same optimal intentional islanding strategy with a total power flow disruption, P_{disrup} , of 897.197 MW, as shown in Table 4.22. The results were compared with those of previously published works [9], [86]. In general, the proposed islanding algorithms were able to determine a better optimal intentional islanding strategy compared with the ant mechanism [86] and similar islanding strategy with the modified ABC [9] algorithm, as shown in Table 4.22. The identical optimal intentional islanding strategies obtained from the proposed algorithms and the modified ABC algorithm [9] are likely because these solutions are the most optimal solution that can be obtained for this case study.

Table 4.22. Comparison of the Optimal Intentional Islanding Strategies for Case Study 6

Algorithm	Optimal intentional islanding strategy	ΣP_{disrup} (MW)
Ant mechanism [86]	1- 2, 4-5, 10-13, 12-13, 15-16, 16-17, 17-18, 25-26	1426.024
Modified ABC [9]	1-39, 3-18, 4-5, 4-14, 14-15, 16-17, 25-26	897.197
MDPSO	1-39, 3-18, 4-5, 4-14, 14-15, 16-17, 25-26	897.197
MDEP	1-39, 3-18, 4-5, 4-14, 14-15, 16-17, 25-26	897.197

The best algorithm was selected based on the convergence curve and computational time. It can be seen from Figure 4.25 that the MDEP and MDPSO algorithms reached convergence within 50 iterations.

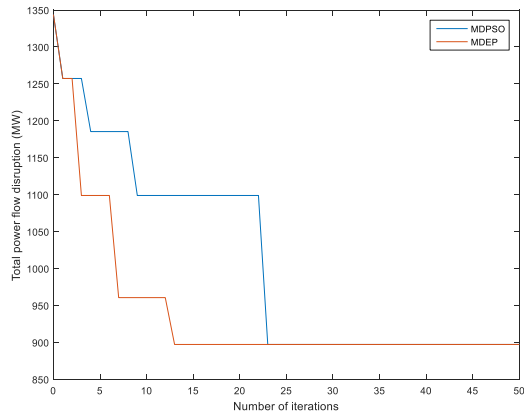


Figure 4.25. Convergence Curves for the MDEP and MDPSO Algorithms for Case Study 6

Although both of the proposed algorithms produced the same optimal intentional islanding strategy, the MDEP algorithm converged faster compared with the MDPSO algorithm, as shown in Figure 4.25. The performance of these algorithms was analyzed and the results are tabulated in Table 4.23.

Table 4.23. Comparison of the Performance Between the MDEP and MDPSO Algorithms

Algorithm	No. of iterations required by the algorithm to reach convergence	Computational time (sec)
MDEP	13	1471.993
MDPSO	24	2791.047

The results showed that the MDEP algorithm attained convergence on the 13th iteration whereas the MDPSO algorithm attained convergence on the 24th iteration. Moreover, the MDEP algorithm consumed less computational time to attain convergence (1471.993 sec) compared with the MDPSO algorithm (2791.047 sec). Based on these results, the MDEP algorithm was selected as the best algorithm for intentional islanding implementation.

4.4.3.3 Determination of the Optimal Intentional Islanding Strategy Using the MDEP Algorithm

In Case Study 6, the optimal intentional islanding strategy obtained from the proposed MDEP algorithm produced four stand-alone islands with eight, 12, 11, and eight buses in Island 1, Island 2, Island 3, and Island 4, respectively. The optimal intentional islanding strategy for this case study was 1–39, 3–18, 4–5, 4–14, 14–15, 16–17, and 25–26, producing a total power flow disruption of 897.197 MW. The one-line diagram of the optimal intentional islanding strategy is shown in Figure 4.26. The graph model of the islanded islands is shown in Appendix A (Figure A.5).

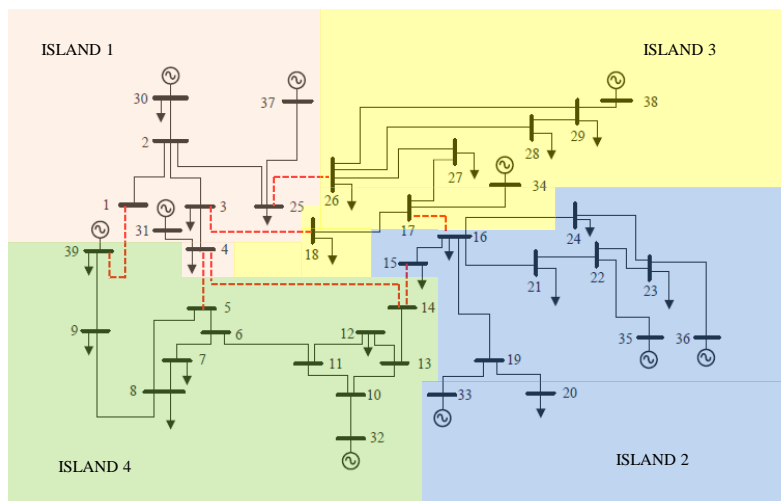


Figure 4.26. Optimal Intentional Islanding Strategy (Red Dashed Lines) for Case Study 6

Next, the power balance criterion was evaluated for each island to ascertain that the total generated power and total load were balanced. Table 4.24 shows the results for Islands 1–4 before and after intentional islanding implementation.

Table 4.24. Results for Islands 1–4 Before and After Intentional Islanding Implementation: Case Study 6

Island 1				
Buses in Island 1	Generator information		Active power (MW)	
			Pre-islanding	Post-islanding
	Generator	Max. limit (MW)	ΣP_{gen}	ΣP_{gen}
1–4, 25, 30, 31, 37	G ₃₀	1040	250.000	250.000
	G _{31*}	646	579.539	374.948
	G ₃₇	564	540.000	540.000
Total generated power, P_{gen} (MW)			1369.539	1164.948
Total load, P_{load} (MW)			1152.800	1152.800
Total power loss, P_{loss} (MW)			10.117	12.148
Total power imbalance, P_{imb} (MW)			206.622	0.000
Total amount of load to be shed, P_{shed} (MW)			—	—
Island 2				
Buses in Island 2	Generator information		Active power (MW)	
			Pre-islanding	Post-islanding
	Generator	Max. limit (MW)	ΣP_{gen}	ΣP_{gen}
15–16, 19–24, 33, 35–36	G ₃₃	652	632.000	652.000
	G _{35*}	687	650.000	671.497
	G ₃₆	580	560.000	580.000
Total generated power, P_{gen} (MW)			1842.000	1903.497
Total load, P_{load} (MW)			2159.100	1885.100
Total power loss, P_{loss} (MW)			15.142	18.397
Total power imbalance, P_{imb} (MW)			–332.242	0.000
Total amount of load to be shed, P_{shed} (MW)			—	274.000
Island 3				
Buses in Island 3	Generator information		Active power (MW)	
			Pre-islanding	Post-islanding
	Generator	Max. limit (MW)	ΣP_{gen}	ΣP_{gen}
17–18, 26–29, 34, 38	G ₃₄	508	508.000	508.000
	G _{38*}	865	830.000	566.797
Total generated power, P_{gen} (MW)			1338.000	1074.797
Total load, P_{load} (MW)			1067.500	1067.500
Total power loss, P_{loss} (MW)			13.103	7.297
Total power imbalance, P_{imb} (MW)			257.397	0.000
Total amount of load shedding, P_{shed} (MW)			—	—
Island 4				
Buses in Island 4	Generator information		Active power (MW)	
			Pre-islanding	Post-islanding
	Generator	Max. limit (MW)	ΣP_{gen}	ΣP_{gen}
5–14, 32, 39	G ₃₂	725	650.000	725.000
	G _{39*}	1100	1000.000	925.355
Total generated power, P_{gen} (MW)			1650.000	1650.355
Total load, P_{load} (MW)			1874.830	1641.030
Total power loss, P_{loss} (MW)			5.397	9.325
Total power imbalance, P_{imb} (MW)			–230.227	0.000
Total amount of load to be shed, P_{shed} (MW)			—	233.800

*slack bus

It can be seen from Table 4.24 that there was a power surplus of 206.622 MW in Island 1 before intentional islanding. The slack bus was available in Island 1 and therefore, load flow analysis was carried out to obtain the system parameters. The slack bus, G_{31} , reduced its generated power to compensate for the power surplus in Island 1. The power balance criterion in Island 1 was met, as shown in Table 4.24 (post-islanding column for Island 1) and therefore, the load shedding scheme was not executed. Island 1 was balanced and it could operate as a stand-alone island.

In Island 2, there was a power deficit of 332.242 MW in the pre-islanding condition. There was no slack bus available in Island 2 and therefore, generator bus, G_{35} was selected as the slack bus because it had the highest maximum power limit of 687 MW. Load flow analysis was then performed. The slack bus, G_{35} , was unable to compensate for the high power deficit in the island because the value exceeded its maximum power limit. To overcome this problem, generator buses, G_{33} and G_{36} were operated at their maximum power limits. However, the generator buses were still unable to fulfil the total load. Hence, the MDEP-based load shedding scheme was executed, where the load at Bus 21 (274.000 MW) was shed to achieve load-generation balance in the island. This action is important to ensure successful intentional islanding implementation and produce a balanced, stand-alone island. The execution of the load shedding scheme enables the island to fulfil the power balance criterion, as shown in Table 4.24 (post-islanding column for Island 2).

In contrast, there was a power surplus of 257.397 MW in Island 3 in the pre-islanding condition. Similar to Island 2, a new slack bus needs to be assigned owing to the absence of a slack bus in this island. Generator bus, G_{38} was selected as the slack bus for the load flow analysis. The slack bus, G_{38} , reduced its generated power from 830.000 MW to 566.797 MW to compensate for the power surplus in Island 3. Finally, the power balance criterion was met ($P_{imb} = 0.000$ MW), as shown in Table 4.24 (post-islanding column for Island 3). Thus, the load shedding scheme was not executed and the island could operate as a balanced, stand-alone island.

In Island 4, there was a power deficit of 230.227 MW prior to intentional islanding. Since there was no slack bus available in this island, generator bus, G_{39} was selected

as the slack bus and load flow analysis was then carried out to obtain the system parameters in the island. It was found that the slack bus, G_{39} , was not able to compensate for the high power deficit in the island because the value exceeded its maximum power limit. To address this problem, generator bus, G_{32} was operated at its maximum power limit. However, the generator was still unable to fulfil the total load. Similar to Island 2, the MDEP-based load shedding scheme was executed, where the load at Bus 7 (233.800 MW) was shed to attain load-generation balance in the island. By executing the load shedding scheme, a balanced, stand-alone island was attained. Detail information on the load, P_{load} and generated power, P_{gen} connected to each bus for each island are shown in Appendix A (Table A.23).

Next, the voltage of each bus was checked for all islands, as in the previous case studies. The voltage of each bus for Islands 1–4 was found to be within the allowable voltage limits, as shown in Appendix A (Table A.24). The power system was also checked to determine if there were violations in the transmission line capacity. It was found that the power flow in each transmission line for all islands was less than the transmission line capacity limit. The results of the transmission line power flow analysis for Case Study 6 are provided in Appendix A (Table A.25).

4.5 Analysis of the IEEE 118-Bus Test System

Similar analysis were conducted on the IEEE 118-bus test system and the results are presented in this section. Figure 4.27 shows the graph model of the IEEE 118-bus test system obtained from the graph theory approach.

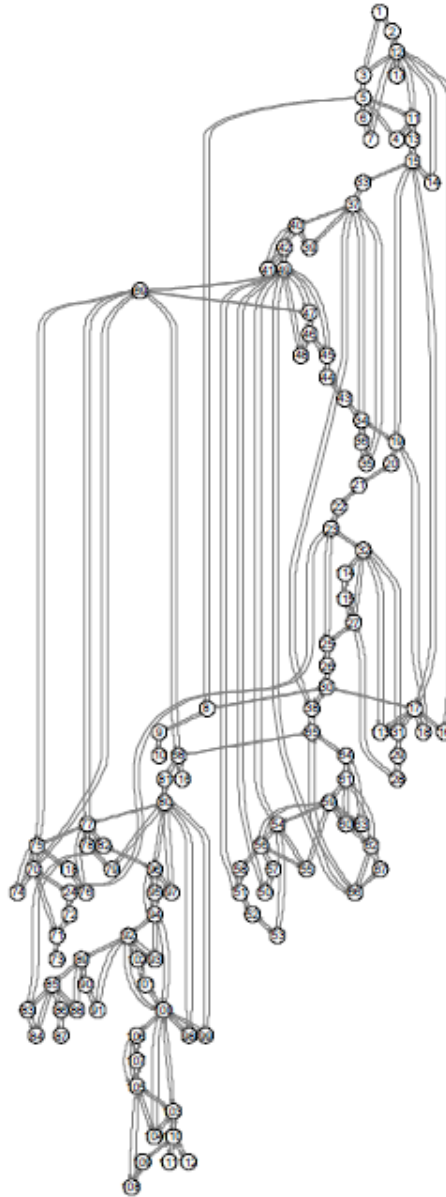


Figure 4.27. Representation of the IEEE 118-Bus Test System as a Graph Model

4.5.1 Case Study 7

For Case Study 7, the optimal intentional islanding strategy was analyzed based on previously published works [9], [102]. In this case study, the system was split into two islands based on the coherent groups of generators: $G_1 = \{10, 12, 25, 26, 31, 46, 49, 54, 59, 61, 65, 66, 69, 80\}$ and $G_2 = \{87, 89, 100, 103, 111\}$.

4.5.1.1 Determination of the Initial Intentional Islanding Solution

The graph model of the initial intentional islanding solution (red lines) for the IEEE 118-bus test system and the corresponding total power flow disruption, P_{disrup} , are shown in Figure 4.28 and Table 4.25, respectively.

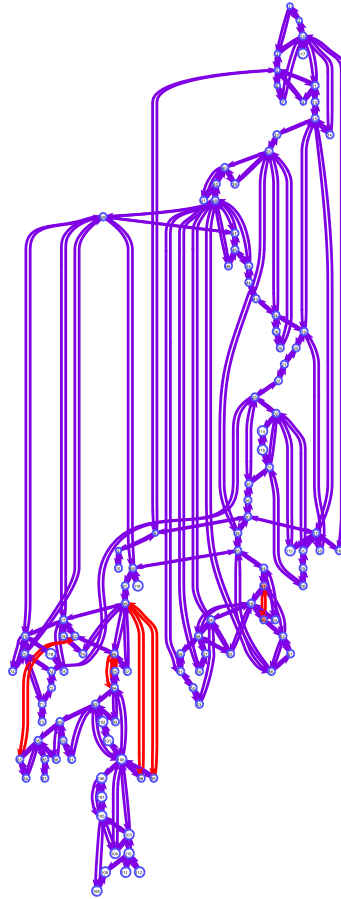


Figure 4.28. Graph Model of the Initial Intentional Islanding Solution (Red Lines) for Case Study 7

Table 4.25. Initial Intentional Islanding Solution for Case Study 7

Initial intentional islanding solution	Total power flow disruption, P_{disrup} (MW)
82–83, 94–96, 80–98, 80–99, 95–96	116.724

It can be observed from Table 4.25 that the initial intentional islanding solution consisting of five cutsets obtained from the graph theory approach yielded a total power flow disruption, P_{disrup} , of 116.724 MW. The results indicate that the graph theory approach is capable of reducing the initial search space of all possible transmission lines ($2^{186}-1 \approx 9.808 \times 10^{55}$) to five lines as the initial solution. This initial solution was used to facilitate the MDEP and MDPSO algorithms in determining the optimal intentional islanding strategy.

4.5.1.2 Evaluation of the MDEP and MDPSO Algorithms

The MDEP and MDPSO algorithms were analyzed using the IEEE 118-bus test system. Both of these algorithms yielded the same optimal intentional islanding strategy with five cutsets, resulting in a total power flow disruption, P_{disrup} , of 93.373 MW, as shown in Table 4.26. The results were compared with those of previously published works [9], [102]. The proposed islanding algorithms were capable of determining a better islanding strategy compared with the AMPSO algorithm [102] and similar islanding strategy with the modified ABC [9] algorithm, as shown in Table 4.26. The identical optimal intentional islanding strategies obtained from the proposed MDEP and MDPSO algorithms and the modified ABC algorithm [9] are likely because these solutions are the most optimal solution that can be obtained for this case study.

Table 4.26. Comparison of the Optimal Intentional Islanding Strategies for Case Study 7

Algorithm	Optimal intentional islanding strategy	ΣP_{disrup} (MW)
AMPSO [102]	80–96, 80–97, 80–98, 82–96, 83–84, 83–85, 99–100	174.523
Modified ABC [9]	82–83, 94–96, 80–99, 95–96, 98–100	93.373
MDPSO	82–83, 94–96, 80–99, 95–96, 98–100	93.373
MDEP	82–83, 94–96, 80–99, 95–96, 98–100	93.373

Because both of the proposed algorithms produced the same optimal intentional islanding strategy for Case Study 7, the best algorithm was determined based on the convergence curve and computational time. It can be seen from Figure 4.29 that the MDEP and MDPSO algorithms reached convergence within 50 iterations.

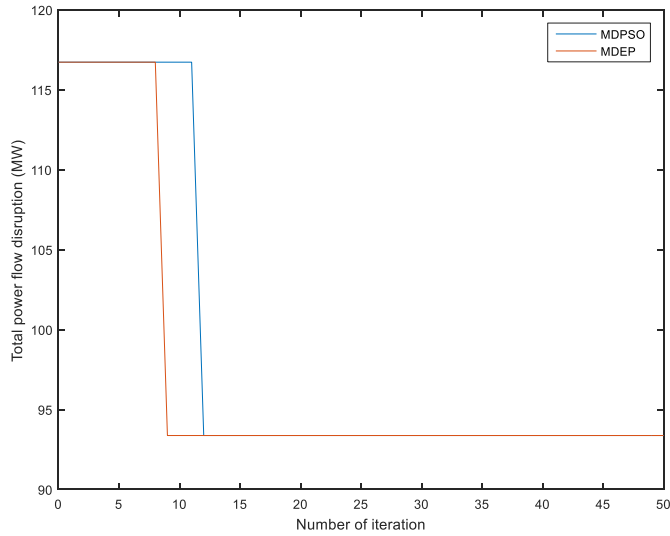


Figure 4.29. Convergence Curves for the MDEP and MDPSO Algorithms for Case Study 7

Although both of the proposed algorithms produced the same optimal intentional islanding strategy, the MDEP algorithm converged faster compared with the MDPSO algorithm. The performance of these algorithms was analyzed and the results are presented in Table 4.27.

Table 4.27. Comparison of the Performance between the MDEP and MDPSO Algorithms

Algorithm	No. of iterations required by the algorithm to reach convergence	Computational time (sec)
MDEP	9	2526.371
MDPSO	12	3592.73

It is apparent from Table 4.27 that the MDEP algorithm attained convergence on the 9th iteration while the MDPSO algorithm attained convergence on the 12th iteration. In addition, the time taken by the MDEP algorithm to achieve convergence was shorter (2526.371 sec) compared with that for the MDPSO algorithm (3592.73 sec). Thus, the MDEP algorithm was proposed as the best algorithm for intentional islanding implementation.

4.5.1.3 Determination of the Optimal Intentional Islanding Strategy Using the MDEP Algorithm

In this case study, the optimal intentional islanding strategy obtained from the proposed MDEP algorithm produced two stand-alone islands with 91 and 27 buses in Island 1 and Island 2, respectively. The optimal intentional islanding strategy for this case study was 82–83, 94–96, 80–99, 95–96, and 98–100, producing a total power flow disruption of 93.373 MW. The one-line diagram of the optimal intentional islanding strategy is shown in Figure 4.30. The graph model of the islanded islands is shown in Appendix A (Figure A.6).

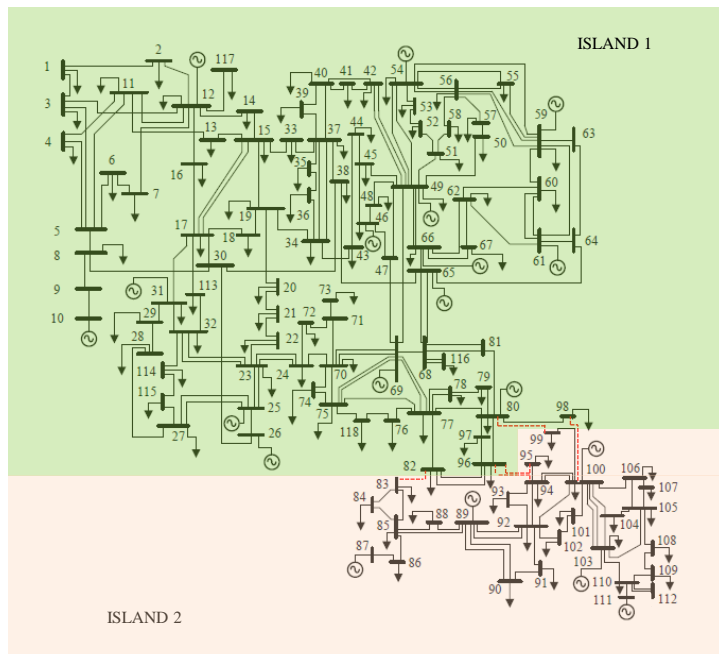


Figure 4.30. Optimal Intentional Islanding Strategy (Red Dashed Lines) for Case Study 7

As in the previous case studies, the power balance criterion was assessed for each island. Table 4.28 shows the results for Island 1 and Island 2 before and after intentional islanding implementation.

Table 4.28. Results for Island 1 and Island 2 Before and After Intentional Islanding Implementation: Case Study 7

Island 1				
Buses in Island 1	Generator information		Active power (MW)	
	Generator	Max. limit (MW)	Pre-islanding	Post-islanding
			ΣP_{gen}	ΣP_{gen}
1-82, 96-98, 113-118	G ₁₀	550	450.000	450.000
	G ₁₂	185	85.000	85.000
	G ₂₅	320	220.000	220.000
	G ₂₆	414	314.000	314.000
	G ₃₁	107	7.000	7.000
	G ₄₆	119	19.000	19.000
	G ₄₉	304	204.000	204.000
	G ₅₄	148	48.000	48.000
	G ₅₉	255	155.000	155.000
	G ₆₁	260	160.000	160.000
	G ₆₅	491	391.000	391.000
	G ₆₆	492	392.000	392.000
G _{69*}	805.2	511.920	566.117	
G ₈₀	577	477.000	477.000	
Total generated power, P_{gen} (MW)			3433.920	3488.117
Total load, P_{load} (MW)			3388.000	3388.000
Total power loss, P_{loss} (MW)			97.844	100.117
Total power imbalance, P_{imb} (MW)			-51.924	0.000
Total amount of load to be shed, P_{shed} (MW)			—	—
Island 2				
Buses in Island 2	Generator information		Active power (MW)	
	Generator	Max. limit (MW)	Pre-islanding	Post-islanding
			ΣP_{gen}	ΣP_{gen}
83-95, 99-112	G ₈₇	104	4.000	4.000
	G _{89*}	707	607.000	551.258
	G ₁₀₀	352	252.000	252.000
	G ₁₀₃	140	40.000	40.000
	G ₁₁₁	136	36.000	36.000
Total generated power, P_{gen} (MW)			939.000	883.258
Total load, P_{load} (MW)			854.000	854.000
Total power loss, P_{loss} (MW)			32.347	29.258
Total power imbalance, P_{imb} (MW)			52.653	0.000
Total amount of load to be shed, P_{shed} (MW)			—	—

*slack bus

In Island 1, there was a power deficit of 51.924 MW prior to intentional islanding. The slack bus, G₆₉, was located in Island 1 and thus, load flow analysis was performed to obtain the new system parameters in the island. The results showed that the slack bus, G₆₉, increased its generated power from 511.920 MW to 566.117 MW to compensate for the power deficit in the island. Finally, the power balance criterion in Island 1 was met, as shown in Table 4.28 (post-islanding column for Island 1) and load shedding scheme was not executed.

In Island 2, there was a power surplus of 52.653 MW in the pre-islanding condition. There was no slack bus available in this island and thus, generator bus, G_{89} was selected as the slack bus for the load flow analysis because it had the highest maximum power limit of 707 MW. The results showed that the slack bus reduced its generated power from 607.000 MW to 551.258 MW to fulfil the power balance criterion in the island, as shown in Table 4.28 (post-islanding column for Island 2). The power balance criterion was finally fulfilled and the island was capable of operating as a balanced, stand-alone island. Detail information on the load, P_{load} and generated power, P_{gen} connected to each bus for each island are presented in Appendix A (Table A.26).

Similar to previous case studies, the voltage of each bus was checked for Island 1 and Island 2. The voltage of each bus for both islands was determined to be within the allowable voltage limits, as shown in Appendix A (Table A.27). The power system was also checked to verify if there were violations in the transmission line capacity. The power flow in each transmission line for both islands was found to be less than the transmission line capacity limit. The results of the transmission line power flow analysis for Case Study 7 are given in Appendix A (Table A.28).

4.5.2 Case Study 8

For Case Study 8, the optimal intentional islanding strategy was analyzed based on previously published works [9], [10], [92]. In this case study, the system was partitioned into two islands based on the coherent groups of generators: $G_1 = \{10, 12, 25, 26, 31\}$ and $G_2 = \{46, 49, 54, 59, 61, 65, 66, 69, 80, 87, 89, 100, 103, 111\}$.

4.5.2.1 Determination of the Initial Intentional Islanding Solution

The graph model of the initial intentional islanding solution (red lines) for the IEEE 118-bus test system (Case Study 8) and the corresponding total power flow disruption, P_{disrup} , for this case study are shown in Figure 4.31 and Table 4.29, respectively.

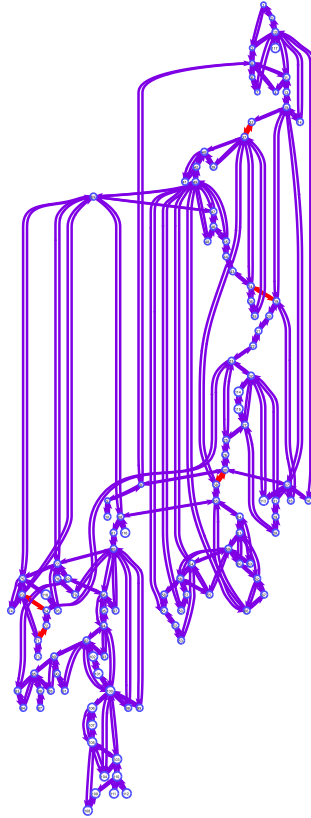


Figure 4.31. Graph Model of the Initial Intentional Islanding Solution (Red Lines) for Case Study 8

Table 4.29. Initial Intentional Islanding Solution for Case Study 8

Initial intentional islanding solution	Total power flow disruption, P_{disrup} (MW)
19–34, 33–37, 30–38, 24–70, 71–72	100.164

It can be seen from Table 4.29 that the initial intentional islanding solution with five cutsets obtained from the graph theory approach resulted in a total power flow disruption, P_{disrup} , of 100.164 MW. This initial solution was used to aid the MDEP and MDPSO algorithms in determining the optimal intentional islanding strategy.

4.5.2.2 Evaluation of the MDEP and MDPSO Algorithms

The MDEP and MDPSO algorithms were analyzed using the IEEE 118-bus test system. The MDEP algorithm provided the best optimal intentional islanding

strategy with five cutsets, resulting in a total power flow disruption, P_{disrup} , of 81.448 MW, as shown in Table 4.30. Furthermore, the MDEP algorithm was capable of determining the optimal intentional islanding strategy with a lower minimal fitness function value compared with the proposed MDPSO algorithm and other algorithms [9], [10], [92].

Table 4.30. Comparison of the Optimal Intentional Islanding Strategies for Case Study 8

Algorithm	Optimal intentional islanding strategy	ΣP_{disrup} (MW)
Controlled islanding [92]	24–70, 34–43, 38–65, 40–41, 40–42, 71–72	232.772
Tabu search [10]	22–23, 23–25, 23–32, 33–37, 34–36, 34–37, 34–43, 37–38, 38–65	890.73
Modified ABC [9]	24–70, 24–72, 34–43, 38–65, 40–41, 40–42	224.148
MDPSO	15–33, 19–34, 30–38, 23–24	83.797
MDEP	15–33, 19–34, 30–38, 24–70, 24–72	81.448

The convergence curves for the MDEP and MDPSO algorithms are shown in Figure 4.32. It can be observed from Figure 4.32 that the MDEP algorithm was able to determine the optimal intentional islanding strategy with a lower minimal fitness function value compared with the MDPSO algorithm. Hence, the MDEP technique was proposed as the best algorithm for intentional islanding implementation.

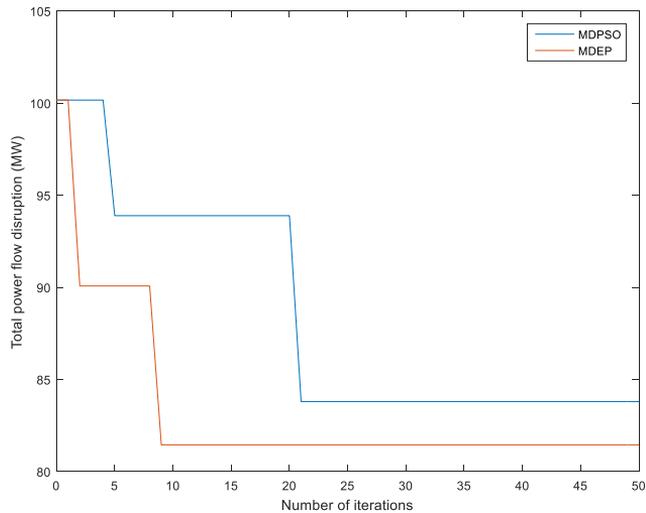


Figure 4.32. Convergence Curves for the MDEP and MDPSO Algorithms for Case Study 8

4.5.2.3 Determination of the Optimal Intentional Islanding Strategy Using the MDEP Algorithm

For Case Study 8, the optimal intentional islanding strategy obtained from the MDEP algorithm produced two stand-alone islands with 36 and 82 buses in Island 1 and Island 2, respectively. The optimal intentional islanding strategy for this case study was 15–33, 19–34, 30–38, 24–70, and 24–72, yielding a total power flow disruption of 81.448 MW. The one-line diagram of the optimal intentional islanding strategy is shown in Figure 4.33. The graph model of the islanded islands is shown in Appendix A (Figure A.7).

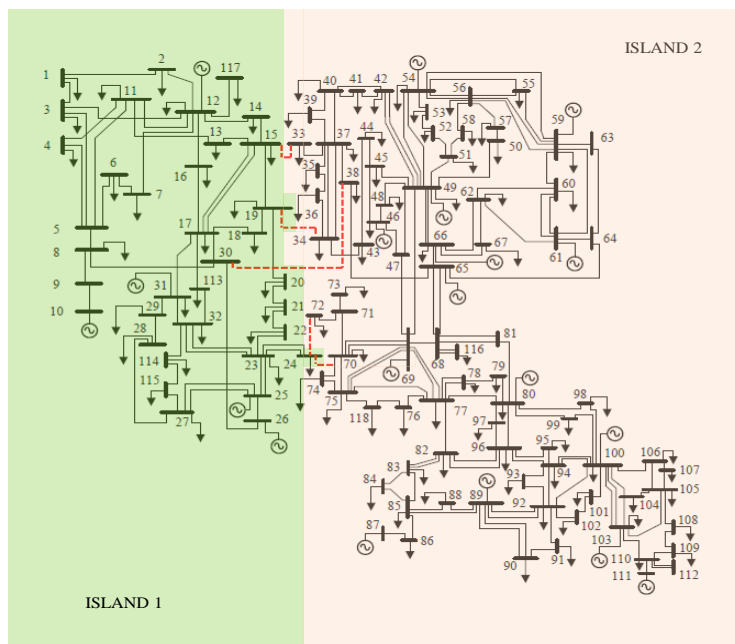


Figure 4.33. Optimal Intentional Islanding Strategy (Red Dashed Lines) for Case Study 8

Next, the power balance criterion was assessed for each island. Table 4.31 shows the results for Island 1 and Island 2 before and after intentional islanding implementation.

Table 4.31. Results for Island 1 and Island 2 Before and After Intentional Islanding Implementation: Case Study 8

Island 1				
Buses in Island 1	Generator information		Active power (MW)	
	Generator	Max. limit (MW)	Pre-islanding	Post-islanding
			ΣP_{gen}	ΣP_{gen}
1–32, 113–115, 117	G _{10*}	550	450.000	385.153
	G ₁₂	185	85.000	85.000
	G ₂₅	320	220.000	220.000
	G ₂₆	414	314.000	314.000
	G ₃₁	107	7.000	7.000
Total generated power, P_{gen} (MW)			1076.000	1011.153
Total load, P_{load} (MW)			976.000	976.000
Total power loss, P_{loss} (MW)			37.980	35.153
Total power imbalance, P_{imb} (MW)			62.020	0.000
Total amount of load to be shed, P_{shed} (MW)			—	—
Island 2				
Buses in Island 2	Generator information		Active power (MW)	
	Generator	Max. limit (MW)	Pre-islanding	Post-islanding
			ΣP_{gen}	ΣP_{gen}
33–112, 116, 118	G ₄₆	119	19.000	19.000
	G ₄₉	304	204.000	204.000
	G ₅₄	148	48.000	48.000
	G ₅₉	255	155.000	155.000
	G ₆₁	260	160.000	160.000
	G ₆₅	491	391.000	391.000
	G ₆₆	492	392.000	392.000
	G _{69*}	805.2	511.920	578.901
	G ₈₀	577	477.000	477.000
	G ₈₇	104	4.000	4.000
	G ₈₉	707	607.000	607.000
	G ₁₀₀	352	252.000	252.000
	G ₁₀₃	140	40.000	40.000
G ₁₁₁	136	36.000	36.000	
Total generated power, P_{gen} (MW)			3296.920	3363.901
Total load, P_{load} (MW)			3266.000	3266.000
Total power loss, P_{loss} (MW)			92.644	97.901
Total power imbalance, P_{imb} (MW)			-61.724	0.000
Total amount of load to be shed, P_{shed} (MW)			—	—

*slack bus

It can be seen from Table 4.31 that there was a power surplus of 62.020 MW in Island 1. Since there was no slack bus available in this island, generator bus, G₁₀ was selected as the slack bus to perform the load flow analysis. The slack bus, G₁₀, reduced its generated power from 450.000 MW to 385.153 MW to compensate for the power surplus in the island. Finally, the power balance criterion was met ($P_{imb} = 0.000$ MW), as shown in Table 4.31 (post-islanding column for Island 1). Hence, the

load shedding scheme was not executed. Thus, the island could operate as a balanced, stand-alone island.

In Island 2, there was power deficit of 61.724 MW. Load flow analysis was carried out and it was found that the slack bus, G_{69} , increased its generated power from 511.920 MW to 578.901 MW to compensate for the power deficit in the island. The power balance criterion was met ($P_{imb} = 0.000$ MW), as shown in Table 4.31 (post-islanding column for Island 2). Thus, the island could operate as a balanced, stand-alone island. Detail information on the load, P_{load} and generated power, P_{gen} connected to each bus for each island are shown in Appendix A (Table A.29).

Next, the voltage profiles for each island after intentional islanding were checked. The voltage of each bus for Island 1 and Island 2 was determined to be within the allowable voltage limits, as shown in Appendix A (Table A.30). The power system was also checked to determine if there were violations in the transmission line capacity. The power flow in each transmission line in these islands was found to be less than the transmission line capacity limit. The results of the transmission line power flow analysis for Case Study 8 are provided in Appendix A (Table A.31).

4.5.3 Case Study 9

For Case Study 9, the optimal intentional islanding strategy was analyzed based on a previous work [92]. In this case study, the system was partitioned into three islands based on the coherent groups of generators: $G_1 = \{10, 12, 25, 26, 31\}$, $G_2 = \{46, 49, 54, 59, 61, 65, 66, 69\}$, and $G_3 = \{80, 87, 89, 100, 103, 111\}$.

4.5.3.1 Determination of the Initial Intentional Islanding Solution

The graph model of the intentional islanding initial solution (red lines) for the IEEE 118-bus test system (Case Study 9) and the corresponding total power flow disruption, P_{disrup} , for this case study are shown in Figure 4.34 and Table 4.32, respectively.

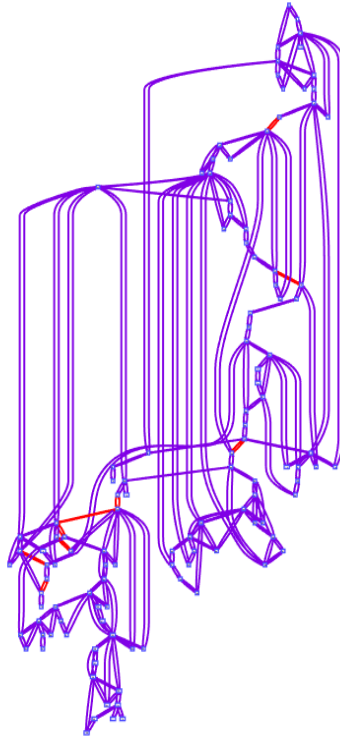


Figure 4.34. Graph Model of the Initial Intentional Islanding Solution (Red Lines) for Case Study 9

Table 4.32. Initial Intentional Islanding Solution for Case Study 9

Initial intentional islanding solution	Total power flow disruption, P_{disrup} (MW)
19–34, 33–37, 30–38, 24–70, 71–72, 78–79, 77–80, 77–80, 80–81, 77–82	314.934

It can be seen from Table 4.32 that the initial intentional islanding solution with 10 cutsets obtained from the graph theory approach produced a total power flow disruption, P_{disrup} , of 314.934 MW. This initial solution was used to facilitate the MDEP and MDPSO algorithms in determining the optimal intentional islanding strategy.

4.5.3.2 Evaluation of the MDEP and MDPSO Algorithms

The MDEP and MDPSO algorithms were analyzed using the IEEE 118-bus test system. The MDEP algorithm provided the best optimal intentional islanding

strategy with five cutsets, producing a total power flow disruption, P_{disrup} , of 296.061 MW, as shown in Table 4.33. It can be deduced that the MDEP algorithm was capable of obtaining a better optimal intentional islanding strategy with a lower minimal fitness function value compared with the proposed MDPSO algorithm and controlled islanding algorithm [92].

Table 4.33. Comparison of the Optimal Intentional Islanding Strategies for Case Study 9

Algorithm	Optimal intentional islanding strategy	ΣP_{disrup} (MW)
Controlled islanding [92]	40–41, 40–42, 34–43, 38–65, 71–72, 24–70, 75–77, 76–118, 69–77, 68–81	385.817
MDPSO	15–33, 19–34, 30–38, 24–70, 71–72, 78–79, 77–80, 77–80, 68–81, 77–82	304.685
MDEP	15–33, 19–34, 30–38, 24–70, 24–72, 78–79, 77–80, 77–80, 68–81, 77–82	296.061

The convergence curves for the MDEP and MDPSO algorithms developed in this research is shown in Figure 4.35. In general, the MDEP algorithm was able to determine a better optimal intentional islanding strategy with a lower minimal fitness function value compared with the MDPSO algorithm. Thus, the MDEP algorithm was the best algorithm to implement intentional islanding for Case Study 9.

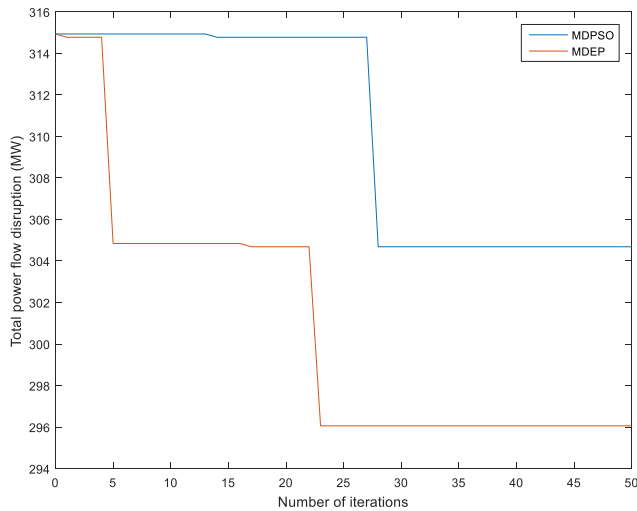


Figure 4.35. Convergence Curves for the MDEP and MDPSO Algorithms for Case Study 9

4.5.3.3 Determination of the Optimal Intentional Islanding Strategy Using the MDEP Algorithm

The optimal intentional islanding strategy obtained from the MDEP algorithm produced three stand-alone islands with 36, 48, and 34 buses in Island 1, Island 2, and Island 3, respectively. The optimal intentional islanding strategy for this case study was 15–33, 19–34, 30–38, 24–70, 24–72, 78–79, 77–80, 77–80, 68–81, and 77–82, resulting in a total power flow disruption of 296.061 MW. The one-line diagram of the optimal intentional islanding strategy is shown in Figure 4.36. The graph model of the islanded islands is shown in Appendix A (Figure A.8).

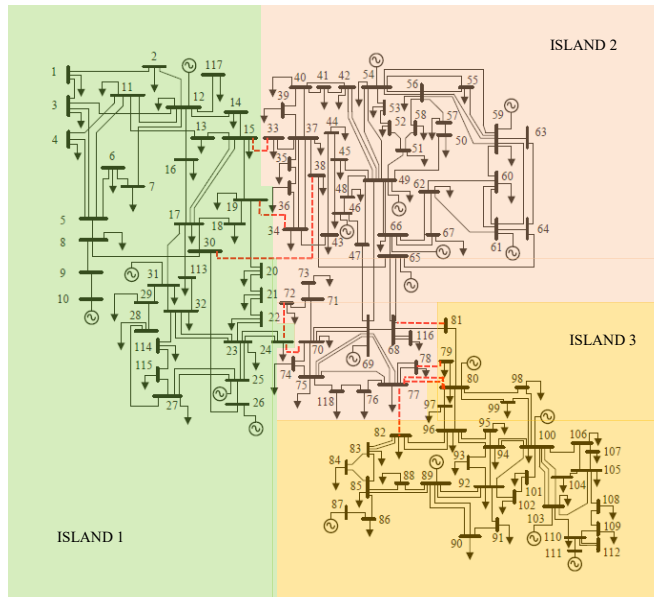


Figure 4.36. Optimal Intentional Islanding Strategy (Red Dashed Lines) for Case Study 9

Next, the power balance criterion was evaluated for each island. Table 4.34 shows the results for Islands 1–3 before and after intentional islanding implementation.

Table 4.34. Results for Islands 1–3 Before and After Intentional Islanding Implementation: Case Study 9

Island 1				
Buses in Island 1	Generator information		Active power (MW)	
	Generator	Max. limit (MW)	Pre-islanding ΣP_{gen}	Post-islanding ΣP_{gen}
1–32, 113–115, 117	G _{10*}	550	450.000	385.153
	G ₁₂	185	85.000	85.000
	G ₂₅	320	220.000	220.000
	G ₂₆	414	314.000	314.000
	G ₃₁	107	7.000	7.000
Total generated power, P_{gen} (MW)			1076.000	1011.153
Total load, P_{load} (MW)			976.000	976.000
Total power loss, P_{loss} (MW)			37.980	35.153
Total power imbalance, P_{imb} (MW)			62.020	0.000
Total amount of load to be shed, P_{shed} (MW)			—	—
Island 2				
Buses in Island 2	Generator information		Active power (MW)	
	Generator	Max. limit (MW)	Pre-islanding ΣP_{gen}	Post-islanding ΣP_{gen}
33–78 116, 118	G ₄₆	119	19.000	19.000
	G ₄₉	304	204.000	204.000
	G ₅₄	148	48.000	48.000
	G ₅₉	255	155.000	155.000
	G ₆₁	260	160.000	160.000
	G ₆₅	491	391.000	391.000
	G ₆₆	492	392.000	392.000
	G _{69*}	805.2	511.920	804.212
Total generated power, P_{gen} (MW)			1880.920	2173.212
Total load, P_{load} (MW)			2102.000	2102.000
Total power loss, P_{loss} (MW)			55.256	71.212
Total power imbalance, P_{imb} (MW)			-276.336	0.000
Total amount of load to be shed, P_{shed} (MW)			—	—
Island 3				
Buses in Island 3	Generator information		Active power (MW)	
	Generator	Max. limit (MW)	Pre-islanding ΣP_{gen}	Post-islanding ΣP_{gen}
79–112	G ₈₀	577	477.000	477.000
	G ₈₇	104	4.000	4.000
	G _{89*}	707	607.000	383.906
	G ₁₀₀	352	252.000	252.000
	G ₁₀₃	140	40.000	40.000
	G ₁₁₁	136	36.000	36.000
Total generated power, P_{gen} (MW)			1416.000	1192.906
Total load, P_{load} (MW)			1164.000	1164.000
Total power loss, P_{loss} (MW)			34.664	28.906
Total power imbalance, P_{imb} (MW)			217.336	0.000
Total amount of load to be shed, P_{shed} (MW)			—	—

*slack bus

It can be seen from Table 4.34 that there was a power surplus of 62.020 MW in Island 1. A new slack bus was assigned from the existing generator buses because there was no slack bus available in this island. Generator bus, G_{10} was selected as the slack bus and load flow analysis is then performed. The results showed that the slack bus, G_{10} , decreased its generated power from 450.000 MW to 385.153 MW to compensate for the power surplus in the island. Finally, the power balance criterion was met ($P_{imb} = 0.000$ MW), as shown in Table 4.34 (post-islanding column for Island 1). Therefore, the load shedding scheme was not executed. Thus, the island could operate as a balanced, stand-alone island.

In Island 2, there was a power deficit of 276.336 MW in the pre-islanding condition. The slack bus was located in this island and therefore, load flow analysis was performed to obtain the system parameters. The results showed that the slack bus, G_{69} , increased its generated power to 804.212 MW to compensate for the power deficit in the island. As such, the power balance criterion was met and the island could operate as a balanced, stand-alone island.

In Island 3, there was a power surplus of 217.336 MW in the pre-islanding condition. Because there was no slack bus available in the island, generator bus, G_{89} was selected as the slack bus and load flow analysis is then carried out. The slack bus, G_{89} , decreased its generated power from 607.000 MW to 383.906 MW to compensate for the power surplus in the island. Finally, the power balance criterion was met ($P_{imb} = 0.000$ MW), as shown in Table 4.34 (post-islanding column for Island 3), and therefore, the load shedding scheme was not executed. Thus, the island could operate as a balanced, stand-alone island. Detail information on the load, P_{load} and generated power, P_{gen} connected to each bus for each island are shown in Appendix A (Table A.32).

Next, the voltage profiles for each island after intentional islanding were checked, as in the previous case studies. The voltage of each bus for all islands was determined to be within the allowable voltage limit, as shown in Appendix A (Table A.33). Transmission line power flow analysis was then performed for Islands 1–3 to identify if there were violations in the transmission line capacity. It was found that

the power flow in each transmission line for these islands was less than the transmission line capacity limit. The results of the transmission line power flow analysis Case Study 9 is provided in Appendix A (Table A.34).

4.6 Chapter Summary

In this chapter, the metaheuristic algorithms developed in this research, MDEP and MDPSO algorithms were implemented to determine the optimal intentional islanding strategy. Nine case studies were conducted using three IEEE test systems: IEEE 30-bus, IEEE 39-bus, and IEEE 118-bus test systems. For each case study, the initial intentional islanding solution was obtained using graph theory. The MDEP and MDPSO algorithms were used to determine the optimal intentional islanding strategy, facilitated by the initial solution obtained from the graph theory-based initialization. The results were compared with those obtained by other researchers. In general, the MDEP and MDPSO algorithms were able to determine a better optimal intentional islanding strategy for six case studies and whereas these algorithms produced a similar strategy (the most optimal solution) with modified ABC algorithm [9] for three case studies (Case Studies 1, 6, and 7). Although the developed algorithms and the modified ABC algorithm [9] were able to determine the most optimal intentional islanding strategy for Case Studies 1, 6, and 7; however, the MDEP and MDPSO algorithms were less complex than the modified ABC algorithm.

Next, the best algorithm was chosen between the MDEP and MSPSO algorithms. Based on the results, the MDEP and MDPSO algorithms produced the same optimal intentional islanding strategies for seven case studies. However, the MDEP algorithm produced a better optimal intentional islanding strategy than the MDPSO algorithm for Case Studies 8 and 9. This shows that MDEP is the best algorithm especially when the size of the test system increases. Furthermore, the convergence test results showed that the MDEP algorithm consistently achieved faster convergence compared with the MDPSO algorithm for all case studies. Therefore, the MDEP algorithm was proposed as the best algorithm for intentional islanding implementation in this research.

The MDEP algorithm was then integrated with a load shedding scheme, bus voltage checking scheme, and transmission line power flow analysis to ensure that each island formed could operate as a balanced, stand-alone island. The optimal intentional islanding strategy obtained from the MDEP algorithm is considered optimal only if the power balance (i.e. load-generation balance) criterion, allowable bus voltage limits, and allowable transmission line capacity limit are fulfilled. In this research, the load shedding scheme was developed based on the MDEP technique. Validation of the MDEP-based load shedding scheme is presented in the following chapter. The optimal intentional islanding strategies considering critical line outages are also presented in Chapter 5.

CHAPTER 5

PROPOSED INTENTIONAL ISLANDING ALGORITHM WITH CONTINGENCY ANALYSIS AND LOAD SHEDDING SCHEME

5.1 Introduction

In this chapter, the proposed intentional islanding algorithm, MDEP algorithm was implemented in contingency scenarios with critical line outages, and the results are presented and discussed in detail. The critical line outages were identified from the N-1 contingency analysis. The overloading criterion in [38] was used to identify the critical line, which can trigger cascading failures. Nine case studies were carried out based on the IEEE 30-bus, IEEE 39-bus, and IEEE 118-bus test systems. The three most critical line outages for each test system were considered in the intentional islanding implementation. The steps described in Chapter 4 were also implemented for the case studies presented in this chapter. For each case study, the initial intentional islanding solution was first determined following a critical line outage. The proposed Modified Discrete Evolutionary Programming (MDEP) algorithm was then used to determine the optimal intentional islanding strategy. The developed Modified Discrete Particle Swarm Optimization (MDPSO) algorithm was used as a benchmark to validate the performance of the MDEP algorithm in determining the optimal intentional islanding strategy. In addition, the MDEP-based load shedding scheme was executed when there were load-generation imbalances in the islands formed.

5.2 IEEE Test Systems

Three IEEE test systems (IEEE 30-bus, IEEE 39-bus, and IEEE 118-bus test systems) were used to analyze the performance of the MDEP and MDPSO algorithms in determining the optimal intentional islanding strategy following a critical line outage. These test systems were also used for the case studies presented in Chapter 4. Three sets of coherent groups of generators were evaluated for each test

system, resulting in a total of nine case studies. Some modifications were made to the maximum power limit of the generators for each test system to increase the complexity of the intentional islanding implementation. In this manner, the performance of the MDEP-based load shedding scheme could be assessed for each case study. This will demonstrate the capability of the proposed algorithms in determining the optimal intentional islanding strategy and the optimal amount of load that needs to be shed. The modified data for each test system are provided in Appendix B (Table B.1- Table B.3).

5.3 N-1 Contingency Analysis and Determination of Critical Lines

In this research work, N-1 contingency analysis was performed for each test system to identify the critical line outages that could result in severe cascading failures if the critical lines were tripped due to failure. As described in Section 3.2.2 of Chapter 3, a line is considered as a critical line when it reaches its maximum overload (MVA) of 130%. Once the first critical line is tripped, this will cause other lines to overload and trip. The complete results obtained for the critical line outages for each test system are provided in Appendix B (Table B.4- Table B.6).

5.4 Critical Line Outages for the IEEE 30-Bus Test System

In this section, the three most critical line outages for the IEEE 30-bus test system with three different coherent groups of generators were analyzed for intentional islanding implementation. The three most critical line outages for the IEEE 30-bus test system are presented in Table 5.1.

Table 5.1. Three Most Critical Line Outages for the IEEE 30-Bus Test System

Critical line	MVA violation (%) of the corresponding overloaded lines	Coherent groups of generators
Line 1-2	Line 1-3 (218.3641) Line 3-4 (194.2109) Line 4-6 (174.0935) Line 6-8 (108.5869)	$G_1 = \{1,2,5,13\}$ $G_2 = \{8,11\}$
Line 1-3	Line 1-2 (190.4687) Line 2-6 (132.2086) Line 2-4 (123.6725)	$G_1 = \{1, 2, 5, \}$ $G_2 = \{8, 11, 13\}$
Line 3-4	Line 1-2 (188.2437) Line 2-6 (130.7388) Line 2-4 (121.7634)	$G_1 = \{1,2,5,13\}$ $G_2 = \{8\}$ $G_3 = \{11\}$

According to Table 5.1, the first critical line obtained from the N-1 contingency analysis was Line 1–2. The failure (tripping) of this line would cause other lines (Lines 1–3, 3–4, 4–6, 4–6, and 6–8) to overload and trip. The second critical line was Line 1–3, where the failure of this line would cause Lines 1–2, 2–6, and 2–4 to overload and trip. Finally, the third critical line was Line 3–4, which would cause Line 1–2, 2–6, and 2–4 to overload and trip. Without a proper intentional islanding strategy, when each of these critical lines trip, the system may experience severe cascading failures, culminating in a partial or total system blackout.

The results obtained from this analysis, including the determination of the initial intentional islanding strategy following a critical line outage based on graph theory and the determination of the optimal intentional islanding strategy using the proposed MDEP algorithm for each case study are presented in the following subsections.

5.4.1 Case Study C1

For Case Study C1, the optimal intentional islanding strategy was determined following the outage of Critical Line 1–2. In this case study, intentional islanding was implemented by splitting the system into two islands based on the coherent groups of generators: $G_1 = \{1, 2, 5, 13\}$ and $G_2 = \{8, 11\}$.

5.4.1.1 Determination of the Initial Intentional Islanding Strategy Following a Critical Line Outage

Once the critical line was removed (disconnected) from the IEEE 30-bus test system, the initial intentional islanding solution was determined using graph theory based on the desired number of islands and coherent groups of generators. As described in Section 4.4.1.1 of Chapter 4, the initial intentional islanding solution generally indicates the total number of transmission lines that needs to be disconnected in order to form the desired number of islands based on the coherent groups of generators. The graph model of the initial intentional islanding solution (red lines) following a critical line outage for the IEEE 30-bus test system is shown in Figure 5.1 and the corresponding total power flow disruption, P_{disrup} , is shown in Table 5.2.

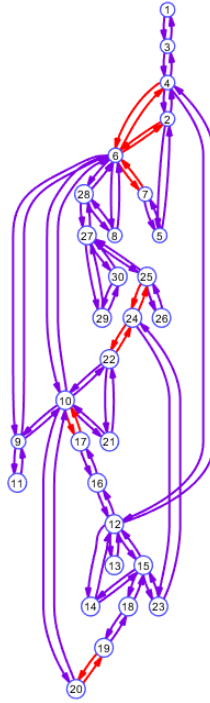


Figure 5.1. Initial Intentional Islanding Solution (Red Lines) for Case Study C1

Table 5.2. Initial Intentional Islanding Solution for Case Study C1

Initial intentional islanding solution	Total power flow disruption, P_{disrup} (MW)
2-6, 4-6, 6-7, 19-20, 10-17, 22-24, 24-25	213.921

It can be seen from Table 5.2 that the initial intentional islanding solution consisting of seven cutsets obtained from the graph theory approach produced a total power flow disruption, P_{disrup} , of 213.921 MW. This indicates the graph theory can reduce the initial search space of all possible transmission lines ($2^{40} \approx 1.0995 \times 10^{12}$) to seven lines as the initial solution. This initial solution was used to facilitate the proposed MDEP algorithm in determining the optimal intentional islanding strategy.

5.4.1.2 Evaluation of the MDEP Algorithm

The MDEP algorithm was evaluated using the IEEE 30-bus test system in order to determine the optimal intentional islanding strategy following a critical line outage. The result was then compared with the developed MDPSO algorithm as presented in

Table 5.3. Both of these algorithms produced the same optimal intentional islanding strategy and total power flow disruption, P_{disrup} , of 185.236 MW. Furthermore, the total number of disconnected lines (cutsets) was reduced to six cutsets in the optimal solution whereas the initial solution consisted of seven cutsets.

Table 5.3. Comparison of the Optimal Intentional Islanding Strategies for Case Study C1

Algorithm	Optimal intentional islanding strategy	ΣP_{disrup} (MW)
MDPSO	2-6, 4-6, 5-7, 10-17, 18-19, 23-24	185.236
MDEP	2-6, 4-6, 5-7, 10-17, 18-19, 23-24	185.236

Since the MDEP and MDPSO provided the same optimal intentional islanding strategy, the performance of these algorithms was assessed in terms of the number of iterations required by the algorithm to reach convergence and computational time. Figure 5.2 shows the convergence curves for the MDEP and MDPSO algorithms. The maximum number of iterations for the convergence test was set at 50.

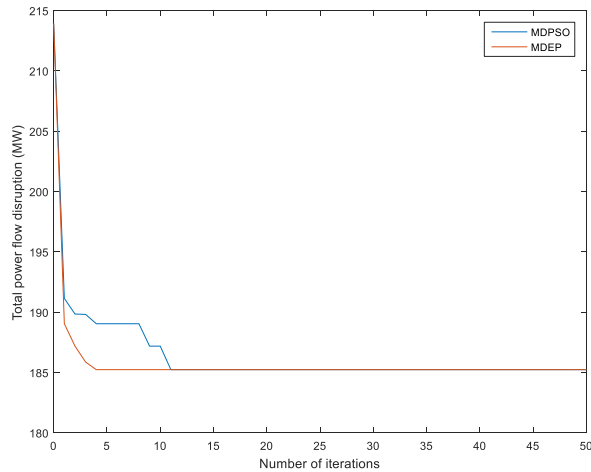


Figure 5.2. Convergence Curves for the MDEP and MDPSO Algorithms for Case Study C1

It can be observed from Figure 5.2 that the MDEP and MDPSO algorithms reached convergence within 50 iterations. However, the MDEP algorithm converged faster than the MDPSO algorithm. The performance of these algorithms was analyzed and the results are tabulated in Table 5.4.

Table 5.4. Comparison of the Performance between the MDEP and MDPSO Algorithms

Algorithm	No. of iterations required by the algorithm to reach convergence	Computational time (sec)
MDEP	4	296.531
MDPSO	11	816.810

Based on the results, the MDEP algorithm achieved convergence on the 4th iteration whereas the MDPSO algorithm achieved convergence on the 11th iteration. The corresponding computational times for the MDEP and MDPSO algorithms were 296.531 sec and 816.810 sec, respectively. The results proved that the proposed MDEP algorithm was capable of producing the optimal intentional islanding strategy within a fewer number of iterations and thereby reducing the computational time.

5.4.1.3 Determination of the Optimal Intentional Islanding Strategy Using the MDEP Algorithm

For Case Study C1, the optimal intentional islanding strategy obtained from the MDEP algorithm produced two stand-alone islands with 13 and 17 buses in Island 1 and Island 2, respectively. The optimal islanding strategy for this case study was 2–6, 4–6, 5–7, 10–17, 18–19, and 23–24, resulting in a total power flow disruption of 185.236 MW. The one-line diagram and graph model of the islanded islands are shown in Figure 5.3 and Figure 5.4, respectively.

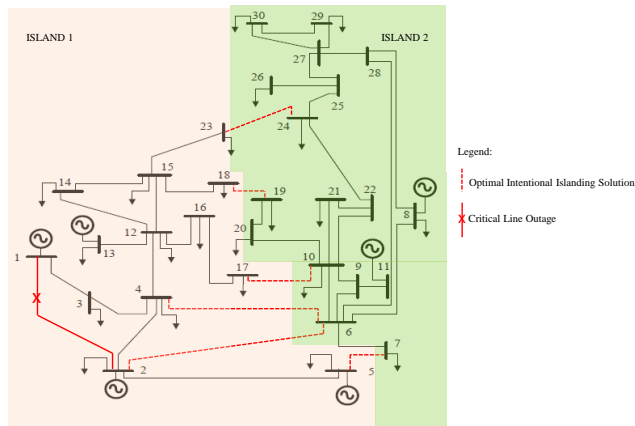


Figure 5.3. One-Line Diagram for Case Study C1

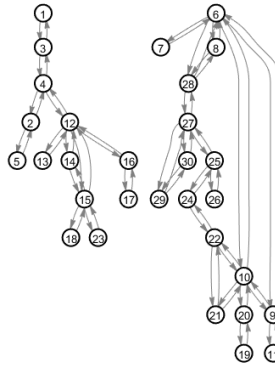


Figure 5.4. Graph Model of the Islanded Islands for Case Study C1

The two stand-alone islands formed after intentional islanding must be balanced in terms of the total generated power and total load. Hence, the power balance criterion was assessed for each island, as in the previous case studies presented in Chapter 4. Table 5.5 shows the results for Island 1 and Island 2 before and after intentional islanding implementation.

It can be seen from Table 5.5 that there was a power surplus of 109.753 MW in Island 1 prior to intentional islanding. The slack bus, G_1 , was located in this island and therefore, load flow analysis was performed to obtain the new system parameters in the island. The slack bus, G_1 , reduced its generated power from 277.423 MW to 139.446 MW in order to fulfil the power balance criterion in the island, as shown in Table 5.5 (post-islanding column for Island 1). Finally, the power balance criterion in Island 1 was met and therefore, the load shedding scheme was not executed. Island 1 was capable of operating as a balanced, stand-alone island.

In Island 2, there was a power deficit of 105.054 MW, which may be due to the absence of a slack bus in this island, considering that the original slack bus was situated in Island 1. Thus, a new slack bus was assigned in the island based on the highest maximum power limit ($P_{gen,max}$) among the available PV (generators) buses, as in the previous case studies presented in Chapter 4. Generator bus, G_8 was selected as the slack bus because it had the highest maximum power limit of 50 MW. However, the slack bus, G_8 , was unable to compensate for the high power deficit in the island because the value exceeded its maximum power limit. To overcome this

problem, generator bus, G_{11} was operated at its maximum power limit. However, the generator bus was still unable to fulfil the power balance criterion in the island. Thus, the MDEP-based load shedding scheme was executed, where the loads at buses 19, 20, 21, 26, and 29 (total amount: 35.100 MW) were shed to achieve load-generation balance in the island. This action is important to ensure successful islanding implementation and produce a balanced, stand-alone island. Furthermore, the execution of the load shedding scheme allows the island to fulfil the power balance criterion, as shown in Table 5.5 (post-islanding column for Island 2). Detail information on the load, P_{load} and generated power, P_{gen} connected to each bus for each island are presented in Appendix B (Table B.7).

Table 5.5. Results for Island 1 and Island 2 Before and After Intentional Islanding Implementation: Case Study C1

Island 1				
Buses in Island 1	Generator information		Active power (MW)	
	Generator	Max. limit (MW)	Pre-islanding ΣP_{gen}	Post-islanding ΣP_{gen}
1–5, 12–18, 23	G_{1^*}	300	277.423	139.446
	G_2	40	40.000	40.000
	G_5	40	10.000	10.000
	G_{13}	40	0.000	0.000
Total generated power, P_{gen} (MW)			327.423	189.446
Total load, P_{load} (MW)			170.400	170.400
Total power loss, P_{loss} (MW)			47.270	19.046
Total power imbalance, P_{imb} (MW)			109.753	0.000
Total amount of load to be shed, P_{shed} (MW)			—	—
Island 2				
Buses in Island 2	Generator information		Active power (MW)	
	Generator	Max. limit (MW)	Pre-islanding ΣP_{gen}	Post-islanding ΣP_{gen}
6–11, 19–22, 24–30	G_{8^*}	50	10.000	48.517
	G_{11}	30	0.000	30.000
Total generated power, P_{gen} (MW)			10.000	78.517
Total load, P_{load} (MW)			113.000	77.900
Total power loss, P_{loss} (MW)			2.054	0.617
Total power imbalance, P_{imb} (MW)			–105.054	0.000
Total amount of load to be shed, P_{shed} (MW)			—	35.100

*slack bus

The voltage profiles were checked for each island to ensure that there were no voltage violations after intentional islanding. The voltage of each bus in all islands

was found to be within the allowable voltage limits, as shown in Appendix B (Table B.8).

Furthermore, the power flow in each transmission line was analyzed for both islands to ensure that there were no violations in the transmission line capacity. The power flow, P_{flow} , in each transmission line for Island 1 and Island 2 was determined to be less than the transmission line capacity limit. The results of the transmission line power flow analysis for Case Study C1 are provided in Appendix B (Table B.9).

Overall, the results obtained for this case study indicate that the MDEP algorithm is capable of determining the optimal intentional islanding strategy following a critical line outage, which fulfils the specified system constraints. The intentional islanding strategy is only considered as successful when the power balance criterion, bus voltage limits, and transmission line capacity limit are fulfilled for each island formed. Furthermore, the implementation of intentional islanding will prevent the power system from experiencing further cascading failures, which can ultimately result in system blackout.

5.4.2 Case Study C2

For Case Study C2, the optimal intentional islanding strategy was determined following the outage of Critical Line 1–3. In this case study, intentional islanding was implemented by partitioning the system into two islands based on the coherent groups of generators: $G_1 = \{1, 2, 5\}$ and $G_2 = \{8, 11, 13\}$.

5.4.2.1 Determination of the Initial Intentional Islanding Solution Following a Critical Line Outage

The initial intentional islanding solution following a critical line outage and the corresponding total power flow disruption, P_{disrup} , for this case study are shown in Table 5.6. The graph model of the initial intentional islanding solution for Case Study C2 is given in Appendix B (Figure B.1).

Table 5.6. Initial Intentional Islanding Solution for Case Study C2

Initial intentional islanding solution	Total power flow disruption, P_{disrup} (MW)
2-6, 4-6, 6-7	188.358

It can be seen from Table 5.6 that the initial intentional islanding solution with three cutsets obtained from the graph theory approach produced a total power flow disruption, P_{disrup} , of 188.358 MW. This initial solution was used to aid the proposed MDEP algorithm in determining the optimal intentional islanding strategy.

5.4.2.2 Evaluation of the MDEP Algorithm

The proposed MDEP algorithm was analyzed using the IEEE 30-bus test system and the result was then compared with the MDPSO algorithm as presented in Table 5.7. Both of the algorithms yielded the same optimal intentional islanding strategies, resulting in a total power flow disruption, P_{disrup} , of 153.474 MW.

Table 5.7. Comparison of the Optimal Intentional Islanding Strategies for Case Study C2

Algorithm	Optimal intentional islanding strategy	$\sum P_{disrup}$ (MW)
MDPSO	2-6, 4-6, 5-7, 4-12	153.474
MDEP	2-6, 4-6, 5-7, 4-12	153.474

Because the MDEP and MDPSO algorithms yielded the same optimal intentional strategies, the performance of these algorithms was evaluated in order to validate the effectiveness of the proposed MDEP algorithm compared to the MDPSO algorithm. Figure 5.5 shows the convergence curves for the MDEP and MDPSO algorithms.

Referring to Figure 5.5, it can be observed that the MDEP and MDPSO algorithms reached convergence within 50 iterations. However, the MDEP algorithm converged faster than the MDPSO algorithm. The performance of these algorithms was analyzed and the results are summarized in Table 5.8.

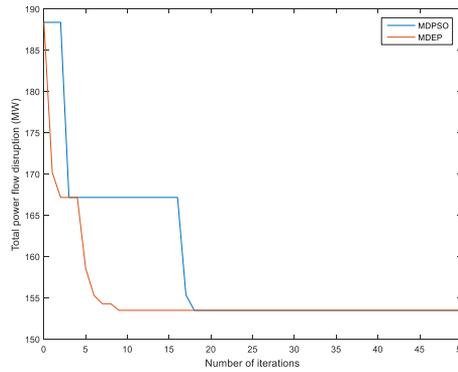


Figure 5.5. Convergence Curves for the MDEP and MDPSO Algorithms for Case Study C2

Table 5.8. Comparison of the Performance between the MDEP and MDPSO Algorithms

Algorithm	No. of iterations required by the algorithm to reach convergence	Computational time (sec)
MDEP	9	341.514
MDPSO	18	683.791

Based on the results, the MDEP algorithm attained convergence on the 9th iteration whereas the MDPSO attained convergence on the 18th iteration. Furthermore, the time taken by the MDEP algorithm to attain convergence was 341.514 sec, which was faster compared with the MDPSO algorithm (683.791 sec). Thus, the proposed MDEP algorithm was superior to the MDPSO algorithm because it produced the optimal intentional islanding strategy within a fewer number of iterations and computational time.

5.4.2.3 Determination of the Optimal Intentional Islanding Strategy Using the MDEP Algorithm

The optimal intentional islanding strategy obtained from the MDEP algorithm yielded two stand-alone islands with five and 25 buses in Island 1 and Island 2, respectively. The optimal intentional islanding strategy for this case study was 2–6, 4–6, 5–7, and 4–12, resulting in a total power flow disruption of 153.474 MW. The one-line diagram for the optimal intentional islanding strategy is shown in Figure 5.6 while the graph model of the islanded islands is shown in Appendix B (Figure B.2).

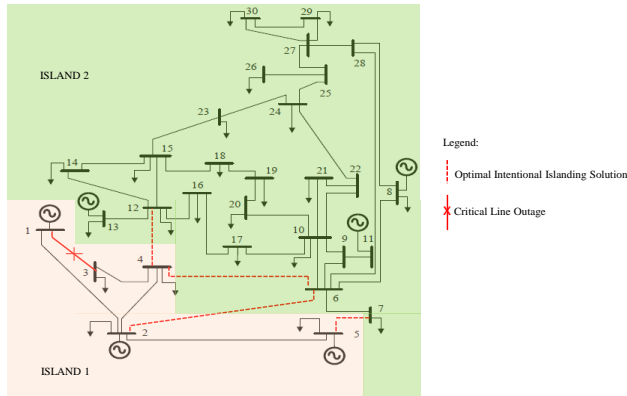


Figure 5.6. One-Line Diagram for Case Study C2

Next, the power balance criterion was evaluated for each island. Table 5.9 shows the results for Island 1 and Island 2 before and after intentional islanding implementation.

Table 5.9. Results for Island 1 and Island 2 Before and After Intentional Islanding Implementation: Case Study C2

Island 1				
Buses in Island 1	Generator information		Active power (MW)	
	Generator	Max. limit (MW)	Pre-islanding ΣP_{gen}	Post-islanding ΣP_{gen}
1–5	G _{1*}	300	247.640	80.580
	G ₂	40	40.000	40.000
	G ₅	40	10.000	10.000
Total generated power, P_{gen} (MW)			297.640	130.580
Total load, P_{load} (MW)			125.900	125.900
Total power loss, P_{loss} (MW)			18.266	4.6800
Total power imbalance, P_{imb} (MW)			153.474	0.000
Total amount of load to be shed, P_{shed} (MW)			—	—
Island 2				
Buses in Island 2	Generator information		Active power (MW)	
	Generator	Max. limit (MW)	Pre-islanding ΣP_{gen}	Post-islanding ΣP_{gen}
6–30	G _{8*}	50	10.000	49.655
	G ₁₁	30	0.000	30.000
	G ₁₃	40	0.000	40.000
Total generated power, P_{gen} (MW)			10.000	119.655
Total load, P_{load} (MW)			157.500	118.400
Total power loss, P_{loss} (MW)			1.523	1.255
Total power imbalance, P_{imb} (MW)			-149.023	0.000
Total amount of load to be shed, P_{shed} (MW)			—	39.1

*slack bus

Referring to Table 5.9, there was a power surplus of 153.474 MW in Island 1 prior to intentional islanding. The slack bus, G_1 , was located in this island and hence, load flow analysis was carried out to obtain the new system parameters in the island. It was found that the slack bus, G_1 , reduced its generated power from 247.640 MW to 80.580 MW in order to fulfil the power balance criteria in the island, as shown in Table 5.9 (post-islanding column for Island 1). Finally, the power balance criterion in Island 1 was met and therefore, the load shedding scheme was not executed. Island 1 was capable of operating as a balanced, stand-alone island.

In Island 2, there was a power deficit of 149.023 MW in the pre-islanding condition. Because there was no slack bus available in the island, generator bus, G_8 was selected as the slack bus to perform the load flow analysis. However, the slack bus, G_8 , was not able to compensate for the high power deficit in the island because the value exceeded its maximum power limit. To solve this problem, generator buses, G_{11} and G_{13} were operated at their maximum power limits. However, these generator buses were still unable to fulfil the loads in the island. Hence, the MDEP-based load shedding scheme was executed, where the loads at buses 14, 17, 19, 20, 24, and 26 (total amount: 39.100 MW) were shed to attain load-generation balance in the island. With the load shedding scheme, Island 2 fulfils the power balance criterion and it could operate as a balanced, stand-alone island, as shown in Table 5.9 (post-islanding column for Island 2). Detail information on the load, P_{load} and generated power, P_{gen} connected to each bus for each island are shown in Appendix B (Table B.10).

Following this, the voltage of each bus was checked for all islands, as in the previous case studies. The voltage of each bus for all islands was determined to be within the allowable voltage limits, as shown in Appendix B (Table B.11). The islands were also checked to identify if there were violations in the transmission line capacity. The power flow for each transmission line in these islands was found to be less than transmission line capacity limit. The results of the transmission line power flow analysis for Case Study C2 are presented in Appendix B (Table B.12).

5.4.3 Case Study C3

For Case Study C3, the optimal intentional islanding strategy was determined following the outage of critical line 3–4. Intentional islanding was implemented by splitting the system into three islands based on the coherent groups of generators: $G_1 = \{1, 2, 5, 13\}$, $G_2 = \{8\}$, and $G_3 = \{11\}$.

5.4.3.1 Determination of the Initial Intentional Islanding Solution Following a Critical Line Outage

The initial intentional islanding solution following a critical line outage and the corresponding total power flow disruption, P_{disrup} , are shown in Table 5.10. The graph model of the initial intentional islanding solution for Case Study C3 is given in Appendix B (Figure B.3).

Table 5.10. Initial Intentional Islanding Solution for Case Study C3

Initial intentional islanding solution	Total power flow disruption, P_{disrup} (MW)
6–8, 6–9, 6–10, 19–20, 10–17, 22–24, 24–25, 6–28	107.411

It can be seen from Table 5.10 that the initial intentional islanding solution consisting of eight cutsets obtained from the graph theory approach produced a total power flow disruption, P_{disrup} , of 107.411 MW. This initial solution was used to facilitate the MDEP algorithm in determining the optimal intentional islanding strategy.

5.4.3.2 Evaluation of the MDEP Algorithm

The proposed MDEP algorithm was analyzed using the IEEE 30-bus test system and the result was then compared with the MDPSO algorithm as presented in Table 5.11. Both of these algorithms yielded the same optimal intentional islanding strategy, where the total power flow disruption, P_{disrup} , was 92.353 MW.

Table 5.11. Comparison of the Optimal Intentional Islanding Strategies for Case Study C3

Algorithm	Optimal intentional islanding strategy	$\sum P_{disrup}$ (MW)
MDPSO	6–8, 6–9, 6–10, 16–17, 18–19, 23–24, 24–25, 6–28	92.353
MDEP	6–8, 6–9, 6–10, 16–17, 18–19, 23–24, 24–25, 6–28	92.353

Because the MDEP and MDPSO algorithms produced the same optimal intentional islanding strategy, the performance of these algorithms was assessed in terms of the number of iterations required by the algorithm to reach convergence and the computational time. Figure 5.7 shows the convergence curves for the MDEP and MDPSO algorithms.

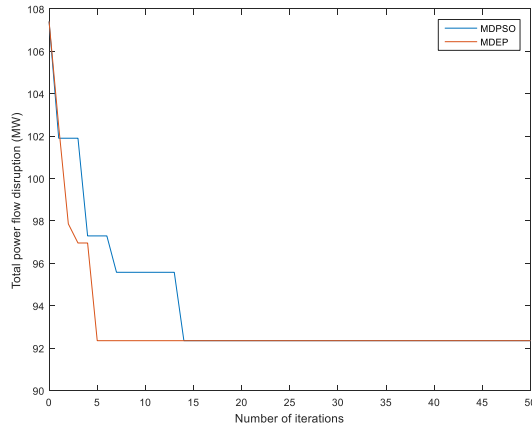


Figure 5.7. Convergence Curves for the MDEP and MDPSO Algorithms for Case Study C3

It can be observed that both algorithms achieved convergence within 50 iterations. As in the previous case studies, the MDEP algorithm converged faster than the MDPSO algorithm. The performance of the MDEP and MDPSO algorithms was analyzed and the results are summarized in Table 5.12.

Table 5.12. Comparison of the Performance Between the MDEP and MDPSO Algorithms

Algorithm	No. of iterations required by the algorithm to reach convergence	Computational time (sec)
MDEP	5	427.325
MDPSO	14	1200.235

Based on the results, the MDEP algorithm achieved convergence on the 5th iteration whereas the MDPSO algorithm achieved convergence on the 14th iteration. Furthermore, the MDEP consumed less computational time to achieve convergence (427.325 sec) compared with the MDPSO algorithm (1200.235 sec). The results indicated that the proposed MDEP algorithm was superior to the MDPSO algorithm because it attained the optimal solution within a fewer number of iterations and computational time.

5.4.3.3 Determination of the Optimal Intentional Islanding Strategy Using the MDEP Algorithm

The optimal intentional islanding strategy obtained from the MDEP algorithm resulted in three stand-alone islands with 14, seven, and nine buses in Island 1, Island 2, and Island 3, respectively. The optimal intentional islanding strategy for this case study was 6–8, 6–9, 6–10, 16–17, 18–19, 23–24, 24–25, and 6–28, producing a total power flow disruption of 92.353 MW. The one-line diagram for the optimal intentional islanding strategy is shown in Figure 5.8 while the graph model of the islanded islands is shown in Appendix B (Figure B.4).

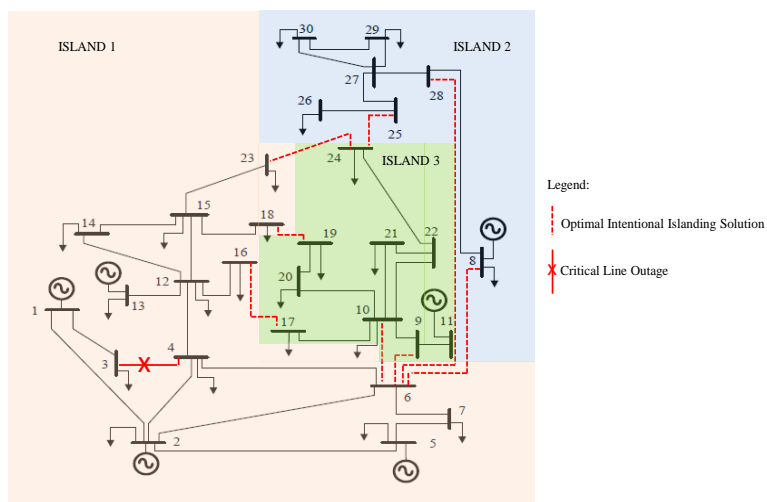


Figure 5.8. One-Line Diagram for Case Study C3

Next, the power balance criterion was assessed for each island. Table 5.13 shows the results for Islands 1–3 before and after intentional islanding implementation.

Table 5.13. Results for Islands 1–3 Before and After Intentional Islanding Implementation: Case Study C3

Island 1				
Buses in Island 1	Generator information		Active power (MW)	
	Generator	Max. limit (MW)	Pre-islanding ΣP_{gen}	Post-islanding ΣP_{gen}
1–7, 12–16, 18, 23	G _{1*}	300	247.153	143.057
	G ₂	40	40.000	40.000
	G ₅	40	10.000	10.000
	G ₁₃	40	0.000	0.000
Total generated power, P_{gen} (MW)			297.153	193.057
Total load, P_{load} (MW)			184.200	184.200
Total power loss, P_{loss} (MW)			22.770	8.857
Total power imbalance, P_{imb} (MW)			90.183	0.000
Total amount of load to be shed, P_{shed} (MW)			—	—
Island 2				
Buses in Island 2	Generator information		Active power (MW)	
	Generator	Max. limit (MW)	Pre-islanding ΣP_{gen}	Post-islanding ΣP_{gen}
8, 25–30	G _{8*}	50	10.000	47.064
Total generated power, P_{gen} (MW)			10.000	47.064
Total load, P_{load} (MW)			46.500	46.500
Total power loss, P_{loss} (MW)			0.411	0.564
Total power imbalance, P_{imb} (MW)			–36.911	0.000
Total amount of load to be shed, P_{shed} (MW)			—	—
Island 3				
Buses in Island 3	Generator information		Active power (MW)	
	Generator	Max. limit (MW)	Pre-islanding ΣP_{gen}	Post-islanding ΣP_{gen}
9–11, 17, 19–22, 24	G ₁₁	30	0.000	29.731
Total generated power, P_{gen} (MW)			0.000	29.731
Total load, P_{load} (MW)			52.700	29.400
Total power loss, P_{loss} (MW)			0.379	0.331
Total power imbalance, P_{imb} (MW)			–53.079	0.000
Total amount of load to be shed, P_{shed} (MW)			—	23.300

*slack bus

It can be observed from Table 5.13 that there was a power surplus of 90.183 MW in Island 1 prior to intentional islanding. The slack bus, G₁, was located in this island and thus, load flow analysis was carried out to obtain the new system parameters. The slack bus, G₁, reduced its generated power from 247.153 MW to 143.057 MW in order to fulfil the power balance criterion in the island, as shown in Table 5.13 (post-

islanding column for Island 1). Finally, the power balance criterion in Island 1 was met ($P_{imb} = 0.000$ MW) and thus, the load shedding scheme was not executed. Island 1 was capable of operating as a balanced, stand-alone island.

In Island 2, there was a small power deficit of 36.911 MW in the pre-islanding condition. Since there was no slack bus available in the island, the only generator bus available in the island, G_8 , was selected as the slack bus. Load flow analysis was then carried out and it was found that the slack bus was able to compensate for the power deficit in the island, as shown in Table 5.13 (post-islanding column for Island 2). Finally, the power balance criterion was met and thus, the load shedding scheme was not executed. Island 2 could operate as a balanced, stand-alone island.

In Island 3, there was a power deficit of 53.079 MW in the pre-islanding condition. Likewise, there was no slack bus available in this island and therefore, generator bus, G_{11} was selected as the slack bus because it was the only generator bus available in the island. However, generator bus, G_{11} was unable to fulfil the loads in the island because the value exceeded its maximum power limit. Hence, the MDEP-based load shedding scheme was executed, where the loads at buses 10 and 21 (total amount: 23.300 MW) were shed to achieve the load-generation balance in the island. The execution of the load shedding scheme produced a balanced, stand-alone island that fulfilled the power balance criterion, as shown in Table 5.13 (post-islanding column for Island 3). Detail information on the load, P_{load} and generated power, P_{gen} connected to each bus for each island are shown in Appendix B (Table B.13).

The voltage profiles were checked for all islands, as in the previous case studies. The voltage of each bus for all islands was found to be within the allowable voltage limits, as shown in Appendix B (Table B.14). Transmission line power flow analysis was performed for both islands to ensure that there were no violations in the transmission line capacity. The power flow in each transmission line for all islands was determined to be less than the transmission line capacity limit. The results of the transmission line power flow analysis for Case Study C3 are provided in Appendix B (Table B.15).

5.5 Critical Line Outages for the IEEE 39-Bus Test System

In this section, the three most critical lines outage for the IEEE 39-bus test system with three different coherent groups of generators were analyzed for intentional islanding implementation. The three most critical line outages for the IEEE 39-bus test system are shown in Table 5.14.

Table 5.14. Three Most Critical Line Outages for the IEEE 39-Bus Test System

Critical line	MVA violation (%) of the corresponding overloaded lines	Coherent groups of generators
Line 13–14	Line 4–5 (201.0256) Line 5–6 (130.8519) Line 6–11 (113.1314)	$G_1 = \{30,31,32,37,38,39\}$ $G_2 = \{33,34,35,36\}$
Line 4–5	Line 13–14 (186.4672) Line 10–13 (173.1765) Line 4–14 (136.7750) Line 6–11 (126.1351)	$G_1 = \{30,37,38\}$ $G_2 = \{31,32,39\}$ $G_3 = \{33,34,35,36\}$
Line 10–13	Line 4–5 (168.5445) Line 5–6 (115.8914)	$G_1 = \{30,31,37\}$ $G_2 = \{33,35,36\}$ $G_3 = \{34,38\}$ $G_4 = \{32,39\}$

The first critical line obtained from the N-1 contingency analysis for the IEEE 39-bus test system was Line 13–14, as shown in Table 5.14. The failure (tripping) of this line would cause other lines (Lines 4–5, 5–6, and 6–11) to overload and trip. The second critical line was Line 4–5, where the failure of this line would cause Lines 13–14, 10–13, 4–14, and 6–11 to overload and trip. Finally, the third critical line identified was Line 10–13, which would cause Lines 4–5 and 5–6 to overload and trip. Without a suitable intentional islanding strategy, when each of these critical lines trips, the system may experience severe cascading failures, resulting in a partial or total system blackout.

The results obtained from this analysis, including the determination of the initial intentional islanding strategy following a critical line outage based on graph theory and the determination of the optimal intentional islanding strategy using the proposed MDEP algorithm for each case study are presented in the following subsections.

5.5.1 Case Study C4

For Case Study C4, the optimal intentional islanding strategy was determined following the outage of Critical Line 13–14. In this case study, intentional islanding was implemented by partitioning the system into two islands based on the coherent groups of generators: $G_1 = \{30, 31, 32, 37, 38, 39\}$ and $G_2 = \{33, 34, 35, 36\}$.

5.5.1.1 Determination of the Initial Intentional Islanding Solution Following a Critical Line Outage

As in the previous case studies, the initial intentional islanding solution following a critical line outage was determined based on the desired number of islands and coherent groups of generators. The initial solution and the corresponding total power flow disruption, P_{disrup} , are presented in Table 5.15. The graph model of the initial intentional islanding solution following a critical line outage for Case Study C4 is shown in Appendix B (Figure B.5).

Table 5.15. Initial Intentional Islanding Solution for Case Study C4

Initial intentional islanding solution	Total power flow disruption, P_{disrup} (MW)
14–15, 17–18, 17–27	526.440

It can be seen from Table 5.15 that the initial intentional islanding solution with three cutsets produced a total power flow disruption, P_{disrup} , of 526.440 MW. This initial solution was used to aid the MDEP algorithm in determining the optimal intentional islanding strategy.

5.5.1.2 Evaluation of the MDEP Algorithm

The proposed MDEP algorithm was analyzed using the IEEE 39-bus test system in order to determine the optimal intentional islanding strategy following a critical line outage. The result was then compared with the developed MDPSO algorithm as tabulated in Table 5.16. Both of these algorithms yielded the same optimal

intentional islanding strategy with a total power flow disruption, P_{disrup} , of 136.718 MW.

Table 5.16. Comparison of the Optimal Intentional Islanding Strategies for Case Study C4

Algorithm	Optimal intentional islanding strategy	$\sum P_{disrup}$ (MW)
MDPSO	15–16, 17–18, 26–27	136.718
MDEP	15–16, 17–18, 26–27	136.718

The MDEP and MDPSO algorithms produced the same optimal intentional islanding strategy and therefore, the performance of these algorithms was analyzed in order to validate the effectiveness of the proposed MDEP algorithm compared to the MDPSO algorithm. Figure 5.9 shows the convergence curves for the MDEP and MDPSO algorithms.

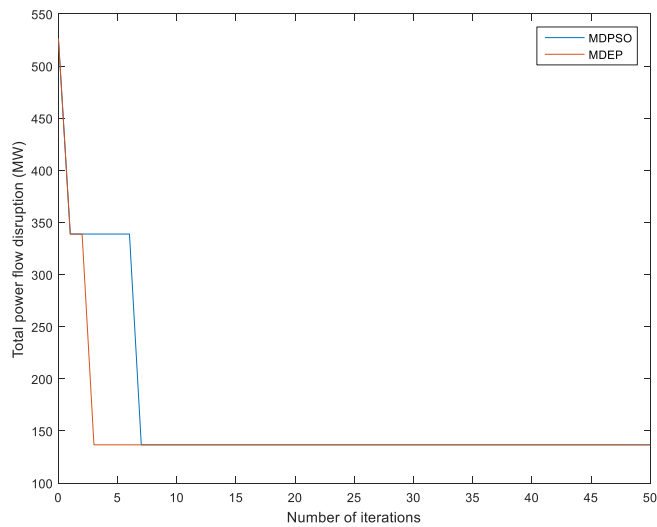


Figure 5.9. Convergence Curves for the MDEP and MDPSO Algorithms for Case Study C4

It can be observed the MDEP algorithm converged faster compared with the MDPSO algorithm. The performance of the MDEP and MDPSO algorithms was analyzed and the results are shown in Table 5.17.

Table 5.17. Comparison of the Performance Between the MDEP and MDPSO Algorithms

Algorithm	No. of iterations required by the algorithm to reach convergence	Computational time (sec)
MDEP	3	136.170
MDPSO	7	318.007

Based on the results, the MDEP algorithm attained convergence on the 3rd iteration whereas the MDPSO algorithm attained convergence on the 7th iteration. Furthermore, the MDEP algorithm attained convergence within a shorter time (136.170 sec) compared with the MDPSO algorithm (318.007 sec). The results proved that the proposed MDEP algorithm was superior to the MDPSO algorithm because it yielded the optimal intentional islanding strategy within a fewer number of iterations and thereby reducing the computational time.

5.5.1.3 Determination of the Optimal Intentional Islanding Strategy Using the MDEP Algorithm

The optimal intentional islanding strategy obtained from the MDEP algorithm produced two stand-alone islands with 26 and 13 buses in Island 1 and Island 2, respectively. The optimal intentional islanding strategy for this case study was 15–16, 17–18, and 26–27, which produced a total power flow disruption of 136.718 MW. The one-line diagram for the optimal intentional islanding strategy is shown in Figure 5.10. The graph model of the islanded islands is shown in Appendix B (Figure B.6).

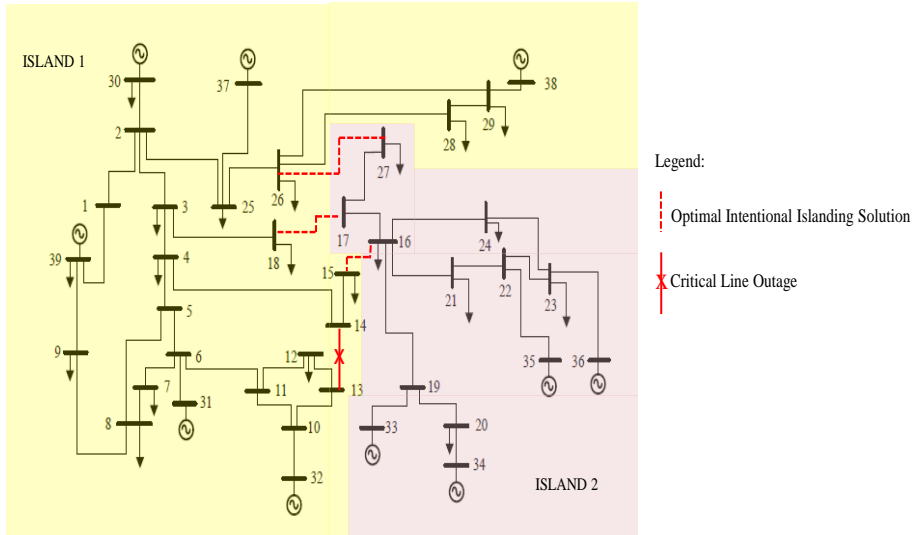


Figure 5.10. One-Line Diagram for Case Study C4

Next, the power balance criterion was evaluated for each island. Table 5.18 shows the results for the Island 1 and Island 2 before and after intentional islanding implementation.

Referring to Table 5.18, there was a power deficit of 1062.462 MW in Island 1 prior to intentional islanding. The slack bus, G_{31} , was located in this island and therefore, load flow analysis was executed to obtain the new system parameters in the island. The slack bus, G_{31} , was unable to compensate for the power deficit because the value was higher than its maximum power limit. To fulfil the loads in the island, generator buses, G_{30} , G_{32} , G_{37} , G_{38} , and G_{39} were operated at their maximum power limits. However, the generator buses were still unable to compensate for the power deficit in the island. Thus, the MDEP-based load shedding scheme was executed, where the loads at buses 1, 9, and 12 (total amount: 112.630 MW) were shed to achieve load-generation balance in the island. This action allows island to fulfil the power balance criteria, as shown in Table 5.18 (post-islanding column for Island 1).

Table 5.18. Results for Island 1 and Island 2 Before and After Intentional Islanding Implementation: Case Study C4

Island 1				
Buses in Island 1	Generator information		Active power (MW)	
	Generator	Max. limit (MW)	Pre-islanding	Post-islanding
			ΣP_{gen}	ΣP_{gen}
1–15, 18, 25, 26, 28–32, 37–39	G ₃₀	500	250.000	500.000
	G _{31*}	650	650.000	643.821
	G ₃₂	650	550.000	650.000
	G ₃₇	540	440.000	540.000
	G ₃₈	730	430.000	730.000
	G ₃₉	1000	800.000	1000.000
Total generated power, P_{gen} (MW)			3120.000	4063.821
Total load, P_{load} (MW)			4134.130	4021.500
Total power loss, P_{loss} (MW)			48.332	42.321
Total power imbalance, P_{imb} (MW)			-1062.462	0.000
Total amount of load to be shed, P_{shed} (MW)			—	112.630
Island 2				
Buses in Island 2	Generator information		Active power (MW)	
	Generator	Max. limit (MW)	Pre-islanding	Post-islanding
			ΣP_{gen}	ΣP_{gen}
16–17, 19–24, 27, 33–36	G ₃₃	632	500.000	500.000
	G ₃₄	508	508.000	508.000
	G _{35*}	670	550.000	566.198
	G ₃₆	560	560.000	560.000
Total generated power, P_{gen} (MW)			2118.000	2134.198
Total load, P_{load} (MW)			2120.100	2120.100
Total power loss, P_{loss} (MW)			13.987	14.098
Total power imbalance, P_{imb} (MW)			-16.087	0.000
Total amount of load to be shed, P_{shed} (MW)			—	—

*slack bus

It can be observed from Table 5.18 that there was a power deficit of 16.087 MW in Island 2. Generator bus, G₃₅ was selected as the slack bus to perform the load flow analysis because there was no slack bus available in this island. The slack bus increased its generated power to fulfil the power balance criterion in the island, as shown in Table 5.18 referring to post-islanding column for Island 2. Finally, the power balance criterion in Island 2 was met and therefore, the load shedding scheme was not executed. Island 2 was capable of operating as a balanced, stand-alone island. Detail information on the load, P_{load} and generated power, P_{gen} connected to each bus for each island are shown in Appendix B (Table B.16).

Next, the voltage profiles were checked for all islands after intentional islanding. The voltage of each bus for both islands was determined to be within the allowable

voltage limits, as shown in Appendix B (Table B.17). In addition, transmission line power flow analysis was performed for both islands to ascertain that there were no violations in the transmission line capacity. It was found that the power flow in each transmission line in Island 1 and Island 2 was less than the transmission line capacity limit. The results of the transmission line power flow analysis for Case Study C4 are shown in Appendix B (Table B.18).

5.5.2 Case Study C5

For Case Study C5, the optimal intentional islanding strategy was determined following the outage of Critical Line 4–5. Intentional islanding was implemented by splitting the system into three islands based on the coherent groups of generators: $G_1 = \{30, 37, 38\}$, $G_2 = \{31, 32, 39\}$, and $G_3 = \{33, 34, 35, 36\}$.

5.5.2.1 Determination of the Initial Intentional Islanding Solution Following a Critical Line Outage

The initial intentional islanding solution following a critical line outage and the corresponding total power flow disruption, P_{disrup} , for Case Study C5 are shown in Table 5.19. The graph model of the initial intentional islanding solution following a critical line outage is presented in Appendix B (Figure B.7).

Table 5.19. Initial Intentional Islanding Solution for Case Study C5

Initial intentional islanding solution	Total power flow disruption, P_{disrup} (MW)
1–39, 4–14, 14–15, 17–18, 17–27	1504.087

It can be seen from Table 5.19 that the initial intentional islanding solution comprising five cutsets obtained from the graph theory approach produced a total power flow disruption, P_{disrup} , of 1504.087 MW. The initial solution was used to facilitate the MDEP algorithm in determining the optimal intentional islanding strategy.

5.5.2.2 Evaluation of the MDEP Algorithm

The proposed MDEP algorithm was analyzed using the IEEE 39-bus test system and the result was then compared with the MDPSO algorithm as summarized in Table 5.20. Both of these algorithms provided the same optimal intentional islanding strategies with five cutsets, yielding a total power flow disruption, P_{disrup} , of 363.895 MW.

Table 5.20. Comparison of the Optimal Intentional Islanding Strategies for Case Study C5

Algorithm	Optimal intentional islanding strategy	ΣP_{disrup} (MW)
MDPSO	1-2, 3-4, 3-18, 15-16, 26-27	363.895
MDEP	1-2, 3-4, 3-18, 15-16, 26-27	363.895

The MDEP and MDPSO algorithms produced the same optimal intentional islanding strategy and therefore, the performance of these algorithms was analyzed in terms of the number of iterations required by the algorithm to reach convergence and the computational time. Figure 5.11 shows the convergence curves for the MDEP and MDPSO algorithms.

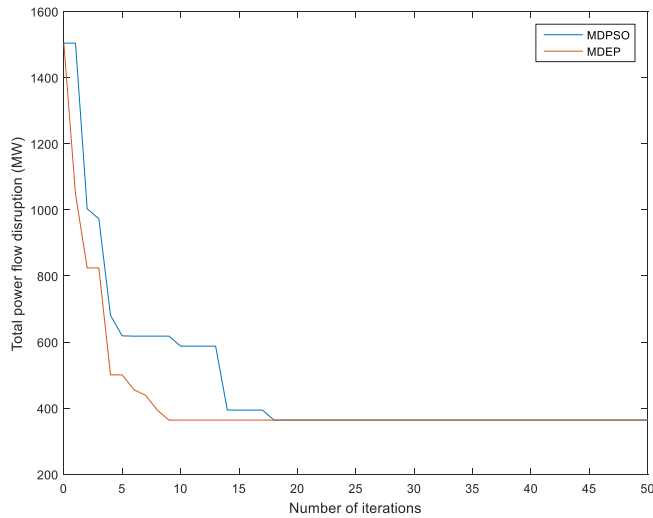


Figure 5.11. Convergence Curves for the MDEP and MDPSO Algorithms for Case Study C5

It can be seen that the MDEP algorithm converged faster compared with the MDPSO algorithm. The performance of the MDEP and MDPSO algorithms was analyzed and the results are tabulated in Table 5.21.

Table 5.21. Comparison of the Performance Between the MDEP and MDPSO Algorithms

Algorithm	No. of iterations required by the algorithm to reach convergence	Computational time (sec)
MDEP	9	617.645
MDPSO	18	1255.706

Based on the results, the MDEP algorithm achieved convergence on the 9th iteration whereas the MDPSO algorithm achieved convergence on the 18th iteration. Furthermore, the time taken by MDEP algorithm to achieve convergence was 617.645 sec, which was approximately twice faster than the MDPSO algorithm (1255.706 sec). The MDEP algorithm was proven to be better than the MDPSO algorithm because it produced the optimal solution within a fewer number of iterations, with significantly reduced computational time.

5.5.2.3 Determination of the Optimal Intentional Islanding Strategy Using the MDEP Algorithm

The optimal intentional islanding strategy obtained from the MDEP algorithm resulted in three stand-alone islands with nine, 16, and 14 buses in Island 1, Island 2, and Island 3, respectively. The optimal intentional islanding strategy for this case study was 1–2, 3–4, 3–18, 15–16, and 26–27 with a total power flow disruption of 363.895 MW. The one-line diagram for the optimal intentional islanding strategy is shown in Figure 5.12. The graph model of the islanded islands is shown in Appendix B (Figure B.8).

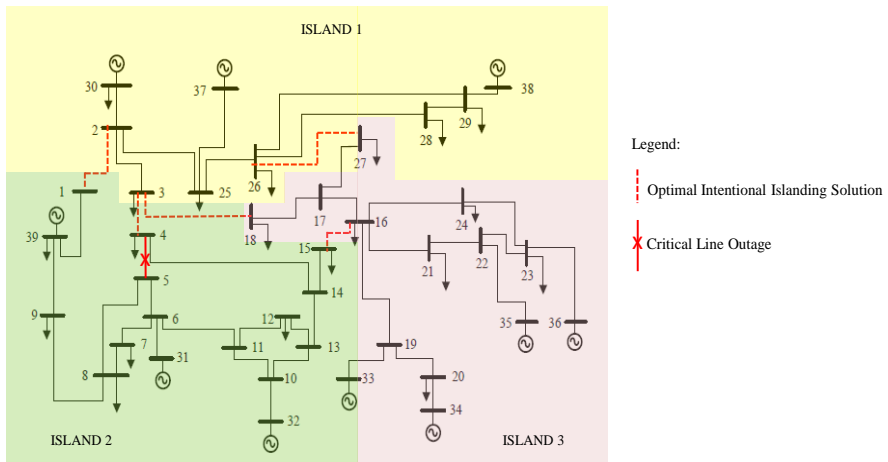


Figure 5.12. One-Line Diagram for Case Study C5

Next, the power balance criterion was assessed for each island. Table 5.22 shows the results for Islands 1–3 before and after intentional islanding implementation.

Referring to Table 5.22, there was a power deficit of 60.009 MW in Island 1 during pre-islanding condition. A new slack bus was assigned because there was no slack bus available in this island. Generator bus, G_{38} was selected as the new slack bus to carry out the load flow analysis. The results showed that the slack bus, G_{38} , increased its generated power from 430.000 MW to 490.841 MW to fulfil the power balance criterion in the island. Finally, the power balance criterion in Island 1 was met, as shown in Table 5.22 (post-islanding column for Island 1). Therefore, the load shedding scheme was not executed and Island 1 could operate as a balanced, stand-alone island.

It can be seen from Table 5.22 that there was a huge power deficit of 844.925 MW in the pre-islanding condition in Island 2. The slack bus, G_{31} , was situated in this island and thus, load flow analysis was executed to obtain the new system parameters. It was found that the slack bus, G_{31} , was not able to compensate for the high power deficit in the island, which exceeded its maximum power limit. To overcome this problem, generator buses, G_{32} and G_{39} were operated at their maximum power limits. However, the generator buses were still unable to fulfil the loads in the island. Therefore, the MDEP-based load shedding scheme was executed, where the loads at

buses 7, 12, 15, and 31 (total amount: 571.530 MW) to attain load-generation balance in the island. This action is important to ensure successful islanding implementation and produce a balanced, stand-alone island. The execution of the load shedding scheme allows the island to fulfil the power balance criterion, as shown in Table 5.22, referring to post-islanding column for Island 2.

Table 5.22. Results for Islands 1–3 Before and After Intentional Islanding Implementation: Case Study C5

Island 1				
Buses in Island 1	Generator information		Active power (MW)	
	Generator	Max. limit (MW)	Pre-islanding	Post-islanding
			ΣP_{gen}	ΣP_{gen}
2–3, 25–26, 28–30, 37–38	G ₃₀	500	250.000	250.000
	G ₃₇	540	440.000	440.000
	G _{38*}	730	430.000	490.841
Total generated power, P_{gen} (MW)			1120.000	1180.841
Total load, P_{load} (MW)			1174.500	1174.500
Total power loss, P_{loss} (MW)			5.509	6.341
Total power imbalance, P_{imb} (MW)			-60.009	0.000
Total amount of load to be shed, P_{shed} (MW)			—	—
Island 2				
Buses in Island 2	Generator information		Active power (MW)	
	Generator	Max. limit (MW)	Pre-islanding	Post-islanding
			ΣP_{gen}	ΣP_{gen}
1, 4–15, 31–32, 39	G _{31*}	650	650.000	590.294
	G ₃₂	650	550.000	650.000
	G ₃₉	1000	800.000	1000.000
Total generated power, P_{gen} (MW)			2000.000	2240.294
Total load, P_{load} (MW)			2801.630	2230.100
Total power loss, P_{loss} (MW)			43.295	10.194
Total power imbalance, P_{imb} (MW)			-844.925	0.000
Total amount of load to be shed, P_{shed} (MW)			—	571.530
Island 3				
Buses in Island 3	Generator information		Active power (MW)	
	Generator	Max. limit (MW)	Pre-islanding	Post-islanding
			ΣP_{gen}	ΣP_{gen}
16–24, 27, 33–36	G ₃₃	632	500.000	587.185
	G ₃₄	508	508.000	508.000
	G _{35*}	670	550.000	640.852
	G ₃₆	560	560.000	560.000
Total generated power, P_{gen} (MW)			2118.000	2296.037
Total load, P_{load} (MW)			2278.100	2278.100
Total power loss, P_{loss} (MW)			14.271	17.937
Total power imbalance, P_{imb} (MW)			-174.371	0.000
Total amount of load to be shed, P_{shed} (MW)			—	—

*slack bus

Similar to Island 2, there was a huge power deficit of 174.371 MW in Island 3 in the pre-islanding condition. Since there was no slack bus available in Island 3, a new slack bus was assigned from the existing generator buses. Generator bus, G_{35} was selected as the slack bus to conduct the load flow analysis. It was found that the slack bus was unable to compensate for the power deficit and therefore, generator buses, G_{33} , G_{34} , and G_{36} shared the loads equally to compensate for the power deficit in the island. Finally, the generated power increased for all generators and the power balance criterion in Island 3 was met ($P_{imb} = 0.000$ MW), as shown in Table 5.22, referring to post-islanding column for Island 3. Detail information on the load, P_{load} and generated power, P_{gen} connected to each bus for each island are shown in Appendix B (Table B.19).

The voltage of each bus was checked for all islands, as in the previous case studies. The voltage profile for each island was determined to be within the allowable voltage limits, as shown in Appendix B (Table B.20). Transmission line power flow analysis was subsequently carried out for Islands 1–3 to ensure that there were no violations in the transmission line capacity. The power flow in each transmission line for all three islands was less than the transmission line capacity limit. The results of the transmission line power flow analysis for Case Study C5 are provided in Appendix B (Table B.21).

5.5.3 Case Study C6

For Case Study C6, the optimal intentional islanding strategy was determined following the outage of Critical Line 10–13. In this case study, intentional islanding was implemented by partitioning the system into four islands based on the coherent groups of generators: $G_1 = \{30, 31, 37\}$, $G_2 = \{33, 35, 36\}$, $G_3 = \{34, 38\}$, and $G_4 = \{32, 39\}$.

5.5.3.1 Determination of the Initial Intentional Islanding Solution Following a Critical Line Outage

The initial intentional islanding solution following a critical line outage and the corresponding total power flow disruption, P_{disrup} , are shown in Table 5.23. The graph model of the initial intentional islanding solution following a critical line outage is presented in Appendix B (Figure B.9).

Table 5.23. Initial Intentional Islanding Solution for Case Study C6

Initial intentional islanding solution	Total power flow disruption, P_{disrup} (MW)
1–39, 5–6, 5–8, 12–13, 14–15, 16–17, 17–18, 25–26	1477.591

It can be seen from Table 5.23 that the initial intentional islanding solution with eight cutsets produced a total power flow disruption, P_{disrup} , of 1477.591 MW. This initial solution was used to aid the MDEP algorithm in determining the optimal intentional islanding strategy.

5.5.3.2 Evaluation of the MDEP Algorithm

The proposed MDEP algorithm was analyzed using the IEEE 39-bus test system and the result was then compared with the MDPSO algorithm as tabulated in Table 5.24. Both of the algorithms produced the same optimal intentional islanding strategy with a total power flow disruption, P_{disrup} , of 1068.291 MW.

Table 5.24. Comparison of the Optimal Intentional Islanding Strategies for Case Study C6

Algorithm	Optimal intentional islanding strategy	ΣP_{disrup} (MW)
MDPSO	1–39, 4–5, 12–13, 15–16, 16–17, 17–18, 25–26	1068.291
MDEP	1–39, 4–5, 12–13, 15–16, 16–17, 17–18, 25–26	1068.291

The convergence curve and computational time for both algorithms were further evaluated in order to validate the effectiveness of the proposed MDEP algorithm

compared to the MDPSO algorithm. Figure 5.13 shows the convergence curves for the MDEP and MDPSO algorithms.

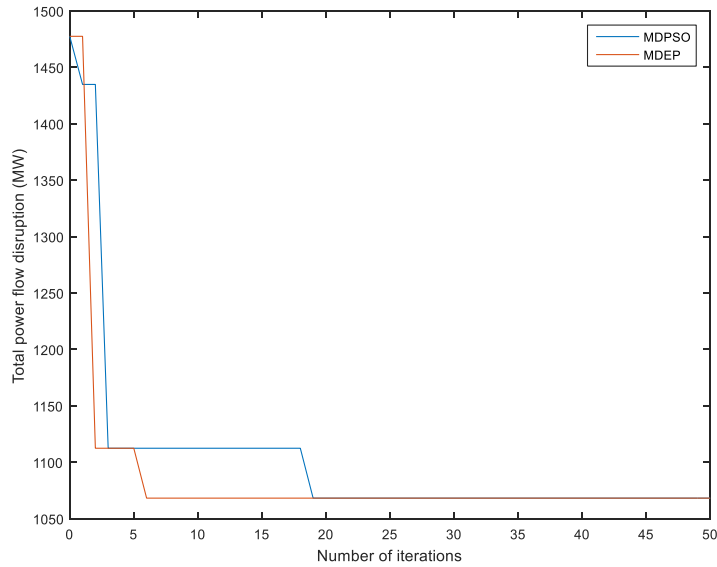


Figure 5.13. Convergence Curves for the MDEP and MDPSO Algorithms for Case Study C6

It can be observed the MDEP algorithm converged faster compared with the MDPSO algorithm. The performance of the MDEP and MDPSO algorithms (in terms of the number of iterations required by the algorithm to reach convergence and the computational time) was compared and the results are summarized in Table 5.25.

Table 5.25. Comparison of the Performance Between the MDEP and MDPSO Algorithms

Algorithm	No. of iterations required by the algorithm to reach convergence	Computational time (sec)
MDEP	6	620.492
MDPSO	19	1981.988

Based on the results, the MDEP algorithm attained convergence on the 6th iteration whereas the MDPSO algorithm attained convergence on the 19th iteration. In addition, the time taken by MDEP algorithm was 620.492 sec, which was approximately three times faster compared with the MDPSO algorithm (1981.988

sec). The results indicated that the proposed MDEP algorithm was superior to the MDPSO algorithm because it was capable of obtaining the optimal solution within a fewer number of iterations and computational time.

5.5.3.3 Determination of the Optimal Intentional Islanding Strategy Using the MDEP Algorithm

The optimal intentional islanding strategy obtained from the MDEP algorithm produced four stand-alone islands with 12, 10, 7, and 10 buses in Island 1, Island 2, Island 3, and Island 4, respectively. The optimal intentional islanding strategy for this case study was 1–39, 4–5, 12–13, 15–16, 16–17, 17–18, and 25–26, resulting in a total power flow disruption of 1068.291 MW. The one-line diagram for the optimal intentional islanding strategy is shown in Figure 5.14. The graph model of the islanded islands is shown in Appendix B (Figure B.10).

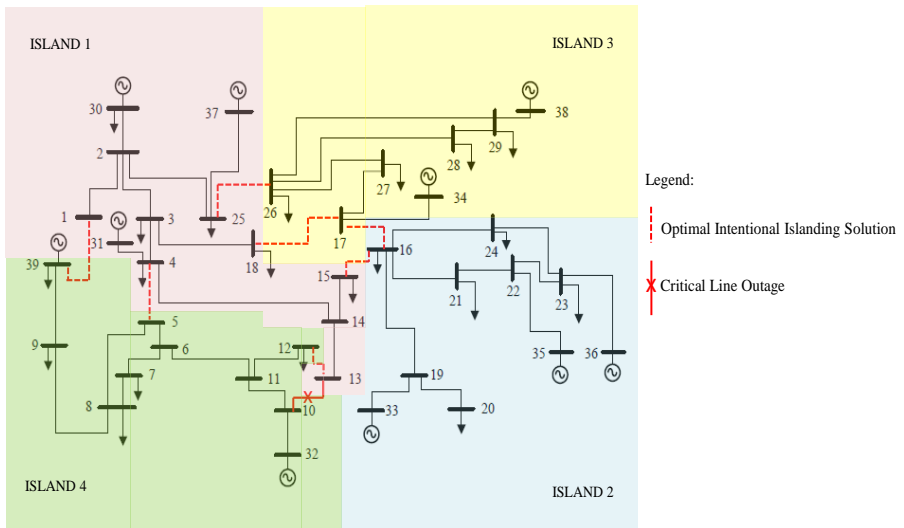


Figure 5.14. One-Line Diagram for Case Study C6

The power balance criterion was evaluated for each island. Table 5.26 shows the results for Islands 1–4 before and after intentional islanding implementation.

Table 5.26. Results for Islands 1–4 Before and After Intentional Islanding Implementation: Case Study C6

Island 1				
Buses in Island 1	Generator information		Active power (MW)	
			Pre-islanding	Post-islanding
	Generator	Max. limit (MW)	ΣP_{gen}	ΣP_{gen}
1–4, 13–15, 18, 25, 30–31, 37	G ₃₀	500	250.000	500.000
	G _{31*}	650	650.000	609.426
	G ₃₇	540	440.000	540.000
Total generated power, P_{gen} (MW)			1340.000	1649.426
Total load, P_{load} (MW)			1630.800	1630.80
Total power loss, P_{loss} (MW)			10.436	18.626
Total power imbalance, P_{imb} (MW)			-301.236	0.000
Total amount of load to be shed, P_{shed} (MW)			—	—
Island 2				
Buses in Island 2	Generator information		Active power (MW)	
			Pre-islanding	Post-islanding
	Generator	Max. limit (MW)	ΣP_{gen}	ΣP_{gen}
16, 19–24, 33, 35–36	G ₃₃	632	500.000	620.875
	G _{35*}	670	550.000	669.442
	G ₃₆	560	560.000	560.000
Total generated power, P_{gen} (MW)			1610.000	1850.317
Total load, P_{load} (MW)			1839.100	1839.100
Total power loss, P_{loss} (MW)			12.651	11.217
Total power imbalance, P_{imb} (MW)			-241.751	0.000
Total amount of load to be shed, P_{shed} (MW)			—	—
Island 3				
Buses in Island 3	Generator information		Active power (MW)	
			Pre-islanding	Post-islanding
	Generator	Max. limit (MW)	ΣP_{gen}	ΣP_{gen}
17, 26–29, 34, 38	G ₃₄	508	508.000	508.000
	G _{38*}	730	430.000	409.310
Total generated power, P_{gen} (MW)			938.000	917.310
Total load, P_{load} (MW)			909.500	909.500
Total power loss, P_{loss} (MW)			5.084	7.810
Total power imbalance, P_{imb} (MW)			23.416	0.000
Total amount of load to be shed, P_{shed} (MW)			—	—
Island 4				
Buses in Island 4	Generator information		Active power (MW)	
			Pre-islanding	Post-islanding
	Generator	Max. limit (MW)	ΣP_{gen}	ΣP_{gen}
5–12, 32, 39	G ₃₂	650	550.000	650.000
	G _{39*}	1000	800.000	998.240
Total generated power, P_{gen} (MW)			1350.000	1648.240
Total load, P_{load} (MW)			1874.830	1641.030
Total power loss, P_{loss} (MW)			8.494	7.210
Total power imbalance, P_{imb} (MW)			-533.324	0.000
Total amount of load to be shed, P_{shed} (MW)			—	233.800

*slack bus

Based on the results in Table 5.26, there was a power deficit of 301.236 MW in Island 1 during pre-islanding condition. The slack bus, G_1 , was located in this island and therefore, load flow analysis was conducted to obtain the new system parameters. The slack bus, G_{31} , was unable to compensate for the power deficit because the value was higher than its maximum power limit. Therefore, generators G_{30} and G_{37} were operated at their maximum power limits to achieve load-generation balance in the island. Finally, the power balance criterion in Island 1 was met and therefore, the load shedding scheme was not executed. Island 1 could operate as a balanced, stand-alone island.

In Island 2, there was a power deficit of 241.751 MW in the pre-islanding condition. Since there was no slack bus available in the island, generator bus, G_{35} was selected as the slack bus to perform the load flow analysis. It was found that the slack bus, G_{35} , was unable to compensate for the power deficit in the island because the power deficit exceeded its maximum power limit. Hence, the generators shared the loads equally to address the power deficit problem in the island. It can be observed from Table 5.26 (post-islanding column for Island 2) that the generated power increased for all generators after intentional islanding. Finally, the power balance criterion in Island 2 was met and thus, the load shedding scheme was not executed. Island 2 was balanced and it could operate as a stand-alone island.

In Island 3, there was a power surplus of 23.416 MW in the pre-islanding condition. Similar to Island 2, there was no slack bus available in the island and therefore, generator bus, G_{38} was selected as the slack bus to conduct the load flow analysis. The slack bus, G_{38} , reduced its generated power from 430.000 MW to 409.310 MW to compensate for the power surplus in the island. Finally, the power balance criterion was met ($P_{imb} = 0.000$ MW), as shown in Table 5.26 (post-islanding column for Island 3). Thus, the load shedding scheme was not executed and the island was capable of operating as a balanced, stand-alone island.

In Island 4, there was a huge power deficit of 533.324 MW during pre-islanding condition. There was no slack bus available in the island and hence, generator bus, G_{39} was selected as the slack bus to perform the load flow analysis. The slack bus,

G_{39} , was unable to compensate for the high power deficit in the island because the value exceeded its maximum power limit. Therefore, Generator G_{32} was operated at its maximum power limit in order to address this problem, but it was still unable to fulfil the loads of the island. Thus, the MDEP-based load shedding scheme was executed, where the load at Bus 7 (233.800 MW) was shed in order to attain load-generation balance in the island. This action is important to ensure successful islanding implementation and produce a balanced, stand-alone island. Moreover, the execution of the load shedding scheme allows Island 4 to fulfil the power balance criterion, as shown in Table 5.26 (post-islanding column for Island 4). Detail information on the load, P_{load} and generated power, P_{gen} connected to each bus for each island are shown in Appendix B (Table B.22).

Next, the voltage profiles for each island after intentional islanding were checked, as in the previous case studies. The voltage of each bus for all islands was found to be within the allowable voltage limits, as shown in Appendix B (Table B.23). Transmission line power flow analysis was also performed for both islands to ensure that there were no violations in the transmission line capacity. The power flow in each transmission line for all islands was determined to be less than the transmission line capacity limit. The results of the transmission line power flow analysis for Case Study C6 are provided in Appendix B (Table B.24).

5.6 Critical Line Outages for the IEEE 118-Bus Test System

In this section, the three most critical line outages for the IEEE 118-bus test system with three different coherent groups of generators were analyzed for intentional islanding implementation. The three most critical line outages for the IEEE 118-bus test system are tabulated in Table 5.27.

The first critical line obtained from the N-1 contingency analysis for the IEEE 118-bus test system was Line 68–69, as shown in Table 5.27. The failure (tripping) of this line would cause other lines (Lines 69–77, 49–69, 47–69, 8–30, and 23–24) to overload and trip. The second critical line was Line 68–81, where the failure of this line would cause Lines 69–77, 8–30, 68–69, and 30–38 to overload and trip. Finally, the third critical line was Line 81–80, which would cause Lines 69–77, 8–30, 68–69,

and 30–38 to overload and trip. Without the appropriate intentional islanding strategy, when each of these critical lines trip, the system may experience severe cascading failures, culminating in a partial or total system blackout.

Table 5.27. Three Most Critical Line Outages for the IEEE 118-Bus Test System

Critical line	MVA violation (%) of the corresponding overloaded lines	Coherent groups of generators
Line 68–69	Line 69–77 (406.5685) Line 49–69 (152.3773) Line 47–69 (150.4911) Line 8–30 (127.9398) Line 23–24 (115.9981)	$G_1 = \{10,12,25,26,31\}$ $G_2 = \{46,49,54,59,61,65,66,69,80,87,89,100,103,111\}$
Line 68–81	Line 69–77 (252.7408) Line 8–30 (128.8497) Line 68–69 (108.0271) Line 30–38 (103.8515)	$G_1 = \{10,12,25,26,31\}$ $G_2 = \{46,49,54,59,61,65,66,69,80\}$ $G_3 = \{87,89,100,103,111\}$
Line 81–80	Line 69–77 (252.7134) Line 8–30 (128.8510) Line 68–69 (108.2306) Line 30–38 (103.9290)	$G_1 = \{10,12,25,26,31\}$ $G_2 = \{46,49,54,59,61,65,66,69,80\}$ $G_3 = \{87,89\}$ $G_4 = \{100,103,111\}$

The results obtained from this analysis, including the determination of the initial intentional islanding strategy following a critical line outage based on graph theory and the determination of the optimal intentional islanding strategy using the proposed MDEP algorithm for each case study are presented in the following subsections.

5.6.1 Case Study C7

For Case Study C7, the optimal intentional islanding strategy was determined following the outage of Critical Line 68–69. In this case study, intentional islanding was implemented by splitting the system into two islands based on the coherent groups of generators: $G_1 = \{10, 12, 25, 26, 31\}$ and $G_2 = \{46, 49, 54, 59, 61, 65, 66, 69, 80, 87, 89, 100, 103, 111\}$.

5.6.1.1 Determination of the Initial Intentional Islanding Solution Following a Critical Line Outage

The initial intentional islanding solution following a critical line outage and the total corresponding power flow disruption, P_{disrup} , are shown in Table 5.28. The graph model of the initial intentional islanding solution following a critical line outage is presented in Appendix B (Figure B.11).

Table 5.28. Initial Intentional Islanding Solution for Case Study C7

Initial intentional islanding solution	Total power flow disruption, P_{disrup} (MW)
19–34, 33–37, 30–38, 24–70, 71–72	406.973

It can be seen from Table 5.28 that the initial intentional islanding solution consisting of five cutsets obtained from graph theory produced a total power flow disruption, P_{disrup} , of 406.973 MW. This initial solution was used to facilitate the MDEP algorithm in determining the optimal intentional islanding strategy.

5.6.1.2 Evaluation of the MDEP Algorithm

The MDEP algorithm was analyzed using the IEEE 118-bus test system and the result was compared with MDPSO algorithm as tabulated in Table 5.29. It can be seen that both of these algorithms produced the same optimal intentional islanding strategy with a total power flow disruption, P_{disrup} , of 345.834 MW.

Table 5.29. Comparison of the Optimal Intentional Islanding Strategies for Case Study C7

Algorithm	Optimal intentional islanding strategy	ΣP_{disrup} (MW)
MDPSO	23–24, 15–33, 19–34, 30–37	345.834
MDEP	23–24, 15–33, 19–34, 30–37	345.834

The convergence curve and computational time were further analyzed in order to validate the performance of the proposed MDEP algorithm compared to the MDPSO algorithm. Figure 5.15 shows the convergence curves for MDEP and MDPSO algorithms.

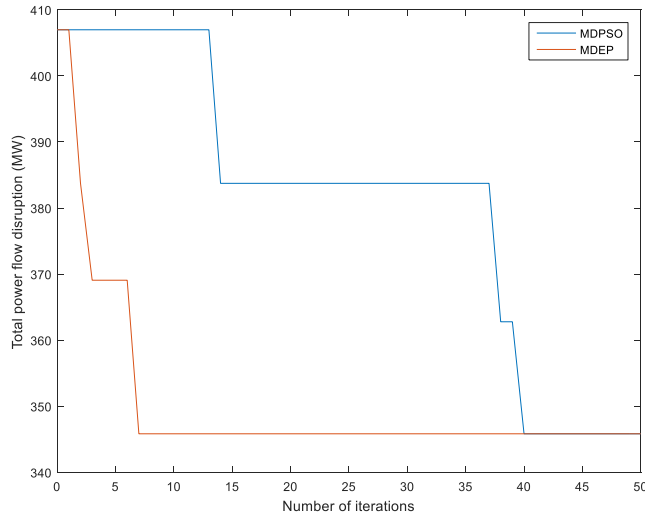


Figure 5.15. Convergence Curves for the MDEP and MDPSO Algorithms for Case Study C7

Based on Figure 5.15, it can be observed that the MDEP and MDPSO algorithms reached convergence within 50 iterations. However, the MDEP algorithm converged faster compared with the MDPSO algorithm. The performance of these algorithms was assessed in terms of the number of iterations required by the algorithm to reach convergence and the computational time and the results are tabulated in Table 5.30.

Table 5.30. Comparison of the Performance Between the MDEP and MDPSO Algorithms

Algorithm	No. of iterations required by the algorithm to reach convergence	Computational time (sec)
MDEP	7	1947.963
MDPSO	40	11431.424

Based on the results, the MDEP algorithm achieved convergence on the 7th iteration whereas the MDPSO algorithm only achieved convergence on the 19th iteration. Furthermore, the time taken by the MDEP algorithm to achieve convergence was 1947.963 sec, which was significantly shorter than that for the MDPSO algorithm (11431.424 sec). The results proved that the proposed MDEP algorithm was superior to the MDPSO algorithm because it was capable of obtaining the optimal solution within a fewer number of iterations and computational time.

5.6.1.3 Determination of the Optimal Intentional Islanding Strategy Using the MDEP Algorithm

The optimal intentional islanding strategy obtained from the MDEP algorithm produced two stand-alone islands with 35 and 83 buses in Island 1 and Island 2, respectively. The optimal intentional islanding strategy for this case study was 23–24, 15–33, 19–34, and 30–38, with a total power flow disruption of 345.834 MW. The one-line diagram for the optimal intentional islanding strategy is shown in Figure 5.16. The graph model of the islanded islands is shown in Appendix B (Figure B.12).

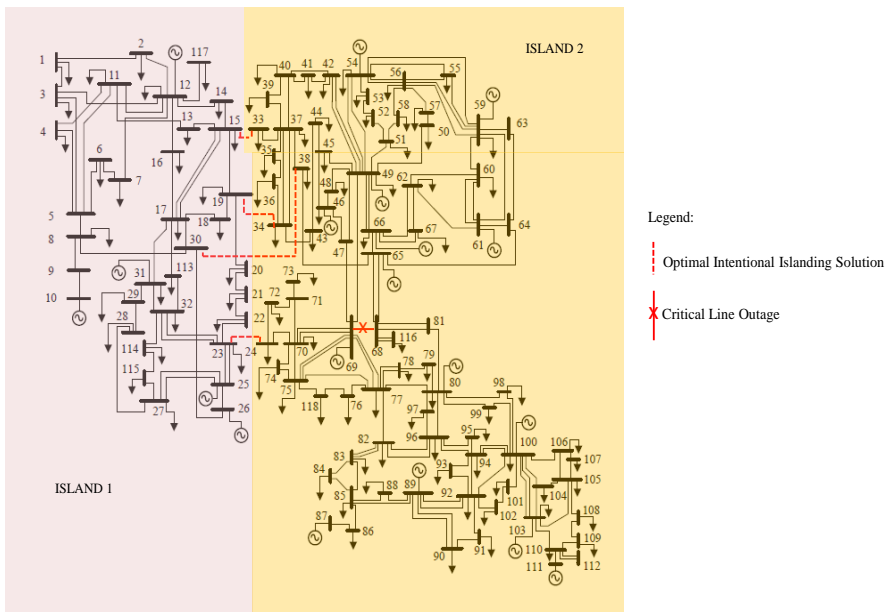


Figure 5.16. One-Line Diagram for Case Study C7

Next, the power balance criterion was assessed for each island. Table 5.31 shows the results for Island 1 and Island 2 before and after intentional islanding implementation.

Table 5.31. Results for Island 1 and Island 2 Before and After Intentional Islanding Implementation: Case Study C7

Island 1				
Buses in Island 1	Generator information		Active power (MW)	
	Generator	Max. limit (MW)	Pre-islanding	Post-islanding
			ΣP_{gen}	ΣP_{gen}
1–23, 25–32, 113–115, 117	G ₁₀	200	30.000	200.000
	G ₁₂	100	100.000	100.000
	G ₂₅	200	200.000	200.000
	G _{26*}	300	220.000	278.724
	G ₃₁	100	100.000	100.000
Total generated power, P_{gen} (MW)			650.000	878.724
Total load, P_{load} (MW)			963.000	853.000
Total power loss, P_{loss} (MW)			32.834	25.724
Total power imbalance, P_{imb} (MW)			-345.834	0.000
Total amount of load to be shed, P_{shed} (MW)			—	110.000
Island 2				
Buses in Island 2	Generator information		Active power (MW)	
	Generator	Max. limit (MW)	Pre-islanding	Post-islanding
			ΣP_{gen}	ΣP_{gen}
24, 33–112, 116, 118	G ₄₆	100	100.000	100.000
	G ₄₉	200	200.000	200.000
	G ₅₄	148	48.000	48.000
	G ₅₉	250	155.000	155.000
	G ₆₁	160	160.000	160.000
	G ₆₅	400	391.000	391.000
	G ₆₆	400	392.000	392.000
	G _{69*}	800	800.000	758.681
	G ₈₀	500	477.000	477.000
	G ₈₇	100	100.000	100.000
	G ₈₉	600	300.000	300.000
	G ₁₀₀	300	252.000	252.000
	G ₁₀₃	140	40.000	40.000
G ₁₁₁	136	36.000	36.000	
Total generated power, P_{gen} (MW)			3451.000	3409.681
Total load, P_{load} (MW)			3279.000	3279.000
Total power loss, P_{loss} (MW)			396.506	130.681
Total power imbalance, P_{imb} (MW)			-224.506	0.000
Total amount of load to be shed, P_{shed} (MW)			—	—

*slack bus

Referring to Table 5.31, there was a huge power deficit of 345.834 MW in Island 1 during pre-islanding condition. There was no slack bus available in this island and therefore, a new slack bus was assigned. Generator bus, G₂₆ was selected as the slack bus and load flow analysis is then carried out to obtain the new system parameters. It was found that the slack bus, G₂₆, was unable to compensate for the high power deficit in the island because the value exceeded its maximum power limit. Therefore, generator buses, G₁₀, G₁₂, G₂₅, and G₃₁ were operated at their maximum power limits

in order to address this problem. However, the generator buses were still unable to fulfil the loads in the island. Therefore, the MDEP-based load shedding scheme was executed, where the loads at Buses 12, 31, and 117 with a total amount of 110.000 MW were shed in order to achieve load-generation balance in the island. This action allows the island to meet the power balance criterion, as shown in Table 5.31, referring to post-islanding column for Island 1. Island 1 was capable of operating as a balanced, stand-alone island.

In Island 2, there was a power deficit of 224.506 MW in the pre-islanding condition. The original slack bus, G_{69} , was located in the island and therefore, load flow analysis was executed. The slack bus, G_{69} , reduced its generated power from 800.000 MW to 758.681 MW in order to fulfil the power balance criterion in the island, as shown in Table 5.31 with respect to post-islanding column for Island 2. Finally, the power balance criterion in Island 2 was met and thus, the load shedding scheme was not executed. Island 2 was capable of operating as a balanced, stand-alone island. Detail information on the load, P_{load} and generated power, P_{gen} connected to each bus for each island are shown in Appendix B (Table B.25).

Similar to the previous case studies, the voltage profiles were checked for each island to ensure that there were no voltage violations. The voltage of each bus for all islands was found to be within the allowable voltage limits, as shown in Appendix B (Table B.26). The islands were also checked to identify if there were violations in the transmission line capacity. The power flow in each transmission line for these islands was determined to be less than the transmission line capacity limit. The results of the transmission line power flow analysis for Case Study C7 are presented in Appendix B (Table B.27).

5.6.2 Case Study C8

For Case Study C8, the optimal intentional islanding strategy was determined following the outage of Critical Line 68–81. In this case study, intentional islanding was implemented by partitioning the system into three islands based on the coherent groups of generators: $G_1 = \{10, 12, 25, 26, 31\}$, $G_2 = \{46, 49, 54, 59, 61, 65, 66, 69, 80\}$, and $G_3 = \{87, 89, 100, 103, 111\}$.

5.6.2.1 Determination of the Initial Intentional Islanding Solution Following a Critical Line Outage

The initial intentional islanding solution following a critical line outage and the corresponding total power flow disruption, P_{disrup} , for this case study are shown in Table 5.32. The graph model of the initial intentional islanding solution following a critical line outage is shown in Appendix B (Figure B.13).

Table 5.32. Initial Intentional Islanding Solution for Case Study C8

Initial intentional islanding solution	Total power flow disruption, P_{disrup} (MW)
19–34, 33–37, 30–38, 24–70, 71–72, 82–83, 94–95, 94–96, 98–100, 99–100	652.544

It can be seen from Table 5.32 that the initial intentional islanding solution consisting of 10 cutsets obtained from the graph theory approach, yielded a total power flow disruption, P_{disrup} , of 652.544 MW. This initial solution was then used to aid the MDEP algorithm in determining the optimal intentional islanding strategy.

5.6.2.2 Evaluation of the MDEP Algorithm

The MDEP algorithm was analyzed using the IEEE 118-bus test system and the result was then compared with the MDPSO algorithm as presented in Table 5.33. It can be seen that the MDEP algorithm provided a better optimal intentional islanding strategy with a lower total power flow disruption ($P_{disrup} = 614.656$ MW) compared with the MDPSO algorithm.

Table 5.33. Comparison of the Optimal Intentional Islanding Strategies for Case Study C8

Algorithm	Optimal intentional islanding strategy	ΣP_{disrup} (MW)
MDPSO	15–33, 19–34, 30–38, 24–70, 71–72, 82–83, 94–95, 94–96, 98–100, 99–100	629.110
MDEP	15–33, 19–34, 30–38, 24–70, 24–72, 82–83, 94–95, 94–96, 98–100, 99–100	614.656

The convergence curves for the MDEP and MDPSO algorithms in this case study are shown in Figure 5.17. It can be observed that the MDEP algorithm was able to obtain

the optimal intentional islanding strategy with a lower minimal fitness function value within a fewer number of iterations compared with the MDPSO algorithm. The results proved that MDEP algorithm was the best algorithm to determine the optimal intentional islanding strategy in this research.

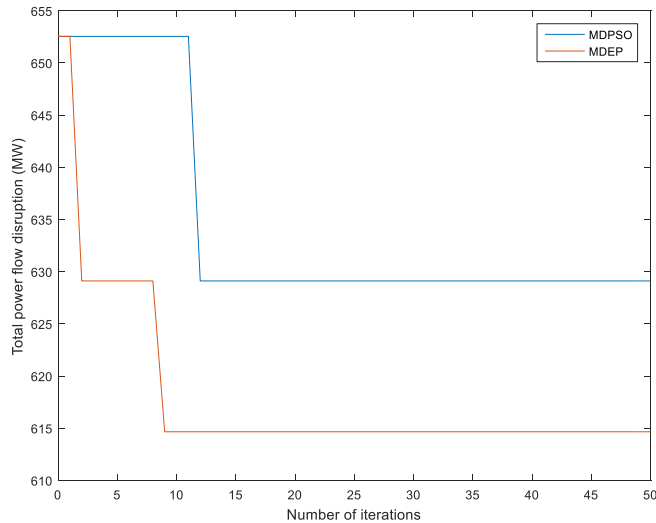


Figure 5.17. Convergence Curves for the MDEP and MDPSO Algorithms for Case Study C8

5.6.2.3 Determination of the Optimal Intentional Islanding Strategy Using the MDEP Algorithm

The optimal intentional islanding strategy obtained from the MDEP algorithm yielded three stand-alone islands with 36, 57, and 25 buses in Island 1, Island 2, and Island 3, respectively. The optimal intentional islanding strategy for this case study was 15–33, 19–34, 30–38, 24–70, 24–72, 82–83, 94–95, 94–96, 98–100, and 99–100, resulting in a total power flow disruption of 614.656 MW. The one-line diagram for the optimal intentional islanding strategy is shown in Figure 5.18. The graph model of the islanded islands is shown in Appendix B (Figure B.14).

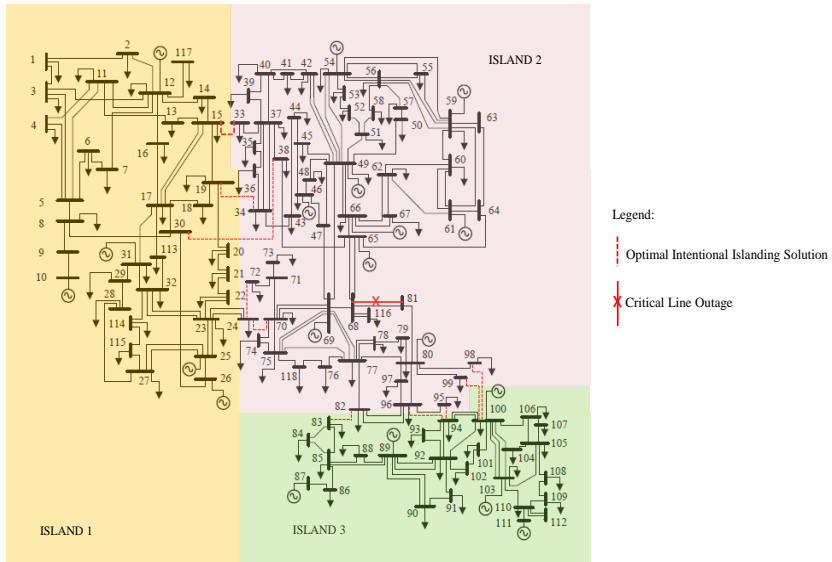


Figure 5.18. One-Line Diagram for Case Study C8

Next, the power balance criterion was evaluated for each island. Table 5.34 shows the results for Islands 1–3 before and after intentional islanding implementation.

Based on the results in Table 5.34, there was a huge power deficit of 355.296 MW in Island 1 prior to intentional islanding. Since there was no slack bus available in the island, generator bus, G_{26} was selected as the slack bus and load flow analysis was then performed to obtain the new system parameters. The slack bus, G_{26} , was unable to compensate for the high power deficit in the island because the value exceeded its maximum power limit. Therefore, generator buses, G_{10} , G_{12} , G_{25} , and G_{31} were operated at their maximum power limits in order to overcome the power deficit in the island. However, the generator buses were still unable to fulfil the loads in the island. Hence, the MDEP-based load shedding scheme was executed, where the loads at Buses 12, 19, and 20 (total amount: 110.000 MW) in order to attain load-generation balance in the island. This action allows the island to fulfil the power balance criterion, as shown in Table 5.34 with respect to post-islanding column for Island 1. Island 1 could operate as a balanced, stand-alone island.

Table 5.34. Results for Islands 1–3 Before and After Intentional Islanding Implementation: Case Study C8

Island 1				
Buses in Island 1	Generator information		Active power (MW)	
	Generator	Max. limit (MW)	Pre-islanding	Post-islanding
			ΣP_{gen}	ΣP_{gen}
1–32, 113–115, 117	G ₁₀	200	30.000	200.000
	G ₁₂	100	100.000	100.000
	G ₂₅	200	200.000	200.000
	G _{26*}	300	220.000	289.881
	G ₃₁	100	100.000	100.000
Total generated power, P_{gen} (MW)			650.000	889.881
Total load, P_{load} (MW)			976.000	866.000
Total power loss, P_{loss} (MW)			29.296	23.881
Total power imbalance, P_{imb} (MW)			-355.296	0.000
Total amount of load to be shed, P_{shed} (MW)			—	110.000
Island 2				
Buses in Island 2	Generator information		Active power (MW)	
	Generator	Max. limit (MW)	Pre-islanding	Post-islanding
			ΣP_{gen}	ΣP_{gen}
33–82, 95–99, 116, 118	G ₄₆	100	100.000	100.000
	G ₄₉	200	200.000	200.000
	G ₅₄	148	48.000	48.000
	G ₅₉	250	155.000	155.000
	G ₆₁	160	160.000	160.000
	G ₆₅	400	391.000	391.000
	G ₆₆	400	392.000	392.000
	G _{69*}	800	800.000	640.732
	G ₈₀	500	477.000	477.000
Total generated power, P_{gen} (MW)			2723.000	2563.732
Total load, P_{load} (MW)			2496.000	2496.000
Total power loss, P_{loss} (MW)			123.317	67.732
Total power imbalance, P_{imb} (MW)			103.683	0.000
Total amount of load to be shed, P_{shed} (MW)			—	—
Island 3				
Buses in Island 3	Generator information		Active power (MW)	
	Generator	Max. limit (MW)	Pre-islanding	Post-islanding
			ΣP_{gen}	ΣP_{gen}
83–94, 100–112	G ₈₇	100	100.000	100.000
	G _{89*}	600	300.000	367.494
	G ₁₀₀	300	252.000	252.000
	G ₁₀₃	140	40.000	40.000
	G ₁₁₁	136	36.000	36.000
Total generated power, P_{gen} (MW)			728.000	795.494
Total load, P_{load} (MW)			770.000	770.000
Total power loss, P_{loss} (MW)			23.096	25.494
Total power imbalance, P_{imb} (MW)			-65.096	0.000
Total amount of load to be shed, P_{shed} (MW)			—	—

*slack bus

It can be seen from Table 5.34 that there was a power surplus of 103.683 MW in the pre-islanding condition in Island 2. The slack bus, G_{31} , was located in this island and thus, load flow analysis was carried out to obtain the new system parameters in the island. It was found that the slack bus, G_{31} , reduced its generated power from 800.000 MW to 640.732 MW to achieve load-generation balance in the island. The power balance criterion in Island 2 was met and thus, the load shedding scheme was not executed. Island 2 could operate as a balanced, stand-alone island.

In Island 3, there was a power deficit of 65.096 MW in the pre-islanding condition. Similar to Island 1, there was no slack bus available in this island. Therefore, generator bus, G_{89} was selected as the slack bus to carry out the load flow analysis. The results showed that the slack bus, G_{89} , increased its generated power from 300.000 MW to 367.494 MW to fulfil the power balance criterion in the island, as shown in Table 5.34 (post-islanding column for Island 3). Thus, the load shedding scheme was not executed and Island 3 could operate as a balanced, stand-alone island. Detail information on the load, P_{load} and generated power, P_{gen} connected to each bus for each island are shown in Appendix B (Table B.28).

Next, the voltage profiles were checked for all islands. The voltage of each bus for all islands was determined to be within the allowable voltage limits, as shown in Appendix B (Table B.29). Following this, transmission line power flow analysis was performed for both islands to ascertain that there were no violations in the transmission line capacity. The power flow in each transmission line for Islands 1–3 was found to be less than the transmission line capacity limit. The results of the transmission line power flow analysis for Case Study C8 are provided in Appendix B (Table B.30).

5.6.3 Case Study C9

For Case Study C9, the optimal intentional islanding strategy was determined following the outage of Critical Line 81–80. Intentional islanding was implemented by splitting the system into four islands based on the coherent groups of generators: $G_1 = \{10, 12, 25, 26, 31\}$, $G_2 = \{46, 49, 54, 59, 61, 65, 66, 69, 80\}$, $G_3 = \{87, 89\}$, and $G_4 = \{100, 103, 111\}$.

5.6.3.1 Determination of the Initial Intentional Islanding Solution Following a Critical Line Outage

The initial intentional islanding solution following a critical line outage and the corresponding total power flow disruption, P_{disrup} , obtained for this case study are shown in Table 5.35. The graph model of the initial intentional islanding solution following a critical line outage is given in Appendix B (Figure B.15).

Table 5.35. Initial Intentional Islanding Solution for Case Study C9

Initial intentional islanding solution	Total power flow disruption, P_{disrup} (MW)
37–40, 39–40, 34–43, 38–65, 24–70, 71–72, 82–83, 92–94, 93–94, 94–95, 94–96, 92–100, 98–100, 99–100, 101–102	870.842

It can be seen from Table 5.35 that the initial intentional islanding solution consisting of 15 cutsets obtained from the graph theory approach produced a total power flow disruption, P_{disrup} , of 870.842 MW. This initial solution was further used to facilitate the MDEP algorithm in determining the optimal intentional islanding strategy.

5.6.3.2 Evaluation of the MDEP Algorithm

The proposed MDEP algorithm was analyzed using the IEEE 118-bus test system and the result was then compared with the MDPSO algorithm as presented in Table 5.36. It is evident that the MDEP algorithm was capable of determining a better optimal intentional islanding strategy with a lower total power flow disruption ($P_{disrup} = 830.253$ MW) compared with the MDPSO algorithm.

Table 5.36. Comparison of the Optimal Intentional Islanding Strategies for Case Study C9

Algorithm	Optimal intentional islanding strategy	ΣP_{disrup} (MW)
MDPSO	37–40, 39–40, 34–43, 38–65, 24–70, 24–72, 82–83, 92–94, 93–94, 94–95, 94–96, 92–100, 98–100, 99–100, 101–102	856.396
MDEP	23–24, 37–40, 39–40, 34–43, 38–65, 82–83, 92–93, 92–94, 94–95, 94–96, 92–100, 98–100, 99–100, 101–102	830.253

Figure 5.19 shows the convergence curves for the MDEP and MDPSO algorithms developed in this research. It can be observed that the MDEP algorithm produced a better optimal intentional islanding strategy with a lower minimal fitness function value compared with the MDPSO algorithm. In addition, the MDEP algorithm achieved the optimal solution within a fewer number of iterations compared with the MDPSO algorithm. Thus, the proposed MDEP algorithm was the best algorithm for intentional islanding in this research.

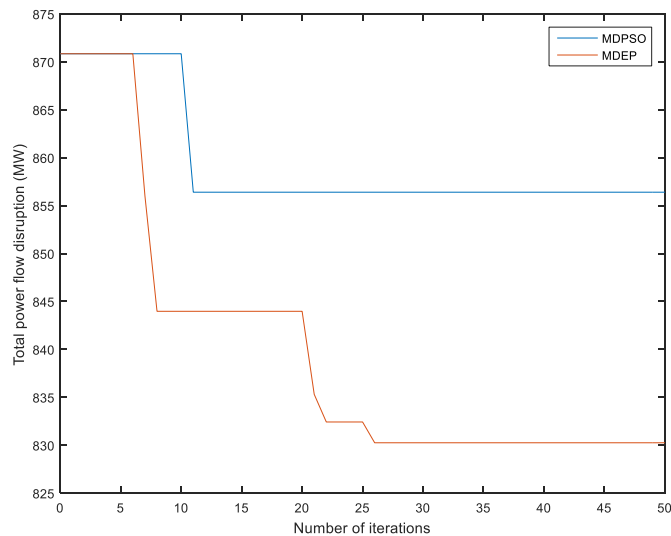


Figure 5.19. Convergence Curves for the MDEP and MDPSO Algorithms for Case Study C9

5.6.3.3 Determination of the Optimal Intentional Islanding Strategy Using the MDEP Algorithm

The optimal intentional islanding strategy obtained from the MDEP algorithm produced four stand-alone islands with 42, 51, 11, and 14 buses in Island 1, Island 2, Island 3, and Island 4, respectively. The optimal intentional islanding strategy for this case study was 23–24, 37–40, 39–40, 34–43, 38–65, 82–83, 92–93, 92–94, 94–95, 94–96, 92–100, 98–100, 99–100, and 101–102, resulting in a total power flow disruption of 830.253 MW. The one-line diagram of the optimal intentional islanding

strategy is shown in Figure 5.20. The graph model of the islanded islands is shown in Appendix B (Figure B.16).

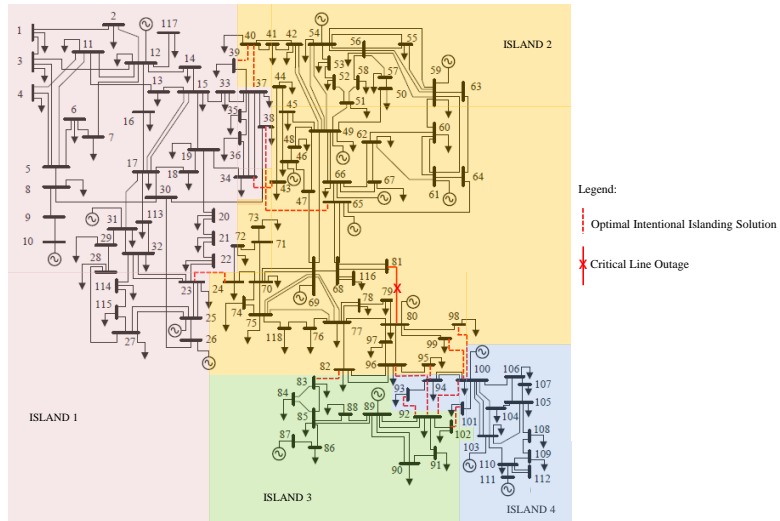


Figure 5.20. One-Line Diagram for Case Study C9

The power balance criterion was assessed for each island. Table 5.37 shows the results for Islands 1–4 before and after intentional islanding implementation.

Based on the results in Table 5.37, there was a power deficit of 533.604 MW in Island 1 during pre-islanding condition. A new slack bus was assigned because there was no slack bus available in the island. Generator bus, G_{26} was selected as the slack bus and load flow analysis was carried out to obtain the new system parameters. The slack bus, G_{26} , was not able to compensate for the high power deficit in the island because the value exceeded its maximum power limit. Therefore, generator buses, G_{10} , G_{12} , G_{25} , and G_{31} were operated at their maximum power limits to address the problem. However, the generator buses were still unable to fulfil the total loads. Thus, the MDEP-based load shedding scheme was executed, where the loads at Buses 7, 11, 13, 15, 17 and 18, with a total amount of 284.000 MW in order to attain load-generation balance in the island. This action allows the island to fulfil the power balance criterion, as shown in Table 5.37, referring to post-islanding column for Island 1. Island 1 could be operated as a balanced, stand-alone island.

Table 5.37. Results for Islands 1–4 Before and After Intentional Islanding Implementation: Case Study C9

Island 1				
Buses in Island 1	Generator information		Active power (MW)	
	Generator	Max. limit (MW)	Pre-islanding	Post-islanding
			ΣP_{gen}	ΣP_{gen}
1–23, 25–39, 113–115, 117	G ₁₀	200	30.000	200.000
	G ₁₂	100	100.000	100.000
	G ₂₅	200	200.000	200.000
	G _{26*}	300	220.000	275.659
	G ₃₁	100	100.000	100.000
Total generated power, P_{gen} (MW)			650.000	875.659
Total load, P_{load} (MW)			1136.000	852.000
Total power loss, P_{loss} (MW)			47.604	23.659
Total power imbalance, P_{imb} (MW)			-533.604	0.000
Total amount of load to be shed, P_{shed} (MW)			—	284.000
Island 2				
Buses in Island 2	Generator information		Active power (MW)	
	Generator	Max. limit (MW)	Pre-islanding	Post-islanding
			ΣP_{gen}	ΣP_{gen}
24, 40–82, 95–99, 116, 118	G ₄₆	100	100.000	100.000
	G ₄₉	200	200.000	200.000
	G ₅₄	148	48.000	48.000
	G ₅₉	250	155.000	155.000
	G ₆₁	160	160.000	160.000
	G ₆₅	400	391.000	391.000
	G ₆₆	400	392.000	392.000
	G _{69*}	800	800.000	486.415
	G ₈₀	500	477.000	477.000
Total generated power, P_{gen} (MW)			2723.000	2409.415
Total load, P_{load} (MW)			2336.000	2336.000
Total power loss, P_{loss} (MW)			124.821	73.415
Total power imbalance, P_{imb} (MW)			262.179	0.000
Total amount of load to be shed, P_{shed} (MW)			—	—
Island 3				
Buses in Island 3	Generator information		Active power (MW)	
	Generator	Max. limit (MW)	Pre-islanding	Post-islanding
			ΣP_{gen}	ΣP_{gen}
83–92, 102	G ₈₇	100	100.000	100.000
	G _{89*}	600	300.000	277.248
Total generated power, P_{gen} (MW)			400.000	377.248
Total load, P_{load} (MW)			367.000	367.000
Total power loss, P_{loss} (MW)			10.782	10.284
Total power imbalance, P_{imb} (MW)			22.218	0.000
Total amount of load to be shed, P_{shed} (MW)			—	—
Island 4				
Buses in Island 4	Generator information		Active power (MW)	
	Generator	Max. limit (MW)	Pre-islanding	Post-islanding
			ΣP_{gen}	ΣP_{gen}
93–94, 100–101, 103–112	G _{100*}	300	252.000	287.428
	G ₁₀₃	140	40.000	65.000
	G ₁₁₁	136	36.000	61.000

Island 4		
	Active power (MW)	
	Pre-islanding	Post-islanding
	$\sum P_{gen}$	$\sum P_{gen}$
Total generated power, P_{gen} (MW)	328.000	413.428
Total load, P_{load} (MW)	403.000	403.000
Total power loss, P_{loss} (MW)	13.017	10.428
Total power imbalance, P_{imb} (MW)	-88.017	0.000
Total amount of load to be shed, P_{shed} (MW)	—	—

*slack bus

It can be observed from Table 5.37 that there was a power surplus of 262.179 MW in the pre-islanding condition in Island 2. The slack bus, G₆₉, was located in the island and thus, load flow analysis was conducted to obtain the new system parameters. After intentional islanding, the slack bus reduced its generated power from 800.000 MW to 486.415 MW to achieve load-generation balance in the island. The power balance criterion in Island 2 was met and therefore, the load shedding scheme was not executed. Island 2 was capable of operating as a balanced, stand-alone island.

In Island 3, there was a small power surplus of 22.218 MW in the pre-islanding condition. A new slack bus was assigned in the island because there was no slack bus available in the island. Generator bus, G₈₉ was selected as the slack bus and load flow analysis was performed to determine the new system parameters. The slack bus, G₈₉, reduced its generated power from 300.000 MW to 277.248 MW in order to fulfil the power balance criterion in the island. Since the power balance was fulfilled, the load shedding scheme was not executed and Island 3 could operate as a balanced, stand-alone island.

In Island 4, there was a small power deficit of 88.017 MW. A new slack bus was assigned from the available generator buses because there was no slack bus available in the island. Hence, generator bus, G₁₀₀ was selected as the slack bus and load flow analysis was carried out to obtain the new system parameters. However, the slack bus, G₁₀₀, was unable to compensate for the high power deficit in the island because the value exceeded its maximum power limit. Therefore, generator buses, G₁₀₃ and G₁₁₁ shared the loads equally to compensate for the power deficit in the island. It is observed that the value of generations on all generator buses has increased in post-islanding column as shown in Table 5.37 (post-islanding column for Island 4).

Finally, the power balance criterion in Island 4 was met and therefore, load shedding scheme was not executed. Island 2 was capable of operating as a balanced, stand-alone island. Detail information on the load, P_{load} and generated power, P_{gen} connected to each bus for each island are shown in Appendix B (Table B.31).

Next, the voltage profiles were checked for all islands, similar to the previous case studies. The voltage of each bus for all islands was found to be within the allowable voltage limits, as shown in Appendix B (Table B.32). Following this, transmission line power flow analysis was performed for both islands to ascertain that there were no violations in the transmission line capacity. The power flow in each transmission line for all islands was determined to be less than the transmission line capacity limit. The results of the transmission line power flow analysis for Case Study C9 are presented in Appendix B (Table B.33).

5.7 Validation of the MDEP-Based Load Shedding Scheme

As described in Chapter 3 (Section 3.3.7), a discrete optimization algorithm was developed for the load shedding scheme in this research. Discrete optimization was chosen because the selection of buses for load shedding was discrete, i.e. Buses 3, 5, and 9. The performance of the MDEP-based load shedding scheme was validated and compared with that of the conventional EP and exhaustive search algorithms. The performance was assessed in terms of computational time and final optimal amount of load to be shed. MATLAB 10 (R2015a) on an Intel[®] Core™ i7-5500U CPU at 2.40 GHz with 8 GB of RAM was used to code these algorithms. In this investigation, four case studies (from Chapters 4 and 5) from the IEEE 30-bus and IEEE 39-bus test systems were used for the validation process. The results obtained for Case Study 6 (Island 2) are summarized in Table 5.38.

Table 5.38. Comparison of the Performance between the Conventional EP, Exhaustive Search, and MDEP Algorithms for Case Study 6 (Island 2) – Chapter 4

Power mismatch = 255.242 MW			
Algorithm	Optimal amount of load to be shed (MW)	Bus(es)	Computational time (sec)
Conventional EP	274.0	21	6.5116
Exhaustive search	274.0	21	0.7149
MDEP	274.0	21	2.3633

Table 5.38 shows the optimal amount of load to be shed obtained from the conventional EP, exhaustive search, and MDEP algorithms. The minimal amount of load to be shed was used as the fitness function for the optimization process. In this investigation, the total number of buses available for load shedding was 6. Based on the results, the conventional EP, exhaustive search, and MDEP algorithms obtained the same optimal amount of load to be shed (274.0 MW) for this case study. However, it can be seen that the exhaustive search algorithm obtains the optimal solution faster compared with the proposed MDEP and conventional EP algorithms. As explained in Chapter 2 (Section 2.10), the exhaustive search algorithm considers all of the possible combinations in order to determine the optimal solution. Since the total number of buses available for load shedding was only 6 in this case study, the exhaustive search algorithm was able to determine the optimal solution faster than the MDEP and conventional EP algorithms. However, the process of determining the optimal amount of load to be shed will be more time-consuming when the total number of available buses, n , increases for this algorithm. In contrast, the time taken by the MDEP algorithm to determine the optimal answer was 2.3633 sec, which was faster compared with that for the conventional EP algorithm (6.5116 sec). Because discrete mutation was used in the MDEP algorithm, this enables the optimum solution to be obtained quickly (less computational time) compared with the conventional EP algorithm.

Table 5.39. Comparison of the Performance between the Conventional EP, Exhaustive Search, and MDEP Algorithms for Case Study 6 (Island 4) – Chapter 4

Power mismatch = 55.227 MW			
Algorithm	Optimal amount of load to be shed (MW)	Bus(es)	Computational time (sec)
Conventional EP	233.8	7	5.5546
Exhaustive search	233.8	7	0.5649
MDEP	233.8	7	2.3484

Table 5.39 shows the optimal amount of load to be shed obtained from the conventional EP, exhaustive search, and MDEP algorithms for Case Study 6 (Island 4). In this case, the total number of buses available for load shedding was 5 and the results showed that all of the three algorithms produced the same optimal amount of load to be shed. As in the previous case study, the exhaustive search algorithm was capable of determining the optimal solution faster compared with the MDEP and

conventional EP algorithms. This can be attributed to the small number of possible load shedding solutions for the exhaustive search algorithm because there were only five buses available for load shedding in this case study. It is evident that the MDEP algorithm obtained the optimal solution within a shorter computational time (2.3484 sec), which was faster compared with the conventional EP algorithm.

Even though the exhaustive search method provides the optimal amount of load to be shed with the least computational time (0.5649 sec) for Case Study 6 (Island 2 and Island 4), the computational time of this algorithm will increase with an increase in the number of available buses. This will be demonstrated in the following case studies.

Case Study C1 (Island 2) from the IEEE 30-bus test system was used to further assess the performance of the conventional EP, exhaustive search, and MDEP algorithms and the results are summarized in Table 5.40.

Table 5.40. Comparison of the Performance between the Conventional EP, Exhaustive Search, and MDEP Algorithms for Case Study C1 (Island 2) – Chapter 5

Power mismatch = 35.054 MW			
Algorithm	Optimal amount of load to be shed (MW)	Bus(es)	Computational time (sec)
Conventional EP	35.7	19,21,24	5.4009
Exhaustive search	35.1	19,20,21,26,29	71.0422
MDEP	35.1	19,20,21,26,29	4.9869

Table 5.40 shows the optimal amount of load to be shed obtained from the conventional EP, exhaustive search, and MDEP algorithms. The total number of buses available for load shedding was 10 in this case study. It can be observed from the results that the exhaustive search and MDEP algorithms were able obtain a better optimal amount of load to be shed compared with conventional EP algorithm. The optimal amount of load to be shed determined from the MDEP algorithm was 35.1 MW with a computational time of 4.9869 sec. In contrast, the optimal amount of load to be shed obtained from the conventional EP algorithm was 35.7 MW with a computational time of 5.4009 sec. This can be attributed to the small changes in the Gaussian function used in the conventional EP algorithm, which does not have a

significant effect on the mutation process. Hence, the final optimal solution obtained from this algorithm is one of the solutions in the random initial population during the optimization process. Both the exhaustive search and MDEP algorithms were able to produce the same optimal amount of load to be shed for this case study. However, the time taken by the MDEP algorithm to obtain the optimal solution was 4.9869 sec, which was faster compared with the exhaustive search algorithm (71.0422 sec). This is likely because the exhaustive search algorithm determines the optimal solution (minimum amount of load to be shed) based on all possible combinations of the available buses in the system, as indicated by Equation 2.4 in Chapter 2. Hence, the computational time needed to determine the optimal amount of load to be shed will increase with an increase in the total number of available buses in the power system. The results indicated that the proposed MDEP algorithm was the best load shedding scheme in this research.

Table 5.41. Comparison of the Performance between the Conventional EP, Exhaustive Search, and MDEP Algorithms for Case Study C4 (Island 1) – Chapter 5

Power mismatch = 112.462 MW			
Algorithm	Optimal amount of load to be shed (MW)	Bus(es)	Computational time (sec)
Conventional EP	115.33	1, 12, 31	8.8957
Exhaustive search	112.63	1, 9, 12	89486.7264
MDEP	112.63	1, 9, 12	3.1935

Table 5.41 shows the optimal amount of load to be shed obtained from the conventional EP, exhaustive search, and MDEP algorithms for Case Study C4 (Island 1). The total number of buses available for load shedding was 15 in this case study. Based on the results, it can be deduced that the proposed MDEP algorithm was capable of determining a better optimal amount of load to be shed (112.63 MW) within shorter a computational time (3.1935 sec) compared with the conventional EP algorithm, where the optimal amount of load to shed and the computational time were 115.33 MW and 8.8957 sec, respectively. Although the exhaustive search algorithm produced the same optimal solution as the MDEP algorithm, the computational time was significantly higher (89486.7264 sec). This is likely because the exhaustive search algorithm considers all possible combinations of available buses ($2^{15}-1 = 32767$) in order to determine the optimal amount of load to be shed. This will impose a higher computational burden as the total number of buses

available for load shedding increases. Therefore, the exhaustive search algorithm was not suitable to be used as the load shedding scheme in this research. The conventional EP algorithm was also not suitable because it was incapable of providing the optimal solution at all times owing to the small changes in the Gaussian function used for the mutation process. Hence, the proposed MDEP algorithm was the best load shedding scheme in this research because of its superior performance (especially in terms of the computational time) compared with the conventional EP and exhaustive search algorithms. For this reason, the MDEP algorithm was used as the load shedding scheme if load shedding was required during intentional islanding in this research.

5.8 Chapter Summary

The proposed MDEP algorithm was used to determine the optimal intentional islanding strategy following a critical line outage and the results are presented and discussed in this chapter. Nine case studies were conducted based on three IEEE test systems: IEEE 30-bus, IEEE 39-bus, and IEEE 118-bus test systems. The three most critical line outages, which would result in severe cascading failures), were investigated. For each case study, the initial intentional islanding solution was determined using graph theory after a critical line was removed from the network. Following this, the steps performed in the case studies presented in Chapter 4 were implemented in this chapter. The initial intentional islanding solution was used to facilitate the proposed MDEP algorithm to determine the optimal intentional islanding strategy, taking into consideration the critical line outage. The results were compared those of the MDPSO algorithm, which was also developed in this research. The results showed that the MDEP algorithm produced the same optimal intentional islanding strategies as the MDPSO algorithm for seven case studies and better optimal solutions for Case Studies C8 and C9. The convergence test results showed that the MDEP algorithm consistently achieved faster convergence compared with the MDPSO algorithm for all nine case studies.

The proposed MDEP algorithm was integrated with a load shedding scheme, bus voltage checking scheme, and transmission line power flow analysis to ensure that each island formed was capable of operating as a balanced, stand-alone island. The

intentional islanding strategy obtained from the MDEP algorithm is regarded as optimal only if the power balance criterion (i.e. load-generation balance), allowable bus voltage limits, and allowable transmission line power flow limit are fulfilled.

Similar to the case studies presented in Chapter 4, the MDEP-based load shedding scheme was executed when the generators were not able to fulfil the power balance criterion in the island after load flow analysis. The MDEP-based load shedding scheme was validated based on four case studies (Case Studies 6 (Islands 2 and 4), Case Study C1 (Island 2), Case Study C4 (Island 1)) and the results have been presented in this chapter. The results proved that the proposed MDEP-based load shedding scheme gave the best performance (especially in terms of the computational time) compared with the conventional EP and exhaustive search algorithms.

CHAPTER 6

CONCLUSIONS AND RECOMMENDATIONS FOR FUTURE WORK

6.1 Conclusions

Cascading failures, which are initiated from the failure or outage of a critical element in the power system, are the main cause of partial or total blackouts. Although the power system is designed to withstand contingencies (single or multiple outages), certain critical line outages may cause the power system to deviate from the normal state, resulting in severe cascading failures. These severe cascading failures cause the system to split into a number of unbalanced islands, which will eventually lead to blackout. Therefore, it is essential to prevent cascading failures from spreading throughout the power system. Intentional islanding is the best approach to prevent severe cascading failures in a power system. This approach involves forming a number of balanced, stand-alone islands that can operate independently and continue to supply electricity to consumers with minimal power disruptions.

Various intentional islanding techniques have been proposed over the years. However, to date, there are no studies on the development of intentional islanding algorithms, taking into account the critical line outages in a power system, which may initiate cascading failures. Hence, in this research, the MDEP and MDPSO algorithms were developed to determine the optimal intentional islanding strategy following a critical line outage. Since intentional islanding is a discrete problem, the algorithms developed to determine the optimal intentional islanding strategy were discrete optimization algorithms, as described in Section 3.3.4. In this research, N-1 contingency analysis was performed to identify the list of critical lines, which can cause severe cascading failures in the power system if these lines trip because of a failure.

The developed MDEP and MDPSO algorithms were evaluated using three IEEE test systems: IEEE 30-bus, IEEE 39-bus, and IEEE 118-bus test systems. The graph theory approach was used to represent the physical connections in a large-scale power system. Because the determination of the optimal solution involves a large

number of possible intentional islanding strategies, the graph theory approach was first used to obtain a suitable initial intentional islanding solution following a critical line outage. The initial intentional islanding solution was used to facilitate the MDEP and MDPSO algorithms to determine the optimal intentional islanding strategy. The optimal intentional islanding strategy obtained from the proposed algorithms must satisfy the specified system constraints (coherent groups of generators, desired number of islands, and load-generation balance). Based on the results obtained for nine case studies presented in Chapter 4 and Chapter 5, the MDEP algorithm was proven to be the best algorithm for intentional islanding in this research. The proposed MDEP algorithm was capable of obtaining an optimal intentional islanding strategy with a lower minimal fitness function value (i.e. lower total power flow disruption) compared with other algorithms, as indicated by the results in Chapter 4 except for Case Studies 1, 6, and 7. As explained previously, the similar optimal intentional islanding strategies determined from the developed algorithms with previously published algorithm [9] for Case Studies 1, 6, and 7 are likely because this strategy are the most optimal solution that can be obtained for these case studies. Furthermore, the proposed MDEP algorithm had the capability to obtain a better optimal intentional islanding strategy with minimal total power disruptions and faster convergence compared to the developed MDPSO algorithm, especially for larger test system.

The proposed MDEP algorithm was used to implement the intentional islanding and integrated with post-islanding schemes in order to determine whether the islands formed fulfil the power balance criterion as well as to check the bus voltage and power flow in each transmission line for all islands. Based on the results obtained for nine case studies, all of the islands formed after intentional islanding fulfilled the power balance criteria, allowable voltage limits, and transmission line capacity limits.

A novel load shedding scheme was developed in this research based on the MDEP technique. With the MDEP-based load shedding scheme, the optimal amount of load to be shed can be obtained in order to achieve load-generation balance in a particular island. The performance of the MDEP algorithm for load shedding scheme (in terms

of the optimal amount of load to be shed and computational time) was compared with that of the conventional EP and exhaustive search algorithms. Based on the results presented in Section 4.3 and Section 5.3, the MDEP-based load shedding scheme was proven to be more effective and efficient in determining the optimal amount of load that needs to be shed within a shorter computational time for cases where load shedding is required, especially when the size of test system increases.

In general, this research has been successfully developed an intentional islanding algorithm to prevent severe cascading failures and blackouts in the power system. The proposed MDEP algorithm is capable of determining the optimal intentional islanding strategy with minimal power flow disruption following a critical line outage. With the optimal intentional islanding strategy, the system can be partitioned into several balanced, stand-alone islands that can operate independently. It is believed that the proposed MDEP algorithm will be very useful to power system operators because the algorithm can be used to simulate and plan successful intentional islanding in the event of a critical line outage. This further can help to reduce wide-area outages and disruptions of electricity supply to the consumers.

6.2 Recommendations for Future Work

Even though the proposed MDEP algorithm is capable of determining the optimal intentional islanding strategy following a critical line outage, there are still avenues for further research in order to improve the proposed algorithm, as follows:

- a) In this research, the coherent groups of generators were obtained based on previously published works. Hence, in future work, a new technique to identify the coherent groups of generators can be explored and incorporated into the MDEP algorithm.
- b) For the proposed MDEP algorithm, the three most common critical line outages for the IEEE 30-bus, IEEE 39-bus, and IEEE 118-bus test systems were solely identified from the N-1 contingency analysis. In future work, other contingency schemes such as N-2, N-3, and N-4 contingency analyzes can be considered to examine the effects of system outages on the intentional islanding implementation.

- c) In this research, only transmission line outages were considered. Hence, in future work, the outages of other critical elements in a power system such as generators and transformers can be explored in order to study their effects on the intentional islanding implementation.
- d) In this research, active power was considered in the determination of the optimal intentional islanding strategy and execution of the load shedding scheme. Reactive power was not considered because it could be compensated locally. In future work, the reactive power can be incorporated into the MDEP algorithm to provide information on the reactive power for each island formed after intentional islanding.
- e) The MDEP algorithm was developed for planning and control action purposes. In future work, a suitable technique can be devised and integrated with the MDEP algorithm for online application.
- f) In this research, the IEEE test systems were used to evaluate the developed islanding MDEP and MDPSO algorithms. In future work, a practical test system such as the 89-bus system can be used to demonstrate the effectiveness of these algorithms for practical applications.

REFERENCES

- [1] H. H. Alhelou, M. E. Hamedani-Golshan, T. C. Njenda, and P. Siano, "A survey on power system blackout and cascading events: Research motivations and challenges," *Energies*, vol. 12, no. 4, pp. 1–28, 2019.
- [2] A. Peiravi and R. Ildarabadi, "A fast algorithm for intentional islanding of power systems using the multilevel kernel k-means approach," *J. Appl. Sci.* 9, pp. 2247–2255, 2009.
- [3] S. Larsson and A. Danell, "The black-out in southern Sweden and eastern Denmark, September 23, 2003," in *2006 IEEE PES Power Systems Conference and Exposition*, 2006.
- [4] G. Andersson *et al.*, "Causes of the 2003 major grid blackouts in North America and Europe , and Recommended Means to Improve System Dynamic Performance," *IEEE Trans. Power Syst.*, vol. 20, no. 4, pp. 1922–1928, 2005.
- [5] K. Yamashita, J. Li, and P. Zhang, "Analysis and control of major blackout events," *Power Systems Conference and Exposition, 2009. PSCE '09. IEEE/PES*, pp. 1–4, 2009.
- [6] S. Matthewman and H. Byrd, "Blackouts: A sociology of electrical power failure," *Soc. Space*, 2014.
- [7] V. Rampurkar, P. Pentayya, H. A. Mangalvedekar, and F. Kazi, "Cascading failure analysis for indian power grid," *IEEE Trans. Smart Grid*, vol. 7, no. 4, pp. 1951–1960, 2016.
- [8] A. Esmailian and M. Kezunovic, "Prevention of power grid blackouts using intentional islanding scheme," *IEEE Trans. Ind. Appl.*, vol. 53, no. 1, pp. 622–629, 2017.
- [9] K. N. Vijayakumar, "Power System Network Splitting and Load Frequency Control Optimization Using ABC Based Algorithms," Ph.D. dissertation, Faculty of Engineering, University of Malaya, Kuala Lumpur, 2015.
- [10] F. Tang, H. Zhou, Q. Wu, H. Qin, J. Jia, and K. Guo, "A tabu search algorithm for the power systemislanding problem," *Energies*, vol. 8, no. 10, pp. 11315–11341, 2015.
- [11] W. Liu, L. Liu, and D. A.Carter, "Binary particle swarm optimization based defensive islanding of large scale power systems," *Int. J. Comput. Sci. Appl.*, vol. 4, no. 3, pp. 69–83, 2007.

- [12] M. Goubko and V. Ginz, "Improved spectral clustering for multi-objective controlled islanding of power grid, " *Energy System*, Springer Berlin Heidelberg, 2017.
- [13] V. Tamilselvan and T. Jayabarathi, "A hybrid method for optimal load shedding and improving voltage stability," *Ain Shams Eng. J.*, vol. 7, no. 1, pp. 223–232, 2016.
- [14] M. F. Orhan, H. Kahraman, and B. S. Babu, "Approaches for integrated hydrogen production based on nuclear and renewable energy sources : Energy and exergy assessments of nuclear and solar energy sources in the United Arab Emirates," *Int. J. Hydrogen Energy*, vol. 42, no. 4, pp. 2601–2616, 2017.
- [15] U. S. Energy Administration, "International Energy Outlook 2017 Overview," 2017.
- [16] Z. Daria and K. Sroka, "The characteristics and main causes of power system failures basing on the analysis of previous blackouts in the world," *2018 Int. Interdiscip. PhD Work.*, pp. 257–262, 2018.
- [17] S. D. Kulkarniirlekar, "Blackouts in the power system," *Int. J. Electr. Electron. Res.*, vol. 3, no. 4, pp. 1–7, 2015.
- [18] L. U. Jinling, C. Yuan, and Z. H. U. Yongli, "Identification of cascading failures based on overload character of transmission lines," *2008 Third Int. Conf. Electr. Util. Deregul. Restruct. Power Technol.*, pp. 1030–1033, 2008.
- [19] Y. E. Xiaohui, Z. Wuzhi, S. Xinli, W. U. Guoyang, L. I. U. Tao, and S. U. Zhida, "Review on power system cascading failure theories and studies," *2016 Int. Conf. Probabilistic Methods Appl. to Power Syst.*, 2016.
- [20] M. Sadeghi, M. A. Sadeghi, S. Nourizadeh, A. M. Ranjbar, and S. Azizi, "Power system security assessment using AdaBoost algorithm," *Proc. NorthAmerican Power Symp. (NAPS 2009)*, 2009.
- [21] J. Srivani and K. S. Swarup, "Power system static security assessment and evaluation using external system equivalents," *Int J Electr Power Energy Syst*, vol. 30, pp. 83–92, 2008.
- [22] C. Joseph, "Power System Contingency Analysis: A study of Nigeria's 330KV transmission grid," in *Proceedings of the Energy Source for Power Generation Conference*, 2013.
- [23] S. Sayah and K. Zehar, "Economic load dispatch with security constraints of the Algerian power system using successive linear programming method,"

- Leonardo J. Sci.*, no. 9, pp. 73–86, 2006.
- [24] P. Hines and S. Talukdar, “Controlling cascading failures with cooperative autonomous agents Paul Hines * Sarosh Talukdar,” *Int. J. Crit. Infrastructures*, vol. 3, pp. 192–220, 2007.
- [25] T. E. D. Y. Liacco, “The adaptive reliability control system,” *IEEE Trans. POWER Appar. Syst.*, vol. PAS-86, no. 5, pp. 517–531, 1967.
- [26] Lester H. Fink; Kjell Carlsen, “Operating under stress and strain,” *IEEE Spectrum*, pp. 48–53, 1978.
- [27] K. Morison, L. Wang, and P. Kundur, “Power system security assessment,” *IEEE power & energy magazine*, no. 2(5), 2004.
- [28] P. Pourbeik, P. S.Kundur, and C. W.Taylor, “The anatomy of a power grid blackout,” *IEEE power & energy magazine*. 2006.
- [29] A. J. Wood and B. F. Wollenberg, *Power Generation, Operation, and Control*. New York, USA: Wiley, 1996.
- [30] P. Kundur *et al.*, “Definition and Classification of Power System Stability IEEE/CIGRE Joint Task Force on Stability Terms and Definitions,” *IEEE Trans. Power Syst.*, vol. 19, no. 3, pp. 1387–1401, 2004.
- [31] D. Bienstock and Abhinav Verma, “The N–k problem in power grids new models,” *SIAM J. Optim.*, vol. 20, no. 5, pp. 2352–2380, 2010.
- [32] V. J. Mishra, “Contingency analysis of power system,” in *2012 IEEE Students’ Conference on Electrical, Electronics and Computer Science*, 2012.
- [33] K. S. Swarup and G. Sudhakar, “Neural network approach to contingency screening and ranking in power systems,” *Neurocomputing*, vol. 70, pp. 105–118, 2006.
- [34] M. D. Khardennis, V. N. Pande, and V. M. Jape, “Transmission network expansion planning using contingency analysis,” in *2011 International Conference on Signal, Image Processing and Applications With workshop of ICEEA 2011*, 2011, vol. 21, pp. 270–274.
- [35] R. Retnamony and I. J. Raglend, “N-1 contingency analysis in a congested power system and enhance the voltage stability using FACTS Devices,” *I J C T A*, vol. 9, no. 7, pp. 3147–3157, 2016.
- [36] X.-F. Wang and J. McDonald, *Modern Power System Planning*. Cambridge, U.K.: McGraw-hill, 1994.
- [37] K. R. Rani, J. Amarnath, and S. Kamakshaiah, “Contingency analysis under

- deregulated power systems,” *Autom. Control Syst. Eng. J.*, vol. 11, no. 2, 2011.
- [38] IEEE PES CAMS Task Force, “Initial review of methods for cascading failure analysis in electric power transmission systems,” *IEEE POWER Eng. Soc. Gen. Meet.*, pp. 1–8, 2008.
- [39] P. Sekhar and S. Mohanty, “Electrical power and energy systems an online power system static security assessment module using multi-layer perceptron and radial basis function network,” *Int. J. Electr. Power Energy Syst.*, vol. 76, pp. 165–173, 2016.
- [40] A. Grothey, W. Bukhsh, K. I. M. Mckinnon, and P. A. Trodden, “Controlled islanding as robust operator response under uncertainty,” in *Handbook of Risk Management in Energy Production and Trading, International Series in Operations Research & Management Science 199*, New York: Springer Science and Business Media, 2013.
- [41] K. M. J. Rahman, M. M. Munnee, and S. Khan, “Largest blackouts around the world: Trends and data analyses,” in *2016 IEEE International WIE Conference on Electrical and Computer Engineering (WIECON-ECE)*, 2016, pp. 19–21.
- [42] Y.K. Wu, S. M. Chang, and Y.L. Hu, “Literature review of power system blackouts,” *Energy Procedia*, vol. 141, pp. 428–431, 2017.
- [43] M. M. Adibi, I. L. Fellow, N. Martins, and I. Fellow, “Impact of power system blackouts,” in *Proceedings of the 2015 IEEE Power & Energy Society General Meeting*, 2015, pp. 1–15.
- [44] M. Singh and K. S. Meera, “Islanding scheme for power transmission utilities,” in *2017 6th International Conference on Computer Applications In Electrical Engineering-Recent Advances (CERA)*, 2017, pp. 69–73.
- [45] G. S.Vassell, “Northeast blackout of 1965,” *Power Eng. Rev. IEEE*, vol. 11, no. 1, pp. 4–8, 1991.
- [46] “U.S.-Canada power system outage task force- causes of august 14th blackout.” 2003.
- [47] U.S.-Canada Power System Outage Task Force, "Final Report on the August 14, 2003 Blackout in the United States and Canada: Causes and Recommendations", April. 2004.
- [48] S. Corsi and C. Sabelli, “General blackout in Italy sunday September 28,

- 2003, h. 03:28:00,” in *Proc. IEEE PES General Meeting*, 2004.
- [49] A. Berizzi, “The Italian 2003 blackout,” in *IEEE Power Engineering Society General Meeting*, 2004.
- [50] “Final report of the investigation committee on the 28 september 2003 blackout in Italy,” 2004.
- [51] M. Sforna, M. Delfanti, and M. Ieee, “Overview of the events and causes of the 2003 Italian blackout,” in *IEEE PES Power Systems Conference and Exposition*, 2006, pp. 301–308.
- [52] A. Gailwad, “Indian blackouts - July 30 & 31, 2012 recommendations and further actions,” in *IEEE PES General Meeting*, 2013.
- [53] L. L. Lai, H. T. Zhang, S. Mishra, C. S. Lai, and F. Y. Xu, “Lessons learned from July 2012 Indian blackout,” in *Proceedings of the 9th IET International Conference on Advances in Power System Control, Operation and Management (APSCOM '12)*, 2012, pp. 1–6.
- [54] T. B. Smith, “Privatising electric power in Malaysia and Thailand : Politics and Infrastructure Development Policy,” vol. 283, pp. 273–283, 2003.
- [55] E. Thomson, Y. Chang, and J. Lee, “Energy conservation policy development in Malaysia,” in *Energy Conservation In East Asia: Towards Greater Energy Security*, Singapore: World Scientific Publishing Co. Pte. Ltd, 2011, pp. 201–208.
- [56] K. Verma and K. R. Niazi, “Preventive control for transient security with generation rescheduling based on rotor trajectory index,” *J. Electr. Eng. Technol.*, vol. 10, no. 2, pp. 465–473, 2015.
- [57] M. K. Maharana and K. S. Swarup, “Graph theoretic approach for preventive control of power systems,” *Int. J. Electr. Power Energy Syst.*, vol. 32, no. 4, pp. 254–261, 2010.
- [58] K. Verma and K. R. Niazi, “A coherency based generator rescheduling for preventive control of transient stability in power systems,” *Int. J. Electr. Power Energy Syst.*, vol. 45, no. 1, pp. 10–18, 2013.
- [59] R. Mageshvaran and T. Jayabarathi, “GSO based optimization of steady state load shedding in power systems to mitigate blackout during generation contingencies,” *Ain Shams Eng. J.*, vol. 6, no. 1, pp. 145–160, 2015.
- [60] M. Giroletti, M. Farina, and R. Scattolini, “A hybrid frequency / power based method for industrial load shedding,” *Int. J. Electr. Power Energy Syst.*, vol.

- 35, no. 1, pp. 194–200, 2012.
- [61] M. Majidi, M. Aghamohammadi, and M. Manbachi, “New design of intelligent load shedding algorithm based on critical line overloads,” *Turk J Elec Eng Comp Sci*, vol. 22, pp. 1395–1409, 2014.
- [62] J. A. Laghari, H. Mokhlis, A. H. A. Bakar, and H. Mohamad, “Application of computational intelligence techniques for load shedding in power systems : A review,” *Energy Convers. Manag.*, vol. 75, pp. 130–140, 2013.
- [63] M. Klaric, I. Kuzle, and T. Tomisa, “Simulation of undervoltage load shedding to prevent voltage collapse,” in *2005 IEEE Russia Power Tech*, 2005.
- [64] R. M. Larik, M. W. Mustafa, S. Qazi, and N. H. Mirjat, “Under voltage load shedding scheme to provide voltage stability,” in *Energy, Environment and Sustainable Development 2016 (EESD 2016)*, 2016.
- [65] M. Javadi and T. Amraee, “Mixed integer linear formulation for undervoltage load shedding to provide voltage stability,” *IET Gener. Transm. Distrib.*, vol. 12, pp. 2095–2104, 2018.
- [66] N. M. Sapari, H. Mokhlis, J. Ahmed, A. H. A. Bakar, and M. R. M. Dahalan, “Application of load shedding schemes for distribution network connected with distributed generation : A review,” *Renew. Sustain. Energy Rev.*, vol. 82, no. September 2017, pp. 858–867, 2018.
- [67] M. Lu, W. A. W. ZainalAbidin, T. Masri, D. H. . Lee, and S. Chen, “Under-Frequency load shedding (UFLS) schemes – A survey,” *Int. J. Appl. Eng. Res.*, vol. 11, no. 1, pp. 456–472, 2016.
- [68] M. Karimi, H. Mohamad, H. Mokhlis, and A. H. A. Bakar, “Electrical power and energy systems under-frequency load shedding scheme for islanded distribution network connected with mini hydro,” *Int. J. Electr. POWER ENERGY Syst.*, vol. 42, no. 1, pp. 127–138, 2012.
- [69] A. Arulampalam and T. K. Saha, “Fast and adaptive under frequency load shedding and restoration technique using rate of change of frequency to prevent blackouts,” Providence, RI, USA, 2010.
- [70] M. Abedini, M. Sanaye-pasand, and S. Azizi, “Adaptive load shedding scheme to preserve the power system stability following large disturbances,” *IET Gener. Transm. Distrib.*, vol. 8, no. 12, pp. 2124–2133, 2014.
- [71] J. Tang and J. Liu, “Adaptive load shedding based on combined frequency and

- voltage stability assessment using synchrophasor measurements,” *IEEE Trans. Power Syst.*, vol. 28, no. 2, pp. 2035–2047, 2013.
- [72] C. Chen, Y. Ke, and C. Hsu, “Protective relay setting of the tie line tripping and load shedding for the industrial power system,” *IEEE Trans. Ind. Appl.*, vol. 36, no. 5, pp. 1226–1234, 2000.
- [73] S. . Huang and C. . Huang, “Adaptive approach to load shedding including pumped-storage units during underfrequency conditions,” *IEE Proc.-Gener. Transm. Distrib.*, vol. 148, no. 2, pp. 165–171, 2001.
- [74] K. Prasertwong, M. Nadarajah, and D. Thakur, “Understanding low-frequency oscillation in power systems,” *Int. J. Electr. Eng. Educ.*, vol. 47, no. July, pp. 248–262, 2010.
- [75] A. M. El-Zonkoly, “Optimal tuning of power systems stabilizers and AVR gains using particle swarm optimization,” *Int. J. Expert Syst. with Appl.*, vol. 31, pp. 551–557, 2006.
- [76] J. Usman, M. W. Mustafa, and G. Aliyu, “Design of AVR and PSS for power system stability based on iteration particle swarm optimization,” *Int. J. Eng. Innov. Technol.*, vol. 2, no. 6, pp. 307–314, 2012.
- [77] G. J. W. Dudgeon *et al.*, “The effective role of AVR and PSS in power systems : frequency response analysis,” *IEEE Trans. POWER Syst.*, vol. 22, no. 4, pp. 1986–1994, 2007.
- [78] C. Y. Chung, L. Wang, F. Howell, and P. Kundur, “Generation rescheduling methods to improve power transfer capability constrained by small-signal stability,” *IEEE Trans. Power Syst.*, vol. 19, no. 1, pp. 524–530, 2004.
- [79] P. Fernández-porras, M. Panteli, and J. Quirós-tortós, “Intentional controlled islanding : when to island for power system blackout prevention,” *IET Gener. Transm. Distrib.*, vol. 12, pp. 3542–3549, 2018.
- [80] Q. Zhao, K. Sun, D. Zheng, J. Ma, and Q. Lu, “A study of system splitting strategies for island operation of power system: a two-phase method based on OBDDs,” *IEEE Trans. Power Syst.*, vol. 18, no. 4, pp. 1556–1565, 2003.
- [81] H. You, V. Vittal, and X. Wang, “Slow coherency-based islanding,” *IEEE Trans. Power Syst.*, vol. 19, no. 1, pp. 483–491, 2004.
- [82] B. Yang, V. Vittal, and G. T. Heydt, “Slow-coherency-based controlled islanding - A demonstration of the approach on the August 14, 2003 blackout scenario,” *IEEE Trans. Power Syst.*, vol. 21, no. 4, pp. 1840–1847, 2006.

- [83] X. Wang, S. Member, and V. Vittal, "System islanding using minimal cutsets with minimum net flow," in *Power System Conference and Exposition*, 2004, pp. 1–6.
- [84] R. Tsukui, H. Watanabe, T. Nakamura, and T. Matsushima, "Islanding protection system with active and reactive power balancing control for tokyo metropolitan power system and actual operational experiences," in *Seventh International Conference on Developments in Power System Protection (IEE)*, 2001, no. 479, pp. 351–354.
- [85] L. Ding, F. M. Gonzalez-longatt, S. Member, P. Wall, V. Terzija, and S. Member, "Two-step spectral clustering controlled islanding algorithm," *IEEE Trans. Power Syst.*, vol. 28, no. 1, pp. 75–84, 2013.
- [86] M. R. Aghamohammadi and A. Shahmohammadi, "Electrical power and energy systems intentional islanding using a new algorithm based on ant search mechanism," *Int. J. Electr. Power Energy Syst.*, vol. 35, no. 1, pp. 138–147, 2012.
- [87] R. E. Bryant, "Algorithms for Boolean function manipulation," *IEEE Trans. Comput.*, vol. C, no. 8, 1986.
- [88] A. K. Singh and A. Mohan, "An efficient method for generating optimal OBDD of boolean functions," *Comput. Inf. Sci.*, vol. 1, no. May, 2008.
- [89] K. Sun, D. Z. Zheng, and Q. Lu, "Splitting strategies for islanding operation of large-scale power systems using OBDD-based methods," *IEEE Trans. Power Syst.*, vol. 18, no. 2, pp. 912–923, 2003.
- [90] K. Sun, D. Zheng, and Q. Lu, "A simulation study of OBDD-based proper splitting strategies for power systems under consideration of transient stability," *IEEE Trans. Power Syst.*, vol. 20, no. 1, pp. 389–399, 2005.
- [91] B. Yang, V. Vittal, and G. T. Heydt, "A novel slow coherency based graph theoretic islanding strategy," *IEEE Trans. Power Syst.*, 2007.
- [92] J. Q. Tortos and V. Terzija, "Controlled islanding strategy considering power system restoration constraints," *IEEE Power Energy Soc. Gen. Meet.*, pp. 1–8, 2012.
- [93] H. Li, G. W. Rosenwald, J. Jung, and C.-C. Liu, "Strategic power infrastructure defense," *Proc. IEEE*, vol. 93, no. 5, 2005.
- [94] L. Ding, P. Wall, and V. Terzija, "Constrained spectral clustering based controlled islanding," *Int. J. Electr. Power Energy Syst.*, vol. 63, pp. 687–694,

- 2014.
- [95] T. S. Ferguson, “Linear Programming: A concise introduction,” [Online]. Available: <http://www.math.ucla.edu/~tom/LP.pdf>, 2009.
- [96] N. Fan, D. Izraelevitz, F. Pan, P. M. Pardalos, and J. Wang, “A mixed integer programming approach for optimal power grid intentional islanding,” *Energy Syst.*, vol. 3, no. 1, pp. 77–93, 2012.
- [97] P. A. Trodden, W. A. Bukhsh, A. Grothey, and K. I. M. Mckinnon, “MILP formulation for islanding of power networks,” *IEEE Trans. POWER Syst.*, vol. 29, pp. 1–8, 2014.
- [98] P. A. Trodden, W. A. Bukhsh, A. Grothey, and K. I. M. McKinnon, “optimization-Based Islanding of Power Networks Using Piecewise Linear AC power flow,” *IEEE Trans. Power Syst.*, vol. 29, no. 3, pp. 1212–1220, 2014.
- [99] P. Demetriou, A. Kyriacou, E. Kyriakides, and C. Panayiotou, “Applying exact MILP formulation for controlled islanding of power systems,” in *51st International Universities Power Engineering Conference (UPEC)*, 2016.
- [100] A. Kyriacou, P. Demetriou, C. Panayiotou, and E. Kyriakides, “Controlled islanding solution for large-scale power systems,” *IEEE Trans. Power Syst.*, vol. 33, no. 2, pp. 1591–1602, 2017.
- [101] C. G. Wang *et al.*, “A novel real-time searching method for power system splitting boundary,” *IEEE Trans. POWER Syst.*, vol. 25, no. 4, pp. 1902–1909, 2010.
- [102] L. Liu, W. Liu, D. A. Cartes, and I. Chung, “Slow coherency and Angle modulated particle swarm optimization based islanding of large-scale power systems,” *Adv. Eng. Informatics*, vol. 23, no. 1, pp. 45–56, 2009.
- [103] R. J. Wilson, Introduction to Graph Theory. Prentice hall, 1996.
- [104] Mathworks, “Directed and Undirected Graphs,” [Online]. Available: <https://www.mathworks.com/help/matlab/math/directed-and-undirected-graphs.html>.
- [105] S. G. Shirinivas, S. Vetrivel, and N. M. Elango, “Applications of graph theory in computer science an overview,” *Int. J. Eng. Sci. Technol.*, vol. 2, no. 9, pp. 4610–4621, 2010.
- [106] S. Desale, A. Rasool, S. Andhale, and P. Rane, “Heuristic and meta-heuristic algorithms and their relevance to the real world: A survey,” *Int. J. Comput.*

- Eng. Res. Trends*, vol. 2, no. 5, pp. 296–304, 2015.
- [107] R. Romero, E. M. C. Franco, and M. Rashidinejad, “Applications of heuristics and metaheuristics in power systems,” *J. Electr. Comput. Eng.*, 2012.
- [108] S. De León-aldaco, H. Calleja, and J. Aguayo, “Metaheuristic optimization methods applied to power converters: A review,” *IEEE Trans. Power Electron.*, vol. 30, no. 12, pp. 6791–6803, 2015.
- [109] M. Gavrilas, “Heuristic and metaheuristic optimization techniques with application to power systems,” in *The 12th International Conference on Mathematical Methods and Computational Techniques in Electrical Engineering*, 2010, pp. 95–103.
- [110] S. Bandaru and K. Deb, “Metaheuristic Techniques,” in *Decision Sciences: Theory and Practice*, CRC Press, Taylor & Francis Group, 2016, pp. 693–750.
- [111] S. A. Syed Mustaffa, I. Musirin, M. M. Othman, and M. H. Mansor, “Chaotic mutation immune evolutionary programming for voltage security with the presence of DGPV,” *Indones. J. Electr. Eng. Comput. Sci.*, vol. 6, no. June, pp. 721–729, 2017.
- [112] M. R. Alrashidi and M. F. Alhajri, “Particle swarm optimization and its applications in power systems,” *Comput. Intell. Power Eng.*, vol. 302, pp. 295–324, 2010.
- [113] Z. Mat Yasin, H. Mohamad, I. Na. Sam’on, N. Ab Wahab, and N. A. Salim, “Optimal undervoltage load shedding using ant lion optimizer,” *Int. J. Simul. Syst. Sci. Technol.*, vol. 17, no. 41, pp. 47.1-47.16, 2017.
- [114] M. M. Aman, G. Jasmon, K. Naidu, A. H. Abu Bakar, and H. Mokhlis, “Discrete evolutionary programming to solve network reconfiguration problem,” in *IEEE 2013 Tencon - Spring*, 2013, pp. 205–509.
- [115] Y. Zhang, S. Wang, and G. Ji, “A comprehensive survey on particle swarm optimization algorithm and its applications,” *Math. Probl. Eng.*, vol. 2015, pp. 1–38, 2015.
- [116] M. Ismail and T. K. Abdul Rahman, “Evolutionary programming optimization technique for solving reactive power planning in power system,” in *Proceedings of the 6th WSEAS Int. Conf. on Evolutionary Computing*, 2005, pp. 239–244.
- [117] N. Sinha, R. Chakrabarti, and P. K. Chattopadhyay, “Evolutionary programming techniques for economic load dispatch,” *IEEE Trans. Evol.*

- Comput.*, vol. 7, no. 1, pp. 83–94, 2003.
- [118] M. A. Abido, “Optimal design of power system stabilizers using evolutionary programming,” *IEEE Trans. Energy Convers.*, vol. 17, no. 4, pp. 429–436, 2002.
- [119] L. J. Fogel, A. J. Owens, and M. J. Walsh, *Artificial Intelligence through Simulated Evolution*. Wiley, New York, 1966.
- [120] J. Brownlee, *Clever Algorithms : Nature - Inspired Programming Recipes*. 2011.
- [121] A. R. Minhat, I. Musirin, and M. M. Othman, “Evolutionary programming based technique for secure operating point identification in static voltage stability assessment,” *J. Artif. Intell.*, vol. 1, pp. 12–20, 2008.
- [122] D. C. Secui, I. Felea, S. Dzitac, and L. Popper, “A swarm intelligence approach to the power dispatch problem,” *Int. J. Comput. Commun. Control*, no. 3, pp. 375–384, 2010.
- [123] A. Jaini *et al.*, “Particle Swarm Optimization (PSO) technique in economic power dispatch problems,” in *The 4th International Power Engineering and Optimization Conference (PEOCO 2010)*, 2010, pp. 308–312.
- [124] D. H. Tungadio, B. P. Numbi, M. W. Siti, and A. A. Jimoh, “Particle swarm optimization for power system state estimation,” *Neurocomputing*, vol. 148, pp. 175–180, 2015.
- [125] H. Su, Y. Hsu, and Y. Chen, “PSO-based voltage control strategy for loadability enhancement in smart power Grids,” *Appl. Sci.*, vol. 6, 2016.
- [126] J. Kennedy and R. Eberhart, “Particle swarm optimization,” in *Proceedings of ICNN’95 - International Conference on Neural Networks*, 1995, pp. 1942–1948.
- [127] S. De León-aldaco, H. Calleja, and J. Aguayo, “Metaheuristic optimization methods applied to power converters: A review,” *IEEE Trans. Power Electron.*, 2015.
- [128] T. Sun and M. Xu, “Applying a new parallelized version of PSO algorithm for electrical power transmission applying a new parallelized version of PSO algorithm for electrical power transmission,” in *IOP Conf. Series: Materials Science and Engineering*, 2017.
- [129] A. Salman, I. Ahmad, and S. Al-madani, “Particle swarm optimization for task assignment problem,” *Microprocess. Microsyst.*, vol. 26, pp. 363–371, 2002.

- [130] J. Nievergelt, “Exhaustive search, combinatorial optimization and enumeration: Exploring the potential of raw computing power,” *Lect. Notes Comput. Sci. (including Subser. Lect. Notes Artif. Intell. Lect. Notes Bioinformatics)*, vol. 1963, no. October, pp. 18–35, 2000.
- [131] K. S. K. Reddy, D. A. K. Rao, A. Kumarraja, and B. R. K. Varma, “Implementation of integer linear programming and exhaustive search algorithms for optimal PMU placement under various conditions,” *2015 IEEE Power, Commun. Inf. Technol. Conf. PCITC 2015 - Proc.*, pp. 850–855, 2016.
- [132] A. C. Adewole, R. Tzoneva, and A. Apostolov, “Adaptive under-voltage load shedding scheme for large interconnected smart grids based on wide area synchrophasor measurements,” *IET Gener. Transm. Distrib.*, pp. 1957–1968, 2016.
- [133] R. Kanimozhi, K. Selvi, and K. M. Balaji, “Multi-objective approach for load shedding based on voltage stability index consideration,” *Alexandria Eng. J.*, vol. 53, no. 4, pp. 817–825, 2014.
- [134] F. HE, Y. Wang, K. W. Chan, Y. Zhang, and S. Mei, “Optimal load shedding strategy based on particle swarm optimization,” in *8th International Conference on Advances in Power System Control, Operation and Management (APSCOM 2009)*, 2009.
- [135] X. Yang, “Firefly algorithms for multimodal optimization,” *Stoch. Algorithms Found. Appl. SAGA*, vol. 5792, pp. 169–178, 2009.
- [136] C. Church, W. G. Morsi, C. P. Diduch, M. E. El-Hawary, and L. Chang, “Voltage collapse detection using ant colony optimization for smart grid applications,” in *2010 IEEE Electrical Power & Energy Conference*, 2010.
- [137] F. M. Gatta, A. Geri, S. Lauria, M. Maccioni, and P. Masato, “Power system adequacy: An efficient procedure based on genetic algorithms,” in *2009 IEEE Bucharest PowerTech*, 2009.
- [138] J. Chen and J. Li, “An application of rough sets to graph theory,” *Inf. Sci. (Ny)*, vol. 201, pp. 114–127, 2012.
- [139] North American Electric Reliability Corporation (NERC), “Standard TPL-001-0.1 — System Performance Under Normal Conditions,” 2011.
- [140] S. Najafi, “Evaluation of Interconnected power systems controlled islanding,” in *IEEE Bucharest Power Tech Conference*, 2009, pp. 1–8.
- [141] S. Skiena, “*Dijkstra ’ s algorithm*,” in *Implementing Discrete Mathematics:*

Combinatorics and Graph Theory with Mathematica, Reading, MA: Addison-Wesley, 1990, pp. 225–227.

- [142] University of Washington, “Power Systems Test Case Archive,”.[Online]. Available: <http://www.ee.washington.edu/research/pstca/>, 1999.
- [143] R. Zimmerman, C. Murillo-Sanchez, and D. Gan, “MATPOWER: A MATLAB power system simulation package 2006,”.[Online].Available: <http://www.pserc.cornell.edu/matpower/>.

APPENDIX A

Table A.1 : IEEE 30-bus generator data

Bus. No	Type	Pmax	Pmin	Qmax	Qmin
1	Slack	360	0	10	0
2	PV	140	0	50	-40
5	PV	100	0	40	-40
8	PV	100	0	40	-10
11	PV	100	0	24	-6
13	PV	100	0	24	-6

Table A.2 : IEEE 39-bus generator data

Bus. No	Type	Pmax	Pmin	Qmax	Qmin
30	PV	1040	0	400	140
31	Slack	646	0	300	-100
32	PV	725	0	300	150
33	PV	652	0	250	0
34	PV	508	0	167	0
35	PV	687	0	300	-100
36	PV	580	0	240	0
37	PV	564	0	250	0
38	PV	865	0	300	-150
39	PV	1100	0	300	-100

Table A.3 : IEEE 118-bus generator data

Bus. No	Type	Pmax	Pmin	Qmax	Qmin
10	PV	550	0	200	-147
12	PV	185	0	120	-35
25	PV	320	0	140	-47
26	PV	414	0	1000	-1000
31	PV	107	0	300	-300
46	PV	119	0	100	-100
49	PV	304	0	210	-85
54	PV	148	0	300	-300
59	PV	255	0	180	-60
61	PV	160	0	300	-100
65	PV	491	0	200	-67
66	PV	192	0	200	-67
69	Slack	805	0	300	-300
80	PV	577	0	280	-165
87	PV	104	0	1000	-100
89	PV	707	0	300	-210
100	PV	352	0	155	-50
103	PV	140	0	40	-15
111	PV	136	0	1000	-100

Table A.4 : Load Flow Analysis Data for IEEE 30-bus Test System

From Line	To Line	P (MW)	Q (MVar)	S (MVA)
1	2	177.7779	22.1476	179.1522
1	3	83.2206	5.126813	83.37837
2	4	45.71185	2.704891	45.79181
2	5	82.9904	1.703486	83.00788
2	6	61.91218	0.95773	61.91958
3	4	78.01242	3.15849	78.07633
4	6	70.12554	17.5259	72.28243

From Line	To Line	P (MW)	Q (MVar)	S (MVA)
4	12	44.12143	14.64569	46.48868
5	7	14.2048	10.50006	17.6643
6	7	37.52314	1.88516	37.57047
6	8	29.52831	3.75408	29.76599
6	9	27.69276	7.32227	28.64445
6	10	15.82275	0.652533	15.8362
6	28	18.81873	9.61847	21.13433
8	28	0.57511	2.36965	2.438439
9	11	5.69E-14	15.6569	15.65694
9	10	27.69276	6.740942	28.50139
10	20	9.027499	3.559709	9.703982
10	17	5.371759	4.413902	6.952577
10	21	15.73312	9.84231	18.55808
10	22	7.583125	4.490381	8.812906
12	13	1.22E-13	10.2909	10.29092
12	14	7.856309	2.441523	8.226945
12	15	17.85738	6.947268	19.16117
12	16	7.207743	3.363219	7.953792
14	15	1.581788	0.68661	1.72438
15	18	6.014306	1.744252	6.262131
15	23	5.001424	2.955944	5.809634
16	17	3.654272	1.450787	3.931728
18	19	2.775236	0.764694	2.878662
19	20	6.72977	2.64544	7.231059
21	22	1.87676	1.5942	2.46246
22	24	5.653933	2.788097	6.304002
23	24	1.770084	1.292639	2.191829
24	25	1.32485	1.601737	2.07865
25	26	3.544513	2.36649	4.261907
25	27	4.87717	0.77838	4.93889
27	28	18.1835	4.15657	18.65254
27	29	6.189382	1.6677	6.410123
27	30	7.091283	1.661445	7.283317
29	30	3.703542	0.60551	3.752715

Table A.5 : Load Flow Analysis Data for Original IEEE 39-bus Test System

From Line	To Line	P (MW)	Q (MVar)	S (MVA)
1	2	133.961	24.0957	136.1108
1	39	36.36099	20.1043	41.54883
2	3	345.0862	91.46759	357.0025
2	25	229.674	160.1417	279.9921
2	30	250	117.697	276.3195
3	4	62.95395	162.2406	174.0265
3	18	41.3611	31.696	52.10932

From Line	To Line	P (MW)	Q (MVar)	S (MVA)
4	5	173.458	56.8185	182.5268
4	14	264.039	38.0571	266.768
5	6	485.444	100.6282	495.7637
5	8	311.7163	20.3445	312.3795
6	7	421.2165	5.449	421.2517
6	11	336.801	53.7638	341.0653
6	31	570.339	162.5022	593.0378
7	8	186.3768	82.2993	203.7387
8	9	24.8217	245.418	246.6702
9	39	32.2919	110.204	114.838
10	11	341.0016	63.62425	346.8864
10	13	308.9984	42.4766	311.9042
10	32	650	21.1476	650.3439
11	12	2.949803	39.44241	39.55256
12	13	5.60436	49.2144	49.53249
13	14	302.9846	81.4992	313.7543
14	15	37.58071	72.3781	81.55307
15	16	282.463	148.28	319.0178
16	17	210.842	198.808	289.7912
16	19	450.645	221.4919	502.1351
16	21	330.52	43.4075	333.3577
16	24	41.9558	131.358	137.8959
17	18	199.6258	12.9537	200.0457
17	27	10.71649	162.342	162.6958
19	20	174.5673	81.29512	192.5685
19	33	629.12	157.0024	648.4147
20	34	505.687	26.7127	506.3918
21	22	605.318	115.659	616.268
22	23	41.98386	73.63855	84.76603
22	35	650	178.597	674.0897
23	24	353.0381	17.1862	353.4562
23	36	558.61	47.42238	560.6197
25	26	79.34413	151.442	170.9683
25	37	538.073	292.2295	612.3079
26	27	271.5706	120.58	297.1365
26	28	141.622	81.0552	163.1767
26	29	189.997	85.0554	208.1661
28	29	348.335	74.28978	356.1686
29	38	825.106	236.8266	858.4213

Table A.6 : Load Flow Analysis Data for Modified IEEE 39-bus Test System

From Line	To Line	P (MW)	Q (MVar)	S (MVA)
1	2	217.492	78.4985	231.2249
1	39	119.8924	34.29855	124.7019

From Line	To Line	P (MW)	Q (MVar)	S (MVA)
2	3	283.5284	95.55842	299.1986
2	25	252.498	142.6477	290.0061
2	30	250	175.84	305.6461
3	4	27.20089	114.4267	117.6153
3	18	66.764	23.76195	70.86646
4	5	258.8078	13.77603	259.1742
4	14	63.1723	45.967	78.12615
4	31	668.671	6.158999	668.6994
5	6	101.117	16.0474	102.3829
5	8	359.4047	17.21107	359.8166
6	7	387.9517	36.87711	389.7004
6	11	489.09	12.1512	489.2407
7	8	153.2616	37.6222	157.8117
8	9	10.4398	166.094	166.4214
9	39	17.3078	24.1112	29.68013
10	11	480.8837	38.16634	482.3959
10	13	169.1163	19.8568	170.278
10	32	650	18.3096	650.2578
11	12	10.7235	41.31767	42.68657
12	13	19.2816	47.4456	51.21389
13	14	149.6829	54.3747	159.2532
14	15	86.2681	38.2272	94.35838
15	16	233.859	115.973	261.0362
16	17	246.102	65.6332	254.7032
16	19	54.96813	168.7988	177.5233
16	21	330.374	71.5276	338.0286
16	24	41.9042	149.455	155.2182
17	18	225.1745	64.4027	234.2035
17	27	33.80656	192.158	195.1091
17	34	505.496	214.5912	549.1588
19	20	683.5053	172.1044	704.84
19	33	629.188	51.47423	631.2901
21	22	605.204	145.478	622.4436
22	23	42.00606	75.75913	86.62537
22	35	650	212.874	683.9703
23	24	353.0513	3.608827	353.0698
23	36	558.604	28.32831	559.3217
25	26	56.19047	135.71	146.8825
25	37	538.146	257.9713	596.783
26	27	248.6259	156.1442	293.5913
26	28	141.765	91.3467	168.6464
26	29	189.912	95.1614	212.42
28	29	348.487	61.07818	353.7989
29	38	825.152	209.9211	851.436

Table A.7 : Load Flow Analysis Data for IEEE 118-bus Test System

From Line	To Line	P (MW)	Q (MVar)	S (MVA)
1	2	12.1867	9.22649	15.28543
1	3	38.8133	10.8616	40.30439
2	12	32.2504	13.6515	35.02072
3	5	68.3948	9.31169	69.02576
3	12	9.64062	10.2446	14.06746
4	5	102.946	22.5752	105.392
4	11	63.94576	2.51179	63.99507
5	6	88.13098	2.800008	88.17545
5	8	337.73	35.1325	339.5521
5	11	76.86416	0.155294	76.86432
6	7	35.20759	5.39882	35.61912
7	12	16.14843	6.58943	17.44111
8	9	440.373	272.679	517.9595
8	30	74.6433	96.016	121.617
9	10	445.52	81.96	452.9963
11	12	33.91582	30.0556	45.31692
11	13	34.83978	4.730216	35.15942
12	14	18.05755	4.3594	18.57632
12	16	7.519328	0.79	7.560714
12	117	20.14533	1.697272	20.2167
13	15	0.552224	8.61149	8.629175
14	15	3.98456	2.04684	4.479538
15	17	103.425	14.9293	104.4969
15	19	11.47222	12.95789	17.30661
15	33	6.469005	8.74687	10.87914
16	17	17.4933	6.65613	18.7168
17	18	80.10502	33.35187	86.77074
17	30	233.289	78.035	245.9946
17	31	16.26395	12.0906	20.2657
17	113	3.371744	20.41535	20.69191
18	19	19.16749	5.32624	19.89376
19	18	19.1219	3.364609	19.41569
19	20	10.0935	0.612708	10.1121
19	15	11.4315	14.7505	18.66166
19	34	4.353	13.7133	14.38758
20	21	28.1238	3.10646	28.29483
21	22	42.2823	1.54609	42.31051
22	23	52.6773	3.6801	52.80569
23	24	9.435105	15.98674	18.56333
23	32	92.22965	6.56346	92.4629
24	70	5.36098	10.4289	11.72613
24	72	1.725031	0.841843	1.919487
25	26	87.4874	69.4481	111.7009

From Line	To Line	P (MW)	Q (MVar)	S (MVA)
25	27	141.0772	14.17901	141.7879
26	30	226.5126	115.357	254.1951
27	28	32.0002	2.93707	32.1347
27	32	11.33385	12.8488	17.13322
27	115	20.56632	4.05274	20.96182
28	29	14.79097	6.84552	16.29828
29	31	9.27045	6.67181	11.42166
30	38	63.53974	61.2462	88.2519
31	32	29.2686	0.106785	29.2688
32	23	89.5436	6.60847	89.78712
32	113	2.738835	14.8255	15.07641
32	114	9.533885	7.233325	11.96729
33	37	16.5603	11.678	20.26374
34	36	30.28665	11.98523	32.57187
34	37	96.708	55.5377	111.5207
34	43	3.005818	0.24811	3.016041
35	36	0.810018	9.745205	9.778811
35	37	33.81	18.7452	38.65876
37	38	250.144	86.1797	264.5736
37	39	56.58091	8.287256	57.1846
37	40	45.85924	1.358131	45.87934
38	65	186.791	84.8917	205.1769
39	37	55.5221	10.0805	56.42983
39	40	28.52214	0.91949	28.53696
40	41	17.11616	1.5087	17.18252
40	42	10.1485	9.18521	13.68798
41	42	19.929	9.36638	22.02032
42	49	63.1712	0.292279	63.17184
42	49	63.1712	0.292279	63.17184
43	44	15.0044	1.028525	15.03963
44	45	31.1747	4.104609	31.44378
45	46	35.5609	8.02315	36.45471
45	49	48.8492	6.49997	49.27977
46	47	30.646	4.77366	31.01551
46	48	14.4482	5.69003	15.52829
47	49	9.48648	8.04644	12.43939
47	69	55.5138	8.563557	56.17039
48	49	34.573	7.44532	35.36554
49	50	53.5261	9.578615	54.37641
49	51	66.46228	15.09963	68.15595
49	54	37.54091	9.22686	38.65818
49	54	37.52506	7.405748	38.24886
49	66	129.571	2.183939	129.5891
49	66	129.571	2.183939	129.5891

From Line	To Line	P (MW)	Q (MVar)	S (MVA)
49	69	46.0869	6.078414	46.486
50	57	35.76411	7.287513	36.49903
51	52	28.43487	3.688284	28.67307
51	58	18.82244	4.01866	19.24666
52	53	10.25568	0.782146	10.28546
53	54	12.7993	3.00621	13.14758
54	55	7.744973	13.1072	15.2244
54	56	17.39252	4.337416	17.9252
54	59	30.4507	10.2134	32.11788
55	56	20.0519	57.22405	60.63555
55	59	35.2378	6.34329	35.80417
56	57	22.8696	12.7404	26.17891
56	58	6.68653	8.42669	10.75727
56	59	27.9791	6.75625	28.78326
56	59	29.33	6.33878	30.00717
59	60	43.6547	4.83438	43.92157
59	61	52.05	3.45507	52.16452
59	63	151.926	58.884	162.9382
60	61	112.952	5.397348	113.0814
60	62	9.32532	8.65258	12.72119
61	62	26.65624	14.6869	30.43451
61	64	32.9108	64.4737	72.38771
62	66	36.3144	16.0677	39.71025
62	67	23.4449	13.2287	26.91958
63	64	151.926	69.4464	167.0459
64	65	185.264	95.6805	208.5126
65	66	1.097587	14.1214	14.16401
65	68	13.91034	75.91108	77.17506
66	67	52.20643	11.48669	53.45517
68	81	47.3801	169.325	175.8291
68	116	184.705	410.2774	449.9372
69	70	108.4365	1.560774	108.4478
69	75	110.0185	7.245128	110.2568
69	77	63.27387	0.96343	63.2812
70	71	16.37702	0.65655	16.39017
70	74	16.78401	11.22473	20.19152
70	75	0.560928	9.416189	9.432882
71	72	10.34951	0.02347	10.34954
71	73	6.003562	0.955953	6.079195
75	77	34.0549	8.33478	35.06005
75	118	41.06219	29.95874	50.82942
76	77	60.4053	22.9713	64.62573
76	118	7.59466	18.0781	19.60856
77	78	46.33686	17.52157	49.53898

From Line	To Line	P (MW)	Q (MVar)	S (MVA)
77	80	95.3337	40.2917	103.4985
77	80	43.7686	21.8917	48.93812
77	82	3.37432	11.95757	12.42455
78	79	24.756	6.23663	25.52954
79	80	63.7911	37.0885	73.78929
80	81	47.53814	0.026558	47.53815
80	96	18.8728	15.15767	24.20615
80	97	26.32172	19.85279	32.96918
80	98	28.77256	4.260743	29.08632
80	99	19.37449	5.250845	20.07342
82	83	47.4284	18.28568	50.8313
82	96	10.0698	17.4008	20.1044
83	84	25.2177	9.319909	26.88477
83	85	42.5232	5.363154	42.86009
84	85	36.7152	6.304046	37.25248
85	86	17.13981	8.11033	18.96182
85	88	50.2173	10.93813	51.39478
85	89	71.4266	4.044047	71.54098
86	87	3.97427	13.0414	13.63355
88	89	98.7645	3.599018	98.83008
89	90	57.93512	7.34582	58.39897
89	90	110.2863	10.7283	110.8069
89	92	202.4728	30.4478	204.7493
89	92	63.48427	15.2413	65.2882
90	91	0.631881	3.623408	3.678091
91	92	9.37673	17.9906	20.28757
92	93	57.8758	10.4956	58.81978
92	94	52.35812	14.0594	54.21291
92	100	31.08585	14.7316	34.39984
92	102	44.44139	8.09418	45.17248
93	94	44.99909	16.0196	47.76553
94	95	40.97774	9.583622	42.0835
94	96	19.88809	8.8927	21.78569
94	100	4.633285	41.0197	41.28059
95	96	1.26022	20.012	20.05167
96	97	11.045	19.6694	22.55832
98	100	5.42151	1.485108	5.621238
100	101	16.651	14.18762	21.87565
100	103	121.0728	7.62463	121.3127
100	104	56.38763	7.827398	56.92831
100	106	60.62196	5.3165	60.85464
101	102	38.808	5.144975	39.14757
103	104	32.29252	6.080115	32.85992
103	105	42.93725	5.28881	43.26175

From Line	To Line	P (MW)	Q (MVar)	S (MVA)
103	110	60.57475	1.077938	60.58434
104	105	48.68217	2.143783	48.72935
105	106	8.676065	0.49031	8.689909
105	107	26.67934	4.55509	27.0654
105	108	23.98186	13.2772	27.4119
106	107	24.05645	4.82831	24.53621
108	109	21.78321	11.3702	24.57212
109	110	13.71719	13.1282	18.98715
110	111	35.7029	0.009406	35.70295
110	112	69.45859	33.549	77.13645
114	115	1.509986	7.192303	7.349101

Table A.8 : Active Power Flow at Each Bus on Island 1 and Island 2- Case Study 1

Active power (MW) at each bus in Island 1				
Bus	Pre-islanding		Post-islanding	
	Pload	Pgen	Pload	Pgen
1	0.000	260.998	0.000	128.075
2	21.700	40.000	21.700	40.000
3	2.400	0.000	2.400	0.000
4	7.600	0.000	7.600	0.000
5	94.200	0.000	94.200	0.000
12	11.200	0.000	11.200	0.000
13	0.000	0.000	0.000	0.000
14	6.200	0.000	6.200	0.000
15	8.200	0.000	8.200	0.000
16	3.500	0.000	3.500	0.000
18	3.200	0.000	3.200	0.000
23	3.200	0.000	3.200	0.000
Active power (MW) at each bus in Island 2				
Bus	Pre-islanding		Post-islanding	
	Pload	Pgen	Pload	Pgen
6	0.000	0.000	0.000	0.000
7	22.800	0.000	22.800	0.000
8	30.000	0.000	30.000	62.189
9	0.000	0.000	0.000	0.000
10	5.800	0.000	5.800	0.000
11	0.000	0.000	0.000	61.000
17	9.000	0.000	9.000	0.000
19	9.500	0.000	9.500	0.000
20	2.200	0.000	2.200	0.000
21	17.500	0.000	17.500	0.000
22	0.000	0.000	0.000	0.000
24	8.700	0.000	8.700	0.000
25	0.000	0.000	0.000	0.000
26	3.500	0.000	3.500	0.000
27	0.000	0.000	0.000	0.000
28	0.000	0.000	0.000	0.000
29	2.400	0.000	2.400	0.000
30	10.600	0.000	10.600	0.000

Table A.9 : Voltage Profile on Island 1 and Island 2- Case Study 1

Island 1		Island 2	
Bus. No	Voltage (p.u)	Bus. No	Voltage (p.u)
1	1.060	6	1.008
2	1.043	7	0.994
3	1.031	8	1.010
4	1.024	9	1.044
5	1.010	10	1.036
12	1.066	11	1.082
13	1.071	17	1.028
14	1.053	19	1.011
15	1.051	20	1.017
16	1.059	21	1.023
18	1.046	22	1.023
23	1.045	24	1.008
		25	1.006
		26	0.989
		27	1.014
		28	1.007
		29	0.994
		30	0.983

Table A.10 : Power Flow Information on Island 1 and Island 2- Case Study 1

Power Flow in ISLAND 1							
From bus	To bus	P _{max} (MW)	P _{flow} (MW)	From bus	To bus	P _{max} (MW)	P _{flow} (MW)
1	2	221	93.864	12	14	54.4	6.834
1	3	221	34.210	12	15	54.4	14.176
2	4	110.5	12.253	12	16	54.4	3.513
2	5	221	98.406	14	15	27.2	0.579
3	4	221	31.307	15	18	27.2	3.211
4	12	110.5	35.723	15	23	27.2	3.212
12	13	110.5	0.000				
Power Flow in ISLAND 2							
From bus	To bus	P _{max} (MW)	P _{flow} (MW)	From bus	To bus	P _{max} (MW)	P _{flow} (MW)
6	7	221	22.968	10	22	54.4	9.559
6	8	54.4	24.772	19	20	54.4	9.534
6	9	110.5	11.454	21	22	54.4	1.115
6	10	54.4	5.481	22	24	27.2	10.599
6	28	54.4	7.705	24	25	27.2	1.771
8	28	54.4	7.421	25	26	27.2	3.546
9	10	110.5	49.546	25	27	27.2	1.794
9	11	110.5	61.00	27	28	110.5	15.081
10	17	54.4	9.035	27	29	27.2	6.192
10	20	54.4	11.874	27	30	27.2	7.095
10	21	54.4	18.758	29	30	27.2	3.704

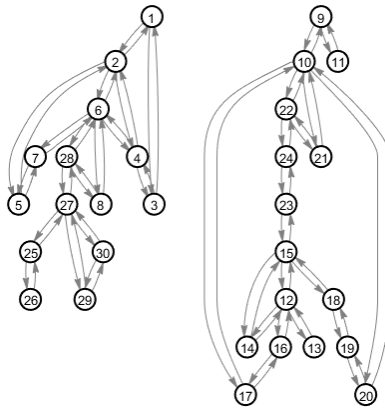


Figure A.1 : Graph model of islanding implementation for Case Study 2

Table A.11 : Active Power Flow at Each Bus on Island 1 and Island 2- Case Study 2

Active power (MW) at each bus in Island 1				
Bus	Pre-islanding		Post-islanding	
	Pload	Pgen	Pload	Pgen
1	0.000	260.998	0.000	163.809
2	21.700	40.000	21.700	40.000
3	2.400	0.000	2.400	0.000
4	7.600	0.000	7.600	0.000
5	94.200	0.000	94.200	0.000
6	0.000	0.000	0.000	0.000
7	22.800	0.000	22.800	0.000
8	30.000	0.000	30.000	0.000
25	0.000	0.000	0.000	0.000
26	3.500	0.000	3.500	0.000
27	0.000	0.000	0.000	0.000
28	0.000	0.000	0.000	0.000
29	2.400	0.000	2.400	0.000
30	10.600	0.000	10.600	0.000
Active power (MW) at each bus in Island 2				
Bus	Pre-islanding		Post-islanding	
	Pload	Pgen	Pload	Pgen
9	0.000	0.000	0.000	0.000
10	5.800	0.000	5.800	0.000
11	0.000	0.000	0.000	90.455
12	11.200	0.000	11.200	0.000
13	0.000	0.000	0.000	0.000
14	6.200	0.000	6.200	0.000
15	8.200	0.000	8.200	0.000
16	3.500	0.000	3.500	0.000
17	9.000	0.000	9.000	0.000
18	3.200	0.000	3.200	0.000
19	9.500	0.000	9.500	0.000
20	2.200	0.000	2.200	0.000
21	17.500	0.000	17.500	0.000
22	0.000	0.000	0.000	0.000
23	3.200	0.000	3.200	0.000
24	8.700	0.000	8.700	0.000

Table A.12 : Voltage Profile on Island 1 and Island 2- Case Study 2

Island 1		Island 2	
Bus. No	Voltage (p.u)	Bus. No	Voltage (p.u)
1	1.060	9	1.050
2	1.043	10	1.045
3	1.034	11	1.082
4	1.028	12	1.025
5	1.010	13	1.051
6	1.019	14	1.011
7	1.008	15	1.013
8	1.010	16	1.026
25	1.017	17	1.034
26	0.999	18	1.012
27	1.025	19	1.014
28	1.016	20	1.021
29	1.005	21	1.031
30	0.994	22	1.031
		23	1.009
		24	1.012

Table A.13 : Power Flow Information on Island 1 and Island 2- Case Study 2

Power Flow in ISLAND 1							
From bus	To bus	P _{max} (MW)	P _{flow} (MW)	From bus	To bus	P _{max} (MW)	P _{flow} (MW)
1	2	221	115.015	6	8	54.4	29.221
1	3	221	48.794	6	28	54.4	17.801
2	4	110.5	22.902	8	28	54.4	0.905
2	5	221	71.411	25	26	27.2	3.545
2	6	110.5	36.739	25	27	27.2	3.564
3	4	221	45.427	27	28	110.5	6.190
4	6	153	60.196	27	29	27.2	7.091
5	7	119	25.364	27	30	27.2	16.845
6	7	221	48.776	29	30	27.2	3.704
Power Flow in ISLAND 2							
From bus	To bus	P _{max} (MW)	P _{flow} (MW)	From bus	To bus	P _{max} (MW)	P _{flow} (MW)
9	10	110.5	90.459	14	15	27.2	2.830
9	11	110.5	90.459	15	18	27.2	6.321
10	17	54.4	27.712	15	23	27.2	5.004
10	20	54.4	21.817	16	17	27.2	18.482
10	21	54.4	22.88	18	19	27.2	9.583
10	22	54.4	12.25	19	20	54.4	19.203
12	13	110.5	0.0	21	22	54.4	5.190
12	14	54.4	3.427	22	24	27.2	17.327
12	15	54.4	0.194	23	24	27.2	8.303
12	16	54.4	14.709				

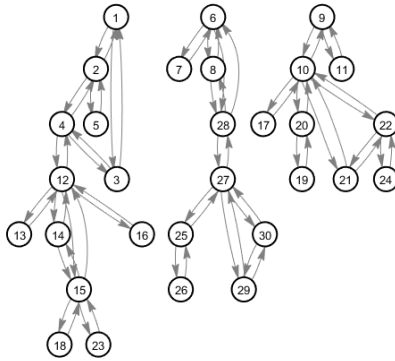


Figure A.2 : Graph model of islanding implementation for Case Study 3

Table A.14 : Active Power Flow at Each Bus on Island 1, Island 2 and Island 3- Case Study 3

Active power (MW) at each bus in Island 1				
Bus	Pre-islanding		Post-islanding	
	Pload	Pgen	Pload	Pgen
1	0.000	260.998	0.000	128.075
2	21.700	40.000	21.700	40.000
3	2.400	0.000	2.400	0.000
4	7.600	0.000	7.600	0.000
5	94.200	0.000	94.200	0.000
12	11.200	0.000	11.200	0.000
13	0.000	0.000	0.000	0.000
14	6.200	0.000	6.200	0.000
15	8.200	0.000	8.200	0.000
16	3.500	0.000	3.500	0.000
18	3.200	0.000	3.200	0.000
23	3.200	0.000	3.200	0.000
Active power (MW) at each bus in Island 2				
Bus	Pre-islanding		Post-islanding	
	Pload	Pgen	Pload	Pgen
6	0.000	0.000	0.000	0.000
7	22.800	0.000	22.800	0.000
8	30.000	0.000	30.000	69.996
25	0.000	0.000	0.000	0.000
26	3.500	0.000	3.500	0.000
27	0.000	0.000	0.000	0.000
28	0.000	0.000	0.000	0.000
29	2.400	0.000	2.400	0.000
30	10.600	0.000	10.600	0.000
Active power (MW) at each bus in Island 3				
Bus	Pre-islanding		Post-islanding	
	Pload	Pgen	Pload	Pgen
9	0.000	0.000	0.000	0.000
10	5.800	0.000	5.800	0.000
11	0.000	0.000	0.000	53.189
17	9.000	0.000	9.000	0.000
19	9.500	0.000	9.500	0.000
20	2.200	0.000	2.200	0.000
21	17.500	0.000	17.500	0.000
22	0.000	0.000	0.000	0.000
24	8.700	0.000	8.700	0.000

Table A.15 : Voltage Profile on Island 1, island 2 and Island 3-
Case Study 3

Island 1		Island 2		Island 3	
Bus. No	Voltage (p.u)	Bus. No	Voltage (p.u)	Bus. No	Voltage (p.u)
1	1.060	6	1.006	9	1.056
2	1.043	7	0.991	10	1.047
3	1.031	8	1.012	11	1.082
4	1.024	25	1.005	17	1.040
5	1.010	26	0.987	19	1.022
12	1.066	27	1.014	20	1.028
13	1.071	28	1.005	21	1.034
14	1.053	29	0.994	22	1.035
15	1.051	30	0.982	24	1.021
16	1.059				
18	1.046				
23	1.045				

Table A.16 : Power Flow Information on Island 1, Island 2 and Island 3- Case Study 3

Power Flow in ISLAND 1							
From bus	To bus	P _{max} (MW)	P _{flow} (MW)	From bus	To bus	P _{max} (MW)	P _{flow} (MW)
1	2	221	93.864	12	14	54.4	6.834
1	3	221	34.210	12	15	54.4	14.176
2	4	110.5	12.253	12	16	54.4	3.513
2	5	221	98.406	14	15	27.2	0.579
3	4	221	31.307	15	18	27.2	3.211
4	12	110.5	35.723	15	23	27.2	3.212
12	13	110.5	0				
Power Flow in ISLAND 2							
From bus	To bus	P _{max} (MW)	P _{flow} (MW)	From bus	To bus	P _{max} (MW)	P _{flow} (MW)
6	7	221	22.969	25	27	27.2	3.546
6	8	54.4	31.124	27	28	110.5	6.193
6	28	54.4	8.041	27	29	27.2	7.095
8	28	54.4	8.873	27	30	27.2	16.853
25	26	27.2	3.565	29	30	27.2	3.704
Power Flow in ISLAND 3							
From bus	To bus	P _{max} (MW)	P _{flow} (MW)	From bus	To bus	P _{max} (MW)	P _{flow} (MW)
9	10	110.5	53.189	10	22	54.4	8.835
9	11	110.5	53.189	19	20	54.4	9.533
10	17	54.4	9.034	21	22	54.4	0.02
10	20	54.4	11.871	22	24	27.2	8.79
10	21	54.4	17.649				

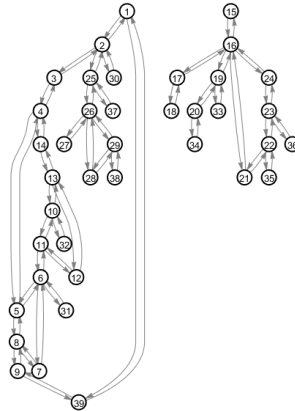


Figure A.3 : Graph model of islanding implementation for Case Study 4

Table A.17 : Active Power Flow at Each Bus on Island 1 and Island 2- Case Study 4

Active power (MW) at each bus in Island 1				
Bus	Pre-islanding		Post-islanding	
	Pload	Pgen	Pload	Pgen
1	97.600	0.000	97.600	0.000
2	0.000	0.000	0.000	0.000
3	322.000	0.000	322.000	0.000
4	500.000	0.000	500.000	0.000
5	0.000	0.000	0.000	0.000
6	0.000	0.000	0.000	0.000
7	233.800	0.000	233.800	0.000
8	522.000	0.000	522.000	0.000
9	6.500	0.000	6.500	0.000
10	0.000	0.000	0.000	0.000
11	0.000	0.000	0.000	0.000
12	8.530	0.000	8.530	0.000
13	0.000	0.000	0.000	0.000
14	0.000	0.000	0.000	0.000
25	224.000	0.000	224.000	0.000
26	139.000	0.000	139.000	0.000
27	281.000	0.000	281.000	0.000
28	206.000	0.000	206.000	0.000
29	283.500	0.000	283.500	0.000
30	0.000	250.000	0.000	269.052
31	9.200	579.539	9.200	601.060
32	0.000	650.000	0.000	669.052
37	0.000	540.000	0.000	559.052
38	0.000	830.000	0.000	849.052
39	1104.000	1000.000	1104.000	1019.052
Active power (MW) at each bus in Island 2				
Bus	Pre-islanding		Post-islanding	
	Pload	Pgen	Pload	Pgen
15	320.000	0.000	320.000	0.000
16	329.000	0.000	329.000	0.000
17	0.000	0.000	0.000	0.000
18	158.000	0.000	158.000	0.000
19	0.000	0.000	0.000	0.000
20	680.000	0.000	680.000	0.000
21	274.000	0.000	274.000	0.000
22	0.000	0.000	0.000	0.000

Active power (MW) at each bus in Island 2				
Bus	Pre-islanding		Post-islanding	
	Pload	Pgen	Pload	Pgen
23	247.500	0.000	247.500	0.000
24	308.600	0.000	308.600	0.000
33	0.000	632.000	0.000	632.000
34	0.000	508.000	0.000	508.000
35	0.000	650.000	0.000	635.223
36	0.000	560.000	0.000	560.000

Table A.18 : Voltage Profile on Island 1 and Island 2- Case Study 4

Island 1		Island 2	
Bus. No	Voltage (p.u)	Bus. No	Voltage (p.u)
1	1.095	15	0.986
2	1.078	16	1.002
3	1.051	17	1.002
4	1.011	18	0.999
5	1.006	19	0.996
6	1.005	20	0.990
7	1.003	21	1.009
8	1.005	22	1.031
9	1.084	23	1.030
10	1.014	24	1.011
11	1.010	33	0.997
12	0.992	34	1.012
13	1.013	35	1.049
14	1.013	36	1.064
25	1.084		
26	1.100		
27	1.100		
28	1.100		
29	1.100		
30	1.099		
31	0.982		
32	1.034		
37	1.028		
38	1.077		
39	1.080		

Table A.19 : Power Flow Information on Island 1 and Island 2- Case Study 4

Power Flow in ISLAND 1							
From bus	To bus	P _{max} (MW)	P _{flow} (MW)	From bus	To bus	P _{max} (MW)	P _{flow} (MW)
1	2	1020	172.081	9	39	1530	11.531
1	39	1700	73.499	10	11	1020	363.962
2	3	850	353.097	10	13	1020	305.090
2	25	850	261.277	10	32	1530	669.052
2	30	1530	269.052	11	12	850	1.556
3	4	850	29.387	12	13	850	7.038
4	5	1020	175.124	13	14	1020	297.689
4	14	850	296.908	25	26	1020	71.700
5	6	2040	509.321	25	37	1530	559.052
5	8	1530	333.670	26	27	1020	281.914
6	7	1530	443.505	26	28	1020	151.433
6	11	816	361.875	26	29	1020	201.284
6	31	3060	591.860	28	29	1020	359.059
7	8	1530	208.536	29	38	2040	849.052
8	9	1530	19.128				

Power Flow in ISLAND 2							
From bus	To bus	P_{max} (MW)	P_{flow} (MW)	From bus	To bus	P_{max} (MW)	P_{flow} (MW)
15	16	1020	321.121	19	33	1530	632.00
16	17	1020	158.352	20	34	1530	508.00
16	19	1020	454.566	21	22	1530	596.875
16	21	1020	320.021	22	23	1020	38.349
16	24	1020	38.150	22	35	1530	635.224
17	18	1020	158.177	23	24	1020	349.342
19	20	1530	174.622	23	36	1530	560.00

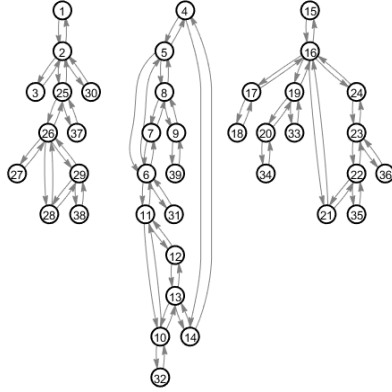


Figure A.4 : Graph model of islanding implementation for Case Study 5

Table A.20 : Active Power Flow at Each Bus on Island 1, Island 2 and Island 3- Case Study 5

Active power (MW) at each bus in Island 1				
Bus	Pre-islanding		Post-islanding	
	Pload	Pgen	Pload	Pgen
4	500.000	0.000	500.000	0.000
5	0.000	0.000	0.000	0.000
6	0.000	0.000	0.000	0.000
7	233.800	0.000	233.800	0.000
8	522.000	0.000	522.000	0.000
9	6.500	0.000	6.500	0.000
10	0.000	0.000	0.000	0.000
11	0.000	0.000	0.000	0.000
12	8.530	0.000	8.530	0.000
13	0.000	0.000	0.000	0.000
14	0.964	0.000	0.000	0.000
31	0.982	579.539	9.200	635.807
32	1.014	650.000	0.000	703.961
39	1.080	1000.000	1104.000	1053.961
Active power (MW) at each bus in Island 2				
Bus	Pre-islanding		Post-islanding	
	Pload	Pgen	Pload	Pgen
1	97.600	0.000	97.600	0.000
2	0.000	0.000	0.000	0.000
3	322.000	0.000	322.000	0.000
25	224.000	0.000	224.000	0.000
26	139.000	0.000	139.000	0.000
27	281.000	0.000	281.000	0.000
28	206.000	0.000	206.000	0.000

Active power (MW) at each bus in Island 2				
Bus	Pre-islanding		Post-islanding	
	Pload	Pgen	Pload	Pgen
29	283.500	0.000	283.500	0.000
30	0.000	250.000	0.000	200.675
37	0.000	540.000	0.000	540.000
38	0.000	830.000	0.000	830.000
Active power (MW) at each bus in Island 3				
Bus	Pre-islanding		Post-islanding	
	Pload	Pgen	Pload	Pgen
15	320.000	0.000	320.000	0.000
16	329.000	0.000	329.000	0.000
17	0.000	0.000	0.000	0.000
18	158.000	0.000	158.000	0.000
19	0.000	0.000	0.000	0.000
20	680.000	0.000	680.000	0.000
21	274.000	0.000	274.000	0.000
22	0.000	0.000	0.000	0.000
23	247.500	0.000	247.500	0.000
24	308.600	0.000	308.600	0.000
33	0.000	632.000	0.000	632.000
34	0.000	508.000	0.000	508.000
35	0.000	650.000	0.000	635.223
36	0.000	560.000	0.000	560.000

Table A.21 : Voltage Profile on Island 1, Island 2 and Island 3-
Case Study 5

Island 1		Island 2		Island 3	
Bus. No	Voltage (p.u)	Bus. No	Voltage (p.u)	Bus. No	Voltage (p.u)
4	0.952	1	1.075	15	0.986
5	0.967	2	1.065	16	1.002
6	0.969	3	1.064	17	1.002
7	0.967	25	1.074	18	0.999
8	0.970	26	1.100	19	0.996
9	1.069	27	1.098	20	0.990
10	0.978	28	1.100	21	1.009
11	0.974	29	1.092	22	1.031
12	0.953	30	1.050	23	1.030
13	0.973	37	1.028	24	1.011
14	0.964	38	1.077	33	0.997
31	0.982			34	1.012
32	1.014			35	1.049
39	1.080			36	1.064

Table A.22 : Power Flow Information on Island 1, Island 2 and Island 3-
Case Study 5

Power Flow in ISLAND 1							
From bus	To bus	P _{max} (MW)	P _{flow} (MW)	From bus	To bus	P _{max} (MW)	P _{flow} (MW)
4	5	1020	189.470	8	9	1530	58.407
4	14	850	311.816	9	39	1530	50.082
5	6	2040	541.768	10	11	1020	383.344
5	8	1530	351.671	10	13	1020	320.617
6	7	1530	465.251	10	32	1530	703.961
6	11	816	381.493	11	12	850	1.222
6	31	3060	626.607	12	13	850	7.378
7	8	1530	230.068	13	14	1020	312.779

Power Flow in ISLAND 2							
From bus	To bus	P_{max} (MW)	P_{flow} (MW)	From bus	To bus	P_{max} (MW)	P_{flow} (MW)
1	2	1020	97.929	26	27	1020	281.925
2	3	850	323.199	26	28	1020	142.142
2	25	850	223.817	26	29	1020	191.861
2	30	1530	200.675	28	29	1020	349.678
25	26	1020	90.326	29	38	2040	830.00
25	37	1530	540.00				

Power Flow in ISLAND 3							
From bus	To bus	P_{max} (MW)	P_{flow} (MW)	From bus	To bus	P_{max} (MW)	P_{flow} (MW)
15	16	1020	321.121	19	33	1530	632.00
16	17	1020	158.352	20	34	1530	508.00
16	19	1020	454.566	21	22	1530	596.875
16	21	1020	320.021	22	23	1020	38.349
16	24	1020	38.150	22	35	1530	635.224
17	18	1020	158.177	23	24	1020	349.342
19	20	1530	174.622	23	36	1530	560.00

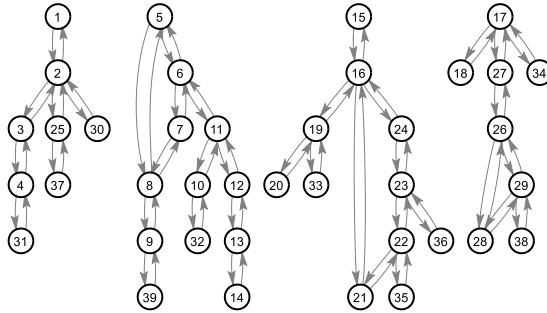


Figure A.5 : Graph model of islanding implementation for Case Study 6

Table A.23 : Active Power Flow at Each Bus on Island 1, Island 2, Island 3 and Island 4- Case Study 6

Active power (MW) at each bus in Island 1				
Bus	Pre-islanding		Post-islanding	
	Pload	Pgen	Pload	Pgen
1	97.600	0.000	97.600	0.000
2	0.000	0.000	0.000	0.000
3	322.000	0.000	322.000	0.000
4	500.000	0.000	500.000	0.000
25	224.000	0.000	224.000	0.000
30	0.000	250.000	0.000	250.000
31	9.200	579.539	9.200	374.948
37	0.000	540.000	0.000	540.000

Active power (MW) at each bus in Island 2				
Bus	Pre-islanding		Post-islanding	
	Pload	Pgen	Pload	Pgen
15	320.000	0.000	320.000	0.000
16	329.000	0.000	329.000	0.000
19	0.000	0.000	0.000	0.000
20	680.000	0.000	680.000	0.000
21	274.000	0.000	0.000	0.000

Active power (MW) at each bus in Island 2				
Bus	Pre-islanding		Post-islanding	
	Pload	Pgen	Pload	Pgen
22	0.000	0.000	0.000	0.000
23	247.500	0.000	247.500	0.000
24	308.600	0.000	308.600	0.000
33	0.000	632.000	0.000	652.000
35	0.000	650.000	0.000	671.497
36	0.000	560.000	0.000	580.000
Active power (MW) at each bus in Island 3				
Bus	Pre-islanding		Post-islanding	
	Pload	Pgen	Pload	Pgen
17	0.000	0.000	0.000	0.000
18	158.000	0.000	158.000	0.000
26	139.000	0.000	139.000	0.000
27	281.000	0.000	281.000	0.000
28	206.000	0.000	206.000	0.000
29	283.500	0.000	283.500	0.000
34	0.000	508.000	0.000	508.000
38	0.000	830.000	0.000	830.000
Active power (MW) at each bus in Island 4				
Bus	Pre-islanding		Post-islanding	
	Pload	Pgen	Pload	Pgen
5	0.000	0.000	0.000	0.000
6	0.000	0.000	0.000	0.000
7	233.800	0.000	0.000	0.000
8	522.000	0.000	522.000	0.000
9	6.500	0.000	6.500	0.000
10	0.000	0.000	0.000	0.000
11	0.000	0.000	0.000	0.000
12	8.530	0.000	8.500	0.000
13	0.000	0.000	0.000	0.000
14	0.000	0.000	0.000	0.000
32	0.000	650.000	0.000	725.000
39	1104.000	1000.000	1104.000	925.355

Table A.24 : Voltage Profile on Island 1, Island 2, Island 3 and Island 4-
Case Study 6

Island 1		Island 2		Island 3		Island 4	
Bus. No	Voltage (p.u)						
1	1.066	15	1.005	17	1.042	5	1.035
2	1.057	16	1.013	18	1.040	6	1.036
3	1.029	19	0.986	26	1.048	7	1.035
4	0.990	20	0.962	27	1.042	8	1.033
25	1.068	21	1.025	28	1.053	9	1.063
30	1.080	22	1.036	29	1.045	10	1.038
31	0.982	23	1.031	34	1.042	11	1.038
37	1.058	24	1.020	38	1.027	12	1.058
		33	0.997			13	1.100
		35	1.049			14	1.100
		36	1.050			32	1.034
						39	1.030

Table A.25 : Power Flow Information on Island 1, Island 2, Island 3 and Island 4 - Case Study 6

Island 1				Island 2			
From bus	To bus	P _{max} (MW)	P _{flow} (MW)	From bus	To bus	P _{max} (MW)	P _{flow} (MW)
1	2	1020	97.931	15	16	1020	320.938
2	3	850	459.663	16	19	1020	34.913
2	25	850	314.431	16	21	1020	582.260
2	30	1530	250.000	16	24	1020	105.289
3	4	850	134.882	19	20	1530	683.579
4	31	3060	365.748	19	33	1530	652.00
25	37	1530	540.00	21	22	1530	584.847
				22	23	1020	86.651
				22	35	1530	617.498
				23	24	1020	417.523
				23	36	1530	580.00
Island 3				Island 4			
From bus	To bus	P _{max} (MW)	P _{flow} (MW)	From bus	To bus	P _{max} (MW)	P _{flow} (MW)
17	18	1020	158.163	5	6	2040	355.353
17	27	1020	347.699	5	8	1530	355.117
17	34	1530	508.00	6	7	1530	355.534
26	27	1020	65.249	6	11	816	714.202
26	28	1020	12.207	7	8	1530	354.826
26	29	1020	61.843	8	9	1530	186.532
28	29	1020	218.893	9	39	1530	179.098
29	38	2040	566.797	10	11	1020	725.000
				10	32	1530	725.000
				11	12	850	8.833
				12	13	850	0.268
				13	14	1020	0.074

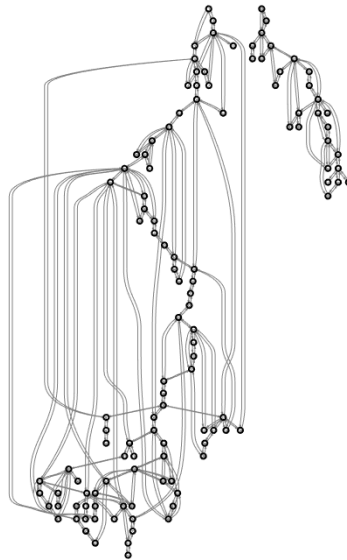


Figure A.6 : Graph model of islanding implementation for Case Study 7

Table A.26 : Active Power Flow at Each Bus on Island 1 and Island 2- Case Study 7

Active power (MW) at each bus in Island 1				
Bus	Pre-islanding		Post-islanding	
	Pload	Pgen	Pload	Pgen
1	51.000	0.000	51.000	0.000
2	20.000	0.000	20.000	0.000
3	39.000	0.000	39.000	0.000
4	39.000	0.000	39.000	0.000
5	0.000	0.000	0.000	0.000
6	52.000	0.000	52.000	0.000
7	19.000	0.000	19.000	0.000
8	28.000	0.000	28.000	0.000
9	0.000	0.000	0.000	0.000
10	0.000	450.000	0.000	450.000
11	70.000	0.000	70.000	0.000
12	47.000	85.000	47.000	85.000
13	34.000	0.000	34.000	0.000
14	14.000	0.000	14.000	0.000
15	90.000	0.000	90.000	0.000
16	25.000	0.000	25.000	0.000
17	11.000	0.000	11.000	0.000
18	60.000	0.000	60.000	0.000
19	45.000	0.000	45.000	0.000
20	18.000	0.000	18.000	0.000
21	14.000	0.000	14.000	0.000
22	10.000	0.000	10.000	0.000
23	7.000	0.000	7.000	0.000
24	13.000	0.000	13.000	0.000
25	0.000	220.000	0.000	220.000
26	0.000	314.000	0.000	314.000
27	71.000	0.000	71.000	0.000
28	17.000	0.000	17.000	0.000
29	24.000	0.000	24.000	0.000
30	0.000	0.000	0.000	0.000
31	43.000	7.000	43.000	7.000
32	59.000	0.000	59.000	0.000
33	23.000	0.000	23.000	0.000
34	59.000	0.000	59.000	0.000
35	33.000	0.000	33.000	0.000
36	31.000	0.000	31.000	0.000
37	0.000	0.000	0.000	0.000
38	0.000	0.000	0.000	0.000
39	27.000	0.000	27.000	0.000
40	66.000	0.000	66.000	0.000
41	37.000	0.000	37.000	0.000
42	96.000	0.000	96.000	0.000
43	18.000	0.000	18.000	0.000
44	16.000	0.000	16.000	0.000
45	53.000	0.000	53.000	0.000
46	28.000	19.000	28.000	19.000
47	34.000	0.000	34.000	0.000
48	20.000	0.000	20.000	0.000
49	87.000	204.000	87.000	204.000
50	17.000	0.000	17.000	0.000
51	17.000	0.000	17.000	0.000
52	18.000	0.000	18.000	0.000
53	23.000	0.000	23.000	0.000
54	113.000	48.000	113.000	48.000

Active power (MW) at each bus in Island 1				
Bus	Pre-islanding		Post-islanding	
	Pload	Pgen	Pload	Pgen
55	63.000	0.000	63.000	0.000
56	84.000	0.000	84.000	0.000
57	12.000	0.000	12.000	0.000
58	12.000	0.000	12.000	0.000
59	277.000	155.000	277.000	155.000
60	78.000	0.000	78.000	0.000
61	0.000	160.000	0.000	160.000
62	77.000	0.000	77.000	0.000
63	0.000	0.000	0.000	0.000
64	0.000	0.000	0.000	0.000
65	0.000	391.000	0.000	391.000
66	39.000	392.000	39.000	392.000
67	28.000	0.000	28.000	0.000
68	0.000	0.000	0.000	0.000
69	0.000	511.920	0.000	566.117
70	66.000	0.000	66.000	0.000
71	0.000	0.000	0.000	0.000
72	12.000	0.000	12.000	0.000
73	6.000	0.000	6.000	0.000
74	68.000	0.000	68.000	0.000
75	47.000	0.000	47.000	0.000
76	68.000	0.000	68.000	0.000
77	61.000	0.000	61.000	0.000
78	71.000	0.000	71.000	0.000
79	39.000	0.000	39.000	0.000
80	130.000	477.000	130.000	477.000
81	0.000	0.000	0.000	0.000
82	54.000	0.000	54.000	0.000
96	38.000	0.000	38.000	0.000
97	15.000	0.000	15.000	0.000
98	34.000	0.000	34.000	0.000
113	6.000	0.000	6.000	0.000
114	8.000	0.000	8.000	0.000
115	22.000	0.000	22.000	0.000
116	184.000	0.000	184.000	0.000
117	20.000	0.000	20.000	0.000
118	33.000	0.000	33.000	0.000
Active power (MW) at each bus in Island 2				
Bus	Pre-islanding		Post-islanding	
	Pload	Pgen	Pload	Pgen
83	20.000	0.000	20.000	0.000
84	11.000	0.000	11.000	0.000
85	24.000	0.000	24.000	0.000
86	21.000	0.000	21.000	0.000
87	0.000	4.000	0.000	4.000
88	48.000	0.000	48.000	0.000
89	0.000	607.000	0.000	551.258
90	163.000	0.000	163.000	0.000
91	10.000	0.000	10.000	0.000
92	65.000	0.000	65.000	0.000
93	12.000	0.000	12.000	0.000
94	30.000	0.000	30.000	0.000
95	42.000	0.000	42.000	0.000
99	42.000	0.000	42.000	0.000
100	37.000	252.000	37.000	252.000

Active power (MW) at each bus in Island 2				
Bus	Pre-islanding		Post-islanding	
	Pload	Pgen	Pload	Pgen
101	22.000	0.000	22.000	0.000
102	5.000	0.000	5.000	0.000
103	23.000	40.000	23.000	40.000
104	38.000	0.000	38.000	0.000
105	31.000	0.000	31.000	0.000
106	43.000	0.000	43.000	0.000
107	50.000	0.000	50.000	0.000
108	2.000	0.000	2.000	0.000
109	8.000	0.000	8.000	0.000
110	39.000	0.000	39.000	0.000
111	0.000	36.000	0.000	36.000
112	68.000	0.000	68.000	0.000

Table A.27 : Voltage Profile on Island 1 and Island 2- Case Study 7

Island 1			
Bus. No	Voltage (p.u)	Bus. No	Voltage (p.u)
1	0.965	47	1.019
2	0.976	48	1.016
3	0.975	49	1.025
4	0.998	50	1.003
5	1.002	51	0.972
6	0.990	52	0.963
7	0.989	53	0.951
8	1.015	54	0.955
9	1.079	55	0.962
10	1.080	56	0.954
11	0.986	57	0.973
12	0.990	58	0.963
13	0.974	59	0.985
14	0.988	60	1.003
15	0.980	61	1.005
16	0.987	62	1.008
17	0.999	63	1.010
18	0.973	64	1.022
19	0.973	65	1.045
20	0.972	66	1.050
21	0.973	67	1.026
22	0.982	68	1.023
23	1.004	69	1.035
24	0.992	70	0.994
25	1.040	71	0.993
26	1.015	72	0.980
27	0.968	73	0.991
28	0.963	74	0.968
29	0.964	75	0.975
30	1.034	76	0.943
31	0.967	77	1.006
32	0.974	78	1.002
33	0.985	79	1.005
34	0.996	80	1.040
35	0.991	81	1.040
36	0.990	82	0.998
37	1.004	96	1.009
38	1.040	97	1.021
39	0.976	98	1.026

Island 1			
Bus. No	Voltage (p.u)	Bus. No	Voltage (p.u)
40	0.970	113	0.993
41	0.968	114	0.967
42	0.985	115	0.966
43	0.988	116	1.005
44	0.981	117	0.976
45	0.983	118	0.954
46	1.005		
Island 2			
Bus. No	Voltage (p.u)	Bus. No	Voltage (p.u)
83	0.973	100	1.017
84	0.977	101	1.000
85	0.985	102	1.002
86	0.990	103	1.001
87	1.015	104	0.971
88	0.990	105	0.965
89	1.005	106	0.963
90	0.985	107	0.952
91	0.980	108	0.967
92	1.003	109	0.968
93	0.992	110	0.973
94	0.989	111	0.980
95	0.970	112	0.975
99	1.010		

Table A.28 : Power Flow Information on Island 1 and Island 2 - Case Study 7

Power Flow in ISLAND 1							
From bus	To bus	P _{max} (MW)	P _{flow} (MW)	From bus	To bus	P _{max} (MW)	P _{flow} (MW)
1	2	297.5	12.188	45	46	297.5	36.276
1	3	297.5	39.034	45	49	297.5	50.517
2	12	297.5	32.485	46	47	297.5	31.311
3	5	297.5	69.590	46	48	297.5	14.449
3	12	297.5	9.710	47	49	297.5	8.380
4	5	850	103.137	47	69	297.5	59.812
4	11	297.5	63.941	48	49	297.5	34.661
5	6	297.5	88.127	49	50	297.5	53.677
5	8	850	337.713	49	51	297.5	66.646
5	11	297.5	76.859	49	54	297.5	37.703
6	7	297.5	35.203	49	54	297.5	37.683
7	12	297.5	16.144	49	66	297.5	131.481
8	9	850	445.520	49	66	297.5	131.481
8	30	297.5	74.660	49	69	297.5	49.886
9	10	850	450.00	50	57	297.5	35.912
11	12	297.5	33.911	51	52	297.5	28.491
11	13	297.5	34.835	51	58	297.5	18.939
12	14	297.5	18.052	52	53	297.5	10.311
12	16	297.5	7.515	53	54	297.5	12.791
12	117	297.5	20.145	54	55	297.5	7.791
13	15	297.5	0.547	54	56	297.5	17.537
14	15	297.5	3.979	54	59	297.5	30.802
15	17	850	104.902	55	56	297.5	20.366
15	19	297.5	11.453	55	59	297.5	35.705
15	33	297.5	6.469	56	57	297.5	23.251

Power Flow in ISLAND 1								
From bus	To bus	P_{max} (MW)	P_{flow} (MW)		From bus	To bus	P_{max} (MW)	P_{flow} (MW)
16	17	297.5	17.643		56	58	297.5	6.833
17	18	297.5	80.093		56	59	297.5	28.546
17	31	297.5	16.232		56	59	297.5	29.939
17	113	297.5	3.340		59	60	297.5	44.184
17	30	850	233.209		59	61	297.5	52.862
18	19	297.5	19.156		59	63	850	151.479
19	20	297.5	10.153		60	61	850	113.141
19	34	297.5	4.418		60	62	297.5	9.395
20	21	297.5	28.312		61	62	297.5	26.525
21	22	297.5	42.707		61	64	850	32.528
22	23	297.5	53.693		62	66	297.5	37.084
23	24	297.5	9.243		62	67	297.5	23.703
23	25	850	166.309		63	64	850	151.904
23	32	238	92.295		64	65	850	185.389
24	70	297.5	5.461		65	66	850	0.653
24	72	297.5	1.633		65	68	850	17.067
25	26	850	87.390		66	67	297.5	52.301
25	27	850	141.081		68	69	850	143.909
26	30	850	226.610		68	81	850	24.133
27	28	297.5	32.010		68	116	850	184.705
27	32	297.5	11.330		69	70	850	112.573
27	115	297.5	20.564		69	75	850	116.567
28	29	297.5	14.800		69	77	297.5	83.370
29	31	297.5	9.275		70	71	297.5	16.471
30	38	297.5	63.730		70	74	297.5	18.438
31	32	297.5	29.567		70	75	297.5	2.598
32	113	850	2.771		71	72	297.5	10.443
32	114	297.5	9.536		71	73	297.5	6.004
33	37	297.5	16.706		74	75	297.5	50.107
34	36	297.5	30.301		75	77	297.5	29.109
34	37	850	96.894		75	118	297.5	45.281
34	43	297.5	2.858		76	77	297.5	58.042
35	36	297.5	0.796		76	118	297.5	11.833
35	37	297.5	33.958		77	78	297.5	45.076
37	39	297.5	56.472		77	80	850	99.775
37	40	297.5	45.754		77	80	850	45.733
37	38	850	249.785		77	82	340	31.123
38	65	850	189.197		78	79	297.5	26.052
39	40	297.5	28.417		79	80	850	65.894
40	41	297.5	17.015		80	96	297.5	34.907
40	42	297.5	10.326		80	97	297.5	42.292
41	42	297.5	20.222		80	98	297.5	34.267
42	49	297.5	66.280		80	81	850	24.133
42	49	297.5	66.280		82	96	297.5	23.285
43	44	297.5	15.325		96	97	297.5	26.956
44	45	297.5	31.563		114	115	297.5	1.512
Power Flow in ISLAND 2								
From bus	To bus	P_{max} (MW)	P_{flow} (MW)		From bus	To bus	P_{max} (MW)	P_{flow} (MW)

Power Flow in ISLAND 2								
From bus	To bus	P_{max} (MW)	P_{flow} (MW)		From bus	To bus	P_{max} (MW)	P_{flow} (MW)
83	84	297.5	6.431		94	100	297.5	17.009
83	85	297.5	13.688		99	100	297.5	42.312
84	85	297.5	17.531		100	101	297.5	17.757
85	86	850	17.174		100	103	850	121.073
85	88	297.5	26.301		100	104	297.5	56.388
85	89	297.5	46.762		100	106	297.5	60.622
86	87	850	4.000		101	102	297.5	40.163
88	89	850	75.089		103	104	297.5	32.293
89	90	850	109.918		103	105	297.5	42.937
89	90	850	57.743		103	110	297.5	60.575
89	92	850	199.280		104	105	297.5	48.682
89	92	850	62.482		105	106	297.5	8.676
90	91	297.5	0.102		105	107	297.5	26.679
91	92	297.5	10.033		105	108	297.5	23.982
92	93	297.5	54.635		106	107	297.5	24.057
92	94	297.5	49.088		108	109	297.5	21.783
92	100	297.5	32.068		109	110	297.5	13.717
92	102	297.5	45.421		110	111	297.5	36.000
93	94	297.5	41.868		110	112	297.5	69.459
94	95	297.5	42.373					

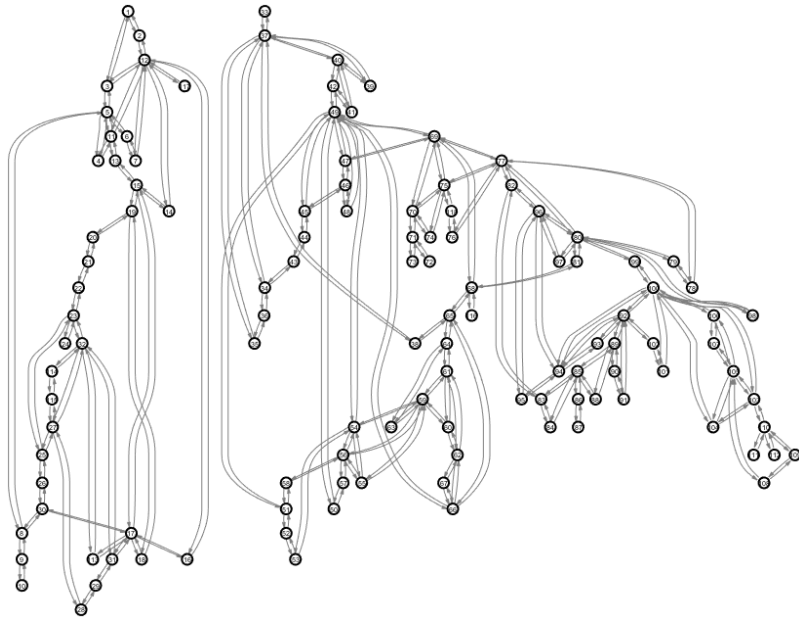


Figure A.7 : Graph model of islanding implementation for Case Study 8

Table A.29 : Active Power Flow at Each Bus on Island 1 and Island 2- Case Study 8

Active power (MW) at each bus in Island 1				
Bus	Pre-islanding		Post-islanding	
	Pload	Pgen	Pload	Pgen
1	51.000	0.000	51.000	0.000
2	20.000	0.000	20.000	0.000
3	39.000	0.000	39.000	0.000
4	39.000	0.000	39.000	0.000
5	0.000	0.000	0.000	0.000
6	52.000	0.000	52.000	0.000
7	19.000	0.000	19.000	0.000
8	28.000	0.000	28.000	0.000
9	0.000	0.000	0.000	0.000
10	0.000	450.000	0.000	385.153
11	70.000	0.000	70.000	0.000
12	47.000	85.000	47.000	85.000
13	34.000	0.000	34.000	0.000
14	14.000	0.000	14.000	0.000
15	90.000	0.000	90.000	0.000
16	25.000	0.000	25.000	0.000
17	11.000	0.000	11.000	0.000
18	60.000	0.000	60.000	0.000
19	45.000	0.000	45.000	0.000
20	18.000	0.000	18.000	0.000
21	14.000	0.000	14.000	0.000
22	10.000	0.000	10.000	0.000
23	7.000	0.000	7.000	0.000
24	13.000	0.000	13.000	0.000
25	0.000	220.000	0.000	220.000
26	0.000	314.000	0.000	314.000
27	71.000	0.000	71.000	0.000
28	17.000	0.000	17.000	0.000
29	24.000	0.000	24.000	0.000
30	0.000	0.000	0.000	0.000
31	43.000	7.000	43.000	7.000
32	59.000	0.000	59.000	0.000
113	6.000	0.000	6.000	0.000
114	8.000	0.000	8.000	0.000
115	22.000	0.000	22.000	0.000
117	20.000	0.000	20.000	0.000
Active power (MW) at each bus in Island 2				
Bus	Pre-islanding		Post-islanding	
	Pload	Pgen	Pload	Pgen
33	23.000	0.000	23.000	0.000
34	59.000	0.000	59.000	0.000
35	33.000	0.000	33.000	0.000
36	31.000	0.000	31.000	0.000
37	0.000	0.000	0.000	0.000
38	0.000	0.000	0.000	0.000
39	27.000	0.000	27.000	0.000
40	66.000	0.000	66.000	0.000
41	37.000	0.000	37.000	0.000
42	96.000	0.000	96.000	0.000
43	18.000	0.000	18.000	0.000
44	16.000	0.000	16.000	0.000
45	53.000	0.000	53.000	0.000
46	28.000	19.000	28.000	19.000
47	34.000	0.000	34.000	0.000

Active power (MW) at each bus in Island 2				
Bus	Pre-islanding		Post-islanding	
	Pload	Pgen	Pload	Pgen
48	20.000	0.000	20.000	0.000
49	87.000	204.000	87.000	204.000
50	17.000	0.000	17.000	0.000
51	17.000	0.000	17.000	0.000
52	18.000	0.000	18.000	0.000
53	23.000	0.000	23.000	0.000
54	113.000	48.000	113.000	48.000
55	63.000	0.000	63.000	0.000
56	84.000	0.000	84.000	0.000
57	12.000	0.000	12.000	0.000
58	12.000	0.000	12.000	0.000
59	277.000	155.000	277.000	155.000
60	78.000	0.000	78.000	0.000
61	0.000	160.000	0.000	160.000
62	77.000	0.000	77.000	0.000
63	0.000	0.000	0.000	0.000
64	0.000	0.000	0.000	0.000
65	0.000	391.000	0.000	391.000
66	39.000	392.000	39.000	392.000
67	28.000	0.000	28.000	0.000
68	0.000	0.000	0.000	0.000
69	0.000	511.920	0.000	578.901
70	66.000	0.000	66.000	0.000
71	0.000	0.000	0.000	0.000
72	12.000	0.000	12.000	0.000
73	6.000	0.000	6.000	0.000
74	68.000	0.000	68.000	0.000
75	47.000	0.000	47.000	0.000
76	68.000	0.000	68.000	0.000
77	61.000	0.000	61.000	0.000
78	71.000	0.000	71.000	0.000
79	39.000	0.000	39.000	0.000
80	130.000	477.000	130.000	477.000
81	0.000	0.000	0.000	0.000
82	54.000	0.000	54.000	0.000
83	20.000	0.000	20.000	0.000
84	11.000	0.000	11.000	0.000
85	24.000	0.000	24.000	0.000
86	21.000	0.000	21.000	0.000
87	0.000	4.000	0.000	4.000
88	48.000	0.000	48.000	0.000
89	0.000	607.000	0.000	607.000
90	163.000	0.000	163.000	0.000
91	10.000	0.000	10.000	0.000
92	65.000	0.000	65.000	0.000
93	12.000	0.000	12.000	0.000
94	30.000	0.000	30.000	0.000
95	42.000	0.000	42.000	0.000
96	38.000	0.000	38.000	0.000
97	15.000	0.000	15.000	0.000
98	34.000	0.000	34.000	0.000
99	42.000	0.000	42.000	0.000
100	37.000	252.000	37.000	252.000
101	22.000	0.000	22.000	0.000
102	5.000	0.000	5.000	0.000

Active power (MW) at each bus in Island 2				
Bus	Pre-islanding		Post-islanding	
	Pload	Pgen	Pload	Pgen
103	23.000	40.000	23.000	40.000
104	38.000	0.000	38.000	0.000
105	31.000	0.000	31.000	0.000
106	43.000	0.000	43.000	0.000
107	50.000	0.000	50.000	0.000
108	2.000	0.000	2.000	0.000
109	8.000	0.000	8.000	0.000
110	39.000	0.000	39.000	0.000
111	0.000	36.000	0.000	36.000
112	68.000	0.000	68.000	0.000
116	184.000	0.000	184.000	0.000
118	33.000	0.000	33.000	0.000

Table A.30 : Voltage Profile on Island 1 and Island 2- Case Study 8

Island 1			
Bus. No	Voltage (p.u)	Bus. No	Voltage (p.u)
1	0.965	19	0.963
2	0.976	20	0.964
3	0.975	21	0.967
4	0.998	22	0.978
5	1.002	23	1.003
6	0.990	24	0.992
7	0.989	25	1.040
8	1.015	26	1.015
9	1.066	27	0.968
10	1.05	28	0.963
11	0.986	29	0.964
12	0.990	30	1.022
13	0.971	31	0.967
14	0.985	32	0.974
15	0.970	113	0.993
16	0.986	114	0.967
17	0.995	115	0.966
18	0.973	117	0.976
Island 2			
Bus. No	Voltage (p.u)	Bus. No	Voltage (p.u)
33	0.974	74	0.958
34	0.986	75	0.970
35	0.981	76	0.943
36	0.98	77	1.006
37	0.993	78	1.002
38	1.020	79	1.005
39	0.972	80	1.040
40	0.970	81	1.040
41	0.968	82	0.990
42	0.985	83	0.987
43	0.980	84	0.988
44	0.976	85	0.995
45	0.980	86	0.996
46	1.005	87	1.015
47	1.019	88	0.993
48	1.016	89	1.005
49	1.025	90	0.985
50	1.003	91	0.980

Island 2			
Bus. No	Voltage (p.u)	Bus. No	Voltage (p.u)
51	0.972	92	1.003
52	0.963	93	0.996
53	0.951	94	0.997
54	0.955	95	0.988
55	0.962	96	0.998
56	0.954	97	1.015
57	0.973	98	1.026
58	0.963	99	1.010
59	0.985	100	1.017
60	1.003	101	1.000
61	1.005	102	1.002
62	1.008	103	1.001
63	1.010	104	0.971
64	1.022	105	0.965
65	1.045	106	0.963
66	1.050	107	0.952
67	1.026	108	0.967
68	1.023	109	0.968
69	1.035	110	0.973
70	0.984	111	0.980
71	0.987	112	0.975
72	0.980	116	1.005
73	0.991	118	0.951

Table A.31 : Power Flow Information on Island 1 and Island 2 - Case Study 8

Power Flow in ISLAND 1							
From bus	To bus	P _{max} (MW)	P _{flow} (MW)	From bus	To bus	P _{max} (MW)	P _{flow} (MW)
1	2	297.5	12.934	17	18	297.5	82.202
1	3	297.5	38.350	17	30	850	242.123
2	12	297.5	33.175	17	31	297.5	16.023
3	5	297.5	67.972	17	113	297.5	3.227
3	12	297.5	10.598	18	19	297.5	21.285
4	5	850	99.910	19	20	297.5	10.192
4	11	297.5	60.725	20	21	297.5	28.350
5	6	297.5	85.111	21	22	297.5	42.752
5	8	850	326.194	22	23	297.5	53.748
5	11	297.5	73.201	23	24	297.5	13.071
6	7	297.5	32.249	23	25	850	169.690
7	12	297.5	13.199	23	32	238	91.625
8	9	850	381.646	25	27	850	142.043
8	30	297.5	23.728	25	26	850	91.733
9	10	850	385.204	26	30	850	222.267
11	12	297.5	30.402	27	28	297.5	32.178
11	13	297.5	31.664	27	32	297.5	11.794
12	14	297.5	14.462	27	115	297.5	20.814
12	16	297.5	3.091	28	29	297.5	14.967
12	117	297.5	20.145	29	31	297.5	9.110
13	15	297.5	2.597	31	32	297.5	29.292
14	15	297.5	0.415	32	113	850	2.846

Power Flow in ISLAND 1								
From bus	To bus	P_{max} (MW)	P_{flow} (MW)		From bus	To bus	P_{max} (MW)	P_{flow} (MW)
15	17	850	107.532		32	114	297.5	9.288
15	19	297.5	13.678		114	115	297.5	1.265
16	17	297.5	22.140					
Power Flow in ISLAND 2								
From bus	To bus	P_{max} (MW)	P_{flow} (MW)		From bus	To bus	P_{max} (MW)	P_{flow} (MW)
33	37	297.5	23.245		70	71	297.5	18.125
34	36	297.5	31.288		70	74	297.5	17.809
34	37	850	87.292		70	75	297.5	1.873
34	43	297.5	3.266		71	72	297.5	12.067
35	36	297.5	0.187		71	73	297.5	6.010
35	37	297.5	32.966		74	75	297.5	50.762
37	38	850	233.692		75	77	297.5	32.526
37	39	297.5	50.467		75	118	297.5	42.467
37	40	297.5	39.721		76	77	297.5	60.885
38	65	850	238.456		76	118	297.5	9.092
39	40	297.5	22.627		77	78	297.5	48.579
40	41	297.5	11.297		77	80	850	92.272
40	42	297.5	16.158		77	80	850	42.134
41	42	297.5	26.020		77	82	340	2.309
42	49	297.5	72.703		78	79	297.5	22.550
42	49	297.5	72.703		79	80	297.5	62.334
43	44	297.5	21.586		80	96	297.5	18.455
44	45	297.5	37.927		80	97	297.5	25.905
45	46	297.5	39.674		80	98	297.5	28.586
45	49	297.5	53.822		80	99	340	19.190
46	47	297.5	34.143		80	81	850	58.124
46	48	297.5	15.093		82	83	340	47.219
47	49	297.5	5.094		82	96	297.5	9.129
47	69	297.5	66.611		83	84	297.5	25.627
48	49	297.5	35.313		83	85	297.5	43.221
49	50	297.5	53.219		84	85	297.5	37.059
49	51	297.5	66.090		85	86	850	17.140
49	54	297.5	37.212		85	88	297.5	50.652
49	54	297.5	37.204		85	89	297.5	72.559
49	66	850	134.422		86	87	850	4.000
49	66	850	134.422		88	89	850	100.029
49	69	297.5	56.443		89	90	850	57.945
50	57	297.5	35.465		89	90	850	110.304
51	52	297.5	28.321		89	92	850	202.629
51	58	297.5	18.586		89	92	850	63.533
52	53	297.5	10.143		90	91	297.5	0.658
53	54	297.5	12.960		91	92	297.5	9.475

Power Flow in ISLAND 2								
From bus	To bus	P _{max} (MW)	P _{flow} (MW)		From bus	To bus	P _{max} (MW)	P _{flow} (MW)
54	55	297.5	7.650		92	93	297.5	57.916
54	56	297.5	17.099		92	94	297.5	52.398
54	59	297.5	31.326		92	100	297.5	31.158
55	56	297.5	20.008		92	102	297.5	44.513
55	59	297.5	36.219		93	94	297.5	45.038
56	57	297.5	22.818		94	95	297.5	40.904
56	58	297.5	6.484		94	96	297.5	19.804
56	59	297.5	28.986		94	100	297.5	4.866
56	59	297.5	30.399		95	96	297.5	1.394
59	60	297.5	44.469		96	97	297.5	10.704
59	61	297.5	53.178		98	100	297.5	5.634
59	63	850	152.835		99	100	297.5	23.113
60	61	850	113.588		100	101	297.5	16.877
60	62	297.5	9.236		100	103	850	121.073
61	62	297.5	26.923		100	104	297.5	56.388
61	64	850	33.689		100	106	297.5	60.622
62	66	297.5	36.797		101	102	297.5	39.265
62	67	297.5	23.423		103	104	297.5	32.293
63	64	850	153.267		103	105	297.5	42.937
64	65	850	187.936		103	110	297.5	60.575
65	66	850	4.656		104	105	297.5	48.682
65	68	850	40.353		105	106	297.5	8.676
66	67	297.5	52.015		105	107	297.5	26.679
68	69	850	167.112		105	108	297.5	23.982
68	81	850	58.124		106	107	297.5	24.056
68	116	850	184.708		108	109	297.5	21.783
69	70	850	107.169		109	110	297.5	13.717
69	75	850	111.490		110	111	297.5	36.000
69	77	297.5	70.076		110	112	297.5	69.459

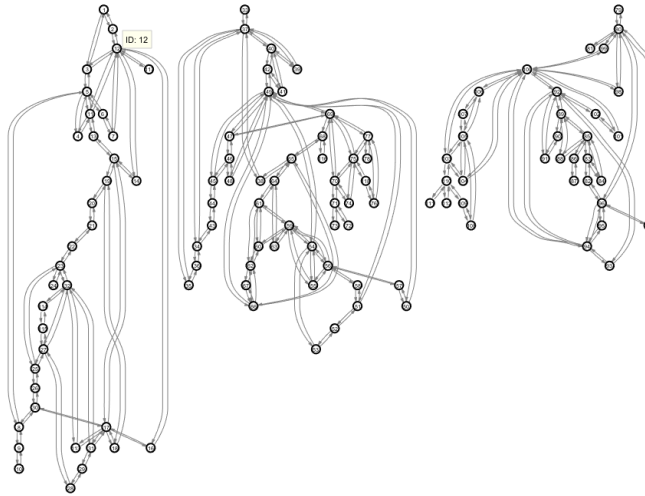


Figure A.8 : Graph model of islanding implementation for Case Study 9

Table A.32 : Active Power Flow at Each Bus on Island 1, Island 2 and Island 3 - Case Study 9

Active power (MW) at each bus in Island 1				
Bus	Pre-islanding		Post-islanding	
	Pload	Pgen	Pload	Pgen
1	51.000	0.000	51.000	0.000
2	20.000	0.000	20.000	0.000
3	39.000	0.000	39.000	0.000
4	39.000	0.000	39.000	0.000
5	0.000	0.000	0.000	0.000
6	52.000	0.000	52.000	0.000
7	19.000	0.000	19.000	0.000
8	28.000	0.000	28.000	0.000
9	0.000	0.000	0.000	0.000
10	0.000	450.000	0.000	385.153
11	70.000	0.000	70.000	0.000
12	47.000	85.000	47.000	85.000
13	34.000	0.000	34.000	0.000
14	14.000	0.000	14.000	0.000
15	90.000	0.000	90.000	0.000
16	25.000	0.000	25.000	0.000
17	11.000	0.000	11.000	0.000
18	60.000	0.000	60.000	0.000
19	45.000	0.000	45.000	0.000
20	18.000	0.000	18.000	0.000
21	14.000	0.000	14.000	0.000
22	10.000	0.000	10.000	0.000
23	7.000	0.000	7.000	0.000
24	13.000	0.000	13.000	0.000
25	0.000	220.000	0.000	220.000
26	0.000	314.000	0.000	314.000
27	71.000	0.000	71.000	0.000
28	17.000	0.000	17.000	0.000
29	24.000	0.000	24.000	0.000
30	0.000	0.000	0.000	0.000
31	43.000	7.000	43.000	7.000
32	59.000	0.000	59.000	0.000

Active power (MW) at each bus in Island 1				
Bus	Pre-islanding		Post-islanding	
	Pload	Pgen	Pload	Pgen
113	6.000	0.000	6.000	0.000
114	8.000	0.000	8.000	0.000
115	22.000	0.000	22.000	0.000
117	20.000	0.000	20.000	0.000
Active power (MW) at each bus in Island 2				
Bus	Pre-islanding		Post-islanding	
	Pload	Pgen	Pload	Pgen
33	23.000	0.000	23.000	0.000
34	59.000	0.000	59.000	0.000
35	33.000	0.000	33.000	0.000
36	31.000	0.000	31.000	0.000
37	0.000	0.000	0.000	0.000
38	0.000	0.000	0.000	0.000
39	27.000	0.000	27.000	0.000
40	66.000	0.000	66.000	0.000
41	37.000	0.000	37.000	0.000
42	96.000	0.000	96.000	0.000
43	18.000	0.000	18.000	0.000
44	16.000	0.000	16.000	0.000
45	53.000	0.000	53.000	0.000
46	28.000	19.000	28.000	19.000
47	34.000	0.000	34.000	0.000
48	20.000	0.000	20.000	0.000
49	87.000	204.000	87.000	204.000
50	17.000	0.000	17.000	0.000
51	17.000	0.000	17.000	0.000
52	18.000	0.000	18.000	0.000
53	23.000	0.000	23.000	0.000
54	113.000	48.000	113.000	48.000
55	63.000	0.000	63.000	0.000
56	84.000	0.000	84.000	0.000
57	12.000	0.000	12.000	0.000
58	12.000	0.000	12.000	0.000
59	277.000	155.000	277.000	155.000
60	78.000	0.000	78.000	0.000
61	0.000	160.000	0.000	160.000
62	77.000	0.000	77.000	0.000
63	0.000	0.000	0.000	0.000
64	0.000	0.000	0.000	0.000
65	0.000	391.000	0.000	391.000
66	39.000	392.000	39.000	392.000
67	28.000	0.000	28.000	0.000
68	0.000	0.000	0.000	0.000
69	0.000	511.920	0.000	804.212
70	66.000	0.000	66.000	0.000
71	0.000	0.000	0.000	0.000
72	12.000	0.000	12.000	0.000
73	6.000	0.000	6.000	0.000
74	68.000	0.000	68.000	0.000
75	47.000	0.000	47.000	0.000
76	68.000	0.000	68.000	0.000
77	61.000	0.000	61.000	0.000
78	71.000	0.000	71.000	0.000
116	184.000	0.000	184.000	0.000
118	33.000	0.000	33.000	0.000

Active power (MW) at each bus in Island 3				
Bus	Pre-islanding		Post-islanding	
	Pload	Pgen	Pload	Pgen
79	39.000	0.000	39.000	0.000
80	130.000	477.000	130.000	477.000
81	0.000	0.000	0.000	0.000
82	54.000	0.000	54.000	0.000
83	20.000	0.000	20.000	0.000
84	11.000	0.000	11.000	0.000
85	24.000	0.000	24.000	0.000
86	21.000	0.000	21.000	0.000
87	0.000	4.000	0.000	4.000
88	48.000	0.000	48.000	0.000
89	0.000	607.000	0.000	383.906
90	163.000	0.000	163.000	0.000
91	10.000	0.000	10.000	0.000
92	65.000	0.000	65.000	0.000
93	12.000	0.000	12.000	0.000
94	30.000	0.000	30.000	0.000
95	42.000	0.000	42.000	0.000
96	38.000	0.000	38.000	0.000
97	15.000	0.000	15.000	0.000
98	34.000	0.000	34.000	0.000
99	42.000	0.000	42.000	0.000
100	37.000	252.000	37.000	252.000
101	22.000	0.000	22.000	0.000
102	5.000	0.000	5.000	0.000
103	23.000	40.000	23.000	40.000
104	38.000	0.000	38.000	0.000
105	31.000	0.000	31.000	0.000
106	43.000	0.000	43.000	0.000
107	50.000	0.000	50.000	0.000
108	2.000	0.000	2.000	0.000
109	8.000	0.000	8.000	0.000
110	39.000	0.000	39.000	0.000
111	0.000	36.000	0.000	36.000
112	68.000	0.000	68.000	0.000

Table A.33 : Voltage Profile on Island 1, Island 2 and Island 3- Case Study 9

Island 1				
Bus. No	Voltage (p.u)		Bus. No	Voltage (p.u)
1	0.965		19	0.963
2	0.976		20	0.964
3	0.975		21	0.967
4	0.998		22	0.978
5	1.002		23	1.003
6	0.990		24	0.992
7	0.990		25	1.040
8	1.015		26	1.015
9	1.066		27	0.968
10	1.050		28	0.963
11	0.986		29	0.964
12	0.990		30	1.022
13	0.971		31	0.967
14	0.985		32	0.974
15	0.970		113	0.993
16	0.986		114	0.967

Island 1				
Bus. No	Voltage (p.u)		Bus. No	Voltage (p.u)
17	0.995		115	0.966
18	0.973		117	0.976
Island 2				
Bus. No	Voltage (p.u)		Bus. No	Voltage (p.u)
33	0.975		57	0.980
34	0.986		58	0.970
35	0.981		59	0.985
36	0.980		60	1.003
37	0.993		61	1.005
38	1.022		62	1.008
39	0.972		63	1.011
40	0.970		64	1.024
41	0.968		65	1.045
42	0.985		66	1.050
43	0.979		67	1.026
44	0.975		68	1.017
45	0.979		69	1.035
46	1.005		70	0.984
47	1.021		71	0.987
48	1.016		72	0.980
49	1.025		73	0.991
50	1.006		74	0.958
51	0.976		75	0.963
52	0.967		76	0.933
53	0.953		77	0.966
54	0.955		78	0.960
55	0.952		116	1.005
56	0.964		118	0.942
Island 3				
Bus. No	Voltage (p.u)		Bus. No	Voltage (p.u)
79	1.013		96	0.992
80	1.040		97	1.010
81	1.040		98	1.024
82	0.974		99	1.010
83	0.974		100	1.017
84	0.978		101	1.001
85	0.985		102	1.003
86	0.990		103	1.001
87	1.015		104	0.971
88	0.990		105	0.965
89	1.005		106	0.963
90	0.985		107	0.952
91	0.980		108	0.967
92	1.003		109	0.968
93	0.996		110	0.973
94	0.996		111	0.980
95	0.984		112	0.975

Table A.34 : Power Flow Information on Island 1, Island 2 and Island 3 - Case Study 9

Power Flow in ISLAND 1								
From bus	To bus	P _{max} (MW)	P _{flow} (MW)		From bus	To bus	P _{max} (MW)	P _{flow} (MW)
1	2	297.5	12.934		17	18	297.5	82.202
1	3	297.5	38.350		17	30	850	242.123
2	12	297.5	33.175		17	31	297.5	16.023

Power Flow in ISLAND 1							
From bus	To bus	P _{max} (MW)	P _{flow} (MW)	From bus	To bus	P _{max} (MW)	P _{flow} (MW)
3	5	297.5	67.972	17	113	297.5	3.227
3	12	297.5	10.598	18	19	297.5	21.285
4	5	850	99.910	19	20	297.5	10.192
4	11	297.5	60.725	20	21	297.5	28.350
5	6	297.5	85.111	21	22	297.5	42.752
5	8	850	326.194	22	23	297.5	53.748
5	11	297.5	73.201	23	24	297.5	13.071
6	7	297.5	32.249	23	25	850	169.690
7	12	297.5	13.199	23	32	238	91.625
8	9	850	381.646	25	27	850	142.043
8	30	297.5	23.728	25	26	850	91.733
9	10	850	385.204	26	30	850	222.267
11	12	297.5	30.402	27	28	297.5	32.178
11	13	297.5	31.664	27	32	297.5	11.794
12	14	297.5	14.462	27	115	297.5	20.814
12	16	297.5	3.091	28	29	297.5	14.967
12	117	297.5	20.145	29	31	297.5	9.110
13	15	297.5	2.597	31	32	297.5	29.292
14	15	297.5	0.415	32	113	850	2.846
15	17	850	107.532	32	114	297.5	9.288
15	19	297.5	13.678	114	115	297.5	1.265
16	17	297.5	22.140				
Power Flow in ISLAND 2							
From bus	To bus	P _{max} (MW)	P _{flow} (MW)	From bus	To bus	P _{max} (MW)	P _{flow} (MW)
33	37	297.5	23.245	54	56	297.5	17.514
34	36	297.5	31.334	54	59	297.5	30.829
34	37	850	86.638	55	56	297.5	20.347
34	43	297.5	3.953	55	59	297.5	35.731
35	36	297.5	0.233	56	57	297.5	23.229
35	37	297.5	32.917	56	58	297.5	6.815
37	38	850	231.833	56	59	297.5	28.569
37	39	297.5	49.886	56	59	297.5	29.963
37	40	297.5	39.148	59	60	297.5	44.357
38	65	850	236.584	59	61	297.5	53.033
39	40	297.5	22.065	60	61	850	113.179
40	41	297.5	10.747	60	62	297.5	9.530
40	42	297.5	16.722	61	62	297.5	26.336
41	42	297.5	26.581	62	66	297.5	37.251
42	49	297.5	73.327	62	67	297.5	23.866
42	49	297.5	73.327	63	59	850	151.246
43	44	297.5	22.295	63	64	850	151.662
44	45	297.5	38.648	64	61	850	32.548
45	46	297.5	40.302	64	65	850	185.122
45	49	297.5	53.944	65	66	850	1.6148
46	47	297.5	35.053	65	68	850	32.546
46	48	297.5	14.828	66	67	297.5	52.467
47	49	297.5	2.179	68	69	850	216.868

Power Flow in ISLAND 2							
From bus	To bus	P _{max} (MW)	P _{flow} (MW)	From bus	To bus	P _{max} (MW)	P _{flow} (MW)
47	69	297.5	70.908	68	116	850	184.323
48	49	297.5	35.045	69	70	850	130.517
49	50	297.5	53.654	69	75	850	148.702
49	51	297.5	66.617	69	77	297.5	178.454
49	54	297.5	37.658	70	71	297.5	18.125
49	54	297.5	37.658	70	74	297.5	27.632
49	66	850	132.448	70	75	297.5	13.870
49	66	850	132.448	71	72	297.5	12.067
49	69	297.5	60.763	71	73	297.5	6.010
50	57	297.5	35.888	74	75	297.5	40.961
51	52	297.5	28.482	75	77	297.5	1.071
51	58	297.5	18.921	75	118	297.5	66.962
52	53	297.5	10.303	76	77	297.5	35.695
53	54	297.5	12.800	76	118	297.5	33.187
54	55	297.5	7.7842	77	78	297.5	71.231
Power Flow in ISLAND 3							
From bus	To bus	P _{max} (MW)	P _{flow} (MW)	From bus	To bus	P _{max} (MW)	P _{flow} (MW)
79	80	297.5	39.369	93	94	297.5	0.483
80	96	297.5	80.406	94	95	297.5	11.081
80	97	297.5	87.798	94	96	297.5	14.256
80	98	297.5	74.590	94	100	297.5	21.679
80	99	340	64.837	95	96	297.5	31.187
81	80	850	0.000	96	97	297.5	71.428
82	83	340	10.547	98	100	297.5	39.365
82	96	297.5	65.287	99	100	297.5	21.062
83	84	297.5	2.121	100	101	297.5	14.307
83	85	297.5	7.388	100	103	850	121.073
84	85	297.5	13.183	100	104	297.5	56.388
85	86	850	17.174	100	106	297.5	60.622
85	88	297.5	20.998	101	102	297.5	7.788
85	89	297.5	41.253	103	104	297.5	32.293
86	87	850	4.000	103	105	297.5	42.937
88	89	850	69.678	103	110	297.5	60.575
89	90	850	97.861	104	105	297.5	48.682
89	90	850	97.861	105	106	297.5	8.676
89	92	850	29.518	105	107	297.5	26.679
89	92	850	29.518	105	108	297.5	23.982
90	91	297.5	17.428	106	107	297.5	24.057
91	92	297.5	27.764	108	109	297.5	21.783
92	93	297.5	11.556	109	110	297.5	13.717
92	94	297.5	5.972	110	111	297.5	36.00
92	100	297.5	0.659	110	112	297.5	69.459
92	102	297.5	12.809				

APPENDIX B

Table B.1 : IEEE 30-bus generator data

Bus. No	Type	Pmax	Pmin	Qmax	Qmin
1	Slack	300	0	10	0
2	PV	40	0	50	-40
5	PV	40	0	40	-40
8	PV	50	0	40	-10
11	PV	30	0	24	-6
13	PV	40	0	24	-6

Table B.2 : IEEE 39-bus generator data

Bus. No	Type	Pmax	Pmin	Qmax	Qmin
30	PV	500	0	400	140
31	Slack	650	0	300	-100
32	PV	650	0	300	150
33	PV	632	0	250	0
34	PV	508	0	167	0
35	PV	670	0	300	-100
36	PV	560	0	240	0
37	PV	540	0	250	0
38	PV	730	0	300	-150
39	PV	1000	0	300	-100

Table B.3 : IEEE 118-bus generator data

Bus. No	Type	Pmax	Pmin	Qmax	Qmin
10	PV	200	0	200	-147
12	PV	100	0	120	-35
25	PV	200	0	140	-47
26	PV	300	0	1000	-1000
31	PV	100	0	300	-300
46	PV	100	0	100	-100
49	PV	200	0	210	-85
54	PV	148	0	300	-300
59	PV	250	0	180	-60
61	PV	160	0	300	-100
65	PV	400	0	200	-67
66	PV	400	0	200	-67
69	Slack	800	0	300	-300
80	PV	500	0	280	-165
87	PV	100	0	1000	-100
89	PV	600	0	300	-210
100	PV	300	0	155	-50
103	PV	140	0	40	-15
111	PV	136	0	1000	-100

Table B.4 : Critical Lines for N-1 Contingency – IEEE-30 bus test system

Line	MVA Violation (%)	Line	MVA Violation (%)
1-2	218.3641	18-19	125.0107
1-3	190.4687	22-24	125.0091
3-4	188.2437	10-22	125.0047
2-5	149.2195	23-24	124.9891
4-6	141.2026	8-28	124.9855
27-28	131.8085	10-17	124.983
6-7	131.7886	14-15	124.9699
4-12	128.904	21-22	124.9654
5-7	128.0918	24-25	124.9322
6-8	127.8516	10-20	124.921
12-16	125.9685	19-20	124.8405
12-14	125.9136	12-13	124.7755
15-18	125.9026	25-27	124.7659
15-23	125.8858	9-11	124.7129
12-15	125.5059	9-10	124.639
27-30	125.2663	6-9	124.6196
27-29	125.19	6-10	124.5664
10-21	125.1711	25-26	123.6203
6-28	125.0546	2-4	119.3892
16-17	125.0538	2-6	114.1995
29-30	125.0393		

Table B.5 : Critical Lines for N-1 Contingency – IEEE-39 bus test system

Line	MVA Violation (%)	Line	MVA Violation (%)
13-14	201.0256	7-8	118.1753
4-5	186.4672	10-11	115.8133
10-13	168.5445	12-13	111.5152
23-36	161.7756	2-3	111.4222
22-35	160.5523	11-12	111.3524
5-6	159.5518	25-26	111.1969
20-34	156.6982	17-18	110.8029
19-33	156.0722	2-25	110.6594
25-37	150.4959	22-23	110.6204
29-38	149.7681	15-16	110.5577
14-15	148.3791	28-29	110.4701
21-22	144.2082	23-24	110.4634
8-9	142.9223	16-21	110.3579
9-39	139.988	26-27	110.1136
16-19	139.615	16-24	110.1
10-32	137.4174	26-28	110.0403
16-17	136.5563	26-29	109.8793
6-7	135.6951	17-27	109.8318
2-30	131.3188	3-18	108.8152
6-31	130.876	3-4	107.8435
4-14	128.8548	1-39	105.9142
6-11	123.5206	1-2	0
5-8	119.1056	19-20	0

Table B.6 : Critical Lines for N-1 Contingency – IEEE-118 bus test system

Line	MVA Violation (%)	Line	MVA Violation (%)	Line	MVA Violation (%)
68-69	406.5685	23-32	180.314	15-19	180.1251
68-81	252.7408	66-67	180.3102	114-115	180.1243
80-81	252.7134	33-37	180.3009	14-15	180.1236
69-75	217.4019	4-5	180.2961	35-36	180.1227
69-70	209.8496	46-47	180.2961	28-29	180.1224
75-118	195.1729	103-105	180.2841	27-32	180.1206
110-111	189.851	17-18	180.2832	53-54	180.1176
38-65	189.6015	56-57	180.2828	7-12	180.1167
76-118	189.0599	5-6	180.2721	31-32	180.1143
47-69	187.7924	51-52	180.2693	92-100	180.1132
49-69	187.5145	85-89	180.2666	37-39	180.1115
37-38	185.3704	90-91	180.2652	109-110	180.1114
80-99	183.6871	100-101	180.2632	60-61	180.1099
75-77	183.525	71-72	180.2482	89-92	180.1025
80-98	183.0583	103-104	180.2463	37-40	180.101
26-30	183.0458	1-3	180.2361	12-14	180.1006
5-8	182.5682	16-17	180.235	61-62	180.0999
8-30	182.5527	2-12	180.2342	17-31	180.0916
98-100	182.3569	62-66	180.2299	17-113	180.086
100-103	182.2986	20-21	180.2249	32-113	180.0845
80-97	182.2844	93-94	180.2207	101-102	180.0759
80-96	181.9183	19-34	180.2186	83-85	180.0758
103-110	181.886	34-37	180.2132	85-88	180.072
47-49	181.8405	105-108	180.2046	48-49	180.0716
99-100	181.5605	51-58	180.203	92-102	180.0599
96-97	181.5442	94-95	180.1971	84-85	180.0568
89-90	181.5181	35-37	180.1897	59-60	180.0443
9-10	181.3052	29-31	180.1883	83-84	180.0368
8-9	181.2755	92-94	180.185	55-59	180.0304
45-46	181.2359	25-26	180.183	59-61	180.0274
86-87	181.1396	108-109	180.1803	54-59	180.0261
100-106	181.1081	62-67	180.1803	42-49	180.0234
30-38	181.0852	5-11	180.1783	42-49	180.0234
100-104	180.9758	46-48	180.1777	56-59	180.0118
43-44	180.902	89-92	180.1706	56-59	180.0048
17-30	180.8211	45-49	180.1692	24-72	179.9809
49-51	180.757	71-73	180.166	61-64	179.9753
88-89	180.7546	40-41	180.1648	94-100	179.9247
24-70	180.6934	15-33	180.1644	70-74	179.8773
70-71	180.6291	4-11	180.1632	70-75	179.8029
49-50	180.6221	52-53	180.1582	59-63	179.7834
34-43	180.5497	92-93	180.1574	63-64	179.7775
25-27	180.5322	105-106	180.1471	82-83	179.6781
23-25	180.5239	13-15	180.1444	65-66	179.6125
104-105	180.5214	11-13	180.1427	79-80	179.3183
23-24	180.5046	55-56	180.1422	77-80	179.0169
22-23	180.4829	54-56	180.1409	49-66	178.8856
95-96	180.4822	1-2	180.1401	49-66	178.8856
89-90	180.4784	3-12	180.1396	77-80	178.643
49-54	180.466	56-58	180.1393	64-65	178.59
49-54	180.4434	34-36	180.1386	12-117	178.4765
44-45	180.4316	27-115	180.1368	82-96	177.99
41-42	180.4208	19-20	180.1347	78-79	177.8064
50-57	180.4051	18-19	180.1344	74-75	176.8481
91-92	180.3833	32-114	180.132	76-77	175.929

Line	MVA Violation (%)	Line	MVA Violation (%)	Line	MVA Violation (%)
105-107	180.3783	12-16	180.131	85-86	175.8088
21-22	180.3722	54-55	180.128	77-78	174.9511
3-5	180.3541	6-7	180.128	77-82	172.9272
40-42	180.3345	27-28	180.1265	69-77	169.4594
106-107	180.3314	11-12	180.126	65-68	164.6093
94-96	180.3203	60-62	180.1256	68-116	163.3672
15-17	180.3177	39-40	180.1253	110-112	162.5807

Table B.7 : Active Power Flow at Each Bus on Island 1 and Island 2- Case Study C1

Active power (MW) at each bus in Island 1				
Bus	Pre-islanding		Post-islanding	
	Pload	Pgen	Pload	Pgen
1	0.000	277.423	0.000	139.446
2	21.700	40.000	21.700	40.000
3	2.400	10.000	2.400	10.000
4	7.600	0.000	7.600	0.000
5	94.200	0.000	94.200	0.000
12	11.200	0.000	11.200	0.000
13	0.000	0.000	0.000	0.000
14	6.200	0.000	6.200	0.000
15	8.200	0.000	8.200	0.000
16	3.500	0.000	3.500	0.000
17	9.000	0.000	9.000	0.000
18	3.200	0.000	3.200	0.000
23	3.200	0.000	3.200	0.000
Active power (MW) at each bus in Island 2				
Bus	Pre-islanding		Post-islanding	
	Pload	Pgen	Pload	Pgen
6	0.000	0.000	0.000	0.000
7	22.800	0.000	22.800	0.000
8	30.000	10.000	30.000	48.517
9	0.000	0.000	0.000	0.000
10	5.800	0.000	5.800	0.000
11	0.000	0.000	0.000	30.000
19	9.500	0.000	0.000	0.000
20	2.200	0.000	0.000	0.000
21	17.500	0.000	0.000	0.000
22	0.000	0.000	0.000	0.000
24	8.700	0.000	8.700	0.000
25	0.000	0.000	0.000	0.000
26	3.500	0.000	0.000	0.000
27	0.000	0.000	0.000	0.000
28	0.000	0.000	0.000	0.000
29	2.400	0.000	0.000	0.000
30	10.600	0.000	10.600	0.000

Table B.8 : Voltage Profile on Island 1 and Island 2- Case Study C1

Island 1		Island 2	
Bus. No	Voltage (p.u)	Bus. No	Voltage (p.u)
1	1.040	6	1.009
2	0.993	7	0.995
3	0.972	8	1.010
4	0.961	9	1.034
5	0.980	10	1.049
12	0.994	11	1.020
13	1.010	19	1.049

Island 1		Island 2	
Bus. No	Voltage (p.u)	Bus. No	Voltage (p.u)
14	0.980	20	1.049
15	0.978	21	1.046
16	0.966	22	1.045
17	0.950	24	1.030
18	0.973	25	1.030
23	0.972	26	1.030
		27	1.030
		28	1.011
		29	1.017
		30	1.002

Table B.9 : Power Flow Information on Island 1 and Island 2- Case Study C1

Power Flow in ISLAND 1							
From bus	To bus	P_{max} (MW)	P_{flow} (MW)	From bus	To bus	P_{max} (MW)	P_{flow} (MW)
1	3	221	139.477	12	15	54.4	14.198
2	4	110.5	73.756	12	16	54.4	12.829
2	5	221	87.918	14	15	27.2	0.580
3	4	221	128.764	15	18	27.2	3.213
4	12	110.5	45.072	15	23	27.2	3.214
12	13	110.5	0.00	16	17	27.2	9.106
12	14	54.4	6.844				
Power Flow in ISLAND 2							
From bus	To bus	P_{max} (MW)	P_{flow} (MW)	From bus	To bus	P_{max} (MW)	P_{flow} (MW)
6	7	221	22.968	19	20	54.4	0.00
6	8	54.4	14.325	21	22	54.4	6.818
6	9	110.5	11.928	22	24	27.2	11.272
6	10	54.4	0.966	24	25	27.2	2.437
6	28	54.4	4.227	25	26	27.2	0.00
8	28	54.4	4.193	25	27	27.2	2.423
9	10	110.5	18.072	27	28	110.5	8.402
9	11	110.5	30.297	27	29	27.2	4.433
10	20	54.4	0.00	27	30	27.2	6.385
10	21	54.4	6.833	29	30	27.2	4.390
10	22	54.4	4.472				

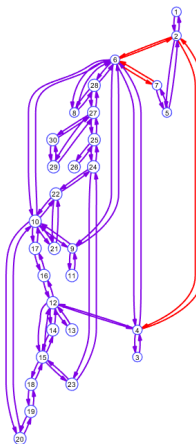


Figure B.1 : Graph model of an initial islanding solution for Case Study C2

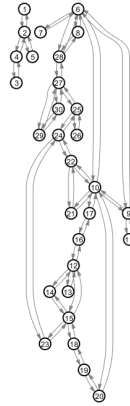


Figure B.2 : Graph model of islanding implementation for Case Study C2

Table B.10 : Active Power Flow at Each Bus on Island 1 and Island 2- Case Study C2

Active power (MW) at each bus in Island 1				
Bus	Pre-islanding		Post-islanding	
	Pload	Pgen	Pload	Pgen
1	0.000	247.640	0.000	80.580
2	21.700	40.000	21.700	40.000
3	2.400	0.000	2.400	0.000
4	7.600	0.000	7.600	0.000
5	94.200	10.000	94.200	10.000
Active power (MW) at each bus in Island 2				
Bus	Pre-islanding		Post-islanding	
	Pload	Pgen	Pload	Pgen
6	0.000	0.000	0.000	0.000
7	22.800	0.000	22.800	0.000
8	30.000	10.000	30.000	49.655
9	0.000	0.000	0.000	0.000
10	5.800	0.000	5.800	0.000
11	0.000	0.000	0.000	30.000
12	11.200	0.000	11.200	0.000
13	0.000	0.000	0.000	40.000
14	6.200	0.000	0.000	0.000
15	8.200	0.000	8.200	0.000
16	3.500	0.000	3.500	0.000
17	9.000	0.000	0.000	0.000
18	3.200	0.000	3.200	0.000
19	9.500	0.000	0.000	0.000
20	2.200	0.000	0.000	0.000
21	17.500	0.000	17.500	0.000
22	0.000	0.000	0.000	0.000
23	3.200	0.000	3.200	0.000
24	8.700	0.000	0.000	0.000
25	0.000	0.000	0.000	0.000
26	3.500	0.000	0.000	0.000
27	0.000	0.000	0.000	0.000
28	0.000	0.000	0.000	0.000
29	2.400	0.000	2.400	0.000
30	10.600	0.000	10.600	0.000

Table B.11 : Voltage Profile on Island 1 and Island 2- Case Study C2

Island 1		Island 2	
Bus. No	Voltage (p.u)	Bus. No	Voltage (p.u)
1	1.040	6	1.004
2	1.043	7	0.990
3	1.037	8	1.010
4	1.038	9	1.018
5	1.010	10	1.018
		11	1.010
		12	1.009
		13	1.010
		14	1.007
		15	1.002
		16	1.008
		17	1.015
		18	1.004
		19	1.008
		20	1.011
		21	1.009
		22	1.010
		23	1.002
		24	1.012
		25	1.013
		26	1.013
		27	1.014
		28	1.006
		29	0.994
		30	0.982

Table B.12 : Power Flow Information on Island 1 and Island 2- Case Study C2

Power Flow in ISLAND 1							
From bus	To bus	P _{max} (MW)	P _{flow} (MW)	From bus	To bus	P _{max} (MW)	P _{flow} (MW)
1	2	221	80.598	2	5	221	87.530
2	4	110.5	10.054	3	4	221	2.401
Power Flow in ISLAND 2							
From bus	To bus	P _{max} (MW)	P _{flow} (MW)	From bus	To bus	P _{max} (MW)	P _{flow} (MW)
6	7	221	22.969	14	15	27.2	3.787
6	8	54.4	15.139	15	18	27.2	4.162
6	9	110.5	11.658	15	23	27.2	6.745
6	10	54.4	0.706	16	17	27.2	5.880
6	28	54.4	4.498	18	19	27.2	0.934
8	28	54.4	4.519	19	20	54.4	0.923
9	10	110.5	18.342	21	22	54.4	4.724
9	11	110.5	30.00	22	24	27.2	0.934
10	17	54.4	5.822	23	24	27.2	3.487
10	20	54.4	0.918	24	25	27.2	4.365
10	21	54.4	12.853	25	26	27.2	0.00
10	22	54.4	5.686	25	27	27.2	4.316
12	13	110.5	40.00	27	28	110.5	8.999
12	14	54.4	3.807	27	29	27.2	6.192
12	15	54.4	15.515	27	30	27.2	7.095
12	16	54.4	9.478	29	30	27.2	3.704

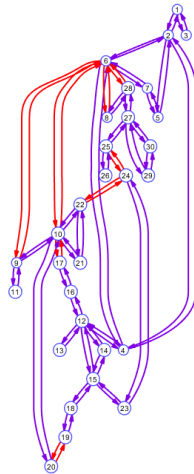


Figure B.3 : Graph model of an initial islanding solution for Case Study C3

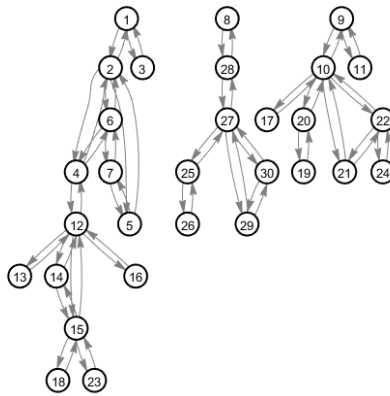


Figure B.4 : Graph model of islanding implementation for Case Study C3

Table B.13 : Active Power Flow at Each Bus on Island 1, Island 2 and Island 3- Case Study C3

Bus	Active power (MW) at each bus in Island 1			
	Pre-islanding		Post-islanding	
	Pload	Pgen	Pload	Pgen
1	0.000	247.153	0.000	143.057
2	21.700	40.000	21.700	40.000
3	2.400	0.000	2.400	0.000
4	7.600	0.000	7.600	0.000
5	94.200	10.000	94.200	10.000
6	0.000	0.000	0.000	0.000
7	22.800	0.000	22.800	0.000
12	11.200	0.000	11.200	0.000
13	0.000	0.000	0.000	0.000
14	6.200	0.000	6.200	0.000
15	8.200	0.000	8.200	0.000
16	3.500	0.000	3.500	0.000
18	3.200	0.000	3.200	0.000
23	3.200	0.000	3.200	0.000

Active power (MW) at each bus in Island 2				
Bus	Pre-islanding		Post-islanding	
	Pload	Pgen	Pload	Pgen
8	30.000	10.000	30.000	47.064
25	0.000	0.000	0.000	0.000
26	3.500	0.000	3.500	0.000
27	0.000	0.000	0.000	0.000
28	0.000	0.000	0.000	0.000
29	2.400	0.000	2.400	0.000
30	10.600	0.000	10.600	0.000
Active power (MW) at each bus in Island 3				
Bus	Pre-islanding		Post-islanding	
	Pload	Pgen	Pload	Pgen
9	0.000	0.000	0.000	0.000
10	5.800	0.000	0.000	0.000
11	0.000	0.000	0.000	29.731
17	9.000	0.000	9.000	0.000
19	9.500	0.000	9.500	0.000
20	2.200	0.000	2.200	0.000
21	17.500	0.000	0.000	0.000
22	0.000	0.000	0.000	0.000
24	8.700	0.000	8.700	0.000

Table B.14 : Voltage Profile on Island 1, Island 2 and Island 3- Case Study C3

Island 1		Island 2		Island 3	
Bus. No	Voltage (p.u)	Bus. No	Voltage (p.u)	Bus. No	Voltage (p.u)
1	1.040	8	1.010	9	1.019
2	1.013	25	0.987	10	1.025
3	1.041	26	0.969	11	1.010
4	0.974	27	0.996	17	1.017
5	0.980	28	0.989	19	0.999
6	0.979	29	0.976	20	1.005
7	0.971	30	0.964	21	1.022
12	1.006			22	1.021
13	1.010			24	1.006
14	0.993				
15	0.991				
16	0.999				
18	0.985				
23	0.984				

Table B.15 : Power Flow Information on Island 1, Island 2 and Island 3- Case Study C3

Power Flow in ISLAND 1							
From bus	To bus	P _{max} (MW)	P _{flow} (MW)	From bus	To bus	P _{max} (MW)	P _{flow} (MW)
1	2	221	140.682	6	7	221	40.753
1	3	221	2.403	12	13	110.5	0.000
2	4	110.5	43.538	12	14	54.4	6.842
2	5	221	69.172	12	15	54.4	14.194
2	6	110.5	42.750	12	16	54.4	3.515
4	6	153	0.934	14	15	27.2	0.580
4	12	110.5	35.751	15	18	27.2	3.212
5	7	119	17.487	15	23	27.2	3.213

Power Flow in ISLAND 2								
From bus	To bus	P_{max} (MW)	P_{flow} (MW)		From bus	To bus	P_{max} (MW)	P_{flow} (MW)
8	28	54.4	17.068		27	29	27.2	6.197
25	26	27.2	3.548		27	30	27.2	7.101
25	27	27.2	3.568		29	30	27.2	3.706
27	28	110.5	16.867					
Power Flow in ISLAND 3								
From bus	To bus	P_{max} (MW)	P_{flow} (MW)		From bus	To bus	P_{max} (MW)	P_{flow} (MW)
9	10	110.5	29.730		10	22	54.4	3.491
9	11	110.5	29.730		19	20	54.4	9.535
10	17	54.4	9.036		21	22	54.4	5.314
10	20	54.4	11.878		22	24	27.2	8.793
10	21	54.4	5.324					

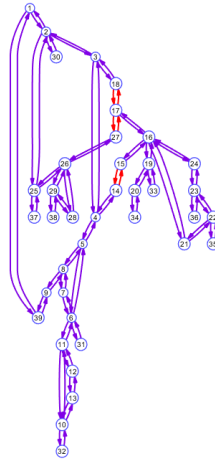


Figure B.5 : Graph model of an initial islanding solution for Case Study C4

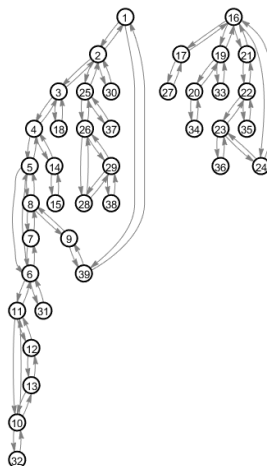


Figure B.6 : Graph model of islanding implementation for Case Study C4

Table B.16 : Active Power Flow at Each Bus on Island 1 and Island 2- Case Study C4

Active power (MW) at each bus in Island 1				
Bus	Pre-islanding		Post-islanding	
	Pload	Pgen	Pload	Pgen
1	97.600	0.000	0.000	0.000
2	0.000	0.000	0.000	0.000
3	322.000	0.000	322.000	0.000
4	500.000	0.000	500.000	0.000
5	0.000	0.000	0.000	0.000
6	0.000	0.000	0.000	0.000
7	233.800	0.000	233.800	0.000
8	522.000	0.000	522.000	0.000
9	6.500	0.000	0.000	0.000
10	0.000	0.000	0.000	0.000
11	0.000	0.000	0.000	0.000
12	8.500	0.000	0.000	0.000
13	0.000	0.000	0.000	0.000
14	0.000	0.000	0.000	0.000
15	320.000	0.000	320.000	0.000
18	158.000	0.000	158.000	0.000
25	224.000	0.000	224.000	0.000
26	139.000	0.000	139.000	0.000
28	206.000	0.000	206.000	0.000
29	283.500	0.000	283.500	0.000
30	0.000	250.000	0.000	500.000
31	9.200	650.000	9.200	643.821
32	0.000	550.000	0.000	650.000
37	0.000	440.000	0.000	540.000
38	0.000	430.000	0.000	730.000
39	1104.000	800.000	1104.000	1000.000
Active power (MW) at each bus in Island 2				
Bus	Pre-islanding		Post-islanding	
	Pload	Pgen	Pload	Pgen
16	329.000	0.000	329.000	0.000
17	0.000	0.000	0.000	0.000
19	0.000	0.000	0.000	0.000
20	680.000	0.000	680.000	0.000
21	274.000	0.000	274.000	0.000
22	0.000	0.000	0.000	0.000
23	247.500	0.000	247.500	0.000
24	308.600	0.000	308.600	0.000
27	281.000	0.000	281.000	0.000
33	0.000	500.000	0.000	500.000
34	0.000	508.000	0.000	508.000
35	0.000	550.000	0.000	566.198
36	0.000	560.000	0.000	560.000

Table B.17 : Voltage Profile on Island 1 and Island 2- Case Study C4

Island 1		Island 2	
Bus. No	Voltage (p.u)	Bus. No	Voltage (p.u)
1	1.061	16	1.028
2	1.053	17	1.025
3	1.026	19	1.015
4	0.996	20	1.001
5	0.992	21	1.026
6	0.992	22	1.039
7	0.988	23	1.036
8	0.989	24	1.034

Island 1		Island 2	
Bus. No	Voltage (p.u)	Bus. No	Voltage (p.u)
9	1.038	27	1.013
10	1.006	33	1.017
11	1.001	34	1.012
12	1.004	35	1.049
13	1.006	36	1.050
14	1.002		
15	0.986		
18	1.023		
25	1.074		
26	1.068		
28	1.042		
29	1.037		
30	1.070		
31	0.982		
32	1.024		
37	1.068		
38	1.027		
39	1.030		

Table B.18 : Power Flow Information on Island 1 and Island 2- Case Study C4

Power Flow in ISLAND 1							
From bus	To bus	P _{max} (MW)	P _{flow} (MW)	From bus	To bus	P _{max} (MW)	P _{flow} (MW)
1	2	1020	149.553	8	9	1530	44.454
1	39	1700	148.821	9	39	1530	44.484
2	3	850	748.722	10	11	1020	620.872
2	25	850	408.636	10	13	1020	29.128
2	30	1530	500.00	10	32	1530	650.00
3	4	850	261.589	11	12	850	29.111
3	18	850	158.263	12	13	850	29.125
4	5	1020	564.888	14	15	1020	321.919
4	14	850	322.788	25	26	1020	94.442
5	6	2040	831.204	25	37	1530	540.00
5	8	1530	264.907	26	28	1020	91.739
6	7	1530	448.873	26	29	1020	143.478
6	11	816	648.429	28	29	1020	298.943
6	31	3060	634.621	29	38	2040	730.00
7	8	1530	213.841				
Power Flow in ISLAND 2							
From bus	To bus	P _{max} (MW)	P _{flow} (MW)	From bus	To bus	P _{max} (MW)	P _{flow} (MW)
16	17	1020	282.554	20	34	1530	508.00
16	19	1020	323.742	21	22	1530	552.803
16	21	1020	276.491	22	23	1020	13.394
16	24	1020	13.680	22	35	1530	566.198
17	27	1020	282.023	23	24	1020	324.437
19	20	1530	174.565	23	36	1530	560.00
19	33	1530	500.00				

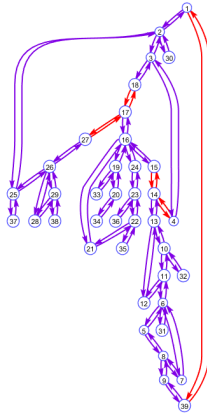


Figure B.7 : Graph model of an initial islanding solution for Case Study C5

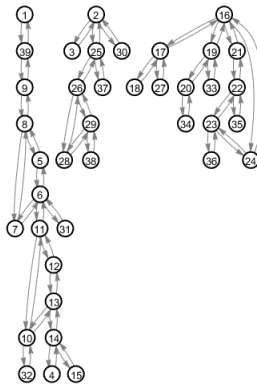


Figure B.8 : Graph model of islanding implementation for Case Study C5

Table B.19 : Active Power Flow at Each Bus on Island 1, Island 2 and Island 3- Case Study C5

Active power (MW) at each bus in Island 1				
Bus	Pre-islanding		Post-islanding	
	Pload	Pgen	Pload	Pgen
2	0.000	0.000	0.000	0.000
3	322.000	0.000	322.000	0.000
25	224.000	0.000	224.000	0.000
26	139.000	0.000	139.000	0.000
28	206.000	0.000	206.000	0.000
29	283.500	0.000	283.500	0.000
30	0.000	250.000	0.000	250.000
37	0.000	440.000	0.000	440.000
38	0.000	430.000	0.000	490.841
Active power (MW) at each bus in Island 2				
Bus	Pre-islanding		Post-islanding	
	Pload	Pgen	Pload	Pgen
1	97.600	0.000	97.600	0.000
4	500.000	0.000	500.000	0.000
5	0.000	0.000	0.000	0.000
6	0.000	0.000	0.000	0.000
7	233.800	0.000	0.000	0.000

Active power (MW) at each bus in Island 2				
Bus	Pre-islanding		Post-islanding	
	Pload	Pgen	Pload	Pgen
8	522.000	0.000	522.000	0.000
9	6.500	0.000	6.500	0.000
10	0.000	0.000	0.000	0.000
11	0.000	0.000	0.000	0.000
12	8.530	0.000	0.000	0.000
13	0.000	0.000	0.000	0.000
14	0.000	0.000	0.000	0.000
15	320.000	0.000	0.000	0.000
31	9.200	650.000	0.000	590.294
32	0.000	550.000	0.000	650.000
39	1104.000	800.000	1104.000	1000.000
Active power (MW) at each bus in Island 3				
Bus	Pre-islanding		Post-islanding	
	Pload	Pgen	Pload	Pgen
16	329.000	0.000	329.000	0.000
17	0.000	0.000	0.000	0.000
18	158.000	0.000	158.000	0.000
19	0.000	0.000	0.000	0.000
20	680.000	0.000	680.000	0.000
21	274.000	0.000	274.000	0.000
22	0.000	0.000	0.000	0.000
23	247.500	0.000	247.500	0.000
24	308.600	0.000	308.600	0.000
27	281.000	0.000	281.000	0.000
33	0.000	500.000	0.000	587.185
34	0.000	508.000	0.000	508.000
35	0.000	550.000	0.000	640.852
36	0.000	560.000	0.000	560.000

Table B.20 : Voltage Profile on Island 1, Island 2 and Island 3-
Case Study C5

Island 1		Island 2		Island 3	
Bus. No	Voltage (p.u)	Bus. No	Voltage (p.u)	Bus. No	Voltage (p.u)
2	1.096	1	1.038	16	1.017
3	1.095	4	0.992	17	1.012
25	1.094	5	1.009	18	1.010
26	1.085	6	1.009	19	1.006
28	1.053	7	1.009	20	0.996
29	1.045	8	1.009	21	1.018
30	1.100	9	1.053	22	1.034
37	1.078	10	1.020	23	1.031
38	1.027	11	1.017	24	1.024
		12	1.018	27	0.999
		13	1.019	33	1.007
		14	1.015	34	1.012
		15	1.023	35	1.049
		31	0.982	36	1.050
		32	1.034		
		39	1.030		

Table B.21 : Power Flow Information on Island 1, Island 2 and Island 3-
Case Study C5

Power Flow in ISLAND 1							
From bus	To bus	P_{max} (MW)	P_{flow} (MW)	From bus	To bus	P_{max} (MW)	P_{flow} (MW)
2	3	850	323.133	26	28	1020	26.420
2	25	850	73.864	26	29	1020	25.123
2	30	1530	250.00	28	29	1020	180.258
25	26	1020	141.111	29	38	2040	490.841
25	37	1530	440.00				
Power Flow in ISLAND 2							
From bus	To bus	P_{max} (MW)	P_{flow} (MW)	From bus	To bus	P_{max} (MW)	P_{flow} (MW)
1	39	1700	97.701	9	39	1530	202.146
4	14	850	502.170	10	11	1020	161.035
5	6	2040	367.244	10	13	1020	488.965
5	8	1530	366.977	10	32	1530	650.00
6	7	1530	367.421	11	12	850	16.366
6	11	816	144.556	12	13	850	16.361
6	31	3060	590.294	13	14	1020	504.402
7	8	1530	366.624	14	15	1020	0.025
8	9	1530	210.014				
Power Flow in ISLAND 3							
From bus	To bus	P_{max} (MW)	P_{flow} (MW)	From bus	To bus	P_{max} (MW)	P_{flow} (MW)
16	17	1020	441.550	19	33	1530	587.185
16	19	1020	410.229	20	34	1530	508.00
16	21	1020	324.173	21	22	1530	600.958
16	24	1020	39.758	22	23	1020	39.893
17	18	1020	158.173	22	35	1530	640.852
17	27	1020	282.051	23	24	1020	350.913
19	20	1530	174.577	23	36	1530	560.00

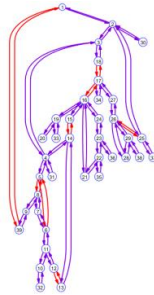


Figure B.9 : Graph model of an initial islanding solution for Case Study C6

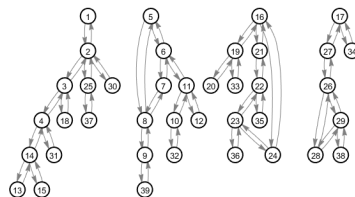


Figure B.10 : Graph model of islanding implementation for Case Study C6

Table B.22 : Active Power Flow at Each Bus on Island 1, Island 2, Island 3 and Island 4-
Case Study C6

Active power (MW) at each bus in Island 1				
Bus	Pre-islanding		Post-islanding	
	Pload	Pgen	Pload	Pgen
1	97.600	0.000	97.600	0.000
2	0.000	0.000	0.000	0.000
3	322.000	0.000	322.000	0.000
4	500.000	0.000	500.000	0.000
13	0.000	0.000	0.000	0.000
14	0.000	0.000	0.000	0.000
15	320.000	0.000	320.000	0.000
18	158.000	0.000	158.000	0.000
25	224.000	0.000	224.000	0.000
30	0.000	250.000	0.000	500.000
31	9.200	650.000	9.200	609.426
37	0.000	440.000	0.000	540.000
Active power (MW) at each bus in Island 2				
Bus	Pre-islanding		Post-islanding	
	Pload	Pgen	Pload	Pgen
16	329.000	0.000	329.000	0.000
19	0.000	0.000	0.000	0.000
20	680.000	0.000	680.000	0.000
21	274.000	0.000	274.000	0.000
22	0.000	0.000	0.000	0.000
23	247.500	0.000	247.500	0.000
24	308.600	0.000	308.600	0.000
33	0.000	500.000	0.000	620.875
35	0.000	550.000	0.000	669.442
36	0.000	560.000	0.000	560.000
Active power (MW) at each bus in Island 3				
Bus	Pre-islanding		Post-islanding	
	Pload	Pgen	Pload	Pgen
17	0.000	0.000	0.000	0.000
26	139.000	0.000	139.000	0.000
27	281.000	0.000	281.000	0.000
28	206.000	0.000	206.000	0.000
29	283.500	0.000	283.500	0.000
34	0.000	508.000	0.000	508.000
38	0.000	430.000	0.000	409.310
Active power (MW) at each bus in Island 4				
Bus	Pre-islanding		Post-islanding	
	Pload	Pgen	Pload	Pgen
5	0.000	0.000	0.000	0.000
6	0.000	0.000	0.000	0.000
7	233.800	0.000	0.000	0.000
8	522.000	0.000	522.000	0.000
9	6.500	0.000	6.500	0.000
10	0.000	0.000	0.000	0.000
11	0.000	0.000	0.000	0.000
12	8.530	0.000	8.530	0.000
32	0.000	550.000	0.000	650.000
39	1104.000	800.000	1104.000	998.240

Table B.23 : Voltage Profile on Island 1, Island 2, Island 3 and Island 4-
Case Study C6

Island 1		Island 2		Island 3		Island 4	
Bus. No	Voltage (p.u)						
1	1.060	16	1.014	17	1.042	5	1.021
2	1.051	19	0.987	26	1.046	6	1.021
3	1.026	20	0.962	27	1.040	7	1.021
4	0.997	21	1.016	28	1.053	8	1.020
13	1.009	22	1.032	29	1.045	9	1.059
14	1.007	23	1.030	34	1.042	10	1.023
15	0.992	24	1.021	38	1.027	11	1.020
18	1.023	33	0.997			12	0.990
25	1.063	35	1.049			32	1.034
30	1.070	36	1.050			39	1.030
31	0.982						
37	1.058						

Table B.24: Power Flow Information on Island 1, Island 2, Island 3 and Island 4 - Case Study C6

Island 1				Island 2			
From bus	To bus	P _{max} (MW)	P _{flow} (MW)	From bus	To bus	P _{max} (MW)	P _{flow} (MW)
1	2	1020	97.933	16	19	1020	62.198
2	3	850	709.859	16	21	1020	342.410
2	25	850	314.435	16	24	1020	49.745
2	30	1530	500.00	19	20	1530	683.575
3	4	850	223.416	19	33	1530	624.500
3	18	850	158.263	21	22	1530	619.388
4	14	850	322.810	22	23	1020	50.055
4	31	3060	600.226	22	35	1530	669.443
13	14	1020	0.000	23	24	1020	361.063
14	15	1020	321.896	23	36	1530	560.00
25	37	1530	540.00				
Island 3				Island 4			
From bus	To bus	P _{max} (MW)	P _{flow} (MW)	From bus	To bus	P _{max} (MW)	P _{flow} (MW)
17	27	1020	505.862	5	6	2040	318.421
17	34	1530	508.00	5	8	1530	318.225
26	27	1020	221.795	6	7	1530	318.591
26	28	1020	66.104	6	11	816	639.777
26	29	1020	16.003	7	8	1530	318.005
28	29	1020	140.395	8	9	1530	113.063
29	38	2040	409.310	9	39	1530	105.988
				10	11	1020	650.00
				10	32	1530	650.00
				11	12	850	8.607

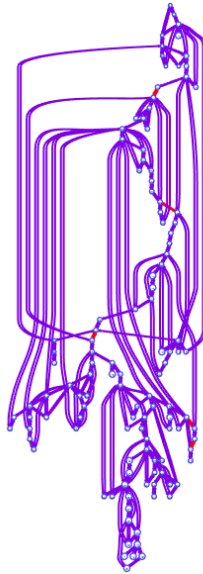


Figure B.11 : Graph model of an initial islanding solution for Case Study C7

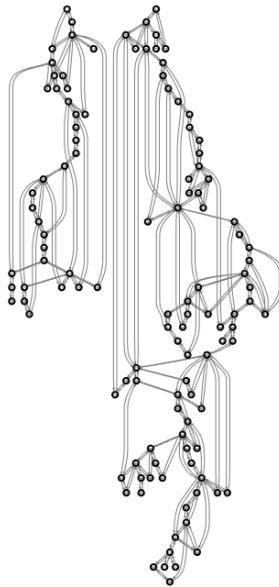


Figure B.12 : Graph model of islanding implementation for Case Study C7

Table B.25: Active Power Flow at Each Bus on Island 1 and Island 2- Case Study C7

Active power (MW) at each bus in Island 1				
Bus	Pre-islanding		Post-islanding	
	Pload	Pgen	Pload	Pgen
1	51.000	0.000	51.000	0.000
2	20.000	0.000	20.000	0.000
3	39.000	0.000	39.000	0.000
4	39.000	0.000	39.000	0.000

Active power (MW) at each bus in Island 1				
Bus	Pre-islanding		Post-islanding	
	Pload	Pgen	Pload	Pgen
5	0.000	0.000	0.000	0.000
6	52.000	0.000	52.000	0.000
7	19.000	0.000	19.000	0.000
8	28.000	0.000	28.000	0.000
9	0.000	0.000	0.000	0.000
10	0.000	30.000	0.000	200.000
11	70.000	0.000	70.000	0.000
12	47.000	100.000	0.000	100.000
13	34.000	0.000	34.000	0.000
14	14.000	0.000	14.000	0.000
15	90.000	0.000	90.000	0.000
16	25.000	0.000	25.000	0.000
17	11.000	0.000	11.000	0.000
18	60.000	0.000	60.000	0.000
19	45.000	0.000	45.000	0.000
20	18.000	0.000	18.000	0.000
21	14.000	0.000	14.000	0.000
22	10.000	0.000	10.000	0.000
23	7.000	0.000	7.000	0.000
25	0.000	200.000	0.000	200.000
26	0.000	220.000	0.000	278.724
27	71.000	0.000	71.000	0.000
28	17.000	0.000	17.000	0.000
29	24.000	0.000	24.000	0.000
30	0.000	0.000	0.000	0.000
31	43.000	100.000	0.000	100.000
32	59.000	0.000	59.000	0.000
113	6.000	0.000	6.000	0.000
114	8.000	0.000	8.000	0.000
115	22.000	0.000	22.000	0.000
117	20.000	0.000	0.000	0.000
Active power (MW) at each bus in Island 2				
Bus	Pre-islanding		Post-islanding	
	Pload	Pgen	Pload	Pgen
24	13.000	0.000	13.000	0.000
33	23.000	0.000	23.000	0.000
34	59.000	0.000	59.000	0.000
35	33.000	0.000	33.000	0.000
36	31.000	0.000	31.000	0.000
37	0.000	0.000	0.000	0.000
38	0.000	0.000	0.000	0.000
39	27.000	0.000	27.000	0.000
40	66.000	0.000	66.000	0.000
41	37.000	0.000	37.000	0.000
42	96.000	0.000	96.000	0.000
43	18.000	0.000	18.000	0.000
44	16.000	0.000	16.000	0.000
45	53.000	0.000	53.000	0.000
46	28.000	100.000	28.000	100.000
47	34.000	0.000	34.000	0.000
48	20.000	0.000	20.000	0.000
49	87.000	200.000	87.000	200.000
50	17.000	0.000	17.000	0.000
51	17.000	0.000	17.000	0.000
52	18.000	0.000	18.000	0.000

Active power (MW) at each bus in Island 2				
Bus	Pre-islanding		Post-islanding	
	Pload	Pgen	Pload	Pgen
53	23.000	0.000	23.000	0.000
54	113.000	48.000	113.000	48.000
55	63.000	0.000	63.000	0.000
56	84.000	0.000	84.000	0.000
57	12.000	0.000	12.000	0.000
58	12.000	0.000	12.000	0.000
59	277.000	155.000	277.000	155.000
60	78.000	0.000	78.000	0.000
61	0.000	160.000	0.000	160.000
62	77.000	0.000	77.000	0.000
63	0.000	0.000	0.000	0.000
64	0.000	0.000	0.000	0.000
65	0.000	391.000	0.000	391.000
66	39.000	392.000	39.000	392.000
67	28.000	0.000	28.000	0.000
68	0.000	0.000	0.000	0.000
69	0.000	800.000	0.000	758.681
70	66.000	0.000	66.000	0.000
71	0.000	0.000	0.000	0.000
72	12.000	0.000	12.000	0.000
73	6.000	0.000	6.000	0.000
74	68.000	0.000	68.000	0.000
75	47.000	0.000	47.000	0.000
76	68.000	0.000	68.000	0.000
77	61.000	0.000	61.000	0.000
78	71.000	0.000	71.000	0.000
79	39.000	0.000	39.000	0.000
80	130.000	477.000	130.000	477.000
81	0.000	0.000	0.000	0.000
82	54.000	0.000	54.000	0.000
83	20.000	0.000	20.000	0.000
84	11.000	0.000	11.000	0.000
85	24.000	0.000	24.000	0.000
86	21.000	0.000	21.000	0.000
87	0.000	100.000	0.000	100.000
88	48.000	0.000	48.000	0.000
89	0.000	300.000	0.000	300.000
90	163.000	0.000	163.000	0.000
91	10.000	0.000	10.000	0.000
92	65.000	0.000	65.000	0.000
93	12.000	0.000	12.000	0.000
94	30.000	0.000	30.000	0.000
95	42.000	0.000	42.000	0.000
96	38.000	0.000	38.000	0.000
97	15.000	0.000	15.000	0.000
98	34.000	0.000	34.000	0.000
99	42.000	0.000	42.000	0.000
100	37.000	252.000	37.000	252.000
101	22.000	0.000	22.000	0.000
102	5.000	0.000	5.000	0.000
103	23.000	40.000	23.000	40.000
104	38.000	0.000	38.000	0.000
105	31.000	0.000	31.000	0.000
106	43.000	0.000	43.000	0.000
107	50.000	0.000	50.000	0.000

Active power (MW) at each bus in Island 2				
Bus	Pre-islanding		Post-islanding	
	Pload	Pgen	Pload	Pgen
108	2.000	0.000	2.000	0.000
109	8.000	0.000	8.000	0.000
110	39.000	0.000	39.000	0.000
111	0.000	36.000	0.000	36.000
112	68.000	0.000	68.000	0.000
116	184.000	0.000	184.000	0.000
118	33.000	0.000	33.000	0.000

Table B.26: Voltage Profile on Island 1 and Island 2- Case Study C7

Island 1				
Bus. No	Voltage (p.u)		Bus. No	Voltage (p.u)
1	0.965		19	0.973
2	0.976		20	0.975
3	0.974		21	0.978
4	0.998		22	0.991
5	1.001		23	1.018
6	0.990		25	1.050
7	0.989		26	1.015
8	1.015		27	0.968
9	1.046		28	0.963
10	1.050		29	0.963
11	0.986		30	1.024
12	0.990		31	0.967
13	0.974		32	0.974
14	0.988		113	0.993
15	0.980		114	0.967
16	0.986		115	0.966
17	0.996		117	0.995
18	0.973			
Island 2				
Bus. No	Voltage (p.u)		Bus. No	Voltage (p.u)
24	0.992		74	0.958
33	0.974		75	0.968
34	0.986		76	0.950
35	0.981		77	1.006
36	0.980		78	1.002
37	0.993		79	1.005
38	1.019		80	1.040
39	0.971		81	1.040
40	0.970		82	0.987
41	0.968		83	0.984
42	0.985		84	0.981
43	0.975		85	0.985
44	0.971		86	0.983
45	0.977		87	1.015
46	1.005		88	0.990
47	1.015		89	1.005
48	1.016		90	0.985
49	1.025		91	0.980
50	1.003		92	1.003
51	0.971		93	0.998
52	0.962		94	0.998
53	0.951		95	0.988
54	0.955		96	0.998
55	0.962		97	1.015

Island 2			
Bus. No	Voltage (p.u)	Bus. No	Voltage (p.u)
56	0.954	98	1.025
57	0.973	99	1.010
58	0.962	100	1.017
59	0.985	101	1.001
60	1.003	102	1.003
61	1.005	103	1.001
62	1.008	104	0.971
63	1.011	105	0.965
64	1.023	106	0.963
65	1.045	107	0.952
66	1.050	108	0.967
67	1.026	109	0.968
68	1.021	110	0.973
69	1.035	111	0.980
70	0.984	112	0.975
71	0.987	116	1.005
72	0.980	118	0.953
73	0.991		

Table B.27: Power Flow Information on Island 1 and Island 2 - Case Study C7

Power Flow in ISLAND 1							
From bus	To bus	P _{max} (MW)	P _{flow} (MW)	From bus	To bus	P _{max} (MW)	P _{flow} (MW)
1	2	297.5	19.293	16	17	297.5	26.296
1	3	297.5	31.992	17	18	297.5	81.923
2	12	297.5	39.616	17	30	850	167.640
3	5	297.5	53.018	17	31	297.5	47.172
3	12	297.5	18.884	17	113	297.5	17.478
4	5	850	74.204	18	19	297.5	21.005
4	11	297.5	35.100	19	20	297.5	15.798
5	6	297.5	57.222	20	21	297.5	34.021
5	8	850	228.609	21	22	297.5	48.524
5	11	297.5	44.165	22	23	297.5	59.719
6	7	297.5	4.825	23	25	297.5	138.047
7	12	297.5	14.195	23	32	238	68.564
8	9	850	198.557	25	26	850	47.644
8	30	297.5	59.292	25	27	850	109.598
9	10	850	200.00	26	30	850	231.080
11	12	297.5	17.304	27	28	297.5	7.798
11	13	297.5	25.862	27	32	297.5	8.068
12	14	297.5	10.971	27	115	297.5	18.810
12	16	297.5	0.980	28	29	297.5	9.241
12	117	297.5	0.004	29	31	297.5	33.369
13	15	297.5	8.364	31	32	297.5	19.459
14	15	297.5	3.077	32	113	850	24.007
15	17	850	111.453	32	114	297.5	11.282
15	19	297.5	8.355	114	115	297.5	3.254
Power Flow in ISLAND 2							
From bus	To bus	P _{max} (MW)	P _{flow} (MW)	From bus	To bus	P _{max} (MW)	P _{flow} (MW)
24	70	297.5	10.488	70	74	297.5	28.779
24	72	297.5	2.540	70	75	297.5	15.423

Power Flow in ISLAND 2								
From bus	To bus	P _{max} (MW)	P _{flow} (MW)		From bus	To bus	P _{max} (MW)	P _{flow} (MW)
33	37	297.5	23.245		71	72	297.5	14.639
34	36	297.5	32.906		71	73	297.5	6.010
34	37	850	72.253		74	75	297.5	39.845
34	43	297.5	20.075		75	77	297.5	10.618
35	36	297.5	1.797		75	118	297.5	75.247
35	37	297.5	31.345		76	77	297.5	27.690
37	39	297.5	67.596		76	118	297.5	41.358
37	40	297.5	56.325		77	78	297.5	84.163
38	37	850	250.763		77	80	850	17.037
38	65	850	256.281		77	80	850	5.992
39	40	297.5	39.105		77	82	340	78.246
40	41	297.5	27.2003		78	79	297.5	12.896
40	42	297.5	0.043		79	80	297.5	26.538
41	42	297.5	9.997		80	96	297.5	48.510
42	49	297.5	115.104		80	97	297.5	55.920
43	44	297.5	39.118		80	98	297.5	61.881
44	45	297.5	55.860		80	99	340	52.201
45	46	297.5	70.206		81	80	850	78.921
45	49	297.5	41.856		82	83	340	3.281
46	47	297.5	10.249		82	96	297.5	19.161
46	48	297.5	11.995		83	84	297.5	4.605
47	49	297.5	52.614		83	85	297.5	12.219
47	69	297.5	105.733		84	85	297.5	15.682
48	49	297.5	8.194		85	86	850	76.232
49	50	297.5	58.052		85	88	297.5	20.544
49	51	297.5	71.944		85	89	297.5	1.638
49	54	297.5	42.387		86	87	850	100.00
49	54	297.5	42.248		88	89	850	27.698
49	66	850	124.834		89	90	850	97.932
49	69	850	102.316		89	90	850	51.474
50	57	297.5	40.167		89	92	850	94.789
51	52	297.5	30.112		89	92	850	29.711
51	58	297.5	22.292		90	91	297.5	17.325
52	53	297.5	11.913		91	92	297.5	27.659
53	54	297.5	11.193		92	93	297.5	9.380
54	55	297.5	9.129		92	94	297.5	3.802
54	56	297.5	21.698		92	100	297.5	1.982
54	59	297.5	25.839		92	102	297.5	15.428
55	56	297.5	23.751		93	94	297.5	2.647
55	59	297.5	30.848		94	95	297.5	0.305
56	57	297.5	27.366		94	96	297.5	26.593
56	58	297.5	10.153		94	100	297.5	2.953
56	59	297.5	25.594		95	96	297.5	42.081
56	59	297.5	24.392		96	97	297.5	40.332
59	60	297.5	42.759		98	100	297.5	27.0361
59	61	297.5	50.810		99	100	297.5	9.041
59	63	850	136.530		100	101	297.5	11.694

Power Flow in ISLAND 2								
From bus	To bus	P_{max} (MW)	P_{flow} (MW)		From bus	To bus	P_{max} (MW)	P_{flow} (MW)
60	61	850	105.590		100	103	850	121.073
60	62	297.5	15.494		100	104	297.5	56.388
61	62	297.5	14.702		100	106	297.5	60.622
61	64	850	11.102		101	102	297.5	10.398
62	66	297.5	46.359		103	104	297.5	32.293
62	67	297.5	32.745		103	105	297.5	42.937
63	64	850	136.883		103	110	297.5	60.575
64	65	850	148.638		104	105	297.5	48.682
65	66	850	120.256		105	106	297.5	8.676
65	68	850	106.338		105	107	297.5	26.679
66	67	297.5	61.551		105	108	297.5	23.982
68	81	850	78.921		106	107	297.5	24.056
68	116	850	184.619		108	109	297.5	21.783
69	70	850	147.606		109	110	297.5	13.717
69	75	850	168.216		110	111	297.5	36.00
69	77	297.5	234.809		110	112	297.5	69.459
70	71	297.5	20.707					

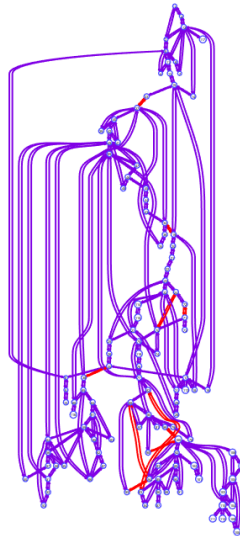


Figure B.13 : Graph model of an initial islanding solution for Case Study C8

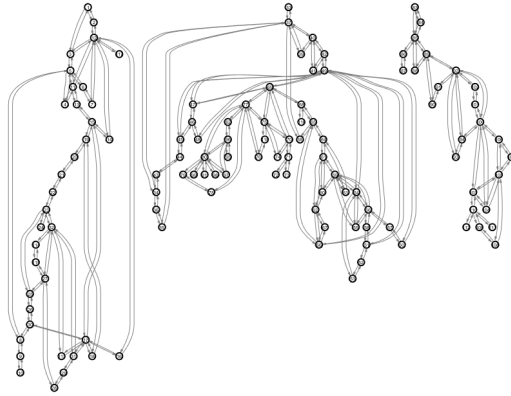


Figure B.14 : Graph model of islanding implementation for Case Study C8

Table B.28: Active Power Flow at Each Bus on Island 1, Island 2 and Island 3 - Case Study C8

Active power (MW) at each bus in Island 1				
Bus	Pre-islanding		Post-islanding	
	Pload	Pgen	Pload	Pgen
1	51.000	0.000	51.000	0.000
2	20.000	0.000	20.000	0.000
3	39.000	0.000	39.000	0.000
4	39.000	0.000	39.000	0.000
5	0.000	0.000	0.000	0.000
6	52.000	0.000	52.000	0.000
7	19.000	0.000	19.000	0.000
8	28.000	0.000	28.000	0.000
9	0.000	0.000	0.000	0.000
10	0.000	30.000	0.000	200.000
11	70.000	0.000	70.000	0.000
12	47.000	100.000	0.000	100.000
13	34.000	0.000	34.000	0.000
14	14.000	0.000	14.000	0.000
15	90.000	0.000	90.000	0.000
16	25.000	0.000	25.000	0.000
17	11.000	0.000	11.000	0.000
18	60.000	0.000	60.000	0.000
19	45.000	0.000	0.000	0.000
20	18.000	0.000	0.000	0.000
21	14.000	0.000	14.000	0.000
22	10.000	0.000	10.000	0.000
23	7.000	0.000	7.000	0.000
24	13.000	0.000	13.000	0.000
25	0.000	200.000	0.000	200.000
26	0.000	220.000	0.000	289.881
27	71.000	0.000	71.000	0.000
28	17.000	0.000	17.000	0.000
29	24.000	0.000	24.000	0.000
30	0.000	0.000	0.000	0.000
31	43.000	100.000	43.000	100.000
32	59.000	0.000	59.000	0.000
113	6.000	0.000	6.000	0.000
114	8.000	0.000	8.000	0.000
115	22.000	0.000	22.000	0.000
117	20.000	0.000	20.000	0.000

Active power (MW) at each bus in Island 2				
Bus	Pre-islanding		Post-islanding	
	Pload	Pgen	Pload	Pgen
33	23.000	0.000	23.000	0.000
34	59.000	0.000	59.000	0.000
35	33.000	0.000	33.000	0.000
36	31.000	0.000	31.000	0.000
37	0.000	0.000	0.000	0.000
38	0.000	0.000	0.000	0.000
39	27.000	0.000	27.000	0.000
40	66.000	0.000	66.000	0.000
41	37.000	0.000	37.000	0.000
42	96.000	0.000	96.000	0.000
43	18.000	0.000	18.000	0.000
44	16.000	0.000	16.000	0.000
45	53.000	0.000	53.000	0.000
46	28.000	100.000	28.000	100.000
47	34.000	0.000	34.000	0.000
48	20.000	0.000	20.000	0.000
49	87.000	200.000	87.000	200.000
50	17.000	0.000	17.000	0.000
51	17.000	0.000	17.000	0.000
52	18.000	0.000	18.000	0.000
53	23.000	0.000	23.000	0.000
54	113.000	48.000	113.000	48.000
55	63.000	0.000	63.000	0.000
56	84.000	0.000	84.000	0.000
57	12.000	0.000	12.000	0.000
58	12.000	0.000	12.000	0.000
59	277.000	155.000	277.000	155.000
60	78.000	0.000	78.000	0.000
61	0.000	160.000	0.000	160.000
62	77.000	0.000	77.000	0.000
63	0.000	0.000	0.000	0.000
64	0.000	0.000	0.000	0.000
65	0.000	391.000	0.000	391.000
66	39.000	392.000	39.000	392.000
67	28.000	0.000	28.000	0.000
68	0.000	0.000	0.000	0.000
69	0.000	800.000	0.000	640.732
70	66.000	0.000	66.000	0.000
71	0.000	0.000	0.000	0.000
72	12.000	0.000	12.000	0.000
73	6.000	0.000	6.000	0.000
74	68.000	0.000	68.000	0.000
75	47.000	0.000	47.000	0.000
76	68.000	0.000	68.000	0.000
77	61.000	0.000	61.000	0.000
78	71.000	0.000	71.000	0.000
79	39.000	0.000	39.000	0.000
80	130.000	477.000	130.000	477.000
81	0.000	0.000	0.000	0.000
82	54.000	0.000	54.000	0.000
95	42.000	0.000	42.000	0.000
96	38.000	0.000	38.000	0.000
97	15.000	0.000	15.000	0.000
98	34.000	0.000	34.000	0.000
99	42.000	0.000	42.000	0.000

Active power (MW) at each bus in Island 2				
Bus	Pre-islanding		Post-islanding	
	Pload	Pgen	Pload	Pgen
116	184.000	0.000	184.000	0.000
118	33.000	0.000	33.000	0.000
Active power (MW) at each bus in Island 3				
Bus	Pre-islanding		Post-islanding	
	Pload	Pgen	Pload	Pgen
83	20.000	0.000	20.000	0.000
84	11.000	0.000	11.000	0.000
85	24.000	0.000	24.000	0.000
86	21.000	0.000	21.000	0.000
87	0.000	100.000	0.000	100.000
88	48.000	0.000	48.000	0.000
89	0.000	300.000	0.000	367.494
90	163.000	0.000	163.000	0.000
91	10.000	0.000	10.000	0.000
92	65.000	0.000	65.000	0.000
93	12.000	0.000	12.000	0.000
94	30.000	0.000	30.000	0.000
100	37.000	252.000	37.000	252.000
101	22.000	0.000	22.000	0.000
102	5.000	0.000	5.000	0.000
103	23.000	40.000	23.000	40.000
104	38.000	0.000	38.000	0.000
105	31.000	0.000	31.000	0.000
106	43.000	0.000	43.000	0.000
107	50.000	0.000	50.000	0.000
108	2.000	0.000	2.000	0.000
109	8.000	0.000	8.000	0.000
110	39.000	0.000	39.000	0.000
111	0.000	36.000	0.000	36.000
112	68.000	0.000	68.000	0.000

Table B.29: Voltage Profile on Island 1, Island 2 and Island 3- Case Study C8

Island 1				
Bus. No	Voltage (p.u)		Bus. No	Voltage (p.u)
1	0.965		19	0.983
2	0.976		20	0.987
3	0.974		21	0.985
4	0.998		22	0.991
5	1.001		23	1.006
6	0.990		24	0.992
7	0.989		25	1.040
8	1.015		26	1.015
9	1.046		27	0.968
10	1.050		28	0.963
11	0.986		29	0.964
12	0.990		30	1.025
13	0.974		31	0.967
14	0.988		32	0.974
15	0.980		113	0.993
16	0.987		114	0.967
17	0.998		115	0.966
18	0.983		117	0.976

Island 2				
Bus. No	Voltage (p.u)		Bus. No	Voltage (p.u)
33	0.974		62	1.008
34	0.986		63	1.008
35	0.981		64	1.019
36	0.980		65	1.035
37	0.992		66	1.050
38	1.019		67	1.026
39	0.972		68	1.016
40	0.970		69	1.035
41	0.968		70	0.984
42	0.985		71	0.987
43	0.978		72	0.980
44	0.975		73	0.991
45	0.979		74	0.958
46	1.005		75	0.970
47	1.020		76	0.950
48	1.016		77	1.006
49	1.025		78	1.002
50	1.003		79	1.005
51	0.972		80	1.040
52	0.963		81	1.040
53	0.951		82	0.982
54	0.955		95	0.960
55	0.962		96	0.9845
56	0.954		97	1.008
57	0.973		98	1.026
58	0.963		99	1.010
59	0.985		116	1.005
60	1.003		118	0.955
61	1.005			
Island 3				
Bus. No	Voltage (p.u)		Bus. No	Voltage (p.u)
83	0.973		101	1.001
84	0.977		102	1.002
85	0.985		103	1.001
86	0.989		104	0.971
87	1.015		105	0.965
88	0.990		106	0.963
89	1.005		107	0.952
90	0.985		108	0.967
91	0.980		109	0.968
92	1.003		110	0.973
93	1.001		111	0.980
94	1.005		112	0.975
100	1.017			

Table B.30: Power Flow Information on Island 1, Island 2 and Island 3 - Case Study C8

Power Flow in ISLAND 1							
From bus	To bus	P_{max} (MW)	P_{flow} (MW)	From bus	To bus	P_{max} (MW)	P_{flow} (MW)
1	2	297.5	18.806	17	18	297.5	61.287
1	3	297.5	32.477	17	30	850	161.497
2	12	297.5	39.122	17	31	297.5	24.534
3	5	297.5	54.155	17	113	297.5	8.539
3	12	297.5	18.249	18	19	297.5	0.793
4	5	850	75.259	19	20	297.5	21.542

Power Flow in ISLAND 1								
From bus	To bus	P _{max} (MW)	P _{flow} (MW)		From bus	To bus	P _{max} (MW)	P _{flow} (MW)
4	11	297.5	36.152		20	21	297.5	21.637
5	6	297.5	59.344		21	22	297.5	35.912
5	8	850	234.118		22	23	297.5	46.648
5	11	297.5	45.360		23	24	297.5	13.101
6	7	297.5	6.918		23	25	850	142.750
7	12	297.5	12.098		23	32	238	72.977
8	9	850	198.557		25	26	850	59.424
8	30	297.5	64.831		25	27	850	116.674
9	10	850	200.00		26	30	850	230.457
11	12	297.5	10.198		27	28	297.5	14.298
11	13	297.5	20.975		27	32	297.5	8.181
12	14	297.5	4.535		27	115	297.5	18.871
12	16	297.5	4.357		28	29	297.5	2.747
12	117	297.5	20.145		29	31	297.5	26.831
13	15	297.5	13.289		31	32	297.5	5.635
14	15	297.5	9.556		32	113	850	14.794
15	17	850	91.839		32	114	297.5	11.221
15	19	297.5	22.215		114	115	297.5	3.193
16	17	297.5	29.761					
Power Flow in ISLAND 2								
From bus	To bus	P _{max} (MW)	P _{flow} (MW)		From bus	To bus	P _{max} (MW)	P _{flow} (MW)
33	37	297.5	23.245		56	59	297.5	27.738
34	36	297.5	31.978		59	60	297.5	42.978
34	37	850	80.722		59	61	297.5	51.502
34	43	297.5	10.544		59	63	850	144.6903
35	36	297.5	0.874		60	61	850	111.015
35	37	297.5	32.272		60	62	297.5	10.304
37	38	850	222.920		61	62	297.5	24.403
37	39	297.5	48.690		61	64	850	26.919
37	40	297.5	37.990		62	66	297.5	38.646
38	65	850	227.30		62	67	297.5	25.228
39	40	297.5	20.906		63	64	850	145.074
40	41	297.5	9.624		64	65	850	172.793
40	42	297.5	17.873		65	66	850	24.058
41	42	297.5	27.725		65	68	850	14.964
42	49	297.5	74.604		66	67	297.5	53.859
42	49	297.5	74.604		68	69	850	169.558
43	44	297.5	29.122		68	116	850	184.322
44	45	297.5	45.615		69	70	850	118.220
45	46	297.5	61.658		69	75	850	129.585
45	49	297.5	39.577		69	77	297.5	126.129
46	47	297.5	1.515		70	71	297.5	18.125
46	48	297.5	8.827		70	74	297.5	22.436
47	49	297.5	15.920		70	75	297.5	7.613
47	69	297.5	50.502		71	72	297.5	12.067
48	49	297.5	11.319		71	73	297.5	6.010
49	50	297.5	55.884		74	75	297.5	46.150
49	51	297.5	69.318		75	77	297.5	16.875
49	54	297.5	40.066		75	118	297.5	54.086
49	54	297.5	39.986		76	77	297.5	48.795
49	66	850	118.219		76	118	297.5	20.595
49	66	850	118.219		77	78	297.5	54.6395
49	69	297.5	46.738		77	80	850	79.336
50	57	297.5	38.059		77	80	850	35.926

Power Flow in ISLAND 2								
From bus	To bus	P_{max} (MW)	P_{flow} (MW)		From bus	To bus	P_{max} (MW)	P_{flow} (MW)
51	52	297.5	29.310		77	82	340	53.663
51	58	297.5	20.633		78	79	297.5	16.500
52	53	297.5	11.120		79	80	297.5	56.191
53	54	297.5	11.983		80	81	850	0.000
54	55	297.5	8.468		80	96	297.5	45.511
54	56	297.5	19.639		80	97	297.5	52.977
54	59	297.5	28.289		80	98	297.5	34.267
55	56	297.5	22.077		80	99	340	42.791
55	59	297.5	33.246		82	96	297.5	1.227
56	57	297.5	25.330		95	96	297.5	42.490
56	58	297.5	8.511		96	97	297.5	37.383
56	59	297.5	26.442					
Power Flow in Island 3								
From bus	To bus	P_{max} (MW)	P_{flow} (MW)		From bus	To bus	P_{max} (MW)	P_{flow} (MW)
83	84	297.5	6.431		94	100	297.5	7.865
83	85	297.5	13.688		100	101	297.5	0.859
84	85	297.5	17.531		100	103	850	121.073
85	86	850	76.232		100	104	297.5	56.388
85	88	297.5	18.904		100	106	297.5	60.622
85	89	297.5	0.072		101	102	297.5	22.991
86	87	850	100.00		103	104	297.5	32.293
88	89	850	29.336		103	105	297.5	42.937
89	90	850	54.056		103	110	297.5	60.575
89	90	850	102.942		104	105	297.5	48.682
89	92	850	137.942		105	106	297.5	8.676
89	92	850	43.234		105	107	297.5	26.679
90	91	297.5	10.116		105	108	297.5	23.982
91	92	297.5	20.331		106	107	297.5	24.056
92	93	297.5	27.977		108	109	297.5	21.783
92	94	297.5	22.445		109	110	297.5	13.717
92	100	297.5	14.684		110	111	297.5	36.000
92	102	297.5	28.090		110	112	297.5	69.459
93	94	297.5	15.766					

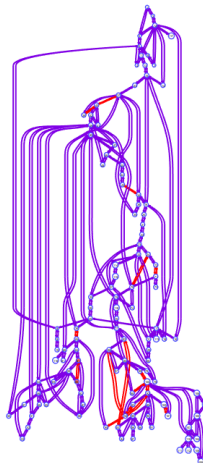


Figure B.15 : Graph model of an initial islanding solution for Case Study C9

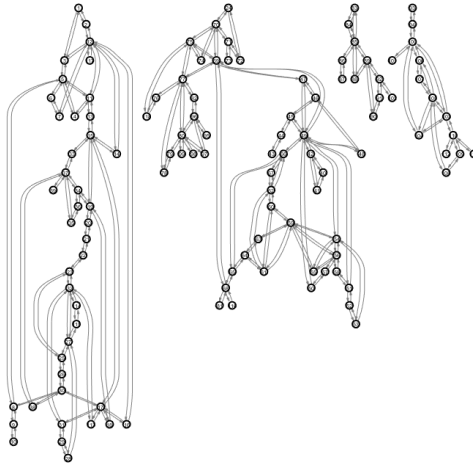


Figure B.16 : Graph model of islanding implementation for Case Study C9

Table B.31: Active Power Flow at Each Bus on Island 1, Island 2, Island 3 and Island 4- Case Study C9

Bus	Active power (MW) at each bus in Island 1			
	Pre-islanding		Post-islanding	
	Pload	Pgen	Pload	Pgen
1	51.000	0.000	51.000	0.000
2	20.000	0.000	20.000	0.000
3	39.000	0.000	39.000	0.000
4	39.000	0.000	39.000	0.000
5	0.000	0.000	0.000	0.000
6	52.000	0.000	52.000	0.000
7	19.000	0.000	0.000	0.000
8	28.000	0.000	28.000	0.000
9	0.000	0.000	0.000	0.000
10	0.000	30.000	0.000	200.000
11	70.000	0.000	0.000	0.000
12	47.000	100.000	47.000	100.000
13	34.000	0.000	0.000	0.000
14	14.000	0.000	14.000	0.000
15	90.000	0.000	0.000	0.000
16	25.000	0.000	25.000	0.000
17	11.000	0.000	0.000	0.000
18	60.000	0.000	0.000	0.000
19	45.000	0.000	45.000	0.000
20	18.000	0.000	18.000	0.000
21	14.000	0.000	14.000	0.000
22	10.000	0.000	10.000	0.000
23	7.000	0.000	7.000	0.000
25	0.000	200.000	0.000	200.000
26	0.000	220.000	0.000	275.659
27	71.000	0.000	71.000	0.000
28	17.000	0.000	17.000	0.000
29	24.000	0.000	24.000	0.000
30	0.000	0.000	0.000	0.000
31	43.000	100.000	43.000	100.000
32	59.000	0.000	59.000	0.000
33	23.000	0.000	23.000	0.000

Active power (MW) at each bus in Island 1				
Bus	Pre-islanding		Post-islanding	
	Pload	Pgen	Pload	Pgen
34	59.000	0.000	59.000	0.000
35	33.000	0.000	33.000	0.000
36	31.000	0.000	31.000	0.000
37	0.000	0.000	0.000	0.000
38	0.000	0.000	0.000	0.000
39	27.000	0.000	27.000	0.000
113	6.000	0.000	6.000	0.000
114	8.000	0.000	8.000	0.000
115	22.000	0.000	22.000	0.000
117	20.000	0.000	20.000	0.000
Active power (MW) at each bus in Island 2				
Bus	Pre-islanding		Post-islanding	
	Pload	Pgen	Pload	Pgen
24	13.000	0.000	13.000	0.000
40	66.000	0.000	66.000	0.000
41	37.000	0.000	37.000	0.000
42	96.000	0.000	96.000	0.000
43	18.000	0.000	18.000	0.000
44	16.000	0.000	16.000	0.000
45	53.000	0.000	53.000	0.000
46	28.000	100.000	28.000	100.000
47	34.000	0.000	34.000	0.000
48	20.000	0.000	20.000	0.000
49	87.000	200.000	87.000	200.000
50	17.000	0.000	17.000	0.000
51	17.000	0.000	17.000	0.000
52	18.000	0.000	18.000	0.000
53	23.000	0.000	23.000	0.000
54	113.000	48.000	113.000	48.000
55	63.000	0.000	63.000	0.000
56	84.000	0.000	84.000	0.000
57	12.000	0.000	12.000	0.000
58	12.000	0.000	12.000	0.000
59	277.000	155.000	277.000	155.000
60	78.000	0.000	78.000	0.000
61	0.000	160.000	0.000	160.000
62	77.000	0.000	77.000	0.000
63	0.000	0.000	0.000	0.000
64	0.000	0.000	0.000	0.000
65	0.000	391.000	0.000	391.000
66	39.000	392.000	39.000	392.000
67	28.000	0.000	28.000	0.000
68	0.000	0.000	0.000	0.000
69	0.000	800.000	0.000	486.415
70	66.000	0.000	66.000	0.000
71	0.000	0.000	0.000	0.000
72	12.000	0.000	12.000	0.000
73	6.000	0.000	6.000	0.000
74	68.000	0.000	68.000	0.000
75	47.000	0.000	47.000	0.000
76	68.000	0.000	68.000	0.000
77	61.000	0.000	61.000	0.000
78	71.000	0.000	71.000	0.000
79	39.000	0.000	39.000	0.000
80	130.000	477.000	130.000	477.000

Active power (MW) at each bus in Island 2				
Bus	Pre-islanding		Post-islanding	
	Pload	Pgen	Pload	Pgen
81	0.000	0.000	0.000	0.000
82	54.000	0.000	54.000	0.000
95	42.000	0.000	42.000	0.000
96	38.000	0.000	38.000	0.000
97	15.000	0.000	15.000	0.000
98	34.000	0.000	34.000	0.000
99	42.000	0.000	42.000	0.000
116	184.000	0.000	184.000	0.000
118	33.000	0.000	33.000	0.000
Active power (MW) at each bus in Island 3				
Bus	Pre-islanding		Post-islanding	
	Pload	Pgen	Pload	Pgen
83	20.000	0.000	20.000	0.000
84	11.000	0.000	11.000	0.000
85	24.000	0.000	24.000	0.000
86	21.000	0.000	21.000	0.000
87	0.000	100.000	0.000	100.000
88	48.000	0.000	48.000	0.000
89	0.000	300.000	0.000	277.248
90	163.000	0.000	163.000	0.000
91	10.000	0.000	10.000	0.000
92	65.000	0.000	65.000	0.000
102	5.000	0.000	5.000	0.000
Active power (MW) at each bus in Island 4				
Bus	Pre-islanding		Post-islanding	
	Pload	Pgen	Pload	Pgen
93	12.000	0.000	12.000	0.000
94	30.000	0.000	30.000	0.000
100	37.000	252.000	37.000	287.428
101	22.000	0.000	22.000	0.000
103	23.000	40.000	23.000	65.000
104	38.000	0.000	38.000	0.000
105	31.000	0.000	31.000	0.000
106	43.000	0.000	43.000	0.000
107	50.000	0.000	50.000	0.000
108	2.000	0.000	2.000	0.000
109	8.000	0.000	8.000	0.000
110	39.000	0.000	39.000	0.000
111	0.000	36.000	0.000	61.000
112	68.000	0.000	68.000	0.000

Table B.32: Voltage Profile on Island 1, Island 2, Island 3 and Island 4- Case Study C9

Island 1				
Bus. No	Voltage (p.u)		Bus. No	Voltage (p.u)
1	0.965		22	1.006
2	0.976		23	1.022
3	0.974		25	1.050
4	0.998		26	1.015
5	1.001		27	0.968
6	0.990		28	0.963
7	0.990		29	0.964
8	1.015		30	1.033
9	1.071		31	0.967
10	1.050		32	0.974

Island 1			
Bus. No	Voltage (p.u)		Voltage (p.u)
11	0.996		0.995
12	0.990		0.986
13	1.004		0.981
14	0.996		0.980
15	1.010		0.992
16	0.990		1.014
17	1.009		0.973
18	1.003		0.993
19	1.003		0.967
20	0.999		0.966
21	0.999		0.976
Island 2			
Bus. No	Voltage (p.u)		Voltage (p.u)
24	0.992		1.035
40	0.970		1.050
41	0.967		1.026
42	0.985		1.020
43	0.948		1.035
44	0.964		0.984
45	0.975		0.987
46	1.005		0.980
47	1.021		0.991
48	1.016		0.958
49	1.025		0.970
50	1.003		0.950
51	0.972		1.006
52	0.963		1.002
53	0.951		1.005
54	0.955		1.040
55	0.962		1.037
56	0.954		0.982
57	0.973		0.960
58	0.963		0.985
59	0.985		1.008
60	1.003		1.026
61	1.005		1.010
62	1.008		1.005
63	1.007		0.954
64	1.018		
Island 3			
Bus. No	Voltage (p.u)		Voltage (p.u)
83	0.973		1.005
84	0.977		0.985
85	0.985		0.980
86	0.989		1.003
87	1.015		1.002
88	0.990		
Island 4			
Bus. No	Voltage (p.u)		Voltage (p.u)
93	0.995		0.964
94	1.002		0.952
100	1.017		0.967
101	0.996		0.968
103	1.001		0.973
104	0.971		0.980
105	0.965		0.975

Table B.33: Power Flow Information on Island 1, Island 2, Island 3 and Island 4 - Case Study C9

Power Flow in ISLAND 1							
From bus	To bus	P _{max} (MW)	P _{flow} (MW)	From bus	To bus	P _{max} (MW)	P _{flow} (MW)
1	2	297.5	20.025	17	113	297.5	5.606
1	3	297.5	31.263	18	19	297.5	35.512
2	12	297.5	40.359	19	20	297.5	7.757
3	5	297.5	51.308	19	34	297.5	18.777
3	12	297.5	19.841	20	21	297.5	25.886
4	5	850	55.116	21	22	297.5	40.220
4	11	297.5	16.049	22	23	297.5	51.075
5	6	297.5	47.951	23	25	850	133.047
5	8	850	177.194	23	32	238	72.426
5	11	297.5	22.819	25	26	850	43.858
6	7	297.5	4.336	25	27	850	110.810
7	12	297.5	4.338	26	30	850	231.801
8	9	850	198.925	27	28	297.5	12.667
8	30	297.5	7.886	27	32	297.5	5.640
9	10	850	200.00	27	115	297.5	17.505
11	12	297.5	40.030	28	29	297.5	4.373
11	13	297.5	1.348	29	31	297.5	28.467
12	14	297.5	5.677	30	38	297.5	125.886
12	16	297.5	2.559	31	32	297.5	7.167
12	117	297.5	20.145	32	113	850	11.769
13	15	297.5	1.353	32	114	297.5	12.583
14	15	297.5	8.407	33	37	297.5	7.050
15	17	850	61.443	34	36	297.5	32.746
15	19	297.5	20.741	34	37	850	43.419
15	33	297.5	30.399	35	36	297.5	1.638
16	17	297.5	22.684	35	37	297.5	31.500
17	18	297.5	35.667	37	38	850	125.161
17	30	850	93.830	37	39	297.5	27.271
17	31	297.5	21.366	114	115	297.5	4.551
Power Flow in ISLAND 2							
From bus	To bus	P _{max} (MW)	P _{flow} (MW)	From bus	To bus	P _{max} (MW)	P _{flow} (MW)
24	70	297.5	10.488	60	61	850	115.477
24	72	297.5	2.540	60	62	297.5	8.712
40	41	297.5	19.335	61	62	297.5	28.383
40	42	297.5	48.078	61	64	850	38.521
41	42	297.5	57.746	62	66	297.5	35.777
42	49	297.5	109.043	62	67	297.5	22.426
42	49	297.5	109.043	63	64	850	158.657
43	44	297.5	18.221	64	65	850	198.216
44	45	297.5	34.505	65	66	850	28.826
45	46	297.5	55.699	65	68	850	163.958
45	49	297.5	33.966	66	67	297.5	50.997
46	47	297.5	6.229	68	69	850	21.161
46	48	297.5	10.072	68	81	850	0.123
47	49	297.5	11.096	68	116	850	184.561
47	69	297.5	40.248	69	70	850	126.135
48	49	297.5	10.089	69	75	850	133.504
49	50	297.5	51.306	69	77	297.5	128.469
49	51	297.5	63.773	70	71	297.5	20.707
49	54	297.5	35.162	70	74	297.5	19.896
49	54	297.5	35.208	70	75	297.5	4.465
49	66	850	147.526	71	72	297.5	14.639
49	66	850	147.526	71	73	297.5	6.010

Power Flow in ISLAND 2								
From bus	To bus	P _{max} (MW)	P _{flow} (MW)		From bus	To bus	P _{max} (MW)	P _{flow} (MW)
49	69	297.5	36.898		74	75	297.5	48.681
50	57	297.5	33.600		75	77	297.5	18.091
51	52	297.5	27.608		75	118	297.5	53.149
51	58	297.5	17.113		76	77	297.5	49.747
52	53	297.5	9.439		76	118	297.5	19.674
53	54	297.5	13.664		77	78	297.5	54.640
54	55	297.5	7.061		77	80	850	79.336
54	56	297.5	15.269		77	80	850	35.926
54	59	297.5	33.524		77	82	340	53.663
55	56	297.5	18.515		78	79	297.5	16.500
55	59	297.5	38.370		79	80	297.5	56.191
56	57	297.5	21.009		80	96	297.5	45.511
56	58	297.5	5.023		80	97	297.5	52.977
56	59	297.5	30.827		80	98	297.5	34.267
56	59	297.5	32.326		80	99	340	42.791
59	60	297.5	45.824		82	96	297.5	1.227
59	61	297.5	54.661		95	96	297.5	42.490
59	63	850	158.2044		96	97	297.5	37.383
Power Flow in ISLAND 3								
From bus	To bus	P _{max} (MW)	P _{flow} (MW)		From bus	To bus	P _{max} (MW)	P _{flow} (MW)
83	84	297.5	6.431		89	90	850	50.428
83	85	297.5	13.688		89	90	850	95.931
84	85	297.5	17.531		89	92	850	77.264
85	86	850	76.232		89	92	850	24.224
85	88	297.5	18.904		90	91	297.5	20.260
85	89	297.5	0.072		91	92	297.5	30.655
86	87	850	100.00		92	102	297.5	5.003
88	89	850	29.336					
Power Flow in ISLAND 4								
From bus	To bus	P _{max} (MW)	P _{flow} (MW)		From bus	To bus	P _{max} (MW)	P _{flow} (MW)
93	94	297.5	12.038		104	105	297.5	42.562
94	100	297.5	42.383		105	106	297.5	14.253
100	101	297.5	22.174		105	107	297.5	27.492
100	103	850	83.907		105	108	297.5	11.794
100	104	297.5	48.164		106	107	297.5	23.247
100	106	297.5	53.810		108	109	297.5	9.739
103	104	297.5	34.084		109	110	297.5	1.724
103	105	297.5	43.212		110	111	297.5	61.000
103	110	297.5	47.513		110	112	297.5	69.459